The Thesis Committee for Rachel Veronica Simon
Certifies that this is the approved version of the following thesis:

Cranial osteology of the long-beaked echidna, and the definition, diagnosis, and origin of Monotremata and its major subclades

APPROVED BY
SUPERVISING COMMITTEE:

Supervisor:

Timothy B. Rowe

Christopher J. Bell

Julia A. Clarke

Matthew W. Colbert

Cranial osteology of the long-beaked echidna, and the definition, diagnosis, and origin of Monotremata and its major subclades

by

Rachel Veronica Simon, B.S.

Thesis

Presented to the Faculty of the Graduate School of

The University of Texas at Austin

in Partial Fulfillment

of the Requirements

for the Degree of

Master of Science in Geological Sciences

The University of Texas at Austin

December 2013

Dedication

I dedicate this thesis to my parents, Joseph Simon and Heather Roskelley, who supported me through the entirety of my thesis, even though it meant moving far away from home. I also dedicate this thesis to my husband, Gerard Wallace, for his endless faith in my capabilities which helped me get to where I am today.

Acknowledgements

I thank my advisor, Tim Rowe, for accepting me into his lab and for his guidance through my thesis with great wisdom and enthusiasm. Tim has talent for asking big-picture questions and communicating science; I would like to think that I have learned from his talent. I thank Tim for his in-depth discussions on mammalian evolution and anatomy which have contributed significantly to this thesis.

I thank my committee for their assistance with my thesis. Thank you, Chris Bell, for access to your extensive library, philosophical discussions on science and paleontology, and attention to detail when reading my thesis. Thank you, Julia Clarke, for your discussions on phylogenetic systematics and valuable input on organization and methods for my thesis. And thank you Matt Colbert, for our many conversations on monotremes, your help with interpreting the CT scans, and the many hours you spent helping me improve my thesis.

Many others outside of my committee deserve my thanks: Matt Colbert and Jessie Maisano, along with the rest of the CT Lab provided CT data of mammal specimens which were used in this thesis. Ernest Lundelius engaged me in many thoughtful discussions about monotremes and the dates of caves in Australia that contain fossils of echidnas. Eileen Westwig of the American Museum of Natural History helped me access monotreme specimens in the Mammalogy Collections. And Anjan Bhullar deserves a big thanks for letting me stay in his apartment when I visited Harvard, teaching me how to observe and compare museum specimens, and bringing the juvenile *Zaglossus bruijni* to the UT campus for it to be scanned in the CT lab.

Work for this thesis was funded by the Jackson School of Geosciences. Travel to the Museum of Comparative Zoology at Harvard and the American Museum of Natural History in New York City was funded by the Ernest L. and Judith W. Lundelius Fund.

Discussions, feedback, and advice on methods and life in general were provided by the ever-talented graduate students at the Jackson School of Geosciences. Thank you to the graduate students, past and present, of the Rowe lab: Eric Ekdale, Heather Ahrens, Jerry Rogers, Adam Marsh, and Zachary Morris. Michelle Stocker, Alicia Kennedy, Robert Burroughs, Will Gelnaw, Travis Wicks of the Bell lab and Zhiheng Li of the Clarke lab also provided me with intellectual feedback and emotional support.

Abstract

Cranial osteology of the long-beaked echidna, and the definition, diagnosis, and origin of Monotremata and its major subclades

Rachel Veronica Simon, M.S. Geo. Sci.

The University of Texas at Austin, 2013

Supervisor: Timothy B. Rowe

Extant monotremes have a combination of plesiomorphic and apomorphic characters that causes ambiguity about their basic anatomy and evolutionary history. The problem is compounded by the lack of extinct and extant specimens of monotremes available for study. Only five species of monotremes are currently recognized, and all are endangered. The most speciose subclade, the long-beaked echidna, *Zaglossus*, has few specimens archived in mammalogy collections relative to the platypus, *Ornithorhynchus anatinus*, and the short-beaked echidna, *Tachyglossus aculeatus*. As a result, researchers sample from *Ornithorhynchus* and *Tachyglossus*, excluding species of *Zaglossus* from analysis. An equally depauperate fossil record consisting primarily of fragmentary jaws and isolated molars over a broad temporal range (~125 Ma) has led to controversies surrounding the origin and evolution of Monotremata and its major subclades. As new fossils attributable to Monotremata have been discovered, they are placed in conflicting positions on either the crown or the stem. I used CT scans of skeletally immature and mature specimens of *Zaglossus bruijni* and *Zaglossus bartoni*, respectively, to describe

the cranial osteology of *Zaglossus* in detail. New insights about the anatomy of *Zaglossus* were then utilized in a phylogenetic analysis. *Zaglossus* and the extinct echidna, *Megalibgwilia* were added to a previously published morphological character matrix, along with 42 new skeletal characters. For the first time, I illustrated the cranial anatomy of *Zaglossus bruijnii* and *Zaglossus bartoni*, and described the endocranial morphology and individual variation among the two species. I described patterns of ossification throughout ontogeny that may explain a preservation bias against echidnas. My phylogenetic analysis placed the Early Cretaceous monotremes either on the stem of Ornithorhynchidae or in the monotreme crown, supporting an Early Cretaceous divergence estimate between platypuses and echidnas. I provide the first phylogenetic definition and diagnosis of Monotremata, Ornithorhynchidae, and Tachyglossidae. Based on the distribution of characters of extant monotremes, the ancestral monotreme was likely a terrestrial, scratch-digger capable of electroreception. The ancestral population gave rise to the semi-aquatic platypuses and the large, terrestrial echidnas. *Tachyglossus* is the most derived of the extant echidnas; it is more appropriate to include *Ornithorhynchus* and *Zaglossus* in future phylogenetic analyses.

Table of Contents

List of Tables

List of Figures

Chapter 1: Description of the cranium of the long-beaked echidna, *Zaglossus*

INTRODUCTION

Since monotremes were introduced to Western science at the end of the 18th century, monotreme taxonomy and affinities remain hotly debated. Contributing factors to this debate include the bizarre morphological specializations of monotremes and their extremely low taxonomic diversity. Although museums house numerous wet and dry specimens, extant monotremes comprise only three genera that include five species (Appendix 1.A). Inclusion of extinct taxa brings monotreme diversity to only nine genera and an uncertain number of species (Appendix 1.B).

Monotremata is defined as the most recent common ancestor of the platypuses, Ornithorhynchidae, and the echidnas, Tachyglossidae, and all of that ancestor's descendants (Fig. 1.1; Chapter 2). Ornithorhynchidae is represented by a single extant species, the duck-billed platypus *Ornithorhynchus anatinus*, and two extinct species *Obdurodon insignis* and *Obdurodon dicksoni* (Chapter 2). *Ornithorhynchus* is semiaquatic and is found in the rivers and lakes of Australia and Tasmania (Fig. 1.2; Griffiths, 1978; Grant, 1992). In the water, *Ornithorhynchus* forages for invertebrates including crustaceans, worms, molluscs, and adult as well as larval-stage insects (Augee et al., 2006). Like its echidna relatives, the platypus is a capable digger, dwelling in burrows when out of the water. Extant Tachyglossidae includes the short-beaked echidna, *Tachyglossus aculeatus*, and the long-beaked echidnas, *Zaglossus*, of which three species

are known. *Tachyglossus* covers the greatest geographic range, occurring throughout parts of Australia, as well as Tasmania and parts of New Guinea (Fig. 1.2) and inhabiting arid environments (Augee et al., 2006). *Tachyglossus* feeds on ants and termites, using curved claws to dig into the hard ground and a long, sticky tongue to gather up prey (Augee et al., 2006).

The taxonomy of *Zaglossus*, the most speciose of the monotreme genera, has been revisited and revised since *Zaglossus bruijnii* was first described in 1876 by Peters and Doria as a species of *Tachyglossus* (see Appendix 1.A). In 1998, Flannery and Groves inspected 75 specimens from 13 museums around the world and divided *Zaglossus* into three species based primarily on claw number, palatal shape, and orbitotemporal size. *Zaglossus bruijnii*, *Zaglossus bartoni*, and *Zaglossus attenboroughi* are still recognized (Wilson and Reeder, 2005). *Zaglossus bartoni* was further divided into four subspecies determined by "size and proportional differences," (Flannery and Groves, 1998: 381) *Zaglossus bartoni bartoni*, *Zaglossus bartoni clunius*, *Zaglossus bartoni diamondi*, and *Zaglossus bartoni smeenki*. All species of *Zaglossus* are found in the humid upper montane regions of New Guinea (Fig. 1.2). *Zaglossus* uses its long, tubular snout to probe moist soils in search of earthworms, centipedes, and soft-bodied insect larvae. Similar to *Tachyglossus*, prey are drawn into the snout using the tongue and are ground between spiny keratinous plates located on the back of the tongue and soft palate (Fig. 1.3; Augee et al., 2006).

Relative to *Ornithorhynchus* and *Tachyglossus*, species of *Zaglossus* have received little academic attention. Although numerous authors described various aspects of the cranial anatomy of *Ornithorhynchus* and *Tachyglossus* (e.g., Van Bemmelen, 1901; Gaupp, 1908; Watson, 1916; Kuhn, 1971; Griffiths, 1978; Kuhn and Zeller, 1987), only two describe *Zaglossus* (Gervais, 1877-1878; Allen, 1912). The first description of a mature specimen of *Zaglossus bruijnii* (referred to as *Acanthoglossus brujnii*, Gervais 1877-1878) included accurate and detailed illustrations, but only a general description of the skull that does not cover every cranial element. The second description (Allen, 1912) covered hard and soft-tissue anatomy and used immature specimens in which visible sutures allowed further identification of cranial elements. Unfortunately, the squamosal was misidentified as the jugal resulting in a cascade of misidentifications. For example, after the squamosal was identified as the jugal, the periotic was reasoned to be the squamosal because it is otherwise "too far anterior to the mastoid region to fulfill the requirements of a squamosal" (Allen, 1912: 291). No qualms were had, however, about calling the orbitosphenoid (positioned medially to the squamosal) the parietal, or identifying the large parietal as the interparietal. This renders Allen's description almost useless.

The taxonomy of extinct echidnas also is convoluted (see Appendix 1.B). Fossil humeri, femora, tibiae, and crania of varying completeness have been discovered in Pleistocene cave deposits in Australia and were variously identified as a species of *Ornithorhynchus*, a species of *Tachyglossus*, a species of *Zaglossus*, or assigned to a new

genus, *Megalibgwilia* (e.g., Krefft, 1868; Owen, 1884; Dun, 1895; Glauert, 1914; Murray, 1978; Griffiths, 1991). In 1978, Murray condensed the numerous names for extinct species into only three (*Zaglossus robusta*, *Zaglossus ramsayi*, and *Zaglossus hacketti*), while at the same time proposing that *Zaglossus hacketti* be assigned to its own genus. Later, *Zaglossus ramsayi* was assigned to a new genus, *Megalibgwilia*, based on morphological differences (Griffiths, 1991). *Zaglossus robusta* may also be a species of *Megalibgwilia* (Griffiths et al., 1991; Musser, 2003). A morphology-based parsimony analysis (Fig. 1.1; Chapter 2) resolves *Megalibgwilia* as the outgroup to Tachyglossidae. The phylogenetic affinities of *Zaglossus hacketti* are uncertain (Griffiths, 1978; Murray, 1978), and additional phylogenetic analysis is required to determine whether it truly represents *Zaglossus*, *Megalibgwilia*, or alternatively requires the establishment of a new genus.

Those fossils highlight the importance of understanding anatomy of extant monotremes, the natural variation within monotreme genera, as well as their similarities and differences. I will describe and illustrate the cranial anatomy of *Zaglossus* by using X-ray Computed Tomography (CT) scans of *Zaglossus bruijnii* and *Zaglossus bartoni*, and by observing specimens in person at mammology collections. My description and detailed illustrations will assist in identifying important anatomical features of skulls of tachyglossids and facilitate meaningful comparisons between the two extant groups of echidnas.

Institutional Abbreviations

AMNH	American Museum of Natural History, New York City, New York
BMNH	Natural History Museum of London, London, United Kingdom
MCZ	Museum of Comparative Zoology, Harvard University, Cambridge, Massachusetts
SAM	South Australian Museum, Adelaide, South Australia

MATERIALS AND METHODS

Resources for Anatomical Identification

The anatomical terminology used here generally follows Kuhn's (1971) comprehensive piece on cranial development and morphology of *Tachyglossus*. For *Ornithorhynchus*, I referenced Zeller's (1989a) extensive monograph on development and morphology of the skull of *Ornithorhynchus*. The anatomy of the secondary cranial wall in Monotremata follows Kuhn and Zeller (1987). Other referenced descriptions of monotremes include: Gervais (1877-1878), Van Bemmelen (1901), Allen (1912), Watson (1916), and Griffiths (1978). Monotreme inner ear anatomy follows Simpson's (1938) *Osteography of the Ear Region in Monotremes*. Descriptions of extinct echidnas were also used from the literature (Murray, 1978; Giffiths, 1991) for comparison with *Zaglossus*.

Referred Specimens

Seven specimens of *Zaglossus bruijnii* and *Zaglossus bartoni* were observed in person in the Mammalogy Collections of the AMNH and the MCZ and are referenced throughout this document (Table 1.1). The specimen referenced primarily for description is a skeletally immature *Zaglossus bruijnii.* MCZ 7397. That specimen has a low degree of skull fusion, with many of its sutures visible. The animal was wild-caught in 1909 from Mt. Arfak in Papua New Guinea. The sex of the specimen is unknown. *Zaglossus bruijnii* MCZ 7397 was observed both in person and from digital CT data. The CT scan of the more skeletally mature *Zaglossus bartoni*, AMNH 157072, was used to compare the internal cranial morphologies that could vary between individuals of different skeletal maturity. See **Computed Tomography** section below, as well as Appendices 1.C and 1.D, for details of the scanning parameters for *Zaglossus bruijnii* MCZ 7397 and *Zaglossus bartoni* AMNH 157072, respectively.

In the revision of the genus *Zaglossus*, morphological differences were reported in the skull between the two species, *Zaglossus bruijnii* and *Zaglossus bartoni* (Flannery and Groves, 1998). The secondary palate of *Zaglossus bruijnii* has a groove that persists through its entire length. In *Zaglossus bartoni*, the back of the secondary palate is flat. *Zaglossus bartoni* tends to have a higher-crowned braincase than *Zaglossus bruijnii*, as well as a shallower orbitotemporal fossa (the fossa between the cranial moiety of the squamosal and the temporal region of the cranial wall). There is, however, overlap in the morphology of *Zaglossus bruijnii* and the subspecies of *Zaglossus bartoni*. Further, the

shape of cranial elements and their contacts are not significantly different between the two species. For this reason, the cranial, comparison between the two species is not discussed. The third species of *Zaglossus*, *Zaglossus attenboroughi*, is based on a single specimen that includes "the rostral portion of a badly crushed skull," (Flannery and Groves, 1998: 387) and is archived at the Nationaal Naturhistorisch Museum, Leiden, in the Netherlands. For those reasons, *Zaglossus attenbouroghi* was excluded from this study.

Specimens of *Ornithorhynchus* and *Tachyglossus* were compared with *Zaglossus* to identify osteological differences between the monotremes. See Table 1.1 for a complete list of specimens of Monotremata observed for this study.

Computed Tomography Methods

X-ray computed tomography scans of *Zaglossus bruijnii* (MCZ 7397), and *Zaglossus bartoni* (AMNH 157072) were extensively used to visualize internal cranial anatomy and to delineate thoroughly the sutures between cranial elements. CT images of *Tachyglossus* and *Ornithorhynchus*, accessed on DigiMorph.org, were also used for a detailed comparison between species of monotremes. All CT data are available on DigiMorph.org. See Table 1.2 for a list of URL web addresses that were accessed for this study.

Zaglossus bruijnii MCZ 7397 was scanned by Dr. Matthew Colbert at The University of Texas at Austin High Resolution X-ray Computed Tomography Facility (UTCT) on April 15, 2008. The high resolution (1024X1024 pixel images) CT scan

covers the skull from the tip of the rostrum to the end of the occiput in 1,139 slices. Each slice is 0.125 millimeters (mm) thick. The field of reconstruction is 57 mm, yielding an inter-pixel value of 0.056 mm/pixel. See Appendix 1.C for complete description of scanning parameters.

Zaglossus bartoni AMNH 157072 was scanned by Dr. Matthew Colbert at UTCT on October 31, 2003. The high resolution (1024X1024 pixel images) CT scan covers the skull from the tip of the rostrum to the end of the occiput in 909 slices. Each slice is 0.175 millimeters (mm) thick. The field of reconstruction is 55 mm. See Appendix 1.D for complete description of scanning parameters.

CT images were visualized using the 3-D rendering software VGStudio MAX v.2.1. Previous descriptions of the cranial anatomy of monotremes were based on disarticulated skulls (e.g., Allen, 1912), serially-sectioned skulls (e.g., Simpson, 1938), or serial-sectioned heads of young specimens (e.g., Gaupp, 1908; Watson, 1916; Kuhn, 1971; Kuhn and Zeller, 1987; Zeller, 1989a). The use of CT data for MCZ 7397 enabled non-destructive digital segmentation (i.e., virtual isolation) and 3-D rendering of individual cranial elements without damaging the specimen. Cranial elements were segmented using the polygon lasso tool for selecting voxels through multiple slices, and using the pen tool for more precise voxel selection on one slice. The skull and its isolated elements were rendered as an isosurface for a brighter image.

Endocranial cavities and spaces were rendered as 3-D volumes, providing information on the shape and size of the cranial endocast, maxillary canals through the

maxillae, inner ear structure within the periotics, and the passage of the arteria diploëtica magna through the temporal regions of the skull. Endocranial spaces were segmented using the region-growing tool for a quick selection through multiple slices. The pen tool was used to adjust the region of interest if the region growing tool selected voxels outside of the endocranial volume of interest. Avizo 7.1 vibrantly renders endocranial volumes and was used for visualizing the blood vessels. Segmentations, volume renderings, and animations will be archived on DigiMorph.org. See Table 1.2 for URL of archived material.

DESCRIPTION

The crania of *Zaglossus bruijnii* MCZ 7397 (Fig. 1.4), *Tachyglossus aculeatus* AMNH 107185 (Fig. 1.5), and *Ornithorhynchus anatinus* AMNH 200255 (Fig. 1.6) are illustrated in dorsal, ventral, and lateral views for general anatomical comparison. Contacts between elements are depicted where sutures are visible, or otherwise indicated at their approximate position. Table 1.3 is a key to the abbreviated skull elements and features labeled in all figures throughout this document.

Overview of the Skull of *Zaglossus*

The skull of *Zaglossus* is characterized by a long snout perforated by numerous foramina for electroreception and a domed cranium enclosing a relatively large brain (Augee et al., 2006). The snout is well over half the length of the entire skull (Table 1.4) and is decurved. The snout of the extinct echidna *Megalibgwilia ramsayi* also is decurved

while the short snout of *Tachyglossus* is recurved (Fig. 1.5). *Ornithorhynchus* and the extinct platypuses of the genus *Obdurodon*, have a long but straight snout that slopes downwards in lateral view (Fig. 1.6). Therefore, although *Zaglossus* is derived for having a longer snout relative to other monotremes, its decurved condition is plesiomorphic for Tachyglossidae, and possibly for Monotremata (based on the phylogenetic analysis presented here in Chapter 2). The snout consists of the dorsal septomaxillae and ventral premaxillae rostrally, the maxillae laterally and ventrally, and the nasals dorsally. The nostrils face dorsally within a single, dorsally positioned external naris as in all other monotremes. The external naris is surrounded by the septomaxillae, a synapomorphy of Tachyglossidae (see Chapter 2), unlike other taxa in which the septomaxillae, when present, are restricted to the posteroventral margins of each external naris. Immediately ventral to the external nares is the palatine fissure (= narial lacuna of Griffiths, 1978, 1991). The palatine fissure in monotremes is a single opening rather than paired as in most other mammals. In tachyglossids, the palatine fissure is bounded by the premaxillae anterolaterally, and the maxillae posteriorly (Figs. 1.4 and 1.5).

Low orbits lie between the snout and braincase. The frontal forms a majority of the orbital wall, but the dorsal exposure of the frontals between the orbits is quite limited, being overlapped by nasals anteriorly, parietals posteriorly, and interfrontals medially (Fig. 1.4). The floor of the orbit comprises the maxilla anteriorly and the palatine posteriorly. The orbit is bounded by the maxilla anteriorly, the nasal anterodorsally, the parietal posterodorsally, and the orbitosphenoid and squamosal posteriorly (Fig. 1.4). A

low zygomatic arch frames the ventrolateral margin of the orbit. The jugal is absent in tachyglossids, and the zygomatic arch is formed by the maxilla anteroventrally and the squamosal posterodorsally. Monotremes lack a lacrimal bone so the lacrimal foramen is positioned between the frontal and maxilla in the anteroventral corner of the orbit.

Endocranially a large, horizontally sloping ethmoid is positioned between the orbits. An anteroposteriorly elongate mesethmoid runs the entire length of the snout dorsal to an elongate vomer. The ethmoid is fused to the orbitosphenoid which contributes to a significant portion of the anterior braincase. Although a small portion of the orbitosphenoid is visible externally in lateral view, it is mostly overlapped by the parietal dorsally and the squamosal ventrally.

The large cerebral cortex of *Zaglossus* is covered dorsally by broad parietals. A facial process of each parietal stretches anteriorly, overlapping the frontal, and in some specimens (e.g., MCZ 7397), it contacts the nasal such that the frontal has two non-contiguous external exposures. Laterally, the cerebral cortex is protected by the orbitosphenoid anteriorly and the lamina ascendens of the periotic posteriorly. Ventrally in the cranial cavity, the hypophysis sits in the sella turcica of the medial basisphenoid. Monotremes lack a presphenoid so the basisphenoid contacts the ethmoid anteriorly. The basisphenoid is bounded laterally by the alisphenoid and posteriorly by the basioccipital.

Between the medial alisphenoid and the lateral periotic and squamosal is the sphenoparietal membrane (Griffiths, 1978), which is not completely ossified in young individuals, thus leaving a membranous gap on the ventral cranium. In skeletally mature

individuals, the membrane is completely ossified such that there are no openings on the ventral surface of the skull except for the foramen ovale.

The back of the skull is rounded and gently slopes anterodorsally such that the occipital condyles protrude further posteriorly than the top of the occiput. The occipital condyles comprise the exoccipitals which frame the foramen magnum laterally. The basisphenoid shapes the ventral border of the foramen magnum, and the dorsal margin is formed by the broad supraoccipital. An incision above the foramen magnum, likely related to an enlarged cerebellum, divides the supraoccipital ventromedially but closes through ontogeny. At incision, the incisura occipitalis, is present in all extant monotremes and *Obdurodon dicksoni* (see Archer et al., 1992, 1993).

The relatively large three middle-ear ossicles and the ectotympanic, are found within the tympanic fossa on the ventral periotic. As in other monotremes, the malleus and ectotympanic lie in a horizontal plane ventrally under the skull. The ectotympanic is thin and ‘C’-shaped.

The lower jaw is formed by the long, gracile and edentulous dentaries. Proximally, the dentaries are more robust than the dentaries of *Tachyglossus*; distally, the dentaries terminate as delicate, pointed splints, differing from the spatulate shape seen in *Tachyglossus* and *Ornithorhynchus*. Although the dentaries of *Zaglossus* are slightly bowed, similar to the dentaries of *Tachyglossus* and *Ornithorhynchus*, they differ from other monotremes in having terminal ends that remain in contact rather than flaring laterally and separating anteriorly as in *Tachyglossus* and *Ornithorhynchus*.

Premaxilla

The edentulous paired premaxillae (Fig. 1.7) contribute to the ventral surface of the rostral tip of the snout. Each premaxilla is shaped as a long 'J;' gently curving anteromedially to meet its counterpart at the midline to form both the pointed anteroventral margin of the snout, and the anterolateral margins of the palatine fissure. The premaxilla lacks both a facial process and internarial bar; instead, it is directly overlain by the septomaxilla anteriorly, and by the maxilla posteriorly. Where the septomaxilla overlies the premaxilla the two elements are fused. This fusion happens early in ontogeny and makes it difficult to distinguish the two elements even in immature specimens. Their separate identities can be discerned in cross-sections, and in embryonic specimens (Kuhn, 1971; Zeller, 1989a). In early-stage embryos of *Tachyglossus,* the premaxilla and septomaxillae are distinct elements separated by the crista marginalis (Kuhn, 1971, figs. 16-19). Posteroventrally, the palatal process of the premaxilla is elongate, thin, and splint-like; it extends the length of the snout beneath the maxilla to where the maxilla begins to flare laterally to form the zygomatic arch. Although longest in *Zaglossus,* the occurrence of anteroposteriorly elongate palatal processes of the premaxillae is a synapomorphy of Monotremata (Simon, Chapter 2). In *Tachyglossus*, the palatal process terminates anterior to the vertical, lateral plate of the squamosal where the squamosal attaches to the cranium, but only extends about half the length of the rostrum in *Ornithorhynchus.*

Monotremes are derived in having an edentulous premaxilla that is restricted to the ventral surface of the snout. In Tritylodontidae, an anterodorsal process of the premaxillae forms an internarial bar that contacts the nasals dorsally, separating the left and right external nares (Sues, 1986). Therian mammals, like monotremes, lack an internarial bar of the premaxillae, but unlike monotremes, retain a facial process that contacts the nasals.

Septomaxilla

The paired septomaxillae (Fig. 1.7) form the anterodorsal rostrum and completely enclose the dorsally opening external naris. The septomaxillae are bordered by the nasals posteriorly, the maxillae posteroventrally, and the premaxillae anteroventrally. Their sutures with the nasals and maxillae remain distinct, unlike their sutures with the premaxillae, which close completely early in ontogeny, rendering the elements indistinguishable. Facial processes of the septomaxillae meet medially and form either a 'V'- or 'U'-shaped posterior margin of the external naris. The facial processes continue dorsomedially for a little under half the length of the rostrum until they contact the nasals. The sutural contact between septomaxillae and nasals is anteriorly convex, each facial process wedging between the anterior nasals and antrerodorsal maxillae. In most specimens of *Tachyglossus*, the external naris is teardrop-shaped, being widest anteriorly and narrow, or even pointed, posteriorly. In *Zaglossus*, the external naris is lenticular, tapering to a rounded end of equal curvature both anteriorly and posteriorly. In *Ornithorhynchus*, the septomaxillae never contact and anteriorly they form the open bill;

posteriorly, facial processes of the septomaxillae taper to a point between the nasals and maxillae (Fig. 1.6).

In Tritylodontidae, the septomaxilla is positioned posterodorsal to the premaxillae, forming the posteroventral margin of the external nares, and bordered by the premaxillae anteroventrally, the maxillae posteroventrally, and the nasals dorsally. A processus intrafenestralis (Sues, 1986) projects dorsally from the rostral end of each septomaxilla into the internarial septum.

In the early mammal, *Hadrocodium wui*, the septomaxilla forms the ventral and lateral margin of the external nares and is bordered by the premaxillae anteroventrally, the maxillae posteroventrally and the nasals dorsally (Luo et al., 2001). There is no evidence of a processus intrafenestralis. The septomaxillae of Tachyglossidae are, therefore, derived for enclosing the external naris, meeting at the midline and forming the anterior roof of the nasal passage, and excluding the nasals from the external naris.

Developmental and paleontological analyses support the hypothesis that monotreme septomaxillae are homologous with the septomaxillae in non-mammalian therapsids and Mesozoic mammals (Wible et al., 1990). Septomaxillae have not been described in the eutriconodont *Jeholodens jenkinsi* (Ji et al., 1999, 2002) but they have in another eutriconodont, *Gobiconodon ostromi* (Jenkins and Schaff, 1988). It is unknown whether septomaxillae are present or absent in the stem metatherian *Sinodelphys szalayi*. Septomaxillae are absent in the stem eutherian *Eomaia scansoria*. The occurrence of septomaxillae in therians is ambiguous (e.g., Wible et al., 1990; Zeller et al., 1993). The

processus ascendens of the intramembranous ossification found in xenarthrans is proposed to be homologous with the central portion of the septomaxillae in monotremes, extinct mammals and mammal relatives, and has been identified from serial sections of prenatal xenarthrans, including: *Tamandua tetradactyla*, *Choloepus hoffmanni*, *Dasypus novemcintus*, and *Zaedyus minutus* (Zeller et al., 1993). It is ambiguous, however, whether the xenarthran 'septomaxillae' are truly homologous with non-therian septomaxillae or are neomorphic (Wible et al., 1990).

Maxilla

The paired maxillae (Fig. 1.8A) form most of the facial skeleton of *Zaglossus* and are the longest bones in the skull. In lateral view, the maxilla forms the lateral wall of the rostrum, the anterior portion of the zygomatic arch, and the anterior border of the orbit. The maxilla contacts the septomaxilla anterodorsally, the premaxilla anteroventrally, and the nasal dorsally. In the orbit, the maxilla contacts the frontal and the palatine. On the palate, the maxilla contacts the premaxilla anteriorly and the palatine posteriorly. The maxilla lacks teeth. It contacts the squamosal on the zygomatic arch. Within the nasopharyngeal passage, the maxilla contacts the vomer ventrally.

The facial process of the maxilla projects posterodorsally between the nasal and the frontal, delineating the anterior and anterodorsal border of the orbit (Fig. 1.8A). The frontomaxillary suture curves gently around the front of the orbit. Anteroventrally in the orbit, the lacrimal canal opens between the maxilla and the frontal. The maxilla forms the ventral border of the orbit and lies ventral to the frontal anteriorly and to the palatine,

posteriorly. The zygomatic process projects ventrolaterally and extends posteriorly, underlying the squamosal for most of the length of the zygomatic arch, terminating just anterior to the glenoid fossa.

The maxillae meet ventromedially to form the secondary palate. The narrow palate is arched and lacks bony palatal ridges, which are present in the fossil echidna *Megalibgwilia*. The anterior palatal margin is 'V'-shaped and terminates considerably posterior to the posterior border of the external nares. Much of the roof of the nasopharyngeal passageway is exposed in *Tachyglossus* as well. In the extinct echidna *Megalibgwilia* the secondary palate extends farther anteriorly so that only a small portion of the roof of the nasopharyngeal passageway is exposed. In *Ornithorhynchus* and *Obdurodon*, the anterior margins of the nasals are posteriorly located relative to the anterior margin of the secondary palate, so that in dorsal view one can see the floor of the nasopharyngeal passageway and the anterior vomer. The maxillopalatine suture in ventral view forms a 'V' that points anteriorly, being bounded by long, laterally positioned posterior extensions of the palatal processes of the maxillae as in *Tachyglossus* (Fig. 1.4 and 1.5, respectively). The processes are shorter in *Tachyglossus* than in *Zaglossus*. In *Tachyglossus* they extend no farther posteriorly than the foramen rotundum. The lengths of these processes vary in *Zaglossus*. In all specimens of *Zaglossus* they traverse a majority of the length of the palatines. In some specimens (e.g., *Zaglossus bruijnii* MCZ 59685, *Zaglossus bartoni* AMNH 157072, and *Zaglossus bartoni* AMNH 190862), the posterior extensions of the palatal processes of the maxilla nearly contact the

ectopterygoids. *Megalibgwilia*, as with *Tachyglossus,* has short posterior extensions (Griffiths et al., 1991, fig. 2, 3). Again, the Kimberly specimen, BMNH 1939.3315, identified as *Zaglossus bruijnii* shares with *Megalibgwilia* short posterior extensions of the palatal processes of the maxillae that terminate considerably anterior to the foramen rotundum (Helgen et al., 2012, fig. 5).

Medially, a crista of the maxilloturbinal contacts the facial process of the maxilla posteroventrally, dorsal to the lacrimal foramen. Moving anteriorly, the maxilloturbinal is positioned further dorsally and begins to branch. In the more skeletally mature *Zaglossus bartoni* AMNH 157052, the branching is elaborated and lies ventral to the complex ethmoturbinal system.

The maxillary canal for the maxillary branch of the trigeminal nerve enters at the crux of the zygomatic process on the maxilla within the orbit. As in *Ornithorhynchus* and *Tachyglossus,* the entrance to the maxillary canal in *Zaglossus* is visible when looking at the skull dorsally and into the anterior corner of the orbit. In *Megalibgwilia*, however, the entrance to the maxillary canal is visible in ventral view (Griffiths, 1991, fig. 2). It is curious to note that the entrance to the maxillary canal in the Kimberly specimen identified as *Zaglossus bruijnii* (BMNH 1939.3315) is also visible in ventral view (Helgen et al., 2012, fig. 5). The branching trigeminal nerve and blood vessels travel through this elaborate canal. In therians the maxillary canal opens anterior to the zygomatic arch as an infraorbital foramen. In Monotremata the maxillary canal persists anteriorly and branches midway through the rostrum, perforating the maxilla with many

maxillary foramina (~10 for *Zaglossus*, ~5-7 for *Tachyglossus*, Fig. 1.9A-C). The maxillary canal of *Ornithorhynchus* divides into three wide branches. The branching pattern in *Zaglossus* manifests as a repeated duplication of the branching pattern present in *Ornithorhynchus*. *Tachyglossus* does not appear to share this duplicated pattern (see AMNH 154457 on DigiMorph.org; Table 1.2). Such a branching pattern is not present in therian mammals, nor in crown mammalian outgroups including *Hadrocodium*, *Morganucodon*, and *Thrinaxodon* that have three exit foramina in the maxillae (Kielan-Jaworowska et al., 2004).

It is likely that the number of maxillary foramina correlates with the degree of electrosensitivity in tachyglossids. Although *Ornithorhynchus* has only three openings for the maxillary nerve, the openings are large to accommodate a thick nerve. The skin that covers the wide bill of *Ornithorhynchus* contains approximately 40,000 electroreceptors (Pettigrew, 1999) that stimulate the maxillary nerve when activated. *Zaglossus* and *Tachyglossus* have fewer electroreceptors in the skin of their narrow snout, and the maxillary nerve, though not as thick as in *Ornithorhynchus*, branches and passes through the numerous foramina that perforate each maxilla. *Zaglossus*, which has more maxillary foramina than *Tachyglossus*, has approximately 2,000 electroreceptors in its snout while *Tachyglossus* has only approximately 400 (Pettigrew, 1999); *Zaglossus* is, therefore, more electrosensitive than *Tachyglossus*. No literature mentions the number of maxillary foramina in *Megalibgwilia* and it is impossible to accurately count them in published figures. It would be worthwhile to CT scan and digitally render the skull of a relatively

complete specimen such as SAM P20488 to accurately count the number of maxillary foramina, reconstruct the maxillary canal, and estimate the electrosensitivity of *Megalibgwilia* relative to extant tachyglossids.

Lacrimal

As with other monotremes, the lacrimal is absent in *Zaglossus*. A lacrimal foramen, however, is present at the anteroventral corner of the orbit, positioned between the frontal and maxilla (Fig. 1.4). The lacrimal canal opens directly into the nasopharyngeal passage, immediately ventral to the posterior end of the maxilloturbinate bones (seen in CT scans of AMNH 157072).

Nasal

The paired nasals occupy the dorsum of the rostrum (Fig. 1.4). The nasal contacts the septomaxilla anteriorly, the maxilla laterally, and the frontal posteriorly. The occurrence of an anteromedial nasoseptomaxillary suture is unique to tachyglossids (the septomaxilla of stem-mammalian taxa only contacts the nasal laterally). In *Ornithorhynchus* and *Obdurodon* the facial process of the septomaxilla projects between the nasal and maxilla (Fig. 1.6). The nasals contact one another at the midline. The nasoseptomaxillary suture is anteriorly convex with the midline extending farther anteriorly than the lateral edges. The nasoseptomaxillary suture is visible in younger individuals but the bones fuse completely in older individuals. Posteriorly, a lateral facial process projects posteriorly. This process nearly contacts, or does contact (e.g., MCZ

7397), the anteriorly directed facial process of the parietal. The anterior half of the nasal is perforated by nasal foramina. Nasal foramina also are present in *Tachyglossus*, as well as *Vincelestes*, multituberculates, and the cynodont, *Thrinaxodon*; nasal foramina are not present in *Ornithorhynchus* and *Obdurodon*, or in therians.

Frontal

The paired frontals (Fig. 1.4) occupy the dorsum of the cranium between the orbits and have an orbital process that contributes to the orbital wall and provides attachment sites for extrinsic muscles of the eye.

On the skull roof, the frontal contacts the nasal anteriorly, the parietal posteromedially and the squamosal posterolaterally. The frontal exposure between the orbits is small because it is overlapped anteriorly by the nasal and posteriorly by the parietal. Two thin bony elements, the interfrontals, lie over the frontals (e.g., MCZ 7397, see below).

The orbital process of the frontal forms a majority of the orbit anterodorsally. Its sutural contact with the facial process of the maxilla defines the anterior border of the orbit. In the orbit, the frontal contacts the maxilla anteriorly, the palatine ventrally, the parietal posterodorsally, and the orbitosphenoid posteriorly. Two foramina, through which pass the vasa diploëtica, perforate the dorsal orbital process of the frontal (Kuhn, 1971).

Interfrontal

The paired interfrontals are positioned medially between the frontals and the parietal (Fig. 1.10A). The interfrontals form a ‘V’, with each interfrontal meeting anteromedially and extending posterolaterally. They are superficial elements, resting above the frontals and parietal and do not contribute to the endocranium (Fig. 1.10B). Because they are only thin ossifications above the frontals and parietals, it is difficult to tell if they are absent in most *Zaglossus* specimens or simply fused with the underlying elements.

The interfrontals were first identified in *Tachyglossus* by Van Bemmelen (1900; see Allen, 1912) and named by Allen (1912). Allen further noted interfrontals in two specimens *Zaglossus bruijnii* and reported interfrontals in an immature *Geomys* (pocket gopher). Although previously thought to be irregular ossifications where the frontals and parietal fail to contact, it is clear from the CT scan of MCZ 7397 that the frontals and parietal contact and that the interfrontals rest on the surface of that area of contact.

Parietal

The parietals (Fig. 1.4) form a single ossified plate with no visible medial suture. In young *Tachyglossus*, the parietals have been observed to originate as individual left and right elements, each with a single center of ossification (Watson, 1916; Kuhn, 1971). A medial suture was observed in a young specimens of *Zaglossus* (Allen, 1912) although the parietals of monotremes fuse together early in development. Early fusion of the parietals has been speculated to be related to the monotreme mode of reproduction, and

that the skull is not required to be flexible to hatch from an egg Kuhn (1971). Alternatively, it could be that stresses from head and neck musculature promote early closure of the midline suture. The parietals form the dorsum of the skull. They are extensive, overlapping the posterior portion of the frontals.

The parietal contacts the frontal anteriorly, the interfrontal anteromedially and the supraoccipital posteriorly. It overlies the midregion of the neocortex. Some of the dorsal gyri of the neocortex make their impression on the medial surface of the parietal. In most specimens, anterior facial processes extend over the frontals nearly contacting the nasals. In some specimens (e.g., MCZ 7397) the facial processes contact the nasals superficially, dividing the facial portion of the frontals from the orbital processes. The posterior margin of the parietal has two broad processes that meet medially and spread laterally, overlapping the supraoccipital. The parietal has a dorsal sculpturing patterning which is also present in the other monotremes, *Tachyglossus*, *Megalibgwilia*, *Ornithorhynchus*, and *Obdurodon*. Parietal sculpturing results from scarring of jaw and neck musculature attachments (Van Bemmelen, 1900).

The parietal spreads ventrolaterally and contributes to a portion of the sidewall of the braincase, contacting the squamosals ventrally, the periotics posteroventrally, and the supraoccipital posteriorly. Contact of the parietal with both the squamosal and periotic is a synapomorphy of Tachyglossidae (Chapter 2). In *Ornithorhynchus*, the temporal process of the periotic is not as expanded, and the periotic does not make contact with the parietal.

Interparietal

The presence of an interparietal in monotremes is debated and remains uncertain. It now seems that interparietal ossification centers are present early in development (see Koyabu et al., 2012). An interparietal fused to the supraoccipital was reported as early as 1901 by Van Bemmelen, and later in embryonic *Zaglossus* as a large element over the back of the braincase (Landry, 1964). However, the report by Van Bemmelen (1901) was later rejected (Kuhn, 1971)[1]. Later, a small, medial membrane bone was later reported in young *Tachyglossus* specimens and has been tentatively identified as an interparietal (Koyabu et al., 2012). It is likely that in tachyglossids either the interparietal begins development as a small, medial membrane bone and fuses with the greatly expanded supraoccipital, or that the interparietal is large and fuses with the smaller supraoccipital.

Jugal

As with *Tachyglossus* and the extinct *Megalibgwilia*, the jugal is absent in *Zaglossus*. The broad squamosal was once proposed to be the jugal, and the mastoid portion of the periotic was proposed to be the squamosal based upon the insertion of the temporalis muscle onto the zygomatic portion of the squamosal (Allen, 1912). No one has followed Allen's hypothesis and it is unlikely to be true because the jugal is present as a reduced element in *Ornithorhynchus*, in which it forms a blunt postorbital process that is completely fused to the maxilla in mature specimens. A reduced jugal is a

[1] The observation of an interparietal in embryonic *Zaglossus* was not cited and discussed by Kuhn (1971) in his monograph on the cranial anatomy of developing *Tachyglossus*.

synapomorphy for Monotremata (Chapter 2). The lack of a jugal is a synapomorphy of Tachyglossidae (Chapter 2).

Squamosal

The paired squamosals (Fig. 1.4) are laterally positioned on the cranium. An anterior zygomatic process overlaps the zygomatic process of the maxilla for nearly the entire length of the zygomatic arch. The cranial portion of the squamosal is greatly expanded and appressed to the cranium, overlapping the orbitosphenoid anteriorly, contacting the parietal dorsally, and overlapping the periotic ventrally. It does not form any part of the wall of the cavum cranii.

The cranial moiety of the squamosal is semi-circular in shape (Allen, 1912). It differs from *Tachyglossus* in which the cranial moiety is relatively low anteriorly, and posteriorly expands dorsally to contact the parietals, covering the contact between the orbitosphenoid and the periotic. There is a small notch on the posterior margin of the squamosal that bounds the entrance to the post-temporal canal. The post-temporal canal contains part of the temporalis musculature, and the arteria diploëtica magna which supplies blood to the meninges and orbit (Rougier et al., 1992). The arteria diploëtica magna runs dorsally through a canal bounded between the medial orbitosphenoid and the lateral squamosal (Fig. 1.11A-D). In some *Zaglossus* and most *Tachyglossus*, the squamosal is so thin over the arteria diploëtica magna that the canal for the artery opens externally leaving a trace on the external surface of the squamosal. More of the medial portion of the glenoid fossa is visible in lateral view in *Zaglossus* than in *Tachyglossus*

because the lateral margin of the glenoid fossa in *Zaglossus* arches dorsally, but it is flat in *Tachyglossus*.

In ventral view, the squamosal forms an anteroposteriorly elongate glenoid fossa for the craniomandibular joint. The glenoid fossa is shallow and almond shaped, widest anteriorly and tapering to a point posteriorly. The glenoid fossa is deeper in *Zaglossus* than in *Tachyglossus*, and more anteroposteriorly elongate. The glenoid fossa in *Ornithorhynchus* differs from tachyglossids, stretching mediolaterally rather than anteroposteriorly, allowing for a complex range of motion by the dentary.

Periotic

The paired periotics (Fig. 1.12A-D) contain the organs for hearing and balance. An endochondral ossification of the otic capsule fuses with an ossified membranous process to form the posterolateral wall of the cavum cranii.

The dorsally expanding process of the periotic contacts the squamosal anteriorly, the parietal anterodorsally, the supraoccipital posterodorsally, and the exoccipital posteriorly (Fig. 1.12A). In medial view, the anterior region of the periotic contacts the orbitosphenoid posteroventrally. In contrast to therian mammals, the periotic in Monotremata contributes to a sizeable portion of the posterolateral wall of the braincase with a broad anterior lamina (Griffiths, 1978).

In ventral view, the periotic contributes to the floor of the cranium. The periotic contacts the exoccipital posterolaterally, the basioccipital posteromedially, the squamosal anterolaterally, and the basisphenoid anteromedially. The morphology of the periotic in

Zalgossus does not differ significantly from *Tachyglossus*, and the periotic and inner ear of monotremes is described in detail (see Van Bemmelen, 1901; Gaupp, 1908; Watson, 1913; Simpson, 1938; Kuhn, 1971). Suspended within the ventrally facing tympanic fossa (Fig. 1.12D) are the ectotympanic and three middle ear ossicles. The tympanic fossa is pierced by three apertures: the fenestra ovalis, or oval window into which the footplate of the stapes fits; the foramen rotundum, or round window; and the aperture tympanica canalis facialis (Griffiths, 1978).

The petrous portion of the periotic in medial view is simple and is perforated posteromedially by the relatively large internal acoustic meatus (Fig. 1.12C), posterolaterally by the vestibular aqueduct (Fig. 1.12B, C), and posteriorly by the metotic fissure (Fig. 1.12D), which represents the combined jugular and condyloid foramina (Simpson, 1938).

Within the bony labyrinth of the periotic, a partially coiled cochlea forms a three-quarter spiral (Fig. 1.13B). Where the canal for the cochlear nerve enters the cochlear fossa it is cribriform as in other mammals. The vestibular nerve leaves the vestibule proper and joins with the cochlear nerve to form the vestibulocochlear nerve which exits the bony labyrinth via the internal acoustic meatus (Fig. 1.13A). The cochlea is positioned ventromedially to the vestibule proper, off of which the horizontal, anterior, and posterior semicircular canals protrude (Fig. 1.13A). The vestibular aqueduct for the endolymphatic duct branches from the vestibule proper just ventral to the crus commune (representing the confluent anterior and posterior semicircular canals; Fig.1.13A). The

vestibular aqueduct is small yet curves dorsally from the vestibule proper, then turns posteromedially before exiting the periotic endocranially. Endocranially, a protruding narrow crest on the petrous portion of the periotic indicates where the vestibular aqueduct arches dorsally from the vestibule proper (Fig. 1.12B, C). The facial canal traverses the bony labyrinth of the periotic from the medial internal acoustic meatus to the lateral opening of the skull where the stylomastoid foramen and metotic fissure open (Fig. 1.12D). In its path, the facial canal crosses anteriorly between the ventral cochlea and dorsal vestibule proper (see sagittal dynamic cutaway animation in supplementary information).

Palatine

The paired palatines (Fig. 1.4) form the posterior end of the secondary bony palate and also the ventral floor of the orbit. In lateral view, the temporal wing of each palatine contacts the maxillae anteriorly, the frontal dorsally, the ethmoid posterodorsally, and the alisphenoids posteriorly. The temporal wing of the palatines contains the foramen pseudosphenoorbitale (Gaupp, 1908; Kuhn and Zeller, 1987), or sphenopalatine foramen, through which passes cranial nerves II through VI, with the exception of the mandibular branch of the trigeminal nerve (Kuhn and Zeller, 1987).

In ventral view, the palatines contact medially and form a triangular shape with the apex directed anteriorly. The apex may either be positioned anterior to the roots of the maxillary zygomatic processes, or nearly aligned. In MCZ 7397, the anterior points of the palatines are positioned slightly posterior to the roots of the maxillary zygomatic

processes, perhaps because the specimen is of a juvenile. The palatines in *Tachyglossus* also form a triangle, which is wider than in *Zaglossus*, either because the palatal processes of the maxillae in *Zaglossus* encroach more on the palatines, or because the palatines extend far anteriorly past the root of the maxillary zygomatic process, depending on the specimen. The rostral ends of the palatines of *Tachyglossus* are noticeably posterior to the root of the maxillary zygomatic processes, though in some specimens the palatines may be closely aligned with these processes (e.g., AMNH 35679). In *Zaglossus*, a small, broad incision divides the posterior end of the left and right palatines. Short posterior processes project posteriorly from the margins of that incision, then flatten out and are contiguous with the posterior margin of the ectopterygoids. In *Tachyglossus*, the posterior process of the palatine is long and forms the entire posterior margin of the palatine; the medial incision is more elongate than in *Zaglossus*. *Megalibgwilia* most closely resembles *Zaglossus* in having a more smoothly bifid posterior palate with a shallower incision. The posterior margins of the palatines in *Ornithorhynchus* are straight and continuous with no incision and no processes present.

Pterygoid

The paired pterygoids are thin strips of bone positioned posteriorly on the lateral walls of the nasopharyngeal passageway, dorsal to palatal processes of the palatines (Fig. 1.15). The pterygoid is short, only a few millimeters in length (Watson, 1916). The pterygoid contacts the basisphenoid/alisphenoid dorsally, the palatine ventrally, and the

periotic laterally. Farther posteriorly, near the choana, the pterygoid contacts the ectopterygoid ventrolaterally (see Fig. 1.15).

Ectopterygoid

The homology of the monotreme ectopterygoids, named the 'echidna pterygoids,' in the early literature, as well as the homology of the pterygoids of therian mammals, is ambiguous and has been referred to as 'The Pterygoid Problem' by many anatomists (see Table 1.5). Monotreme ectopterygoids have been variously proposed to be homologous with the reptilian pterygoid (or both the reptilian and mammalian pterygoid assuming that the mammalian pterygoid is homologous with the reptilian pterygoid; Gaupp, 1908; Fuchs, 1910; De Beer, 1929), the cynodont epipterygoid (Watson, 1916; Kesteven, 1918), and the reptilian ectopterygoid (Broom, 1914; Parrington and Westoll; 1940). The ectopterygoids in basal cynodonts such as *Thrinaxodon* are positioned posterolaterally to the palatines, anterior to the pterygoids and medial to the maxillae, though the ectopterygoids do not contact the maxillae in all cynodont taxa (Parrington and Westoll, 1940). The monotreme ectopterygoid does not contact the maxilla, is posterior to the pterygoid, and contacts the ectotympanic medially. It is defended as an ectopterygoid primarily based on comparisons with its development in *Dasypus*. In *Dasypus*, placental armadillos, the pterygoid develops from two paired elements, a dorsal plate of membrane bone and a ventral endochondrally-derived element that contacts the palatine. Based on position relative to other elements, and based on paleontological evidence (Parrington and Westoll, 1940), the dorsal element is identified as the mammalian pterygoid and is

considered homologous with the reptilian pterygoid, while the ventral element is identified as the ectopterygoid (Presley and Steel, 1978). Because of positional similarities, the monotreme ectopterygoid is considered to be a homolog of the ectopterygoid in the developing *Dasypus*, and is here referred to simply as the ectopterygoid.

The paired ectopterygoids (Fig. 1.4) are positioned posterolaterally on the palate, and contact the palatines anteroventrally and the pterygoids anterodorsally. The shape of the ectopterygoids shows intraspecific variation. Most are semi-circular in shape, though some are round (e.g., AMNH 157072) or anteroposteriorly elongate (e.g., MCZ 7397). In AMNH 190862, the ectopterygoids are rounded posteriorly, but have an anteriorly directed process. The ectopterygoids have been hypothesized to help shape the palate as a suitable surface against which to grind food (Griffiths, 1978). In extinct and extant tachyglossids, the ectopterygoids are large and robust, and form a concave region on the posterior end of the palate; a keratinous pad on the back of the tongue is of the same size as the concave region and is used to grind food against the roof of the mouth (Griffiths, 1978). In *Ornithorhynchus* the ectopterygoids are narrow slips of bone lateral to the palatines. Ectopterygoids are not preserved in *Obdurodon*, though the skull of *Obdurodon dicksoni* was reconstructed with ectopterygoids similar to those of *Ornithorhynchus*, although comparatively more robust because the facets on the palatine are larger and broader (Musser and Archer, 1998).

Elements of the Cavum Epiptericum

The cavum epiptericum is the space between the primary wall of the braincase, which surrounds the dura mater, and the secondary wall that closes the orbitotemporal region of the skull and is positioned lateral to the cranial nerves (Kuhn and Zeller, 1987). Tachyglossids are unique among mammals in their extreme reduction of the primary wall, which consists of the lamina obturatoria periotici (an ossification of the sphenoparietal membrane; Kuhn and Zeller, 1987) and the clinoid processes of the basiphenoid (Van Bemmelen, 1901; Kuhn and Zeller, 1987). This reduction of the primary wall in *Tachyglossus* is thought to accommodate the expanding neocortex during development (see Kuhn and Zeller, 1987). The secondary wall in *Tachyglossus* consists of the alisphenoid, ectopterygoid, squamosal, palatine, appositional bone of the periotic, and intramembranous ossification of lamina obturans. These elements are "morphologically non-uniform" (Kuhn and Zeller, 1987: 60). Development of ossification of the sidewall of the braincase in young *Tachyglossus* specimens was illustrated (Griffiths, 1978), and showed how a lamina ascendens of the alisphenoid grows dorsally and engulfs the temporal wing of the palatine as it contacts the ventrally directed process of the orbitosphenoid. Between the alisphenoid and squamosal the sphenoparietal membrane becomes increasingly ossified forming the dorsal margin of the foramen ovale; in adult specimens, the sphenoparietal fissure is completely ossified and the side wall is enclosed by a plate of bone (Griffiths, 1978). This process of ossification is identical in *Zaglossus* (Griffiths, 1978).

Vomer

The paired vomer (Fig. 1.16A-C) is an anteroposteriorly elongate bone positioned on the dorsal surface of the palatal processes of the maxillae. *Zaglossus* has one of the relatively longest vomers in the Mammalia (Griffiths, 1978), with the anterior end situated about halfway down the length of the rostrum, and its posterior end at the choanae. The vomer is a short, 'V'-shaped bone (Fig. 1.16D), similar to that of other crown mammals. The dorsal processes of the vomer contact the ventral processes of the ethmoid plate. Posteriorly, below the mesethmoid, the processes elongate and extend laterally, forming the dorsum of the nasopharyngeal passageway.

Ethmoid

The ethmoid of *Zaglossus* (Fig. 1.17A-C) ossifies in the nasal septum (Rowe et al., 2008) and consists of an anteroposteriorly elongate ethmoid plate, ethmoturbinals and a large, horizontally sloping mesethmoid perforated with many olfactory foramina (fig. 1.17D). The mesethmoid is cribriform in both *Zaglossus* and *Tachyglossus*, and although the mesethmoid is perforated only by two olfactory foramina in mature *Ornithorhynchus*, it is cribriform early in ontogeny. Olfaction is more sensitive in the terrestrial echidnas than in the semi-aquatic *Ornithorhynchus* (Augee et al., 2006). Endocasts have been used to estimate the proportion of olfactory bulb volume to the rest of the brain. The olfactory bulb fills merely 0.8% of the total brain volume in *Ornithorhynchus* (Augee et al., 2006). Its Miocene relative, *Obdurodon dicksoni*, has a larger olfactory bulb, contributing to 1.9% of the total brain volume (Macrini et al., 2006). In *Tachyglossus*, however, the

olfactory bulb contributes to 2.3% of the endocranial volume; the olfactory bulb in *Zaglossus* contributes 3.1% to the endocranial volume (Macrini et al., 2006). Compared with therians, the olfactory bulb in the echidnas is relatively small (8.4% total brain volume in the gray short-tailed opossum *Monodelphis domestica*). Further, *Tachyglossus* has seven ethmoturbinals but *Ornithorhynchus* and *Obdurodon dicksoni* have three (DeBeer and Fell, 1936). Figure 1.18 (A-D) and figure 1.19 (A-C) illustrate the complex maze of interfingering ethmoturbinals that are well-developed in the skeletally mature *Zaglossus bartoni* AMNH 157072. Reduction in olfaction is likely a trend within Ornithorhynchidae (platypuses) in response to a semi-aquatic habit. If tachyglossids evolved from a semi-aquatic ancestor, then they would have had to have evolved a larger olfactory bulb, complex cribriform plate, and more ethmoturbinals within 15 million years, which would be interesting to explore in the future.

The mesethmoid is externally visible in ventral view through the large, singular palatine fissure. The anterior end of the mesethmoid begins where the septomaxillae fuse dorsomedially. In cross-section, the mesethmoid is in the shape of an upside-down 'Y' with the two processes contacting the tips of the 'U'-shaped vomer (see coronal slice and cut animations archived on DimiMorph.org from the URL in Table 1.2). The mesethmoid traverses the length of the rostrum and ends with the cribriform plate.

Orbitosphenoid

The paired orbitosphenoids in mature specimens of *Zaglossus* are restricted in external view, being largely overlapped by the frontals and parietals dorsally and the

squamosals ventrally (Fig. 1.20A). The orbitosphenoid occupies the posterior margin of the orbit and the lateral temporal region of the skull (Fig. 1.20B). Its exposure on the lateral surface of the skull is modest in comparison with its extensive contribution to the anterolateral portion of the endocranial cavity (Fig. 1.20C). Anteriorly, the orbitosphenoid contacts the lateral surface of the ethmoid. In *Tachyglossus*, the anterior half of the dorsal margin of the squamosal is low and contacts the orbitosphenoid dorsally, while the posterior half stretches farther dorsally and contacts the parietals, obscuring contact of the orbitosphenoid and periotic in lateral view (Fig. 1.5). In some specimens, however (e.g., AMNH 154458), the squamosal never contacts the parietal, and the contact between the orbitosphenoid and periotic is visible in lateral view. In *Ornithorhynchus*, the orbitosphenoid is anteroposteriorly elongate and contacts the periotic posteriorly and ventrally (Fig. 1.6); much of the ventrolateral wall of the braincase consists of the periotic (Griffiths, 1978). In the tritylodontid *Kayentatherium*, the orbitosphenoid contacts the prootic posteriorly, and lies medial to the epipterygoid (alisphenoid; Presley and Steel, 1976), the orbital process of the palatine anteroventrally, and the frontal anteriorly (Sues, 1986), as in *Zaglossus*. The orbitosphenoids of monotremes may not be homologous with the obitosphenoids of other mammals (Kuhn, 1971) but are here referred to as orbitosphenoids by convention.

Alisphenoid

The paired alisphenoids (Fig. 1.21) contribute to the posteroventral wall of the braincase, as in *Tachyglossus* (Watson, 1916; Kuhn, 1971; Griffiths, 1978). The

alisphenoid contacts the palatine posterodorsally, the basisphenoid medially, and the periotic posterolaterally. In skeletally mature individuals, the alisphenoid is indistinguishable from the basisphenoid. As in other monotremes, the alisphenoid is small, forming the floor of the cavum epiptericum and making no contribution to the braincase wall (Kuhn and Zeller, 1987). In young echidnas, a cartilaginous ala temporalis is positioned lateral to the floor of the braincase. A pila antotica grows medial to the ala temporalis and lateral to each carotid foramen, ascending anteriorly to the pila praeoptica. The rostral portion of the ala temporalis ossifies into the alisphenoid while the pila antotica is mostly resorbed. A small ventral portion ossifies as the clinoid process of the basisphenoid. In *Ornithorhynchus*, the alisphenoid does not contribute to the side wall of the braincase (Griffiths, 1978).

Basisphenoid

The basisphenoid is a dorsoventrally compressed element anterior to the basioccipital (Fig. 1.22A, B). It contacts the palatines anteriorly and the alisphenoids ventrolaterally. In some regions the alisphenoids are indistinguishably fused with the basisphenoid. The basisphenoid forms a sella turcica posteriorly. The sella turcica is relatively deeper in *Zaglossus bruijnii* MCZ 7397 than *Zaglossus bartoni* AMNH 157072; this could be explained by developmental stage rather than by species variation. More data from CT scans of specimens of *Zaglossus bruijnii* and *Zaglossus bartoni* at varying stages of ontogeny will clarify if this is species variation, ontogenetic variation, or individual variation. The sella turcica is bordered laterally by the clinoid processes

(Fig. 1.22C). Again, the clinoid processes of *Zaglossus bruijnii* MCZ 7397 are more pronounced than in *Zaglossus bartoni* AMNH 157072, and more data needs to be collected to explain this morphological variation. A carotid canal for the carotid artery runs between the sella turcica and each clinoid process (Fig. 1.22C). The carotid canal passes through the basisphenoid posteroventrally so that the paired carotid foramina are externally visible on the ventral posterlateral surface of the basisphenoid immediately anterior to the basioccipital.

Parasphenoid

As with *Tachyglossus* (Kuhn, 1971) and *Ornithorhynchus* (Zeller, 1989a), the parasphenoid is absent in *Zaglossus*.

Occipital Region

The occipital region of *Zaglossus* remains relatively unfused throughout ontogeny so that the sutures remain visible and the occipital elements remain distinct in mature specimens. The foramen magnum is large and formed by the basioccipital ventrally, and the paired exoccipitals laterally and dorsally. An incisura occipitalis (Gaupp, 1907) is always present in skeletally immature *Zaglossus* as a dorsomedial incision of the foramen magnum (Fig. 1.23A), giving the foramen magnum a distinctive key-hole shape; in one specimen, *Zaglossus bartoni* AMNH 194702, the foramen magnum is closed without an incisura occipitalis, though a foramen in the supraoccipital superior to the foramen magnum is present (Fig. 1.23C). The incisura occipitalis was reported in some therians

(e.g., *Lestodelphys halli*; Voss and Jansa, 2009) as well as pterosaurs (e.g., *Pterodactylus elegans*; Edinger, 1941). The incisura occipitalis inferior of *Pterodactylus elegans* was inferred to have been formed as a consequence of how the occipital bones ossify around the cerebellum (Edinger, 1941) and this could be true for monotremes as well. All monotremes with the exception of the extinct echidna, *Megalibgwilia* (Griffiths et al., 1991), have the incisura occipitalis. The large occipital condyles are doubled and positioned ventrolaterally. They are rounded and bulbous, bulging laterally. The occipital condyles of *Zaglossus* are similar to *Tachyglossus* in that they extend away from the skull (Fig. 1.24 B, C), unlike in *Ornithorhynchus* where the occipital condyles are relatively in line with the occiput (Fig. 1.24A). However, the occipital condyles of *Zaglossus* are similar to *Ornothirhynchus* in that they are positioned ventrally on the skull (Fig. 1.24A, B), unlike in *Tachyglossus* where the occipital condyles are more elevated on the skull (Fig. 1.24C).

Supraoccipital

The supraoccipital (Fig. 1.4) is dorsal to the exoccipitals and usually forms the dorsomedial margin of the foramen magnum. It is broad mediolaterally and convex. There is no lambdoidal crest. The ventromedial margin of the supraoccipital is notched by an incisura occipitalis. The incisura occipitalis is present in some marsupial and placental species; however, it is present in all known extinct and extant monotremes, except for *Megalibgwilia* (Griffiths et al., 1991). Endocranially, the supraoccipital has a medial ridge. In *Ornithorhynchus* and *Obdurodon dicksoni*, the supraoccipital forms the

falx cerebri and midline ridge in place of the ridge in tachyglossids. The supraoccipital is bordered anteriorly by the parietal, ventrolaterally by the petrosals, and posteroventrally by the exoccipitals.

Exoccipital

The paired exoccipitals (Fig. 1.4) are positioned lateral to the formen magnum and form the occipital condyles. In ventral view, the exoccipitals contact the periotics laterally and the basioccipital medially. The occipital condyles are broad and bulbous relative to the occipital condyles of *Tachyglossus* and *Ornithorhynchus* which are thinner and more gracile. The occipital condyles of *Megalibgwilia* are similarly broad. In lateral view, the position of the occipital condyles and foramen magnum are close to the back of the skull, as with *Ornithorhynchus* and *Obdurodon dicksoni*, but unlike *Tachyglossus* and *Megalibgwilia* in which the occipital condyles and foramen magnum protrude from the back of the cranium. In posterior view, the condyles occupy the entire ventral half of the exoccipitals. Anterior to the ventrolateral surface of the occipital condyles are deep depressions. In many specimens, these depressions are open as fissures, and in others (e.g., MCZ 12414, AMNH 194702) one side is closed and the other is open. These fissures are rarely present in *Tachyglossus* (e.g., AMNH 65842) but are consistently present in *Ornithorhynchus* (Fig. 1.6). In *Ornithorhynchus*, they have been identified as the metotic fissure through which pass cranial nerves IX, X, XI, and XII (Zeller, 1989a). In the echidnas, cranial nerves IX, X, XI, and XII pass through the jugular foramen on the periotic (Kuhn, 1971; Fig. 1.4).

Basioccipital

The basioccipital (Fig. 1.4) forms the base of the skull, the anteroventral border of the foramen magnum, and the ventromedial ends of the occipital condyles. In ventral view, the basioccipital has three projections: an anterior projection contacting the basisphenoid anteriorly and the periotics laterally, and two posterolateral projections contacting the periotics anteriorly and the exoccipitals posterolaterally.

Craniofacial Foramina

The sphenopalatine foramen is enclosed by the temporal wings of the palatines. In *Tachyglossus*, cranial nerves II, III, IV, V_1, V_2, and VI pass through this foramen (Kuhn and Zeller, 1987). The maxillary branch of the trigeminal nerve (V_2) enters the rostrum via the infraorbital foramen positioned within the orbit through the maxilla (Kuhn, 1971; Griffiths, 1978; Kuhn and Zeller, 1987). This is likely the case for *Zaglossus* as well. According to Griffiths (1978), the craniofacial nerves listed above, to the exclusion of V_2, pass through the foramen rotundum (formed medially by the palatine and laterally by the temporal wing of the alisphenoid) in tachyglossids (see in Musser and Archer, 1998, table 3, for table of synonyms for major foramina in *Ornithorhynchus* and *Obdurodon dicksoni*). The mandibular branch of V_3 leaves the cavum epiptericum through the foramen ovale (foramen pseudoovale of Kuhn and Zeller, 1987). The foramen ovale is surrounded by the alisphenoid anteriorly, ossification of the sphenoparietal membrane (Griffiths, 1978) posteriorly, and the ectopterygoid ventrally. The geniculate ganglion of the facial nerve (VII) is positioned in the cavum epitpericum (Zeller, 1989b). The facial

nerve passes through the anterior notch of the internal auditory meatus (Kesteven, 1940). The vestibulocochlear nerve (VIII) exits the petrous portion of the periotic endocranially through the internal acoustic meatus. Craniofacial nerves IX, X, XI, and XII pass through the jugular foramen located ventrally on the periotic posterior to the stylomastoid foramen (Kuhn, 1971; Zeller, 1989a; Fig. 1.4).

Malleus, Incus, and Stapes

The middle ear ossicles (the malleus, incus, and stapes), are relatively large and lie in a horizontal plane on the ventral surface of the skull, as in all monotremes (Fig. 1.14A). The ectotympanic is a thin, 'C'-shaped bone associated with the posteromedial margin of the malleus (Fig. 1.14B). In ventral view the malleus, is a relatively more robust, 'L'-shaped bone. The anterior process, forming the long part of the 'L', is dorsoventrally compressed and is directed anteromedially. The incus lies dorsal to the body of the malleus (Fig. 1.14C). The incus and the malleus are already fused in the juvenile *Zaglossus bruijnii* (MCZ 7397). Fusion of the incus and malleus also occurs in *Tachyglossus* (Griffiths, 1978) and is not uncommon in other mammals; it occurs in humans, and also frequently enough in guinea pigs to be considered "one of the characteristics of all hystricomorphs" (Bellmer, 1963: 426). This tight association of the ear ossicles in echidnas was proposed previously as an adaptation for improving the conduction of sound (Augee et al., 2006).

The stapes (Fig. 1.14C, D) is imperforate and columelliform, shaped similar to a thumb tack with the circular footplate fitting into the fenestra ovalis. Because the stapes is imperforate in all monotremes and some therians, an imperforate, columelliform stapes

could be primitive for Mammalia (see Novacek and Wyss, 1986). The ontogeny of the stapes in *Ornithorhynchus* differs from *Tachyglossus*, however, leading some to hypothesize that the monotreme stapes is secondarily imperforate (Goodrich, 1930). In *Ornithorhynchus*, a stapedial foramen pierces the procartilaginous stapes and then disappears while in *Tachyglossus* the stapedial foramen never forms (Kuhn, 1971; see Novacek and Wyss, 1986). Additionally, the variable occurrence of a stapedial foramen within therapsids (Novacek and Wyss, 1986), suggests that it may be primitive for Mammalia.

Dentary

The dentaries of *Zaglossus* (Fig. 1.25B) are significantly more robust at their proximal end than the dentaries of *Tachyglossus* (Fig. 1.25A). Because they contour the long, decurved snout, the dentaries are similarly elongate and decurved. As with *Tachyglossus* and *Ornithorhynchus*, the posterior end of the dentary forms the dentary condyle, reduced coronoid process, and angular process (Fig. 1.25A, B). The dentary condyle is anteroposteriorly elongate with a mediolateral axis of curvature, as with *Tachyglossus*, though more narrow. Similar to *Ornithorhynchus* and *Tachyglossus*, a posteriorly directed process is present on the posterolateral end of the dentary condyle (Fig. 1.25A, B). The dentary condyle is positioned atop an elongate, dorsally-directed dentary peduncle. A gracile dentary peduncle is a synapomorphy for all monotremes, because it is present in the extinct, basally divergent monotreme *Teinolophos trusleri* (Chapter 2). The angular process in *Zaglossus* is well developed and directed ventromedially. In specimen *Zaglossus bartoni* AMNH 190863, the angular process is

more medially directed, as in metatherians. In *Tachyglossus* the angular process is present, though not as robust. The angular process is reduced or absent in *Ornithorhynchus*. The coronoid process in *Zaglossus* is a small, laterally inflected bump on the lateral surface of the dentary (Fig. 1.24B). This is similar to *Tachyglossus* (Fig. 1.24B) whereas the coronoid process in *Ornithorhynchus* is a narrow projection over a hypertrophied masseteric fossa that forms a canal penetrating the mandibular canal. The masseteric fossa is mostly absent in tachyglossids. The mandibular foramen is positioned anterior to the coronoid process in *Zaglossus*, as it is in *Tachyglossus* and *Ornithorhynchus*. The mandibular foramen in *Teinolophos* also is positioned anterior to the coronoid process, which is more developed than in extant monotremes, ruling out the hypothesis that the anterior position of the mandibular foramen is correlated with a reduced coronoid process.

The dentaries merge and contact slightly anterior to the midline of the mandiblar length, and remain in contact until the distal end (Fig. 1.24B). The terminal ends of the dentaries are narrow points (Fig. 1.25B). This differs from both *Tachyglossus* and *Ornithorhynchus*, in which the dentaries contact briefly more distally down their length and then bow laterally so that the terminal ends are not fused (Fig. 1.245). In *Tachyglossus* and *Ornithorhynchus*, the terminal ends of the dentaries are spatulate in shape (Fig. 1.25A), though this is much more the case in *Ornithorhynchus*. The symphysis in all extant genera differs from therians in that only thin ventral margins of the dentaries contact leaving a medial foramen for the exit of the mandibular nerve

visible (Fig. 1.25A, B). In therians, the dentary symphysis covers a majority of the medial face of the dentaries and there is no foramen.

SUMMARY

Skull Fusion and Ossification

Skeletally mature monotremes have highly fused crania, with completely closed sutures and indistinguishable boundaries between most cranial elements. Fusion between some elements starts extremely early. For example, original descriptions of both *Zaglossus* and *Tachyglossus* did not report the septomaxilla because its suture with the premaxilla is generally indistinguishable - even in immature specimens in which most other cranial sutures are obvious (see Gervais, 1877-1878; Van Bemmelen, 1901; Allen, 1912). In the immature *Zaglossus bruijnii* used here (MCZ 7397), the septomaxilla and premaxilla already are fused and are difficult to distinguish (Fig. 1.7) even though the frontals, interfrontals, parietals, orbitosphenoids, and periotics are readily identifiable. CT-based cross-sections reveal widespread fusion between the overlapping septomaxillae and premaxillae. The margins of each element, both on the outside of the skull and inside the cranium, must be the last part to fuse together. The elements of the occiput in MCZ 7397 are well separated, with a large fontanel occurring between the supraoccipital, periotic, and the parietal. Juveniles of *Ornithorhynchus* and *Tachyglossus* do not have a fontanel between the occiput and cranial vault in observed specimens. In ventral view, the palatal process of the premaxilla, the maxilla, palatine, ectopterygoid, squamosal, periotic, basisphenoid, basioccipital, and exoccipital all are distinct with no indication of

fusion. The elements that form the ventral and posterior regions of the braincase are readily distinguishable, being separated by relatively wide sutures and synchondroses. In CT cross-sections the palatines, alisphenoids, basisphenoid, and pterygoids are difficult to delineate, with the alisphenoid and basisphenoid being nearly indistinguishable. In the more skeletally mature *Zaglossus bruijnii* specimen, MCZ 12414, none of the elements are distinguishable, except the ectopterygoids from the palatines. Additional material including more juveniles would be necessary to establish the degree of correlation between sutural closure and age, and the sequence of closure.

Along with degree of fusion, degree of ossification is correlated with age (Griffiths, 1978). In younger individuals, such as *Zaglossus bruijnii* MCZ 7397, the sphenoparietal membrane around the ventral surface of the skull is not ossified, leaving a gap between the palatine, squamosal, and periotic in skeletonized specimens (Fig. 1.26A; Griffiths, 1978). This gap closes as the animal matures (Griffiths, 1978), until there are almost no visible cranial sutures, and the relatively small foramina for craniofacial nerves and blood vessels are the only openings in the ventral surface of the cranium such as seen in *Zaglossus bruijnii* MCZ 12414 (Fig. 1.26B). Thus, it is clear that ossification of the braincase continues late in the lifespan of *Zaglossus*. In specimens that show an intermediate degree of ossification (e.g., *Zaglossus bartoni* AMNH 157072), sutures of the septomaxilla and premaxilla, and frontal, parietal, occiput, periotic and squamosal may no longer be visible or are barely visible, whereas sutures of the palatal process of the premaxilla, maxilla, nasal, palatine, ectopterygoid, and basisphenoid remain visible.

Although the basioccipital, exoccipital, and periotic are fused together, there is a clear synchondrosis between the basioccipital and basisphenoid.

As the individual matures and the cranium becomes increasingly ossified, the incisura occipitalis begins to close. In *Zaglossus bruijnii* MCZ 7397, the incisura occipitalis is an open notch on the dorsomedial margin of the foramen magnum (Fig. 1.23A). In the more skeletally mature specimen, *Zaglossus bartoni* AMNH 157072, processes at the base of the incisura occipitalis grow medially, nearly separating the incisura occipitalis from the foramen magnum (Fig. 1.23B). As described above, *Zaglossus bartoni* AMNH 194702 has a fully enclosed foramen magnum with the remains of the incisura occipitalis expressed as a circular foramen above the foramen magnum (Fig. 1.23C). In the most skeletally mature specimen, MCZ 12414, there is neither incisura occipitalis nor a foramen above the foramen magnum (Fig. 1.23D).

Loss of the incisura occipitalis does not occur in observed specimens of *Ornithorhynchus* and *Tachyglossus*. It is unknown whether this reflects the relative immaturity of museum specimens, or because ontogenetic closure of the incisura occipitalis is unique to *Zaglossus*. The absence of an incisura occipitalis in *Megalibgwilia* may thus reflect the maturity of known specimens at time of death, rather than a character of *Megalibgwilia* throughout its lifespan. The advanced maturity of known specimens of *Megalibgwilia* is indicated by the observation that most sutures are difficult to see with the exception of the sutures between the ectopterygoids and palatines and a portion of the palatines with the maxillae in ventral view (see Griffiths et al., 1991). Furthermore, the

margin of the foramen magnum of *Megalibgwilia* has been described as "slightly thickened," (Griffiths et al., 1991: 90) which may be indicative of a skeletally mature individual. The lack of specimens of *Megalibgwilia* that have an incisura occipitalis may reflect a preservational bias, with mature animals that have thicker, solid, and more heavily fused skulls being more likely to be preserved as fossils.

Lengthening of the rostrum may also occur as *Zaglossus* grows. In Table 1.4 I calculate the ratio of rostrum length to skull length in five individuals of *Zaglossus* representing two species, *Zaglossus bruijnii* and *Zaglossus bartoni*, at different developmental stages. The two smallest specimens, *Zaglossus bruijnii* MCZ 7397 and *Zaglossus bartoni* AMNH 157072, have a rostrum-to-skull length ratio closer to 0.50 than the larger specimens of *Zaglossus*. The larger *Zaglossus* specimens are greater than 17.0 cm in length and have a rostrum-to-skull length ratio that exceeds 0.60. This includes *Zaglossus bruijnii* MCZ 12414, a mature specimen that shows a high degree of skull fusion, ossification of the sphenoparietal membrane, and loss of the incisura occipitalis.

In summary, as in mammals generally, there are three major trends of cranial development in the skull of *Zaglossus*. These trends are fusion of bones, increased ossification, and increased rostrum length relative to skull length. The fusion of bones in *Zaglossus* occurs in three general stages. First, the bones of the anterior rostrum as well as the elements of the cranial vault fuse. Second, the bones of the occiput fuse to each other and to the cranial vault and periotic. Finally, the body of the rostrum and the ventral

surface of the skull fuse. The increased degree of ossification can be recognized by increased ossification of the sphenoparietal membrane leading to complete ossification, ossification of the orbitotemporal region with concomitant reduction of foramina size, and loss of the incisura occipitalis. Future researchers may be able to quantify better the degree of ossification by using CT to characterize bone density. As previously discussed, specimens of *Megalibgwilia* were likely to be skeletally mature at time of death. Therefore, mature *Megalibgwilia* had a rostrum-to-skull length ratio of approximately 0.56 (calculated from Griffiths et al., 1991, table 2). This is less than the ratio calculated for the specimens of *Zaglossus* that have a skull length longer than 17 cm. However, 0.56 is close to the ratio calculated for the smaller specimen, *Zaglossus bartoni* AMNH 157072, that was not skeletally mature at time of death (see Table 1.6). As *Zaglossus* grows, the rostrum grows proportionately longer. A ratio greater than 0.60 is achieved by the time the skull us just over 17.0 cm in length. The skull length of skeletally mature *Zaglossus* individuals does not seem to exceed the range of 17 cm. Measurements of more specimens of *Zaglossus* that vary in size and ontogeny will allow for a more accurate description of rostrum growth.

Comparison with *Tachyglossus* and *Megalibgwilia*

Superficially, the short-beaked echidna, the long-beaked echidna, and the extinct *Megalibgwilia* are morphologically similar. *Zaglossus* and *Megalibgwilia* share with *Ornithorhynchus* and *Obdurodon* a rostrum longer than half the length of the skull. In the platypuses, the rostrum is relatively straight and directed ventrally. In *Megalibwilia* and

Zaglossus, the rostrum is decurved. The rostrum of *Zaglossus*, however, is proportionately longer than the rostrum of any other monotreme. *Tachyglossus* is unique among the monotremes in having a rostrum that is less than half the length of the skull. Both extinct and extant echidnas differ from platypuses by having a maxilla that is perforated with many foramina (between 5 and 10). *Zaglossus* has approximately double the number of foramina piercing the maxillae compared to *Tachyglossus*. Although the number of maxillary foramina in *Megalibgwilia* is not recorded in the literature and is impossible to assess accurately based on published photos, it is clear that it has at least ten foramina for the maxillary branch of the trigeminal nerve, closer in number to *Zaglossus* than *Tachyglossus*. *Zaglossus* has a longer rostrum with more maxillary foramina and greater electrosensitivity than *Tachyglossus* (Manger et al., 1997). If the number of maxillary foramina is correlated with electrosensitivity, then *Tachyglossus* exhibited reduced electrosensitivity. This condition, likely associated with its lifestyle and arid habitat, appears derived relative to the inferred electroreception condition plesiomorphic for echidnas (see Chapter 2).

The length of the posterior extension of the maxillary palatal process is relatively greater in *Zaglossus* than in *Tachyglossus*. In *Tachyglossus*, the process of each maxilla varies in length but extends no farther posterior than anterior to the foramen rotundum (Fig. 1.27A). In *Zaglossus*, the posterior extensions of the maxillary palatine processes also vary in length. In the immature *Zaglossus bruijnii* MCZ 7397, they extend as far posteriorly as the processes in *Tachyglossus*, terminating anterior to the foramen

rotundum. Even in the fully fused and ossified cranium of MCZ 12414, subtle sutures outline the terminus of each process anterior to the foramen rotundum, and accordingly the length of the processes is not correlated with age. Specimens of *Zaglossus* (AMNH 157072 and AMNH 190862) have long processes that extend to the foramen ovale (Fig. 1.27B) and nearly contact the ectopterygoids. The posterior extensions of the maxillary palatine processes of AMNH 194702 are atypically long, making contact with the ectopterygoids. The length of these processes in *Megalibgwilia* cannot be determined from published images.

Two characteristics of the posterior end of the palatines distinguish *Zaglossus* from *Tachyglossus*. Those are shape and size of the palatal incision, and shape and size of the posterior palatine processes. A synapomorphy of Tachyglossidae is the occurrence of a medial incision at the posterior end of the bony palate between the left and right palatines. In *Tachyglossus*, this incision is deep, cutting between the palatines as far anteriorly as the anterior end of the ectopterygoids (Fig. 1.28A). In some specimens such as AMNH 65833 and AMNH 65842, the incision is also wide mediolaterally. Width of the palatal incision does not correlate with degree of cranial ossification but it could correlate with subspecies of *Tachyglossus* because the two specimens named above are identified as *Tachyglossus aculeatus setosus*. In *Zaglossus,* the palatal incision is shallow and not remarkably wide (Fig. 1.28B). Length and width of the incision is not significantly variable and typically it does not extend farther anteriorly than the center of the ectopterygoids. Between the palatal incision and the ectopterygoids are two posterior

processes of the palatines. In *Tachyglossus*, the processes are long, thin splints of bone free from the ectopterygoids (Fig. 1.29A). In *Zaglossus*, the palatal processes are short, blunt, and continuous with the posterior margin of the ectopterygoids (Fig. 1.29B). With the posterior end of the palatine alone, the two genera of echidnas can be instantly identified. In *Megalibgwilia*, the palatines are more similar to *Zaglossus*. The palatal incision is shallow and the posterior processes of the palatines are broad and continuous with the posterior end of the ectopterygoids.

Squamosal shape readily distinguishes *Zaglossus* from *Tachyglossus*: the cranial moiety of the squamosal in *Zaglossus* is semicircular in shape and contacts the frontal anteriorly, covering up a portion of the orbitosphenoid, while in *Tachyglossus* the cranial moiety of the squamosal is low anteriorly, and expands dorsally and posteriorly, making contact with the parietals but not the frontals. Therefore, the squamosals of *Tachyglossus* do not cover up as much of the orbitosphenoids as they do in *Zaglossus*.

The occipital condyles of *Zaglossus* are positioned low on the occiput as in the ornithorhynchids and *Megalibgwilia*. *Tachyglossus* is derived in having the occipital condyles positioned higher on the occiput so that when the cranium is set on a flat surface, the condyles do not touch the surface as they would in *Zaglossus* or other monotremes.

In summary, species of *Zaglossus* can be differentiated from *Tachyglossus* by length of rostrum, number of foramina perforating each maxilla for the trigeminal nerve, length of the posterior extension of the palatal process of the maxilla, size and shape of

the medial palatal incision, size and shape of the posterior process of the palatine, shape of squamosal, and position of the occipital condyles. *Zaglossus* and *Megalibgwilia* share the condition of having a rostrum longer than half the length of its skull, greater than seven maxillary foramina, a shallow palatal incision, short posterior processes of the palatine, and low occipital condyles. The rostrum length of skeletally mature individuals is greater in *Zaglossus*, however, than in *Megalibgwili*a.

Though superficially similar in morphology, extinct and extant echidnas differ from one another by number of maxillary foramina, anatomy of the secondary bony palate, and squamosal shape. Comparison of the skulls of species of *Zaglossus* to the skulls of *Tachyglossus* and *Megalibgwilia* suggest that *Zaglossus* retains more plesiomorphic characters than *Tachyglossus* (Chapter 2). This calls into question the common practice of using *Tachyglossus* as a representative of Tachyglossidae to the exclusion of *Zaglossus* in many phylogenetic analyses.

CONCLUSIONS

The skulls of *Zaglossus* are variable. Proportions of rostrum length to skull length, length of the posterior projections of the palatal processes of the maxillae, shape of the ectopterygoids, degree in ossification of the skull, shape of the sella turcica of the basisphenoid, and height of the clinoid processes are a few examples of the variation seen amongst individuals of *Zaglossus* archived in North American museum collections. Some of this variation is difficult to attribute to sex, ontogeny, species, or individual variation due to a lack of information accompanying skeleton and skin specimens. Future

specimens of *Zaglossus* acquired by mammalogy collections should record location of acquisition of specimen in the wild and sex. An estimation of age would also be informative; any captive *Zaglossus* should be archived in museum collections along with information about the animals' age. Finally, it is important that the geographic ranges of species of *Zaglossus* be confidently established so that any locality information accompanying currently archived specimens can be retroactively accurately assigned to species level and updated on the online mammalogy databases.

With the recent re-discovery of a 20th Century western long-beaked echidna from Australia (Helgen et al., 2012), it is evident that there remains more to learn of these rarest of monotremes. As previously discussed, the specimen identified as *Zaglossus bruijnii* that was collected from the Kimberley region of Australia has a couple of anatomical features inconsistent with specimens of *Zaglossus bruijnii* and *Zaglossus bartoni* that were collected from New Guinea. This either suggests that there is a greater range of morphological variation within *Zaglossus* than previously considered, or that the specimen from Kimberley is not a *Zaglossus*, but some other rare or exctinct species of echidna. Specimens such as the Kimberley specimen, with such aberrant morphology, illustrate the importance of knowing the anatomy that is diagnostic of *Zaglossus* if we are to better understand the natural history and diversity of monotremes.

Table 1.1: List of monotreme specimens referenced throughout document. Data based on specimen labels (geography amended to reflect current political boundaries).

Taxon	Specimen Number	Country	State	County	Location	Sex
Megalibgwilia	SAM P20488	Australia	South Australia	N/A	Ossuary, Victoria Cave	N/A
Ornithorhynchus						
O. anatinus	AMNH 200255	N/A	N/A	N/A	N/A	unknown
Tachyglossus						
T. aculeatus	AMNH 35679	N/A	N/A	N/A	N/A	Female
T. a. setosus	AMNH 65833	Australia	Tasmania	Huon Peninsula	N/A	Male
T. a. setosus	AMNH 65842	Australia	Tasmania	N/A	N/A	Male
T. a. lawesii	AMNH 107185	Australia	Queensland	Dimbulah	N/A	Male
T. a. lawesii	AMNH 154458	Australia	Queensland	Cape York	N/A	Male
T. a. lawesii	AMNH 154457	Australia	Queensland	Cape York	N/A	Male
Zaglossus						
Z. bartoni smeenki	AMNH 157072	Papua New Guinea	N/A	N/A	N/A	Male
Z. bartoni bartoni	AMNH 190862	Papua New Guinea	Morobe District	N/A	N/A	unknown
Z. bartoni bartoni	AMNH 190863	Papua New Guinea	Morobe District	N/A	N/A	unknown
Z. bartoni clunius	AMNH 194702	Papua New Guinea	Morobe District	Huon Peninsula	N/A	unknown
Z. bruijnii	MCZ 7397	Papua New Guinea	N/A	N/A	Mt. Arfak (located in what is now West Papua, Indonesia)	unknown
Z. bruijnii	MCZ 12414	Indonesia	Irian Jaya (now West Papua)	N/A	Fakfak	unknown
Z. bruijnii	MCZ 59685	Papua New Guinea	Eastern Highlands	N/A	Crater Mountain	unknown

Table 1.2: Table of URL web addresses for CT data available on DigiMorph.org.

Specimen	DigiMorph.org URL
Ornithorhynchus anatinus AMNH 200255	http://digimorph.org/specimens/Ornithorhynchus_anatinus/adult/
Ornithorhynchus anatinus AMNH 252512	http://digimorph.org/specimens/Ornithorhynchus_anatinus/juvenile/
Tachyglossus aculeatus AMNH 154457	http://digimorph.org/specimens/Tachyglossus_aculeatus/skull/
Zaglossus bartoni AMNH 157072	http://digimorph.org/specimens/Zaglossus_bartoni/
Zaglossus bruijnii MCZ 7379	http://digimorph.org/specimens/Zaglossus_bartoni/

Table 1.3. Key to anatomical abbreviations.

adm	arteria diploëtica magna
ap	angular process of dentary
asc	anterior semicircular canal
bo	basioccipital
bs	basisphenoid
cf	carotid foramen
clp	clinoid process
cor	coronoid process
cp	crista parotica
cva	crest over vestibular aqueduct
dc	dentary condyle
dcp	process on dentary condyle
dp	dentary peduncle
ect	ectopterygoid
emf	exit for mandibular foramen
en	external naris
et	ectotympanic
eth	ethmoid
ex	exoccipital
fm	foramen magnum
fn	fontanelle
fo	foramen ovale
fov	fenestra ovalis
for	foramen rotundum
fp	facial process of parietal
fr	frontal
gf	glenoid fossa
hsc	horizontal semicircular canal
iam	internal acoustic meatus
if	interfrontal
in	incus
io	incisura occipitalis
iof	infraorbital foramen
jf	jugular foramen
ju	jugal
la	lamina ascendens (of alisphenoid)
lf	lacrimal foramen
lo	lamina obturans
ma	malleus
mc	maxillary canal

Table 1.3 (continued)

mf	maxillary foramen
mff	maxillofacial foramen
mpfa	anterior maxillopalatine foramen
mpfp	posterior maxillopalatine foramen
mtf	metotic fissure
mx	maxilla
na	nasal
nf	nasal foramen
np	nasopharyngeal passageway
oc	occipital condyle
op	orbital process of maxilla
or	orbitosphenoid
os	ossifications of the sphenoparietal membrane
pa	parietal
pal	palatine
pem	palatal process of maxilla (posterior extension)
per	periotic
pf	palatine foramen
pfi	palatine fissure
pi	palatal incision
pmx	premaxilla
pp	palatine process of palatine
ppm	palatal process of maxilla
ppx	palatal process of premaxilla
psc	posterior semicircular canal
pt	pterygoid
ptc	post-temporal canal entrance
sf	stylomastoid foramen
smx	septomaxilla
so	supraoccipital
spf	sphenopalatine foramen
sq	squamosal
st	stapes
sym	dentary symphysis
tf	tympanic fossa
v	vestibule
va	vestibular aqueduct
vd	vasa diplöetica
vo	vomer
zpr	zygomatic process of maxilla
*	dorsal shield foramen

Table 1.4: Rostrum length, skull length, and ratio of rostrum length-to-skull length in centimeters of five *Zaglossus* specimens. Rostrum length is measured from tip of snout to lacrimal foramen (Griffiths et al., 1991). In all specimens, rostrum length is longer than half the length of the skull. The two smallest skulls, MCZ 7397 and AMNH 157072, have the smallest rostrum-to-skull length ratio. Skulls of a length over 17 cm have a rostrum-to-skull length ratio just over 0.60. Both *Z. bruijnii* and *Z. bartoni* reach a skull length of over 17 cm, suggesting that skull size and relative rostrum length are not significantly different between species of *Zaglossus*.

Specimen number	Species name	Rostrum length (cm)	Skull Length (cm)	rostrum length/ skull length (cm)
MCZ 7397	*Z. bruijnii*	7.20	13.80	0.52
MCZ 12414	*Z. bruijnii*	10.50	17.33	0.61
AMNH 157072	*Z. bartoni smeenki*	8.50	15.50	0.55
AMNH 190862	*Z. bartoni bartoni*	11	17.50	0.62
AMNH 194702	*Z. bartoni clunius*	10.80	17.60	0.61

Table 1.5: Summary of proposed homologies for the echidna pterygoid in monotremes with elements in reptile and therian skulls. Table modified from de Beer, 1929.

Authority	Reptile	Monotreme	Therian
Gaupp, 1908	Parasphenoid Pterygoid	=Pterygoid =Echidna pterygoid	=Pterygoid
Lubosch, 1907		Pterygoid =Echidna pterygoid	}=Pterygoid
Fuchs, 1910	 Pterygoid	Pterygoid =Echidna pterygoid	=Perpendicular plate of palatine =Pterygoid
Broom, 1914	Pterygoid Ectopterygoid	=Pterygoid =Echidna pterygoid	=Pterygoid =Ectopterygoid of *Dasypus* (=*Tatusia*)
Watson, 1916	Epipterygoid Epipterygoid*	=Pterygoid =Echidna pterygoid	=Pterygoid =Alisphenoid
Kesteven, 1918	Epipterygoid	Echidna pterygoid	=Alisphenoid tympanic wing
Van Kampen, 1922	Basitemporal Pterygoid	=Pterygoid =Echidna pterygoid	=Tympanic process =Pterygoid
De Beer, 1929	Parasphenoid Pterygoid	=Pterygoid =Echidna pterygoid	}=Pterygoid
Parrington and Westoll, 1940	Cynodont epipterygoid Pterygoid Parasphenoid Ectopterygoid	 =Echidna pterygoid	=Alisphenoid =Pterygoid =Parasphenoid =Ventral ossification of pterygoid

*Watson (1916) is referring to the cynodont epipterygoid which he emphasizes is not homologous with the epipterygoid in 'reptiles'.

Table 1.6: Summary of shape of incisura occipitalis, degree of ossification, and degree of skull fusion for five specimens of *Zaglossus* of varying length. Incisura occipitalis shape recorded as open if the foramen magnum has a keyhole shape, nearly open if medially-directed processes above the foramen magnum constrict the base of the incisura occipitalis, closed if the incisura occipitalis is restricted to a foramen dorsal to the foramen magnum, and absent if the foramen magnum is circular and no indication of an incisura occipitalis is present. Degree of ossification is weakly ossified if the sphenoparietal membrane is not completely ossified and the skull is open on the ventral surface between the palatine and periotic, moderately ossified if the sphenoobturator membrane is ossified between the alisphenoid and periotic but the foramen rotundum and foramen ovale are large, and fully ossified if the sphenoobturator membrane is ossified and the foramen rotundum and foramen ovale are small. Skull fusion is superficially approximated by visibility of sutures. In MCZ 7397, many elements are distinguishable because of clear sutures. In AMNH 157072, AMNH 190862, and AMNH 194702, many sutures on the top of the cranium are no longer visible, but the sutures of the palate, the maxilla, and the squamosal are still visible. In MCZ 12414, no sutures are visible. *Zaglossus bruijnii* and *Zaglossus bartoni* species overlap in size. Though sample size is small, skull length, incisura occipitalis shape, degree of ossification, and degree of fusion may be correlated.

Specimen number	Species name	Length (cm)	Incisura occipitalis shape	Degree of ossification	Skull Fusion
MCZ 7397	*Zaglossus bruijnii*	13.8	open	Weakly ossified	cranial sutures present
MCZ 12414	*Zaglossus bruijnii*	17.33	absent	Fully ossified	cranial sutures absent
AMNH 157072	*Zaglossus bartoni smeenki*	15.5	Nearly closed	Moderately ossified	some cranial sutures present
AMNH 190862	*Zaglossus bartoni bartoni*	17.5	Broken, nearly closed	Moderately ossified	some cranial sutures present
AMNH 194702	*Zaglossus bartoni clunius*	17.6	Closed with foramen above foramen	Moderately ossified	some cranial sutures present

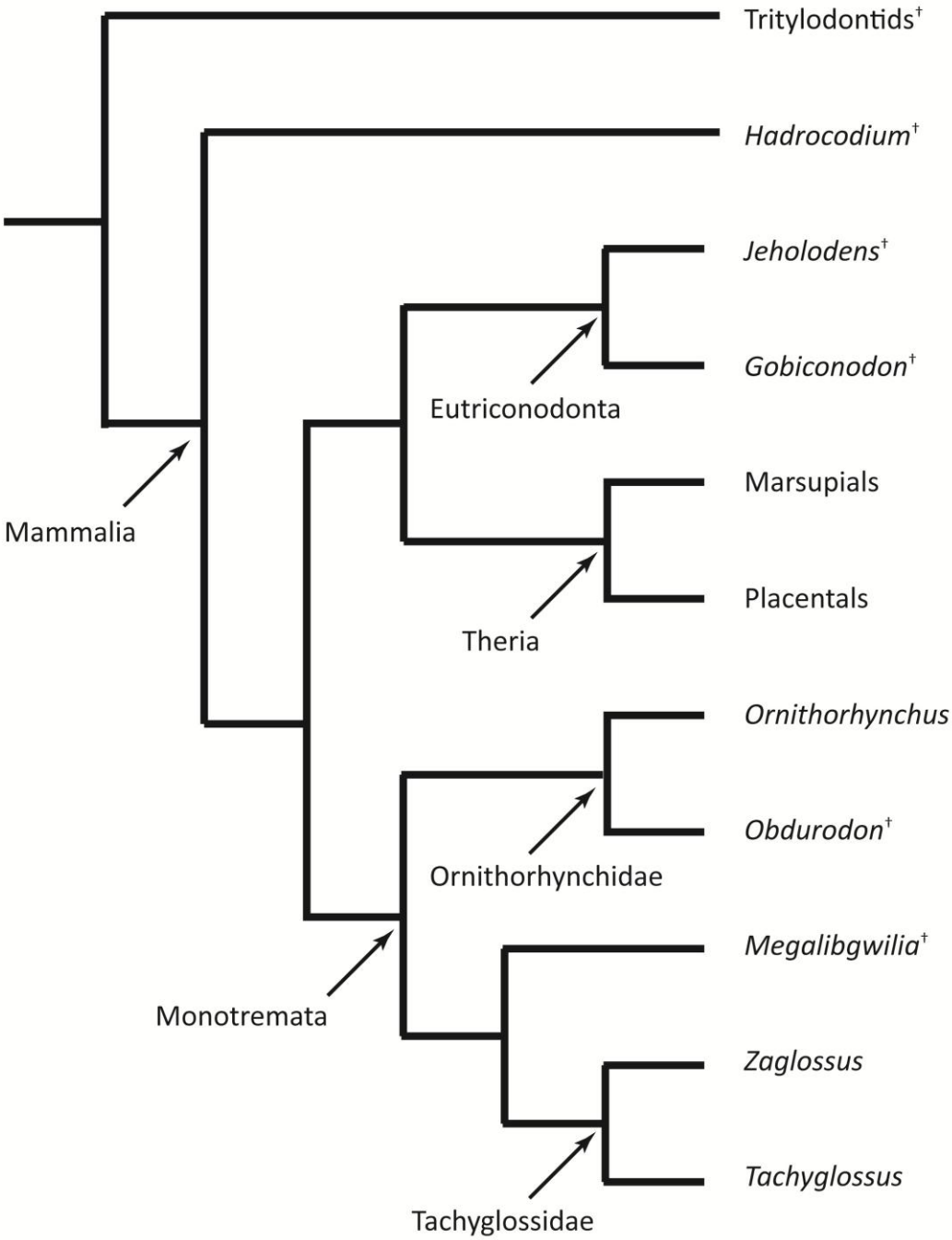

			magnum		

Figure 1.1: Phylogeny of Monotremata in the context of Mammalia. Based on a matrix rescored from Luo and Wible (2005) and Rowe et al. (2008). For more information, see Chapter 2.

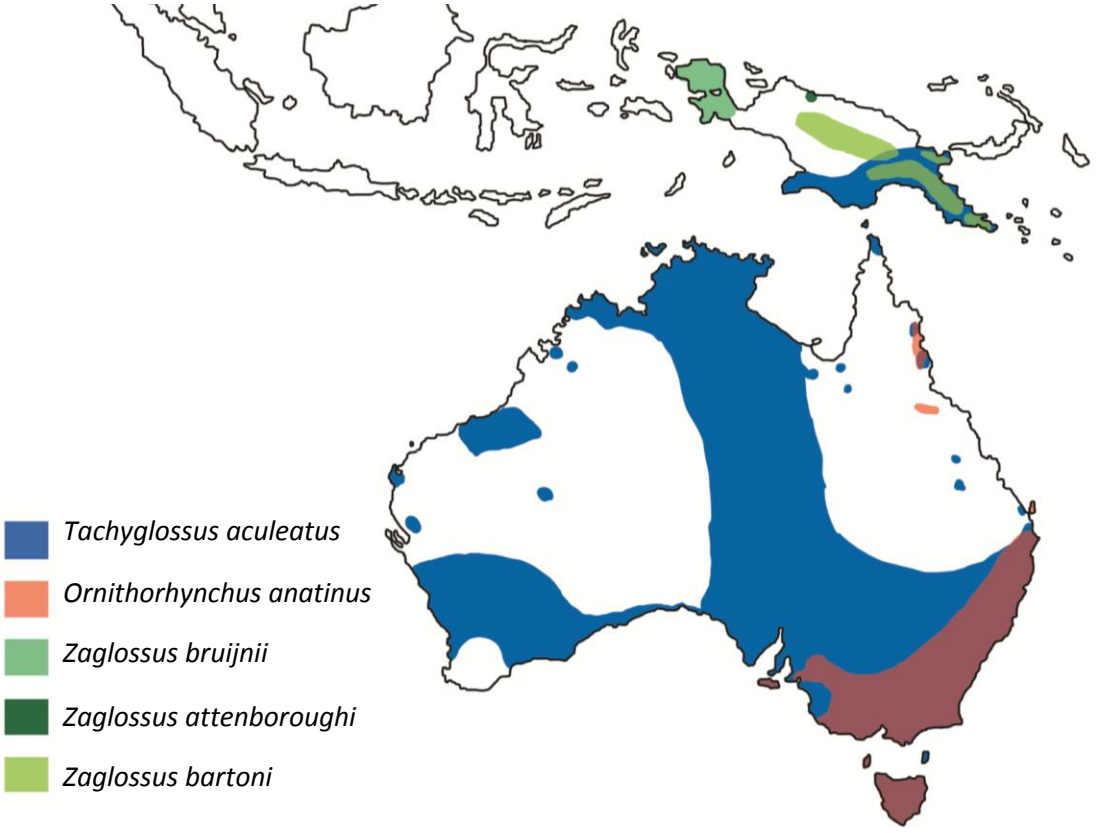

Figure 1.2: Distribution of extant monotremes. Monotremes are restricted to Australia and New Guinea and nearby islands. *Tachyglossus aculeatus* (distribution approximated in blue) has the greatest range, occurring in northern, southern, eastern, western, and central parts of Australia, as well as in Tasmania and other nearby islands, and the southern part of New Guinea. *Ornithorhynchus anatinus* (distribution approximated in red) is found along the eastern edge of Australia, Tasmania, and nearby islands. *Zaglossus* has the narrowest range (distribution approximated in green), occurring only within New Guinea. Sea green represents population distribution of *Zaglossus bruijnii*. Dark green—a small circle on the northern border of New Guinea—represents the population of *Zaglossus attenboroughi*. Lime green represents the population distribution of all four subspecies of *Zaglossus bartoni* (see Flannery and Groves, 1998).

Figure 1.3: Keratinous pads cover the bony palate of *Zaglossus*. Keratinous spines on the ventral surface of the snout (right, indicated by white arrows) and palate (left, seen as rows of light colored spines in a dark patch of membrane) of *Zaglossus bruijnii* AMNH 195373 (specimen broken) and AMNH 190859, respectively. Scale bar = 1 cm.

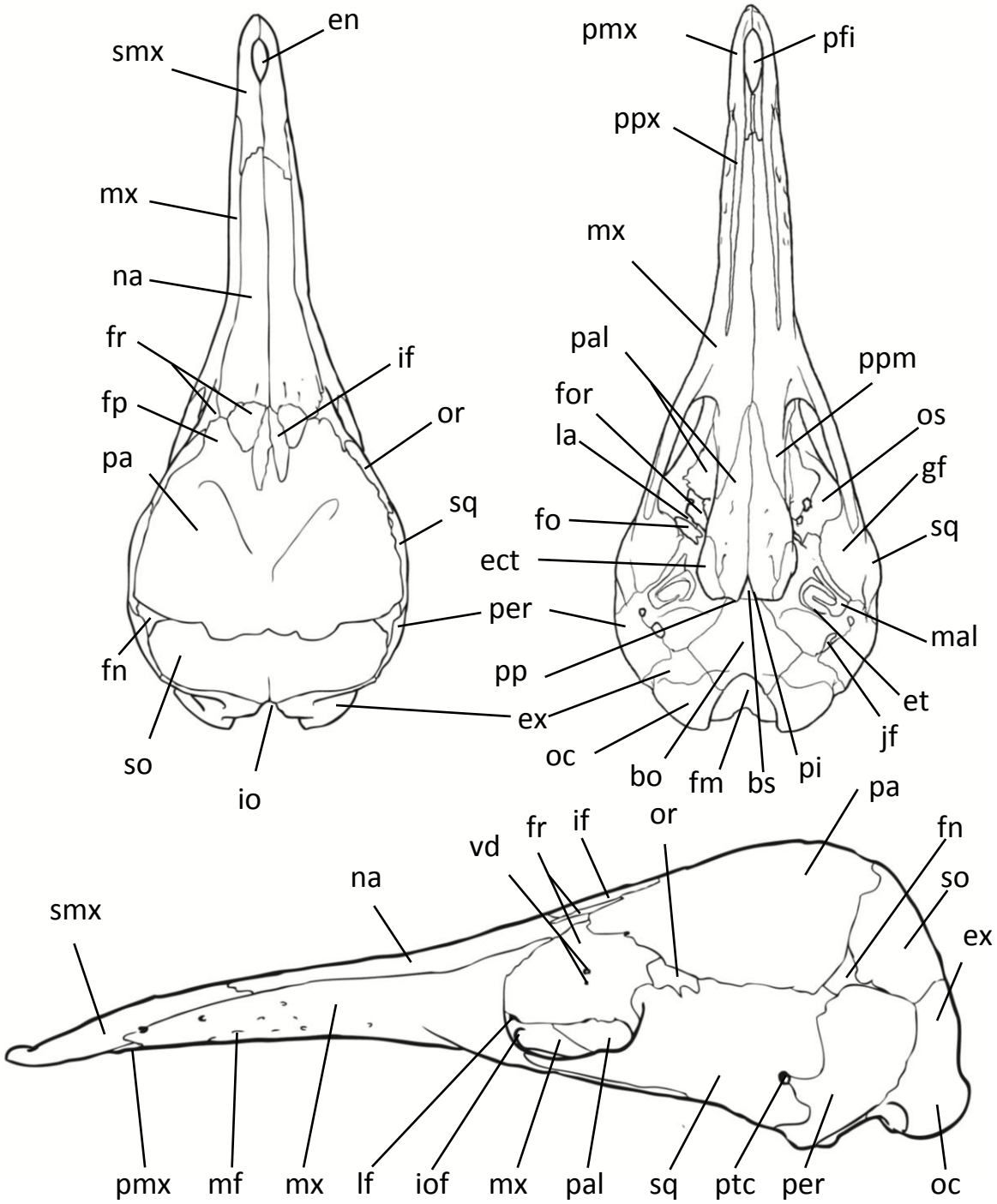

Figure 1.4: *Zaglossus bruijnii* CMZ 7397 skull in dorsal (left), ventral (right), and lateral (bottom) view. For key to abbreviations, see Table 1.3.

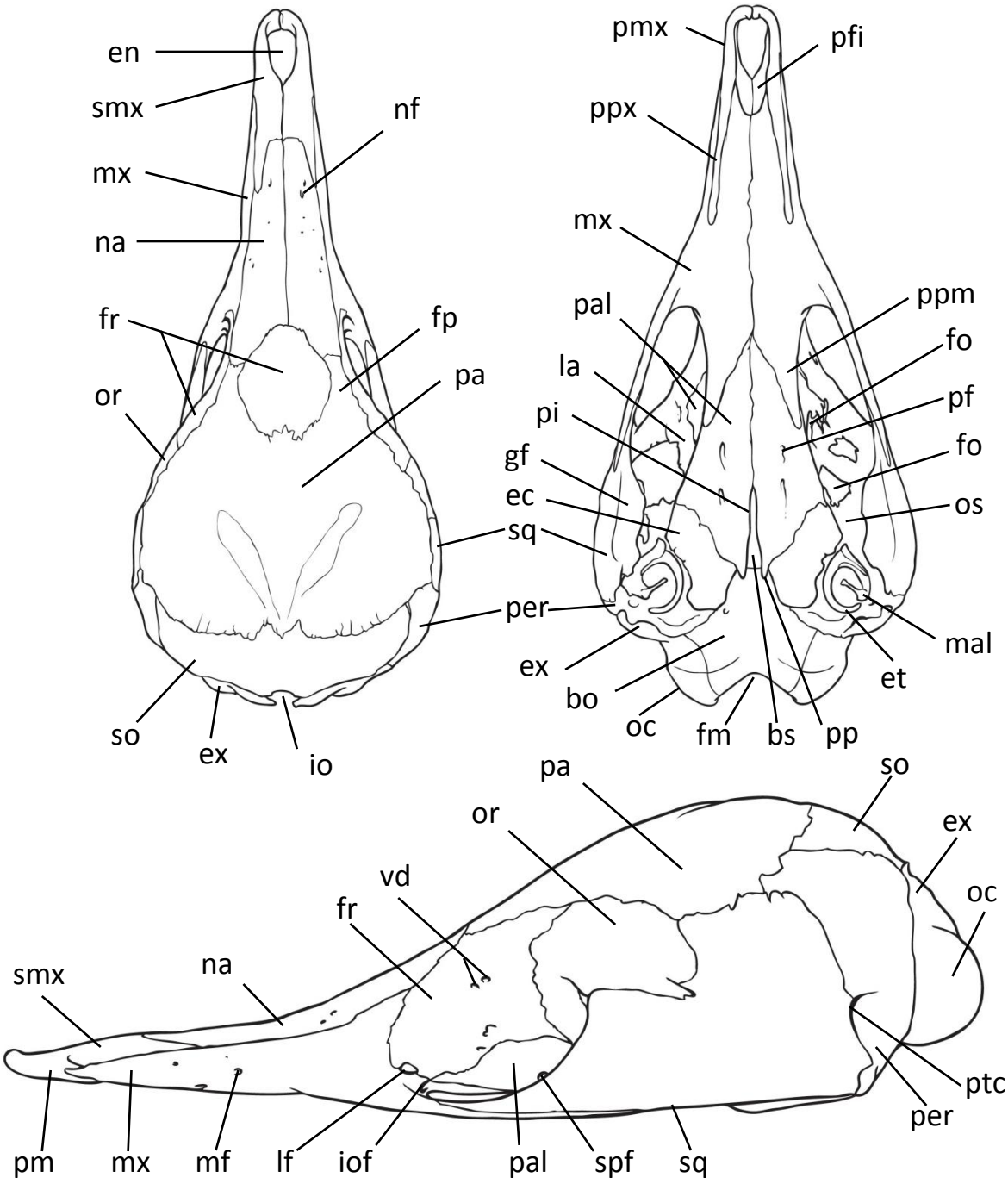

Figure 1.5: *Tachyglossus aculeatus* AMNH 107185 skull in dorsal (left), ventral (right), and lateral (bottom) view. For key to abbreviations, see Table 1.3.

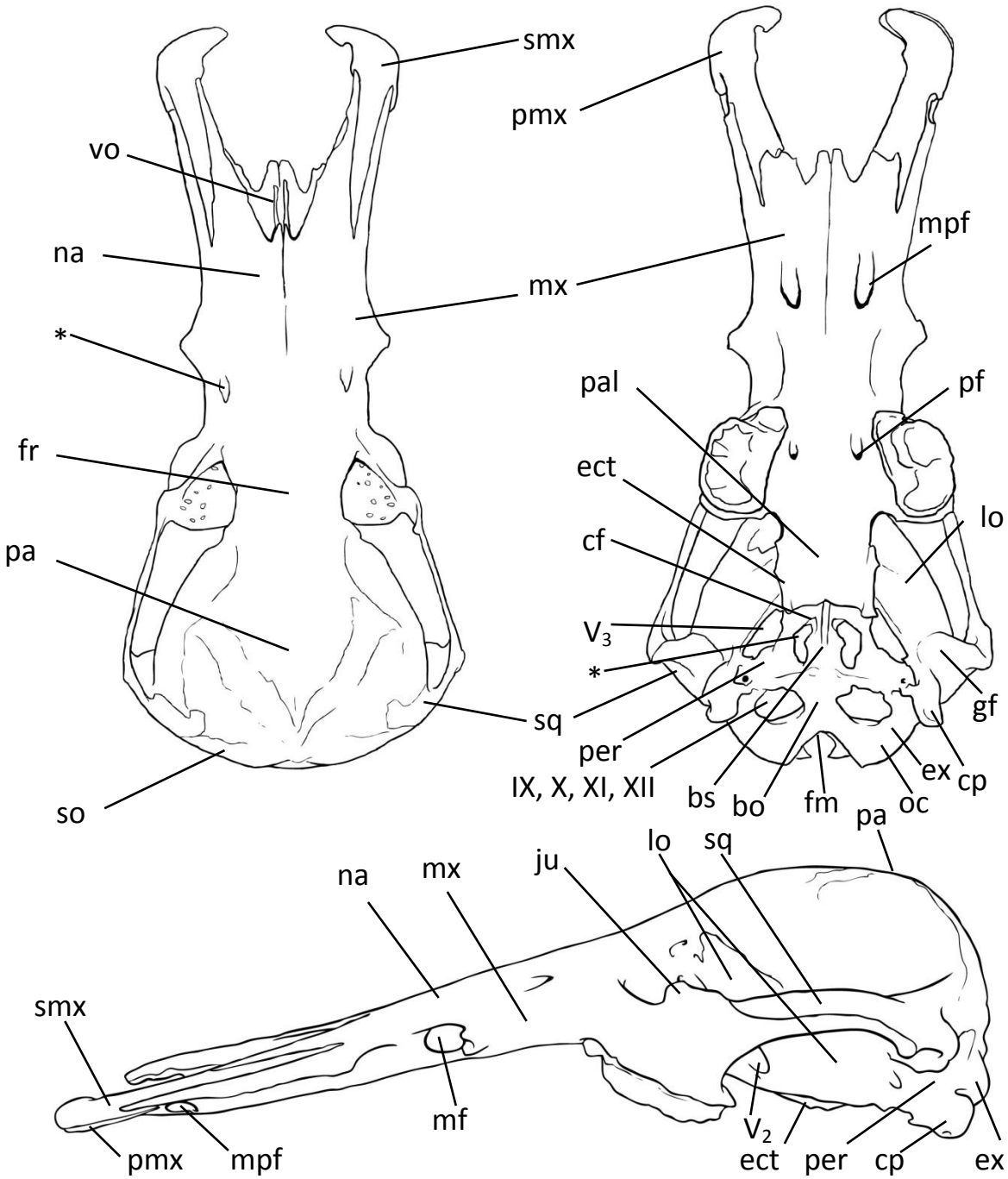

Figure 1.6: *Ornithorhynchus anatinus* AMNH 200255 skull in dorsal (left), ventral (right), and lateral (bottom) view. For key to abbreviations, see Table 1.3.

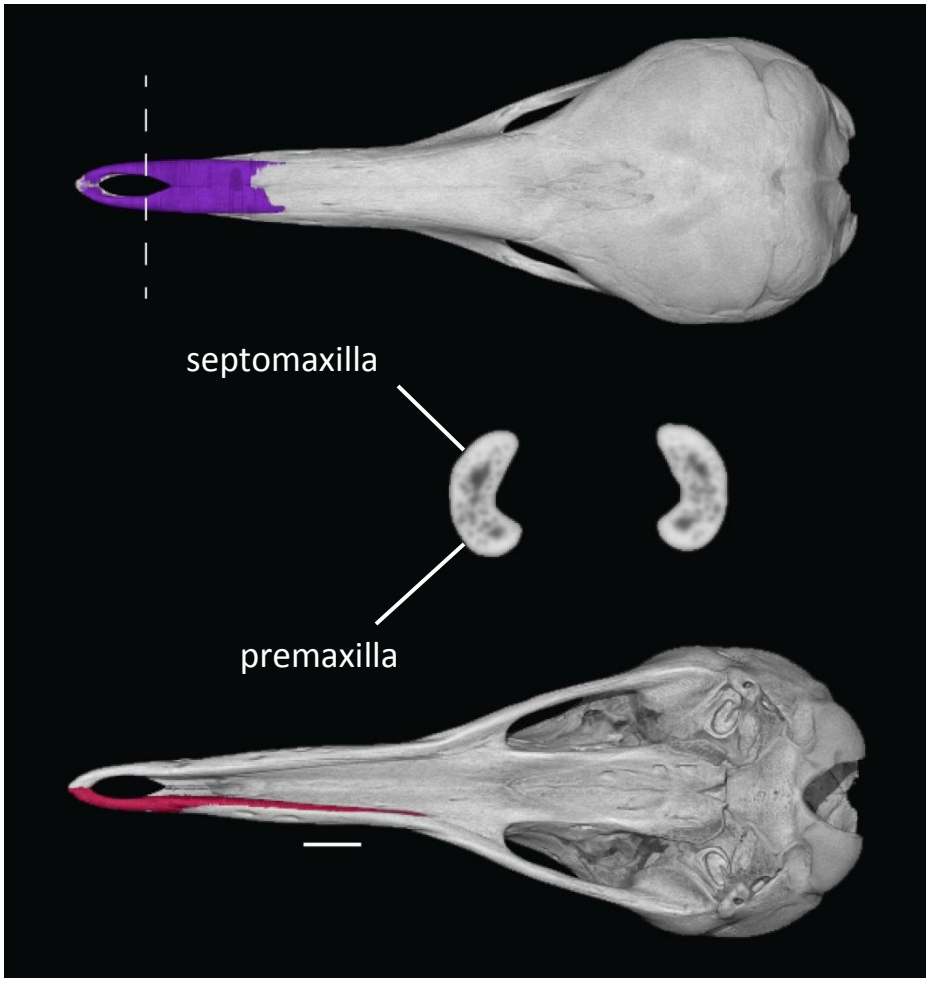

Figure 1.7: Septomaxilla in situ (A) and premaxilla in situ (C) of *Zaglossus bruijnii* MCZ 7397. Dashed line approximates location of cross section (B), illustrating the fusion of the septomaxillae and premaxillae. Scale bar = 10 mm.

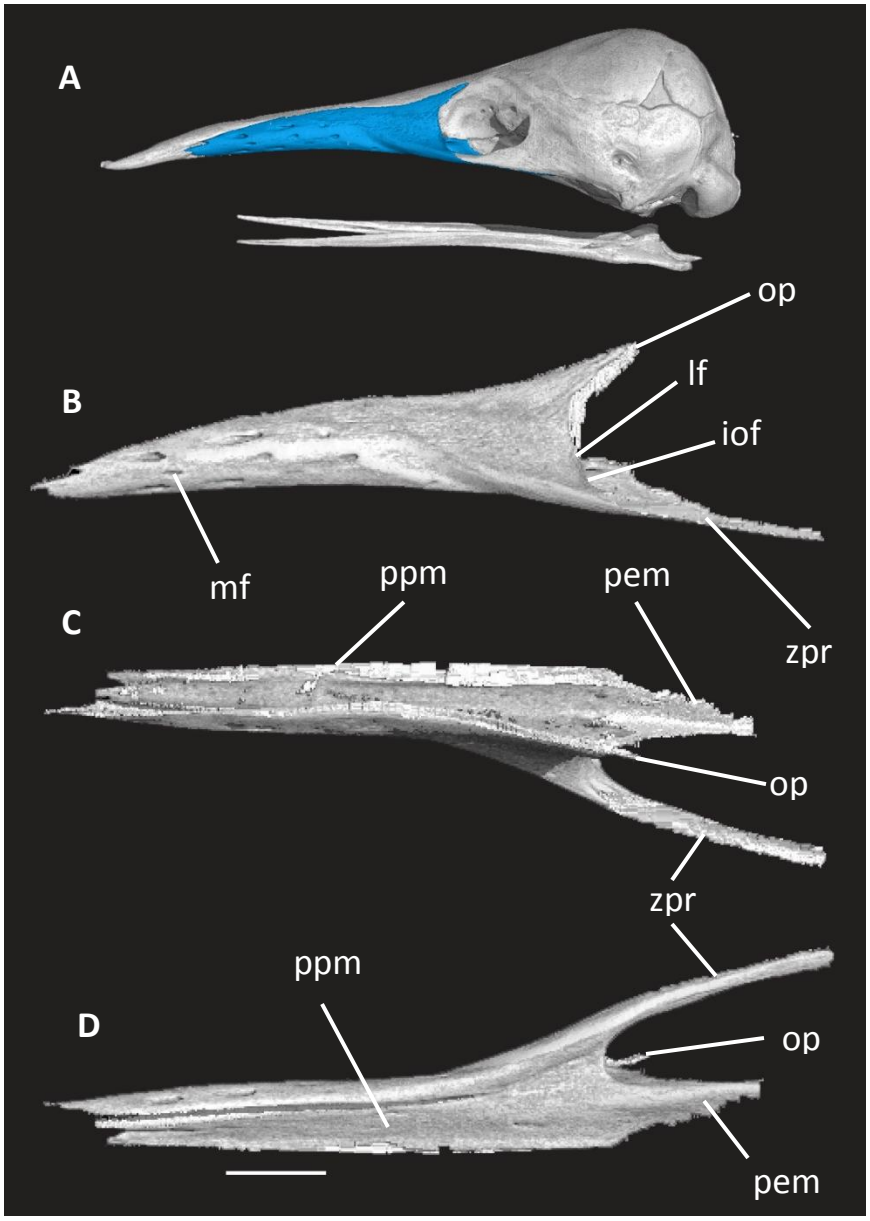

Figure 1.8: Left maxilla of *Zaglossus bruijnii* MCZ 7397 in situ and shaded in blue (A), and in isolation, depicted in lateral view (B), dorsal view (C), and ventral view (D). Scale bar = 10 mm. For key to abbreviations, see Table 1.3.

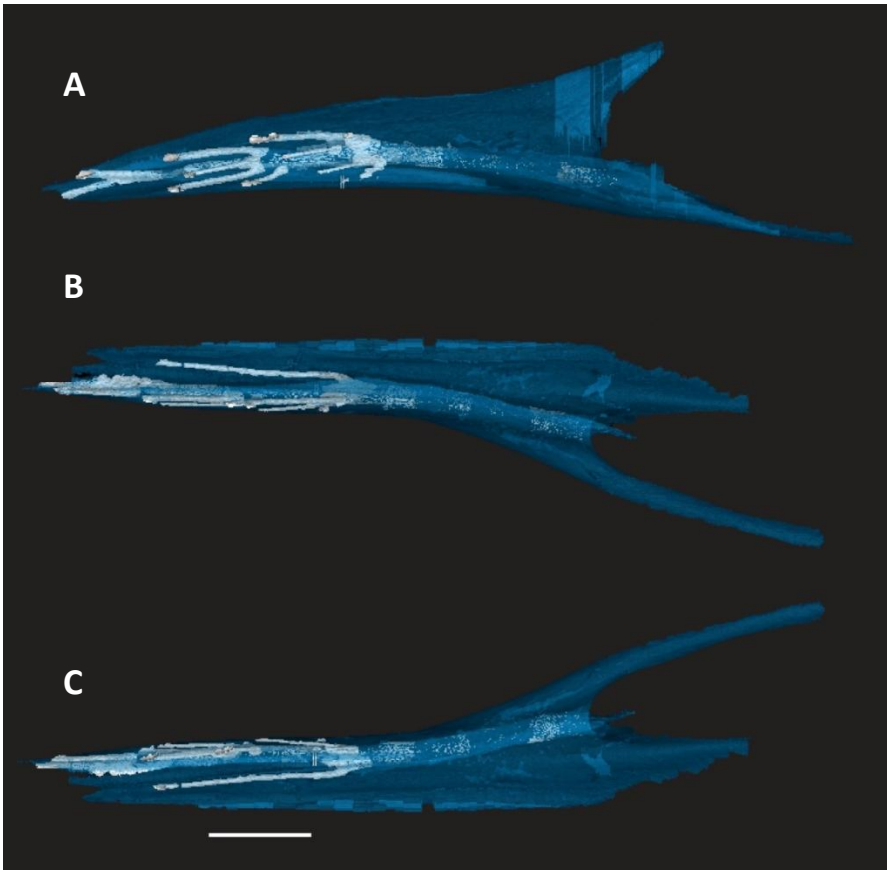

Figure 1.9: Maxillary canal for V_2 digitally colored an opaque white and depicted in situ of the maxilla, which is shaded a transparent blue, shown in left lateral view (A), left dorsal view (B), left ventral view (C). Maxilla and maxillary canal digitally rendered from CT scan of *Zaglossus bruijnii* MCZ 7397. Scale bar = 10 mm.

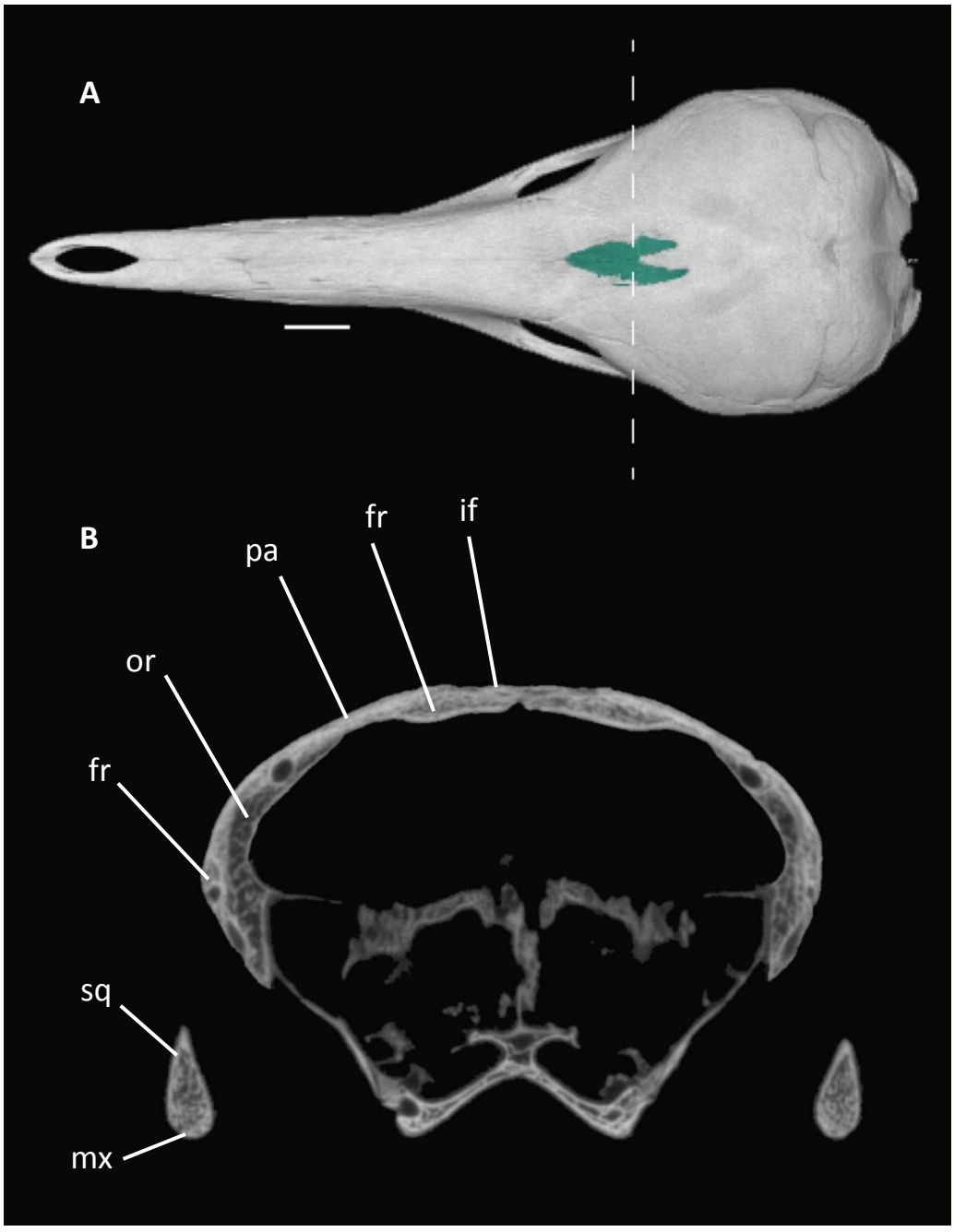

Figure 1.10: Position of interfrontal in situ in dorsal view (A) and cross section (B). Dashed line approximates location of cross section. Whole skull and cross section are of *Zaglossus bruijnii* MCZ 7397. For key to abbreviations, see Table 1.3. Scale bar = 10 mm.

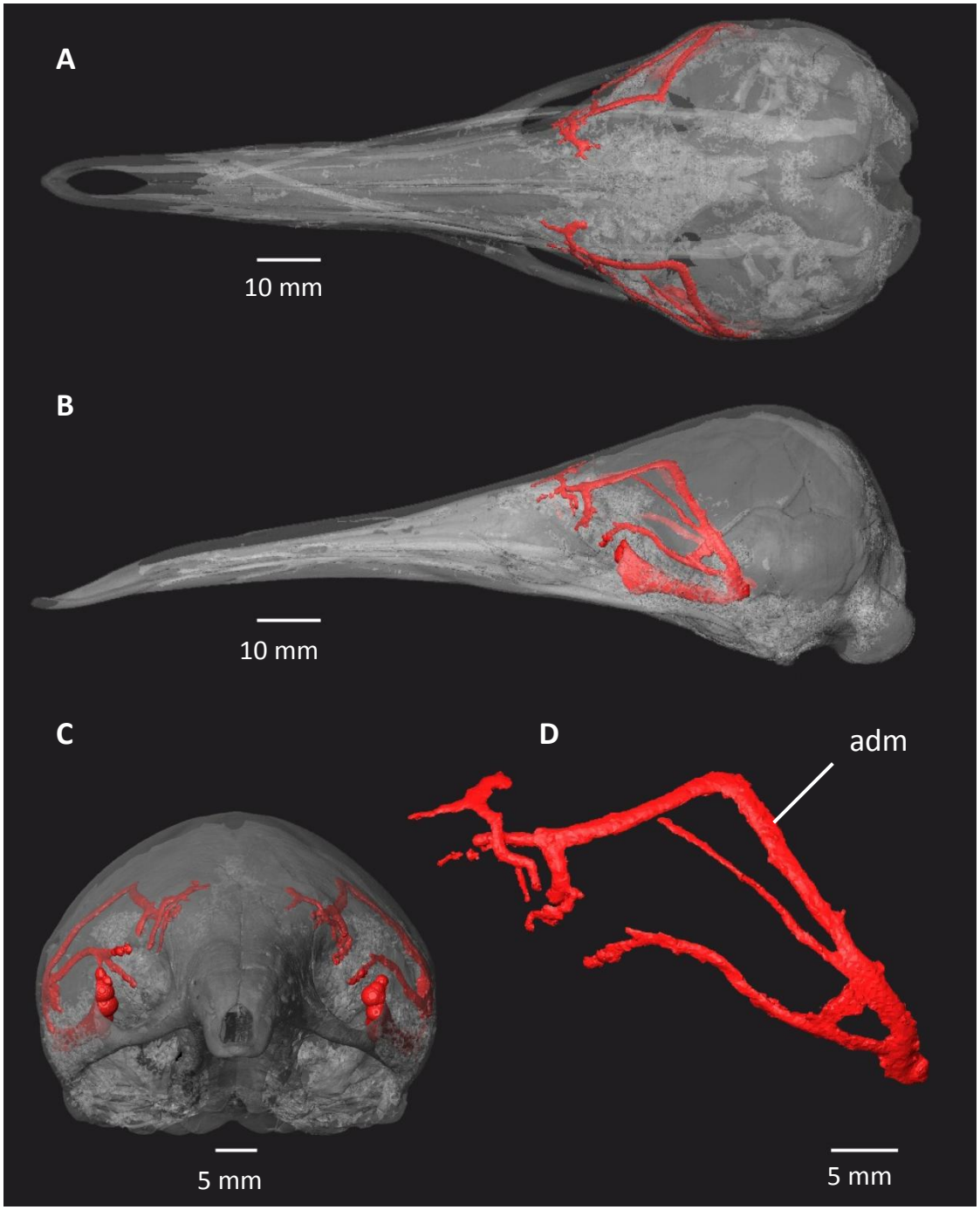

Figure 1.11: The canal for the arteria diploëtica magna (adm) and other blood vessels within the skull of *Zaglossus bruijnii* MCZ 7397 in (A) dorsal, (B) lateral, and (C) anterior view. Isolated blood vessel canals in left lateral view (D).

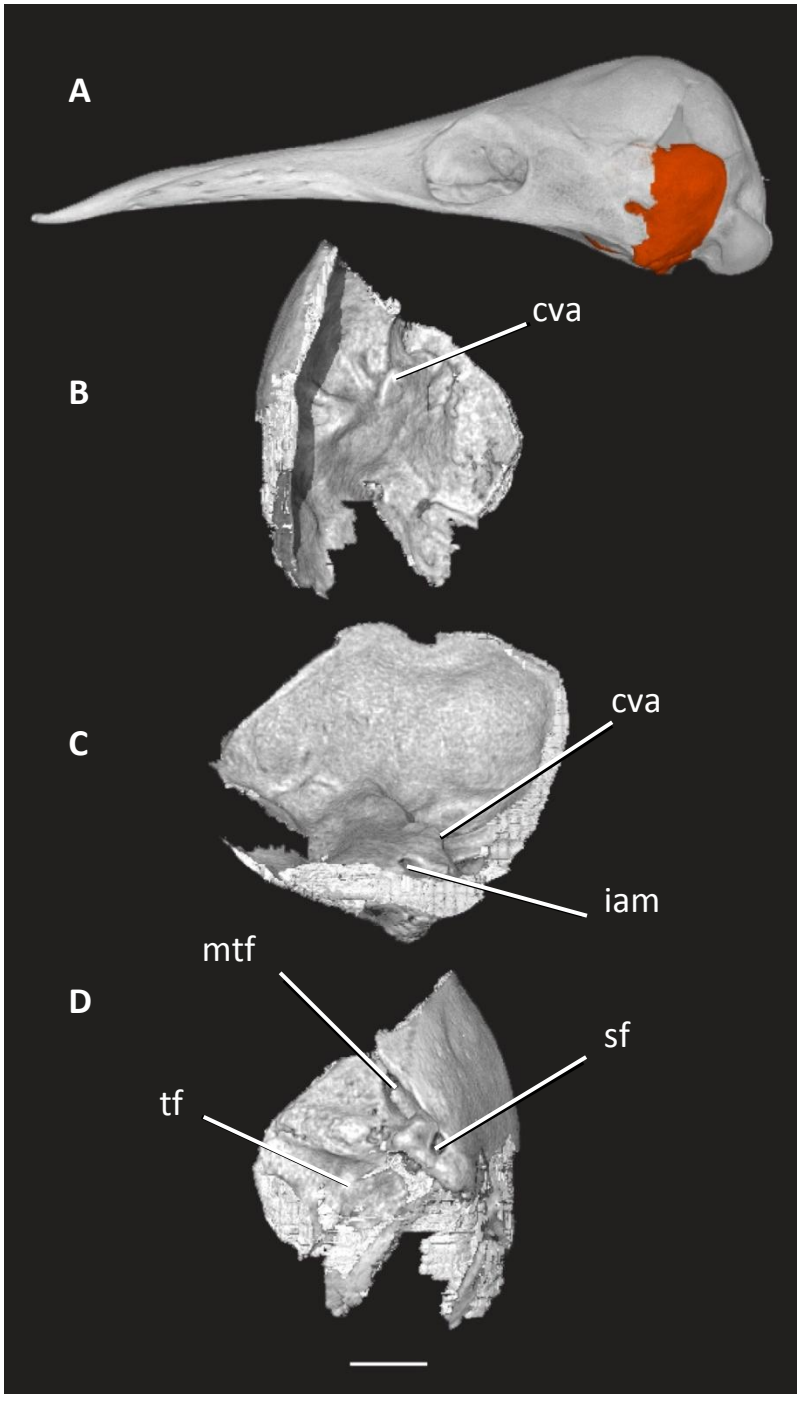

Figure 1.12: Right periotic of *Zaglossus bruijnii* MCZ 7397 in situ (colored orange, A), dorsal (B), medial (C), and ventral (D) view. Scale bar = 5 mm. For key to abbreviations, see Table 1.3.

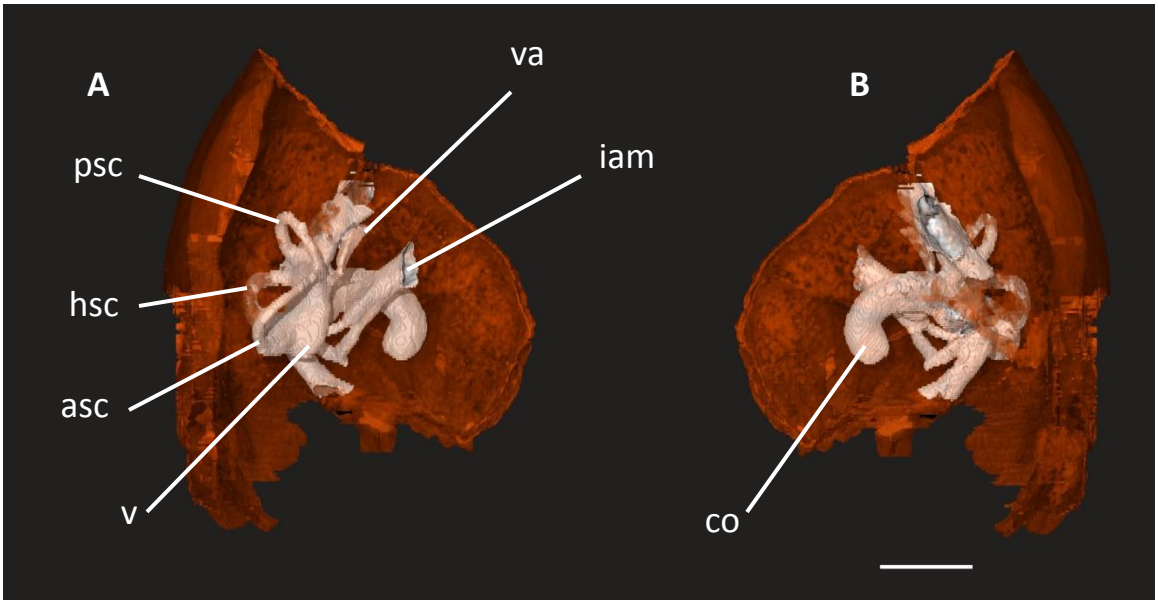

Figure 1.13: Right periotic of *Zaglossus bruijnii* MCZ 7397 showing internal bony labyrinth in dorsal view (A) and ventral view (B). Scale bar = 5 mm. For key to abbreviations, see Table 1.3.

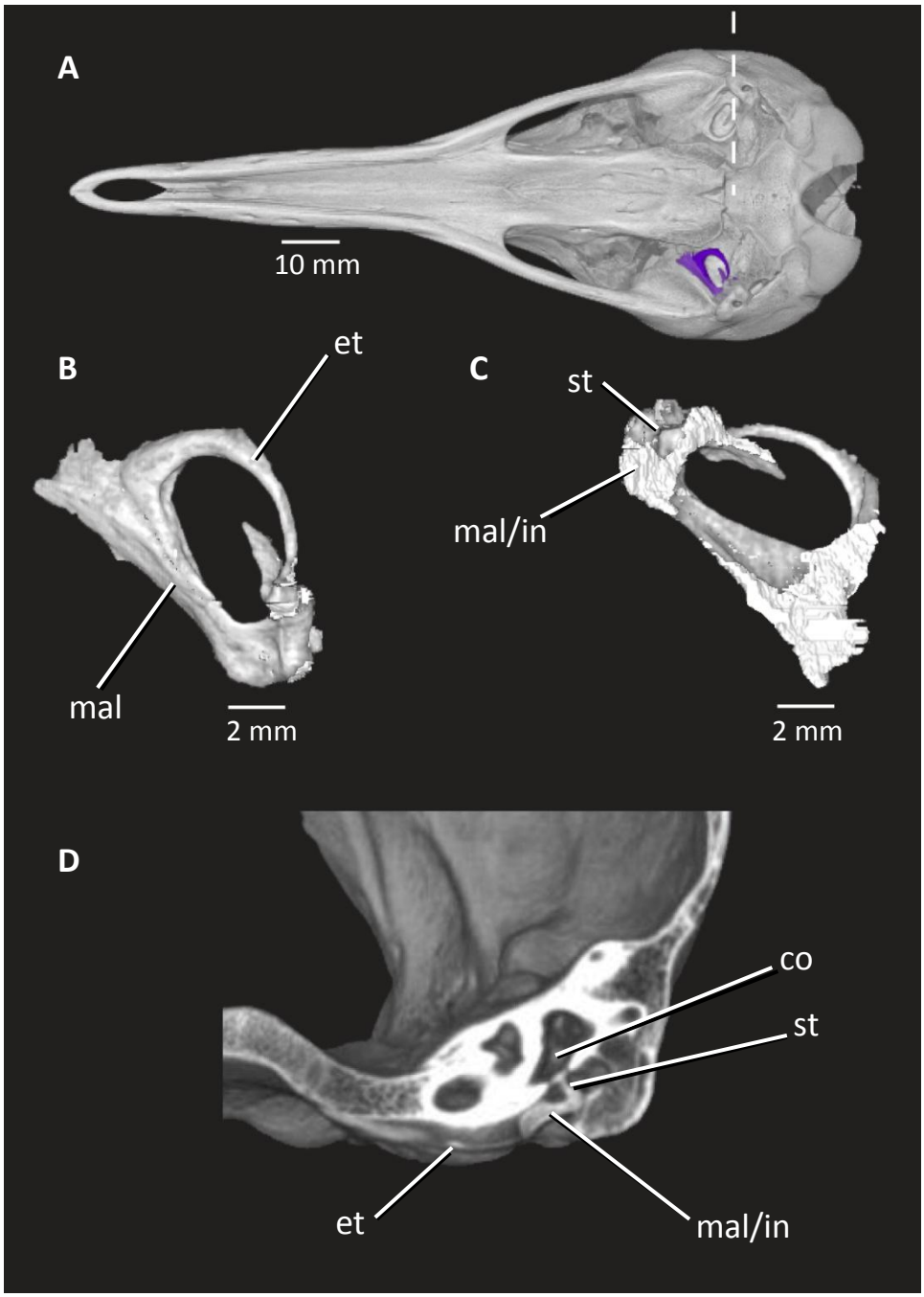

Figure 1.14: Ectotympanic and middle ear ossicles of *Zaglossus bruijnii* MCZ 7397 shown in situ (A) and isolated in ventral (B) and dorsal (C) view. Cross section (D) through lower left portion of skull—approximated with dashed line—to show how the footplate of the stapes fits into the fenestra ovalis and contacts the cochlea. For key to abbreviations, see Table 1.3.

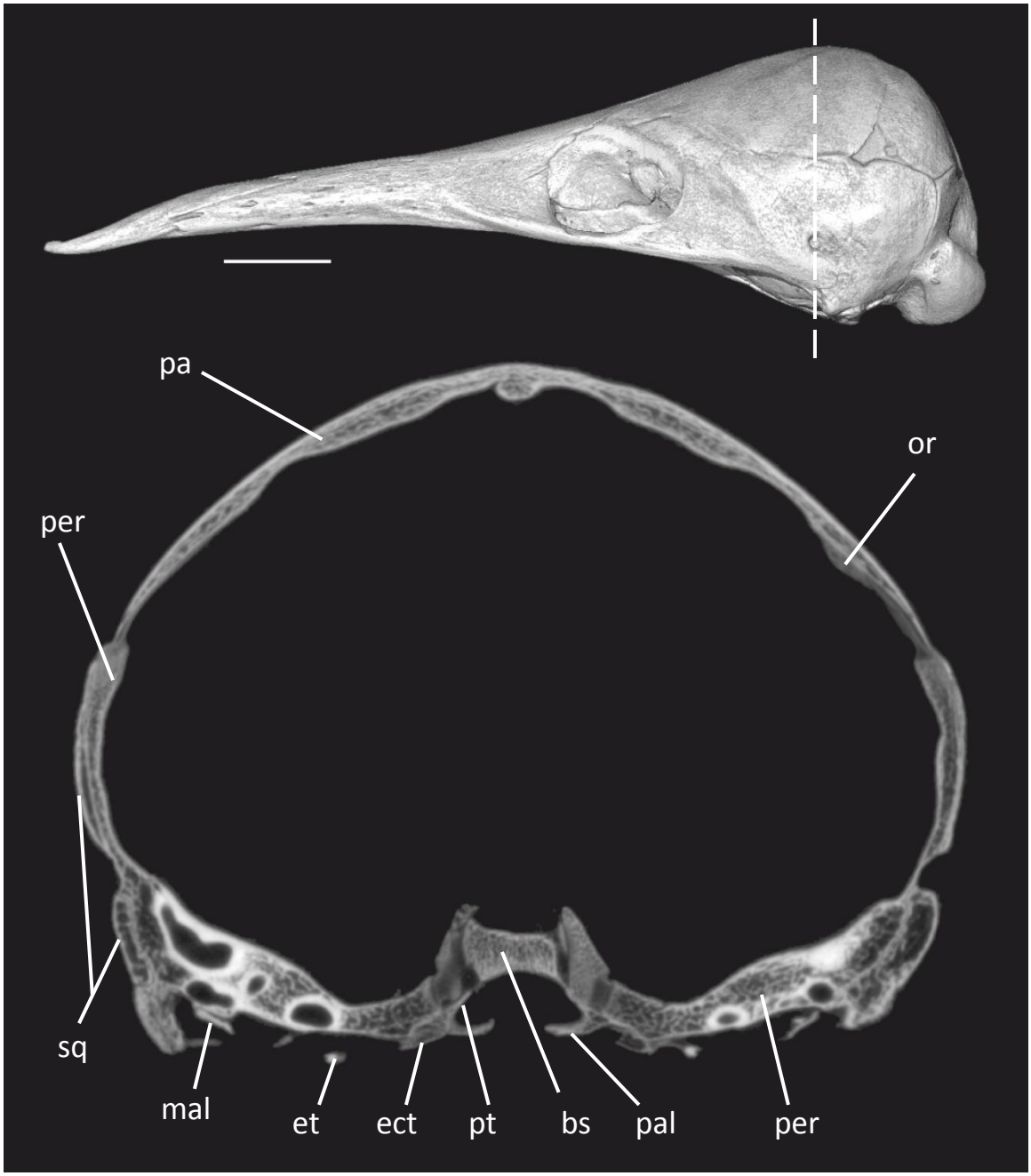

Figure 1.15: The terygoid of *Zaglossus bruijnii* MCZ 7397, visible in cross section. Position of cross section approximated with dotted line. For key to abbreviations, see Table 1.3. Scale bar = 10 mm.

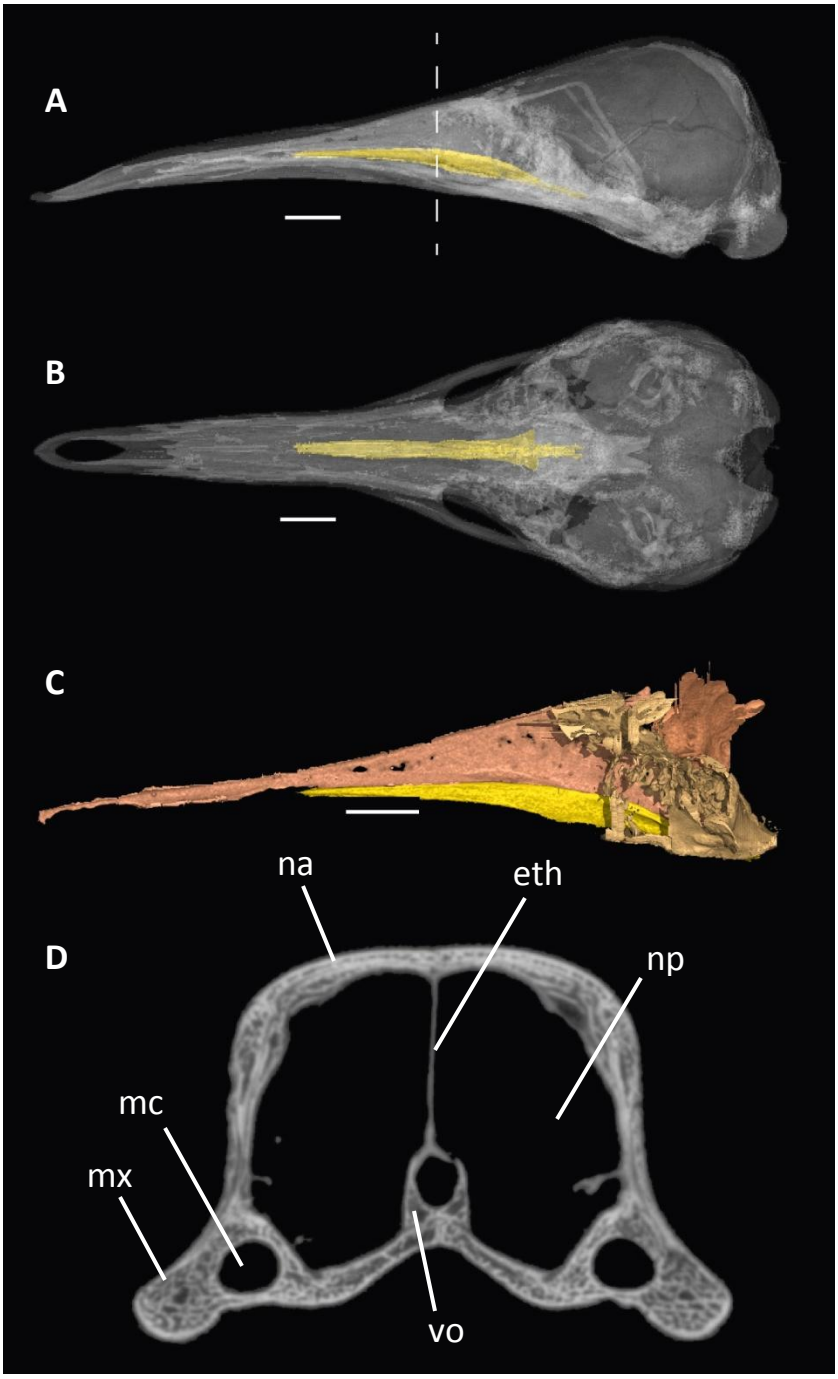

Figure 1.16: Vomer of *Zaglossus bruijnii* MCZ 7397 shown in situ in lateral (A) and ventral view (B); in relation to the ethmoid skeleton viewed laterally (C), and in cross section (D). Scale bar = 10 mm.

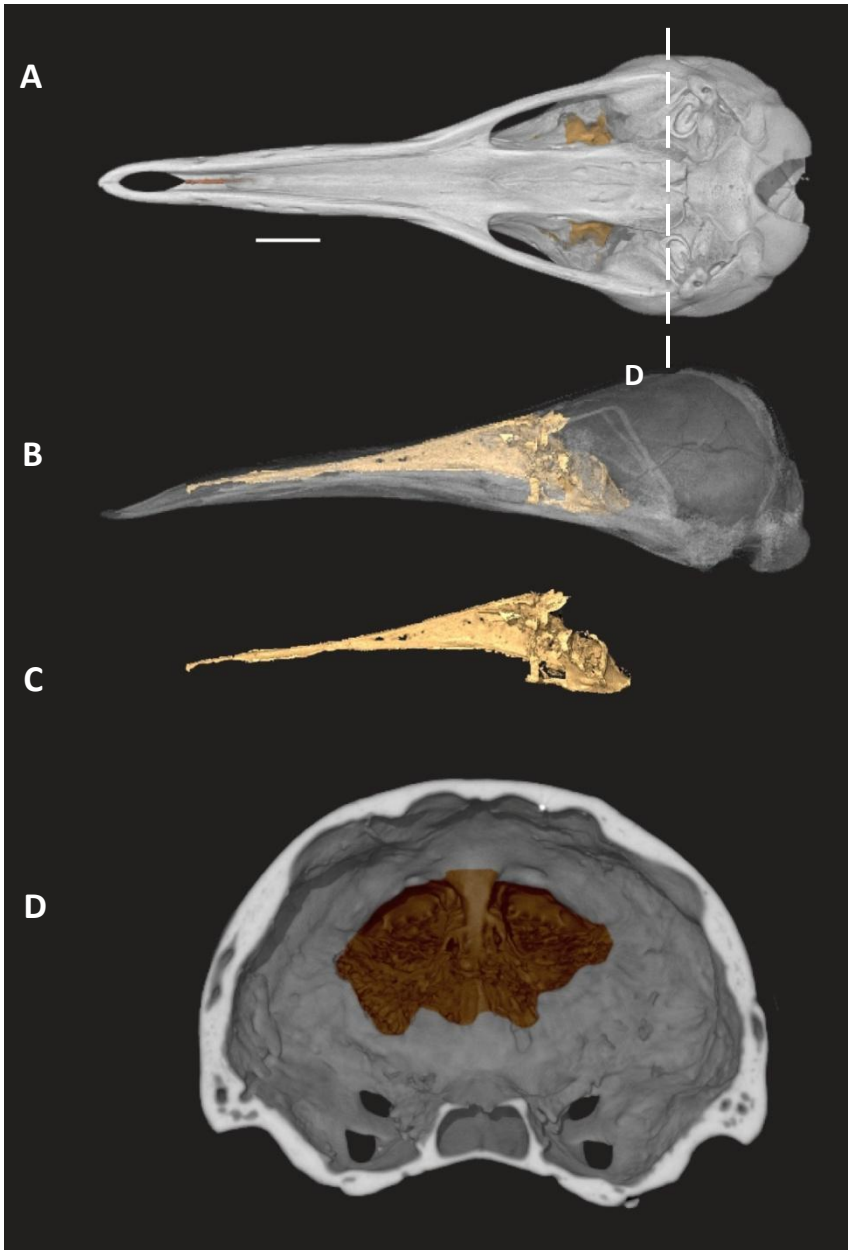

Figure 1.17: Ethmoid. (A) Ethmoid in situ in ventral view, (B) in situ in lateral view with rest of skull made transparent, (C) isolated in left lateral view, and (D) in posterior view with posterior end of cranium cut away. (A)-(C) depict ethmoid in *Zaglossus bruijnii* MCZ 7397. (D) Depicts the cribriform plate of the ethmoid skeleton. Dashed line approximates the location of the cross section through the skull. (A)-(C) are shown to scale. Scale bar = 10 mm.

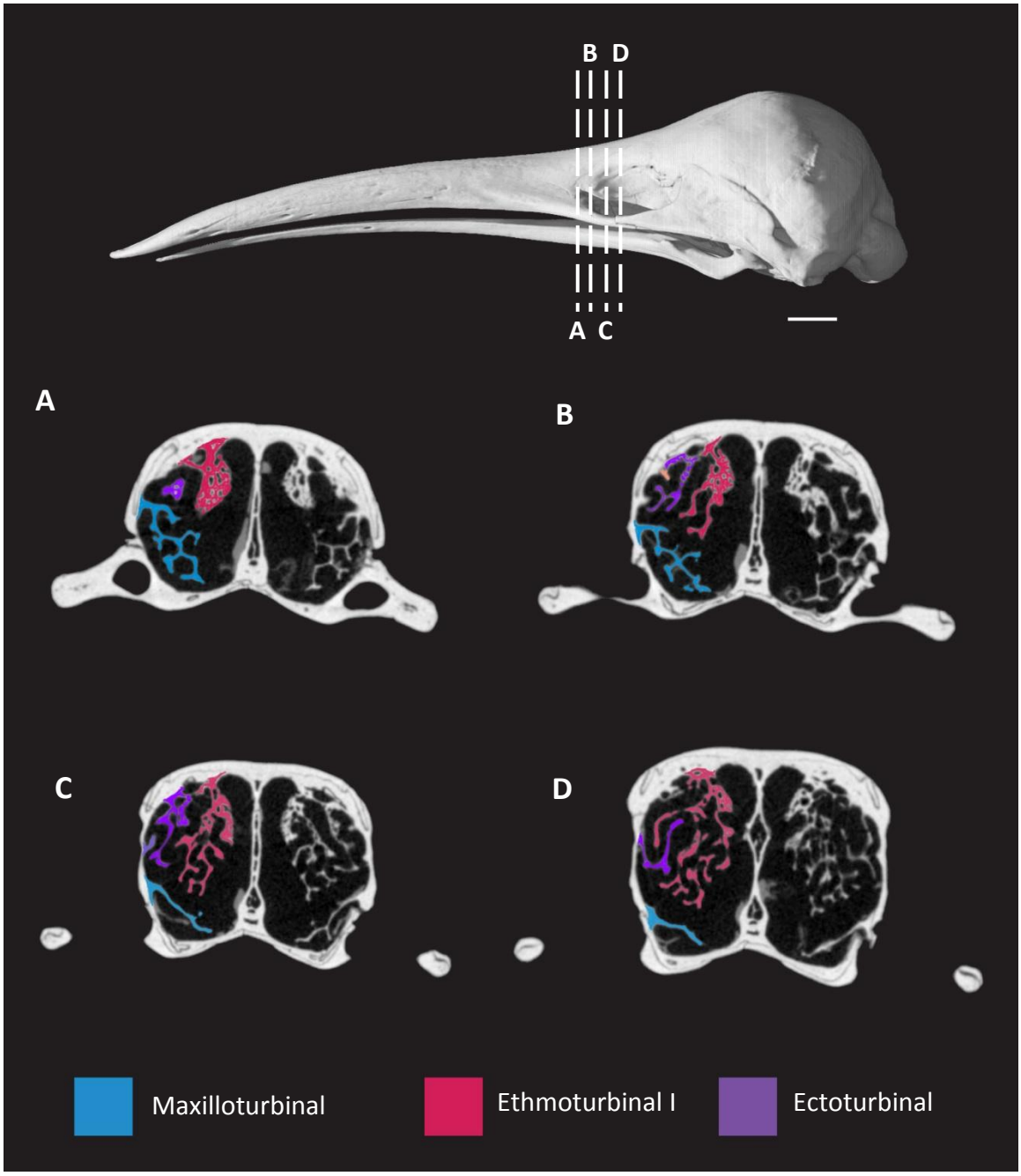

Figure 1.18: Nasal turbinates shown in cross section through the snout of the skeletally mature *Zaglossus bartoni* AMNH 157072. Cross sections (A)-(D) move anterior to posterior. The maxilloturbinal is shaded blue, the ethmothmoturbinal I is shaded red and the ectoturbinal is shaded purple. Position of cross sections are indicated on the whole skull (top). Scale bar = 1 cm. Cross sections are not shown to scale.

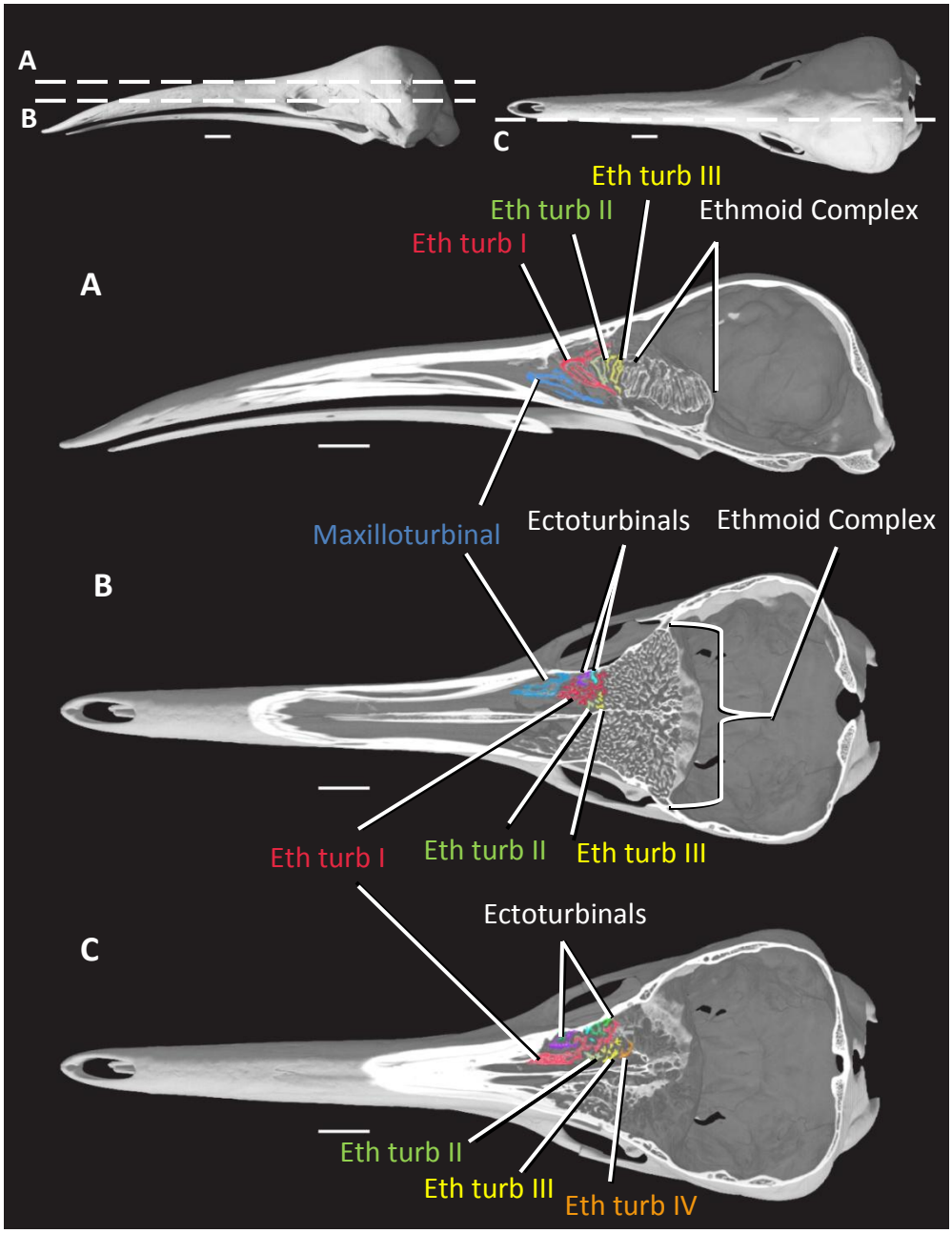

Figure 1.19: Sagittal (A) and horizontal (B, C) cross-sections through the ethmoid skeleton of the skeletally mature *Zaglossus bartoni* AMNH 157072. Cross sections indicated through dorsal and lateral views of the entire skull (top). Ethmoturbinals = Eth turb. Scale bars = 1 cm.

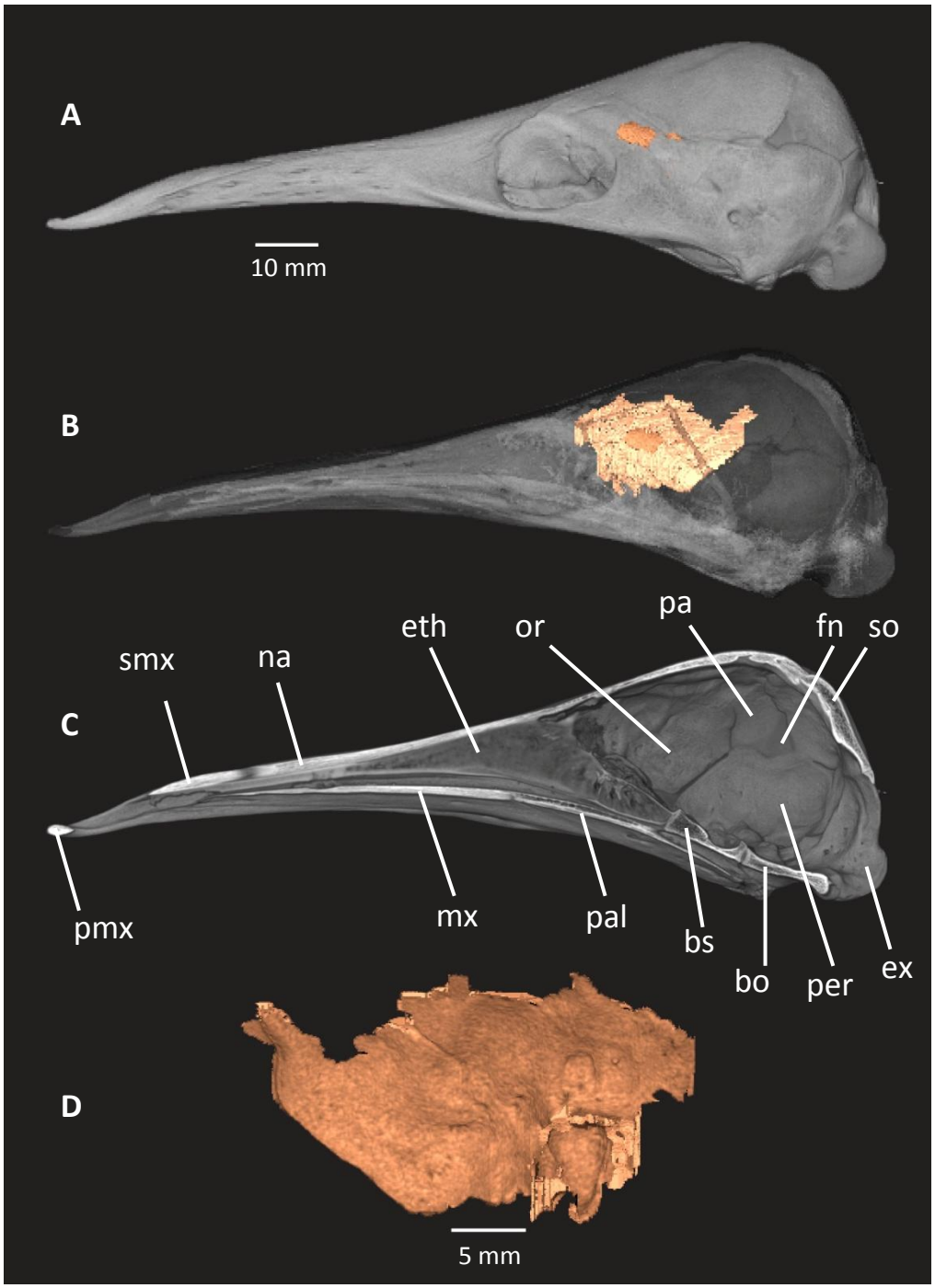

Figure 1.20: Orbitosphenoid of *Zaglossus bruijnii* MCZ 7397 shown in situ in lateral view with the skull opaque (A) and transparent (B), and in situ with half of

skull cut away (C). Left orbitosphenoid is shown isolated in medial view (D). For key to abbreviations, see Table 1.3.

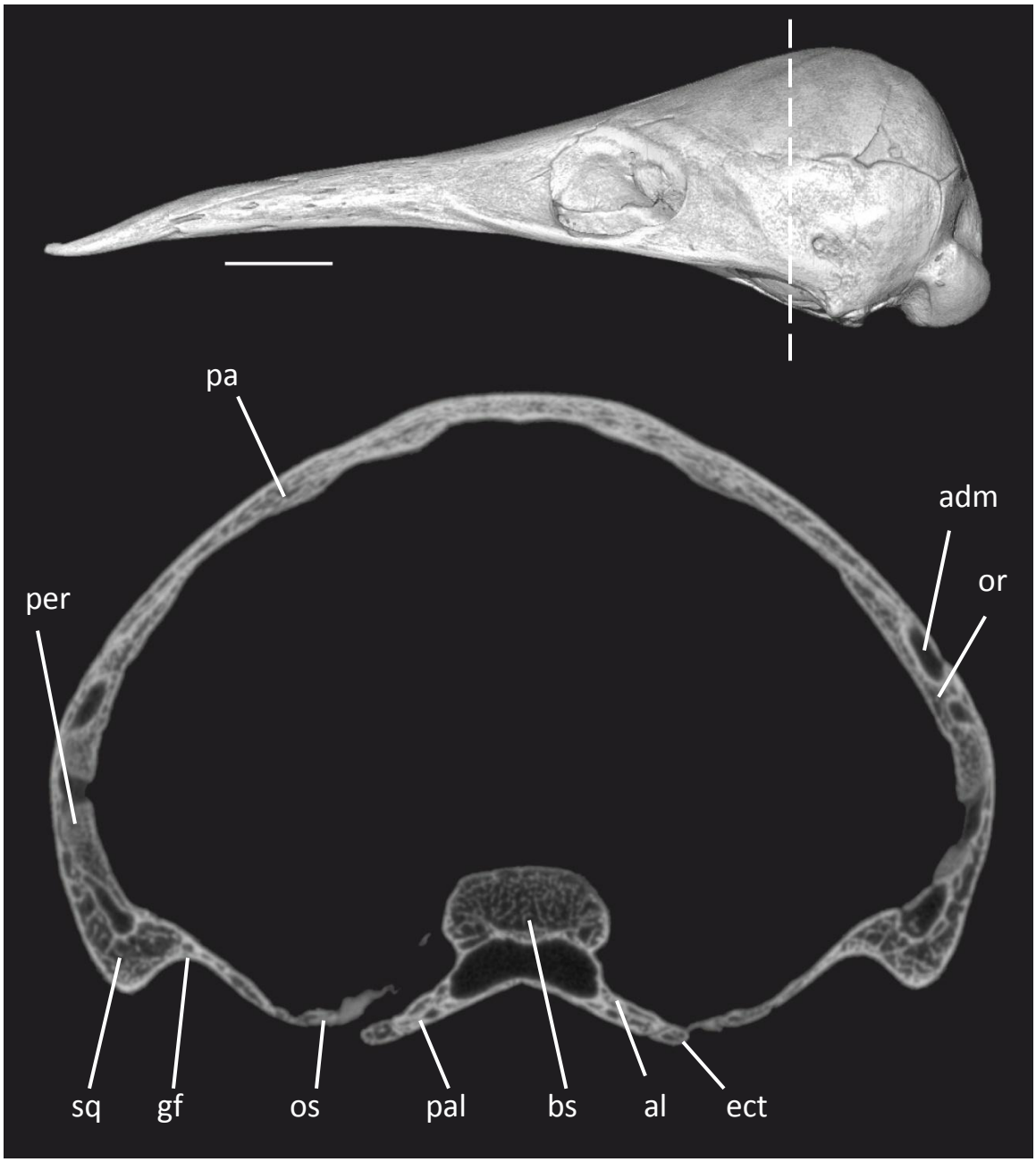

Figure 1.21: Alisphenoid of *Zaglossus bruijnii* MCZ 7397 in cross section. Position of cross section approximated by dashed line. For key to abbreviations, see Table 1.3. Scale bar = 10 mm.

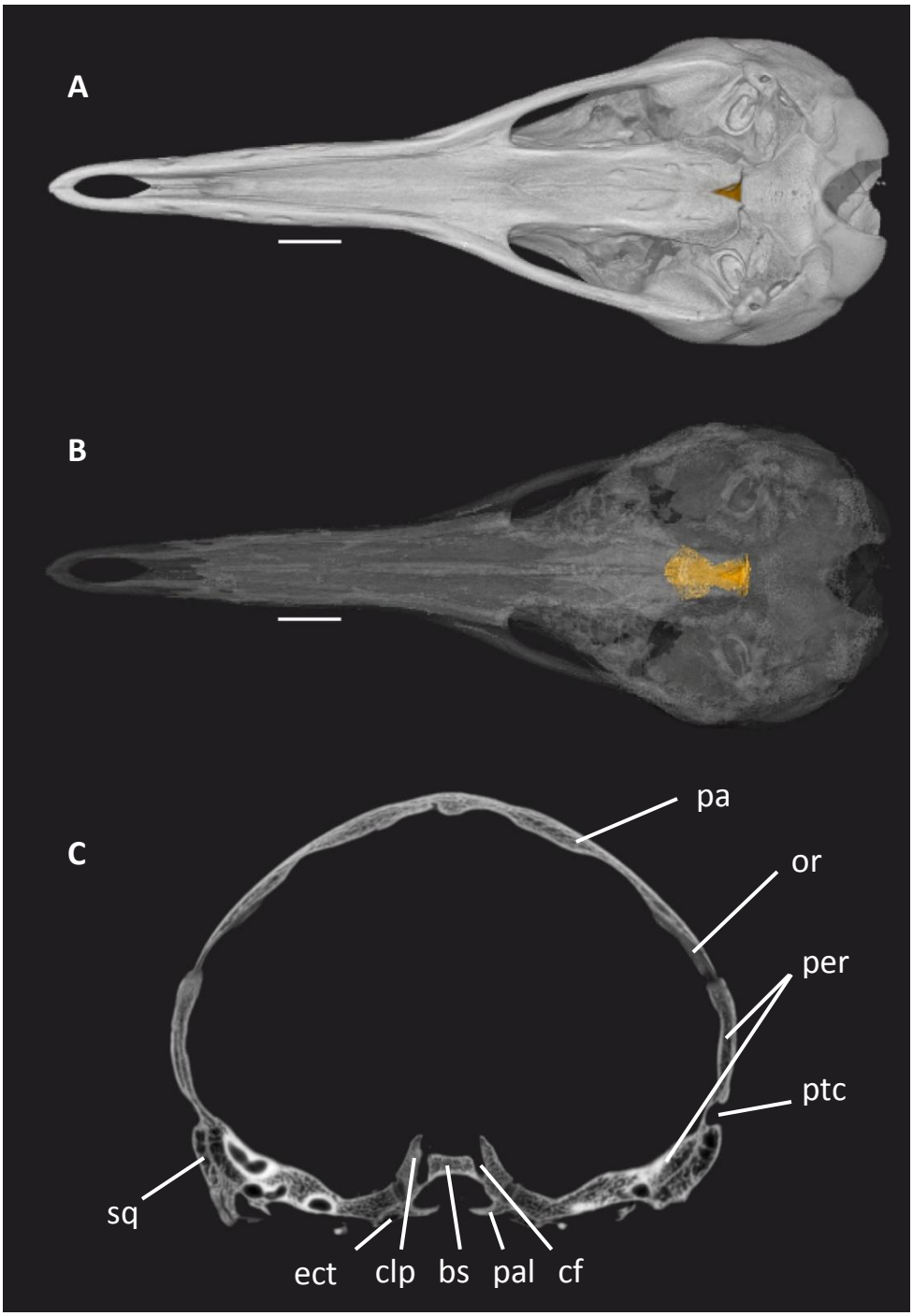

Figure 1.22: Basisphenoid of *Zaglossus bruijnii* MCZ7397 shown in situ (orange) in ventral view (A), with the skull rendered transparent (B), and in cross section (C). For key to abbreviations, see Table 1.3. Scale bar = 10 mm.

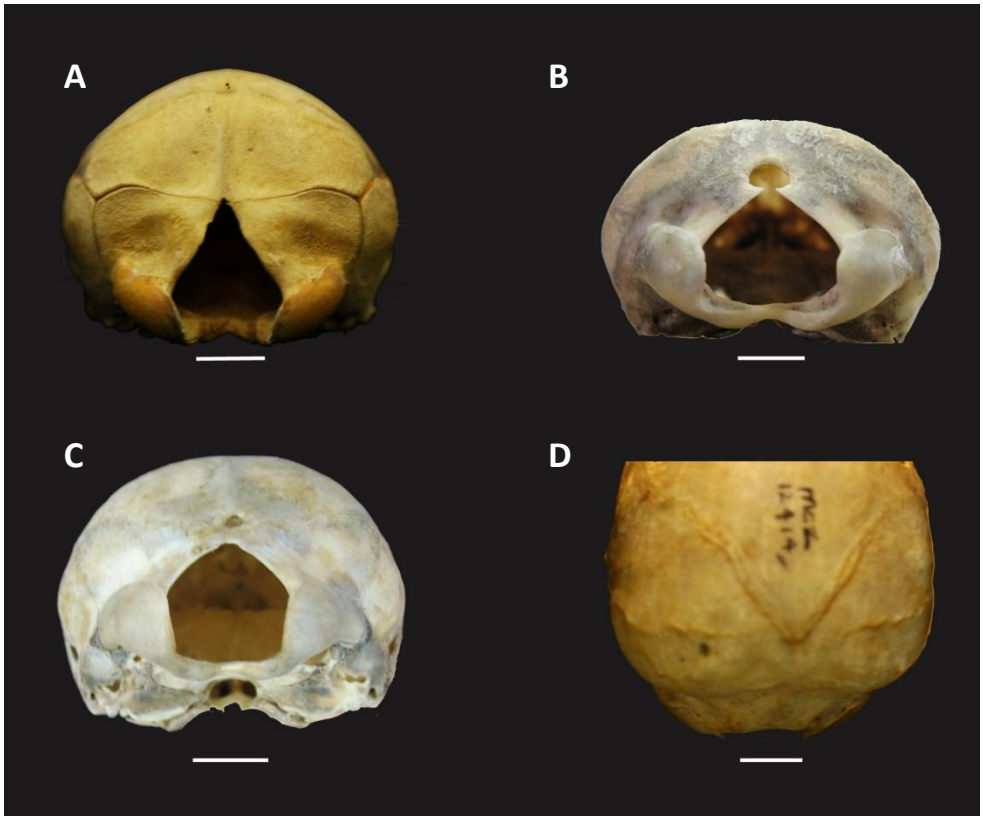

Figure 1.23: Comparison of incisura occipitalis presence and shape in four specimens of *Zaglossus* ranging in skeletal maturity from youngest (A) to oldest (D). Specimens: (A) *Zaglossus bruijnii* MCZ 7397, (B) *Zaglossus bartoni* AMNH 157072, (C) *Zaglossus bartoni* AMNNH 194702, and (D) *Zaglossus bruijnii* MCZ 12414. Scale bars = 1 cm.

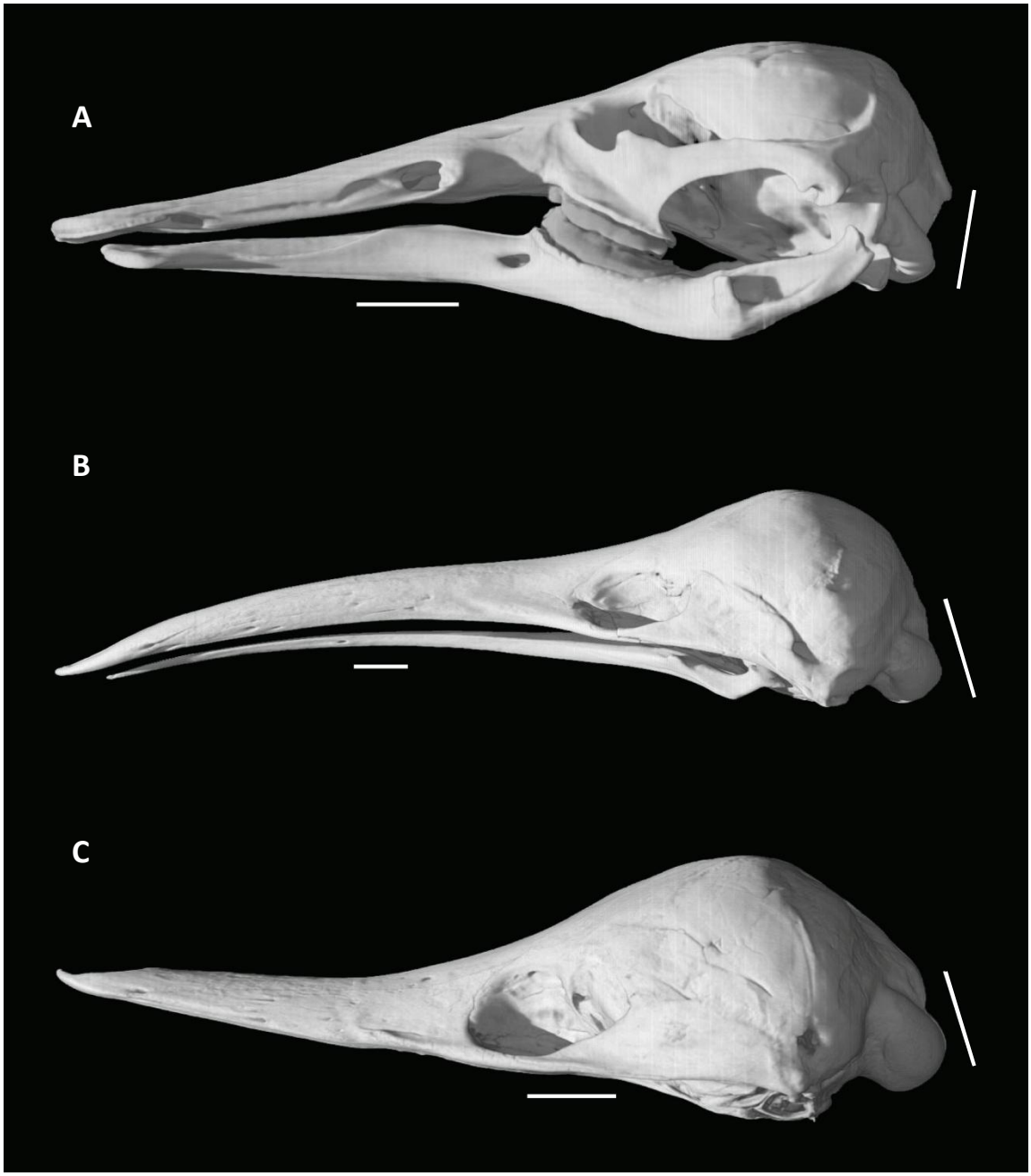

Figure 1.24: Posterior extension of occipital condyles shown in *Ornithorhynchus anatinus* AMNH 200255 (A), *Tachyglossus aculeatus* AMNH 154457 (B), and *Zaglossus bartoni* AMNH 157072 (C). In *Ornithorhynchus*, the occipital condyles are rostral to the occiput whereas in tachyglossids the occipital condyles extend farther caudally. Scale bars = 1 cm.

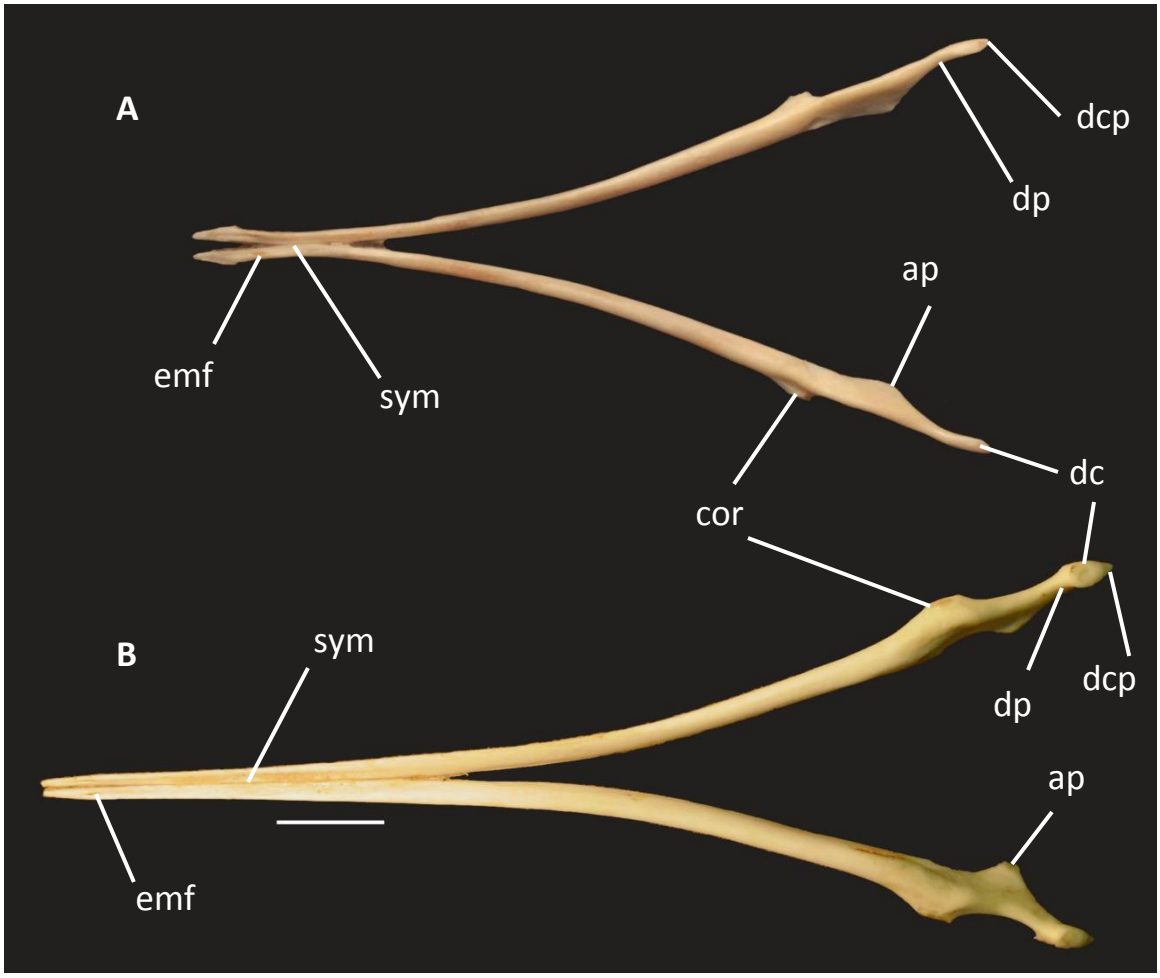

Figure 1.25: Dorsal view of dentaries of *Tachyglossus aculeatus* TMM M-1826 (A) and of *Zaglossus bruijnii* AMNH 197402 (B). The dentaries of *Tachyglossus* are relatively gracile, curve inward, and are free and spatulate in shape at their distal ends. In *Zaglossus*, the proximal end of the dentaries is more robust while the distal ends become very thin. The terminal ends of the dentaries are not as free and spatulate as they are in *Tachyglossus*. Dentaries are shown to scale. Scale bar = 1 cm.

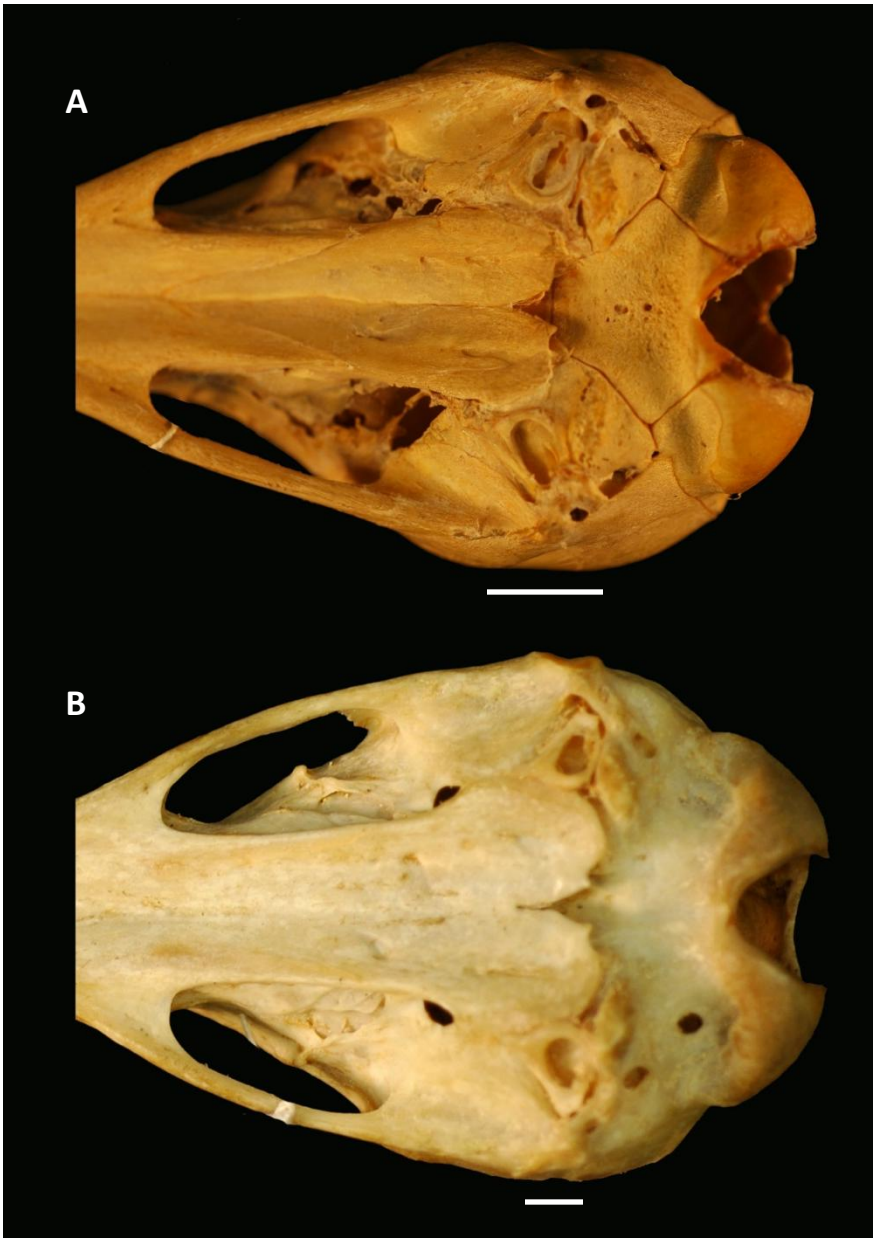

Figure 1.26: Varying degree of ossification and fusion in *Zaglossus*. The skeletally immature skull of *Zaglossus bruijnii* MCZ 7397 (A) is open where the orbitotemoral region is not fully ossified and has visible sutures. In *Zaglossus bruijnii* MCZ 12414 (B), the skull is more thoroughly ossified and sutures are not visible. Scale bars = 1 cm.

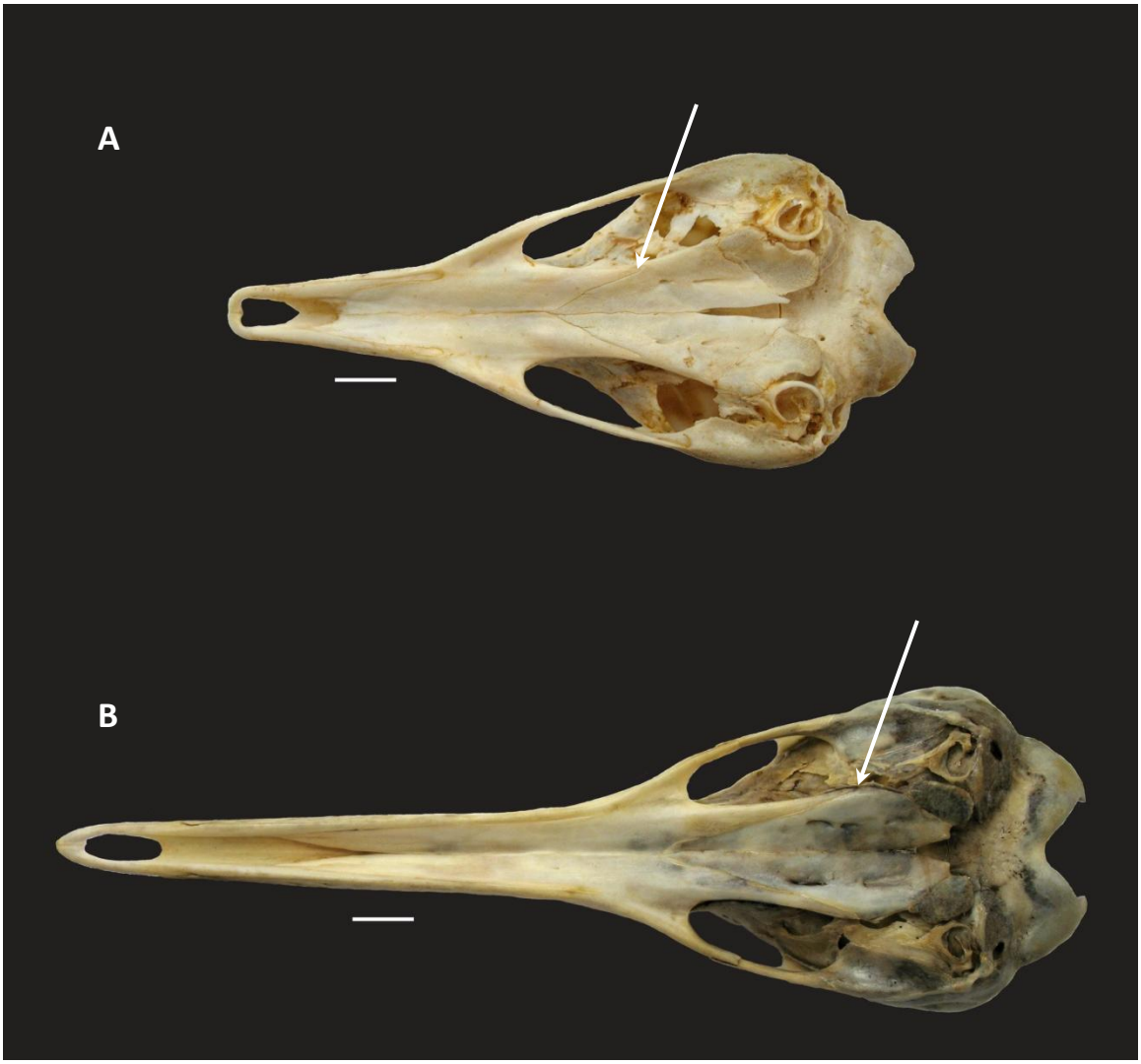

Figure 1.27: Posterior extension of the palatal process of the maxilla in *Tachyglossus aculeatus* AMNH 107185 (A) and *Zaglossus bruijnii* 157072 (B). Terminal end of process is indicated by arrow. Skulls are shown to scale; scale bar = 1 cm.

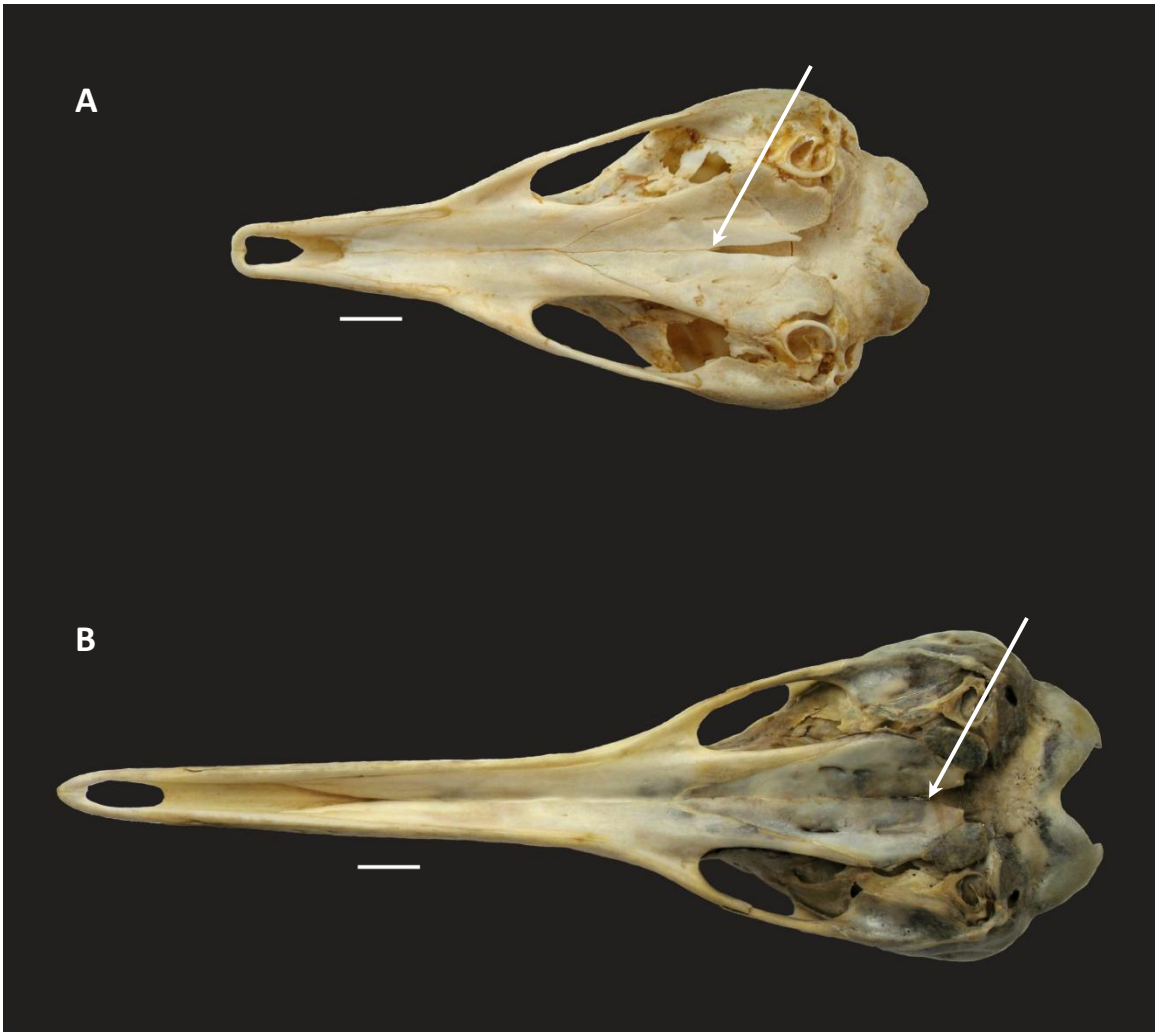

Figure 1.28: The medial palatal incision in *Tachyglossus aculeatus* AMNH 107185 (A) is deeper than the medial palatal incision in *Zaglossus bruijnii* 157072 (B). Anterior-most end of incision is indicated by arrow on both skulls. Skulls are shown to scale; scale bar = 1 cm.

Figure 1.29: Posterior processes of the palatines of *Tachyglossus aculeatus* AMNH 107185 (A) are long and narrow, and in *Zaglossus bruijnii* 157072 (B), the posterior processes of the palatines are short and broad, often not extending further posteriorly than the ectopterygoids. Processes are indicated by arrows on both skulls. Skulls are shown to scale; scale bar = 1 cm.

Chapter 2: Definition, Diagnosis, and Origin of Monotremata and its Major Subclades

INTRODUCTION

In recent decades, most problems and controversies surrounding the origin and evolution of Monotremata revolved around Mesozoic and Paleogene fossils of isolated teeth and jaws recovered at localities in the Southern Hemisphere. Little attention was given to the potential phylogenetic signal preserved in the skull, and even less to the postcranium, of extant monotremes, or to the systematic implications of the few fossil monotremes that are relatively complete. Thanks to advances in the resolution of computed tomography, new data can be extracted from extant monotreme skeletons. In Chapter 1, I studied the skull of *Zaglossus* in detail using that technique. In this chapter, I focus on describing and illustrating cranial and postcranial data that are relevant to the problem of monotreme evolution. This new information was used to conduct a preliminary analysis of relationships among living and putative extinct monotremes in which cranial and/or postcranial evidence is preserved.

The literature on the dentitions of taxa seemingly relevant to this question is quite extensive. It is complicated by two entirely separate vocabularies developed in reference to monotreme dental characters, with little agreement on which terms refer to potentially homologous character states. It was beyond the scope of this thesis to attempt a resolution of this tangled problem. Taxa represented solely by dentitions were not included in the analysis. However, in the interest of systematic completeness, the general controversies

surrounding these taxa are discussed briefly below. In retrospect, this rationale for selecting which taxa to analyze and which to exclude seems justified by the large body of cranial and postcranial data assembled below and by the robust support that cranial and postcranial characters provide to certain nodes of the resulting tree. Perhaps the strength of the phylogenetic results may provide a platform upon which dental characters can be optimized in a future study that attempts to resolve this tenacious problem.

The primary question addressed in this chapter is phylogenetic, and it encompasses the questions of monotreme monophyly, the relationships of extant species of monotremes to each other and to other living mammals, and finally the relationships of fossils of putative crown- and stem-monotreme to the living monotremes. The second question is diagnostic, concerning what osteological characters diagnose Monotremata and its two major subclades, Tachyglossidae and Ornithorhynchidae.

The answers to these questions afford a basis to examine diametrically opposed views regarding the circumstances surrounding the origin of monotremes. Was the ancestral monotreme aquatic, as was recently postulated by Phillips et al. (2009, 2010)? If this hypothesis is true, it implies that the echidna lineage is secondarily terrestrial. Or was the ancestral monotreme a terrestrial thrust-digger? If monotremes had a terrestrial origin, the platypus clade would, therefore, be secondarily aquatic.

In addition to addressing this controversy, the diagnoses of Monotremata and its major subclades presented below enable more rigorous conclusions regarding the

placement of fossils, and more detailed estimations of the ecology of the ancestral monotreme, along with a more nuanced understanding of evolution of its subclades.

Composition

Monotremata comprises five extant species of mammals (Chapter 1, Fig. 1.1) whose geographic distribution is confined to the continent and surrounding islands of Australia (Chapter 1, Fig. 1.2), otherwise known as the 'Greater Australian continent,' or as 'Meganesia' or the 'Sahul' region (Helgen et al., 2012). Each of the living species of monotreme has a complex history of nomenclatural revision that is summarized in Table 1. In the following account, my focus is to introduce the entities currently viewed as valid species of extant Monotremata, using contemporary and widely accepted taxonomic nomenclature.

Living monotremes include *Ornithorhynchus anatinus*, the enigmatic, semiaquatic duck-billed platypus whose distribution is limited to sub-tropical eastern Australia, Tasmania, King Island, and Kangaroo Island (Griffiths, 1978; Grant, 1992; Helgen et al., 2012). *Ornithorhynchus* is the only surviving member of Ornithorhynchidae, a clade that includes at least one and possibly several more named extinct taxa that are discussed below.

The remaining four living monotreme species are all members of Tachyglossidae, the echidnas. The most abundant and best-known of these is the short-beaked echidna *Tachyglossus aculeatus*, which is distributed over a wide range of habitats across much of Australia, Tasmania, and the larger neighboring islands in the Bass Strait, including King

Island, Kangaroo Island, and Flinders Island, and the island of New Guinea (Griffiths, 1968; Helgen et al., 2012). *Tachyglossus aculeatus* is by far the most abundantly represented of all the echidna species in the biological research collections in the US and Europe. One subtle but important consequence is that most of the anatomical knowledge gathered to date on Tachyglossidae is based solely on *Tachyglossus aculeatus* rather than all members of the clade. One aim of this thesis was to mitigate that bias by describing in detail the cranial anatomy of the long-beaked echidna (Chapter 1).

Tachyglossidae also includes three currently recognized species of the long-beaked echidna, *Zaglossus* (Flannery and Groves, 1998). These include *Zaglossus attenboroughi* (possibly now extinct; see Flannery and Groves, 1998: 390), *Zaglossus bartoni*, and *Zaglossus bruijni* (sometimes spelled *bruijnii*). Specimens of *Zaglossus* are rare in biological research collections. Most of the research collections of *Zaglossus* were made early in the 20th century and museum records reflect the taxonomy of that time, which recognized only *Zaglossus bruijni*, regardless of provenance of the specimens.

Today, the species of *Zaglossus* are known only from New Guinea, where they are all rare and difficult to observe. However, *Zaglossus bruijni* may have been a member of the historical fauna of continental Australia, and hopes were recently expressed that it might still be found living in the remote Kimberley district of northern Western Australia (Helgen et al., 2012). That conclusion was based on several observations including a skin with associated skull, mandibles, and distal right forelimb elements collected near Mount Anderson in the West Kimberly region by the Australian naturalist John T. Tunney in

1901. The specimen was collected for the wealthy amateur naturalist Walter Rothschild and placed in his Tring Museum, and later transferred to the Natural History Museum in London. The circumstances surrounding the collections and subsequent handling of the specimen were detailed by Helgen et al. (2012), who personally examined the specimen and confirms its identification as *Zaglossus bruijni*. Additional evidence supporting the existence of *Zaglossus* on the Australian continent in historic times includes Australian ectoparasites from the above-mentioned skin, rock art in the West Kimberly region depicting a long-beaked echidna, and living-memory accounts by aboriginal inhabitants of Kununurra in East Kimberley of long-beaked echidnas in the region. Tunney's tag indicated that the specimen represented a rare species for the region. Given the remoteness of the area, it is conceivable that *Zaglossus* may still live on the continent, or that it was extirpated there during the 20th century (Helgen, et al., 2012).

Based on ongoing field work in New Guinea, Dr. Kristopher Helgen of the U.S. National Museum (pers. comm.) is undertaking detailed molecular, anatomical, and biogeographic analyses of the various surviving populations of *Zaglossus*, and expects his work to lead to further refinements in the species-level taxonomy of *Zaglossus*. Consequently, in this study I record species-level identifications as they appeared on the tags of vouchered museum specimens that I studied, as a means of preserving historical continuity for each specimen, while treating the three nominal species of *Zaglossus* as a clade and doing so without regard to their interrelationship. Given the variation I observed in the specimens of *Zaglossus* used in this analysis, and in light of the

characters scored in my matrix, it seems doubtful that the lack of an alpha-level phylogeny for *Zaglossus* will have any major impact on my larger conclusions. The composition of Monotremata with respect to extinct taxa is the subject of much debate, and this topic is treated separately below (see Materials).

Relationships

Ornithorhynchidae and Tachyglossidae are the two sister lineages that together make up crown Monotremata. In turn, Monotremata is the sister lineage of Theria (i.e., Marsupialia + Placentalia), the lineage that includes the more than 5,000 species that make up the remainder of extant Mammalia (Chapter 1, Fig. 1.1), plus several thousand named extinct species (Rowe, 1988; McKenna and Bell, 1997; Wilson and Reeder, 2005).

This phylogenetic picture, that Monotremata is monophyletic and is the sister taxon of Theria, summarizes what will be referred to as the 'conventional' view of relationships of monotremes. But that conventional view by no means presents a unanimous scientific opinion, because some scientists in recent years argued that one or the other of the two monotreme sister clades is more closely related to, or even nested within, therian mammals (see Kullberge et al., 2008). If true, this would render the conventional Monotremata paraphyletic. As detailed below, my analysis strongly supports the conventional view of the composition and relationships of extant Monotremata. Nevertheless, the conventional view took many years to emerge, and it faced a number of challenges over the last two centuries and even in recent decades. A

brief survey of this convoluted history, involving both taxonomic and conceptual problems, offers an informative context in which to interpret the problems and questions addressed in my analysis.

The first publication on a monotreme was on the short-beaked echidna *Tachyglossus aculeatus* (Shaw, 1792), but it was originally referred to *Myrmecophaga aculeata*, which allied it with the Giant Anteater, a placental mammal. The echidna's close relationship with the duck-billed platypus *Ornithorhynchus anatinus* (then named *Ornithorhynchus paradoxus* Shaw, 1799) was soon realized after Sir Everard Home published dissections on both the platypus (Home, 1802a) and echidna (Home, 1802b)[2]. In the second paper, Home (1802b) named the echidna as a species of *Ornithorhynchus*, *Ornithorhynchus hystrix*, admitting: "When more of this extraordinary tribe of animals, which, although quadrupeds, are not Mammalia, shall have been discovered, and naturalists thereby enabled to divide them properly, the two which I have described will doubtless be arranged under different genera…" (1802b: 361). Not long after Home's publications, monotremes were proposed as a missing link between turtles and mammals (Fitzinger, 1826).

[2] footnote: According to Sir Richard Owen (1861), Everard Home commonly plagiarized the voluminous unpublished papers and dissections of his late mentor and father-in-law, the great 18th century surgeon and anatomist John Hunter (1728-1793). Home reportedly burned many of Hunter's papers, and the Hunterian Museum suffered further loss of records and specimens during the London blitz of WW II. It is possible that John Hunter was the first to dissect and compare a platypus and echidna, and that observations attributed to Home were in fact made by John Hunter. See Owen 1861 for details.

In the pre-cladistic paleontological literature, the lack of robust analytic techniques and the absence of a robust diagnosis for either Mammalia or Monotremata presented a murky picture of the evolution of the two groups. A good deal of attention was devoted to speculation on whether Mammalia was a grade rather than a clade. An entire school of thought, influenced by the great 20th century paleontologist George Gaylord Simpson, favored the view that Mammalia was a grade instead of a clade (e.g., Simpson, 1971). Within that school there was a protracted argument over which 'defining' characteristic was most apt or essential (see historical summaries by Rowe, 1987, 1988; Rowe and Gauthier, 1992). In the context of such arguments, and in an intellectual climate that presumed extremely slow rates of morphological evolution, it seemed reasonable that therians and monotremes might have independently evolved mammalian-grade characteristics from a non-mammalian common ancestor among extinct Permian-Triassic Therapsida, or an even deeper ancestor among Carboniferous-Permian stem-synapsids (e.g., Olson, 1944; Young, 1962; MacIntyre, 1967; Parrington, 1974; Crompton and Jenkins, 1979; Carroll, 1988 fig. 18-14).

Those opinions and arguments notwithstanding, a broad majority of post-Darwinian mammalogists considered monotremes and therians to form the most fundamental division within Mammalia and that the two lineages shared a common ancestor which was itself a mammal (e.g., Flower and Lydekker, 1891; Haeckel 1897; see historical reviews in Gregory 1910, 1947; Rowe 1986; Rowe and Gauthier, 1992; de

Quieiroz, 1994; McKenna and Bell, 1997). But that conclusion begs the question of how the various fossils of purported relevance are related to living species of monotremes.

Of the authors cited above, one stands out in his life-long interest and focus on the importance of monotremes to understanding mammalian evolution in general. This is William King Gregory (1876-1970), who indisputably stands among the greatest paleontologists of the 20th century. Over the course of his career, he aimed explicitly at the question of monotreme monophyly and was virtually alone in including first-hand observation of all three nominal monotreme genera in his comparative studies over the entire course of a long career that played out entirely before the rise of cladistic principles (Gregory, 1910, 1947). *Zaglossus* held the name '*Proechidna*' in Gregory's early masterpiece, *The Orders of Mammals* (Gregory, 1910). Gregory's last scientific monograph, *The Monotremes and the Palimpsest Theory* (Gregory, 1947), included a lengthy discussion regarding the diagnostic osteological features of monotremes, and as will be seen, many of his diagnostic features were corroborated as apomorphies of Monotremata by my analysis. However, Gregory came to the odd conclusion that monotremes were secondarily primitive in many of the features that united them, including such seemingly profound characters as ovipary. Although Gregory found that *Ornithorhynchus* and tachyglossids clustered together, he posited that monotremes were the closest relatives of Marsupialia, and together monotremes and marsupials constituted the taxon 'Marsupionta.' In turn, Marsupionta was the sister taxon to Placentalia. That hypothesis became known as the 'Marsupionta hypothesis.' Only a few morphologists

ever endorsed the idea (e.g., Kühne, 1973, 1974), and it was rejected by an overwhelming majority in the paleontological community on a variety of grounds (e.g., Parrington, 1974; Rowe, 1988; McKenna and Bell, 1997); the name soon disappeared from the systematic literature.

In the following decades, the early emergence of molecular systematics surprised morphologists with the finding that either *Tachyglossus* or *Ornithorhynchus* was phylogenetically nested within, or was sister taxon to, Marsupialia. Evidence came from sequence analyses of 18s rRNA (Janke et al., 2002), and both mitochondrial DNA (Janke et al., 1996, 1997; Penny and Hasegawa, 1997; Zardoya and Meyer, 1998; Kumanzawa and Nishida, 1999; Penny et al., 1999; Nilsson et al., 2004) and nuclear genes (Kirsch and Mayer, 1998; Vernesson et al. 2002; Nowack et al., 2004). To the consternation of morphologists, that work either resurrected the Marsupionta hypothesis and/or implied that Monotremata was paraphyletic. If either finding were true, it would radically alter the most basic framework in which mammalian history has been interpreted since before the start of Gregory's career.

More recent work showed that these early molecular results suffered a sampling bias that led to the mistaken splitting of monotremes (Rowe et al., 2008). When both the platypus and an echidna were sampled simultaneously, the two taxa inevitably clustered as sister taxa (Toyasawa et al. 1998; Phillips and Penny, 2003; Reyes et al., 2004; van Rheede et al., 2006; Bininda-Emonds et al., 2007). However, even some of those analyses recovered the Marsupionta hypothesis (Toyasawa et al., 1998; Janke et al., 2002;

Phillips and Penny, 2003), or were equivocal in placement of monotremes with respect to the therian clades (Reyes et al., 2004). Thus, the relationship of living monotremes to other living mammals remains in question.

The Monophyly of Monotremata

Living monotremes were regarded as a natural group of some sort by many naturalists for the last two centuries (e.g., Home, 1802b; Gregory, 1910, 1947; Burrell, 1927; Griffiths, 1968, 1978; Rowe, 1988; McKenna and Bell, 1997; Kielan-Jaworowska et al., 2004). However, many authors noted that historically, the rationale for recognizing Monotremata as a natural group is problematic (e.g., Griffiths, 1978; Rowe, 1988; Gauthier et al., 1988; Musser, 2003; Rowe, in press-a). For example, the retention of plesiomorphic features in the monotremes such as egg-laying (ovipary) and plesiomorphic skeletal features such as the interclavicle, procoracoid, and epipubis were used as evidence for their close relationship. Another problematic rationale for the monophyly of Monotremata is that monotremes lack diagnostic therian autapomorphies such as nipples, vibrissae and a rhinarium, or epiphyses on the vertebral centra. From today's cladistics perspective, neither rationale presents a valid defense of monotreme monophyly. Additional circumstantial evidence, such as their biogeographic restriction to the continent and surrounding islands of Australia (Meganesia), has been cited in support of their 'naturalness' (e.g., Flower and Lydekker, 1891: 117) but invokes circular reasoning in defense of monophyly (e.g., Bever, 2005; Bell et al., 2010).

To put it another way, a major ambiguity plaguing a clear understanding of monotreme history is the lack of rigorous, phylogenetic diagnoses (Rowe, 1987) of Monotremata, and of the clades within it, based on shared derived features. Without such diagnoses, it is difficult or impossible to identify with rigor fossils that lie within the monotreme crown or along its stem. If one follows the growing popularity of apomorphy-based identifications in the taxonomic allocation of fossils (e.g., Gauthier et al., 1988; Rowe, 1988; Bever, 2005; Bell, et al. 2010), then the monophyly of Monotremata should not be taken for granted. At first glance, moreover, the platypus and echidnas can seem outwardly as different from each other as each is from any living therian mammal (Rowe et al., 2008). Ambiguity in phylogenetic placement of fossils cascades to an ambiguous divergence time for the monotremes from other mammals, and between clades within Monotremata. Accordingly, rate-related evolutionary properties of monotremes, their historical biogeography and its calibration, and other fundamental questions about their origin and subsequent evolution are matters of debate (Rowe, 1987, 1988; Rowe et al., 2008; Phillips et al., 2009, 2010; Camen, 2010).

To date, a number of authors of widely scattered studies on disparate anatomical systems anecdotally mentioned shared derived characters that collectively present a robust defense of monotreme monophyly. The following list was assembled from a search of recent literature and is presented to offer some measure of the confidence that one can place in monotreme monophyly; undoubtedly this list is incomplete. Osteological features are noted here in general terms only; these are described elsewhere in greater

detail and in many cases were parsed into individual characters for the taxon/character matrix used in my phylogenetic analysis. The monophyly of Monotremata, as defined as a node-based crown-clade (see **Taxonomic Conventions**, below) is potentially supported by the following:

1) Unique cranial developmental patterns (Kuhn, 1971; Kuhn and Zeller, 1987; Zeller, 1989).
2) Unique skeletal ossification sequences (Weisbecker, 2011; Werneburg and Sánchez-Villagra, 2011)
3) Numerous features of mature cranial anatomy (Gregory, 1910, 1947; Rowe, 1986, 1988)
4) A unique pattern of facial musculature and its pathway of embryological differentiation (Huber, 1930a, b; Lightoller, 1942)
5) Unique mandibular depressor musculature (Edgeworth, 1935; Rowe, 1986)
6) A unique skeletomuscular basis for behaviors involving feeding and locomotion (Winge, 1941)
7) The timing and sequence of events in brain development (Ashwell, 2012)
8) Distinct developmental pathways and mature sensory neurons associated with pressure reception in and around the oral cavity (Ashwell et al., 2012)
9) The possession of electroreception mediated by the trigeminal nerve (Proske et al., 1998)

10) Unique functional and developmental aspects of electroreception (Proske et al., 1998)

11) Unique architecture of the forebrain (Macrini et al., 2006; Rowe et al., 2011).

12) In the cytoarchitecture of the olfactory bulb, with presumptive projection cell somata spread throughout the external plexiform layer (Switzer and Johnson, 1977; Ashwell, 2006a, b)

13) The possession of approximately 180 miRNAs unique to platypus and echidna (Murchison et al., 2008).

14) Multiple sex chromosomes: male karyotype with an X1Y1X2Y2X3Y3X4Y4X5Y5 sex chromosome constitution (Grutzner et al., 2004; Rens et al., 2004).

15) Unique duplications of the beta-casein genes, which are tied to lactation (Lefèvre et al., 2009).

This survey summarizes the development and anatomy of the soft-tissues that support the conventional view of a monophyletic Monotremata, with *Ornithorhynchus* and extant echidnas being more closely related to each other than either is to therian mammals. A detailed osteological diagnosis is still needed in order to assess the placement of fossils and to calibrate the tree. The persistent inconsistencies seen in molecular-based phylogenies of monotremes and the other major clades of mammals further underscore the necessity for this analysis.

Taxonomic Conventions

In reviewing the literature, as noted above, it is apparent that many previous authors employed the term 'Monotremata' using observations from either *Ornithorhynchus* or *Tachyglossus*, but not both. In effect, the nomenclature was overextended, further complicating an already complicated phylogenetic situation. This underscores the importance of setting out an explicit nomenclatural framework.

In general, I tried to follow the general principles of phylogenetic nomenclature (e.g., Rowe 1987, 1988; Rowe and Gauthier, 1992; de Queiroz, 1994, 2007; de Queiroz and Gauthier, 1992, 1994; Gautheir et al., 1988a, b; ICPN, 2010). Among those principles is a recommended application of widely-known names with deep historic inertia to crown clades. The following definitions set out the meanings of names used in discussing the results of my analysis.

1) Tachyglossidae (Gill, 1872): this is a node-based crown clade designated by the last common ancestor of *Tachyglossus aculeatus* and *Zaglossus bruijni*, and all of its descendants.

2) Ornithorhynchidae (Gray, 1825): This is a node-based clade designated by the last common ancestor of the extant *Ornithorhynchus anatinus* and the extinct *Obdurodon dicksoni*, and all its descendants. In my analysis, the Early Cretaceous fossil *Steropodon galmani*, known from a single opalized mandible with only three teeth preserved, forms an unresolved polytomy with *Obdurodon* and *Ornithorhynchus*. This polytomy is probably a result of missing data because the position of *Steropodon* proved highly labile

in various data partitioning tests run during the course of this analysis. Consequently *Steropodon* is not a specifier in defining the name Ornithorhynchidae.

3) Monotremata (Bonaparte, 1827; converted clade name, Rowe, 1986): a node-based crown clade comprising the last common ancestor of *Orntihorhynchus anatinus* and *Tachyglossus aculeatus*, and all its descendants. Synonyms: Monotrémes Geoffrey 1803; Monotremia Rafinesque, 1815 (cited by Gill, 1903).

4) Theria (Parker and Haswell, 1897; converted clade name, Rowe, 1986): a node-based crown clade comprising the last common ancestor of Placentalia and Marsupialia, and all its descendants. This term has been used variably in the last century to include a range of extinct taxa that now are known with reasonable certainty to lie on the therian stem, or even outside of Mammalia altogether (Rowe, 1993).

5) Mammalia (Linnaeus 1758; converted clade name, see Rowe, 1986, 1987, 1988, 1993, in press-a; Rowe and Gauthier, 1992): a node-based crown clade designated by the last common ancestor of monotremes and therians, and all its descendants. This follows the most common meaning and intention of the name as employed by virtually all mammalogists and by paleontologists working within the phylogenetic system (e.g., Donoghue, et al., 1989; Rowe, 1986, 1987, 1988, 1993; in press-a; Gauthier et al., 1988; Rowe and Gauthier, 1992; de Queiroz, 1994; de Queiroz and Gauthier, 1992, 1994; Mckenna and Bell, 1997). Restricting this name to the crown clade is not a unanimous practice even in today's literature (e.g., Kielan Jaworowska et al., 2004; Luo et al., 2001). Those making exceptions are all paleontologists who prefer to include members of the

mammalian stem as well as the crown under the *nomen* 'Mammalia.' Ironically, although all recognize that monotremes and therians share a common ancestor and constitute a node-based clade, never has an alternative name for that node been suggested (Rowe and Gauthier, 1992).

I also adopt the more controversial convention of attaching the prefix Pan- when using names that include both crown clades and their extinct stem-members (e.g., Rowe, 2004, in press-b). The prefix 'Pan-' means 'all' or 'the whole,' and the pan-clade name is a new convention that designates a converted clade name plus its total branch (*ICPN* Art 10.3; see de Queiroz, 2007).

6) Pan-Mammalia (Rowe, 2004, in press-b): Pan-Mammalia is the total-clade that includes *Homo sapiens* Linnaeus, 1758 (Mammalia) plus all extinct taxa more closely related to *Homo sapiens* than to *Vultur gryphus* Linnaeus, 1758 (Archosauria), *Iguana iguana* Linnaeus, 1758 (Lepidosauromorpha), or *Testudo graeca* Linnaeus, 1758 (Testudines). This is a stem-based name that designates a total branch (de Queiroz, 2007).

There are several approximate synonyms for Pan-Mammalia. These include 'Theromorpha' Cope, 1878 [approximate]; 'Synapsida' Osborn, 1903a [approximate; but see Rowe, 1986; Gauthier et al., 1988a; Donoghue et al., 1989]; 'Theropsida' Goodrich, 1916.

Of these, Synapsida is the most popular approximate synonym in modern parlance. Pan-Mammalia differs from Synapsida in being based on extant specifiers, principally *Homo sapiens* Linnaeus, 1758 (Placentalia, Theria), along with *Didelphis*

marsupialis Linnaeus, 1758 (Marsupialia, Theria), and *Tachyglossus aculeatus* (Shaw, 1792; Monotremata) for the crown. Both the name Pan-Mammalia and its modern specifiers bring a sharper focus on the evolutionary connotation of the name with respect to our own species and to the evolutionary history of the clade Mammalia.

It is worth noting that both names are applicable because they are defined differently. Pan-Mammalia designates the total-clade, whereas Synapsida is an apomorphy-based name in reference to those pan-mammals that possess the lower temporal arch beneath the infratemporal fenestra (Laurin and Reisz, in press). Historically, the name Synapsida was mostly used only among paleontologists, and at present the known contents of Synapsida and Pan-Mammalia are identical. However, it is possible that members of Pan-Mammalia will eventually be uncovered which possess characters that place them at the base of the stem, and yet lack the single diagnostic apomorphy of Synapsida. Designating Synapsida as an apomorphy-based name enables a continued debate among the paleontologists over what is or is not a synapsid, without obscuring the meaning of Pan-Mammalia to the far broader audience of non-specialists who are interested in mammalian evolution.

7) Pan-Theria (= Theriimorpha, Rowe 1993): a stem-based name that includes Theria and all extinct taxa closer to Theria than to Monotremata. Pan-Theria is synonymous with Theriimorpha, which was explicitly defined as a stem-based name for the total therian clade (Rowe, 1993), coined before the Pan- prefix was suggested as a

convention to simplify phylogenetic nomenclature. For the sake of consistency and clarity, I accede to the convention and use the term Pan-Theria throughout.

Both Placentalia and Marsupialia as used here represent crown clades. The terms Eutheria and Metatheria are sometimes used interchangeably with Placentalia and Marsupialia, respectively. However, to carry the Pan- convention to its fullest, I prefer Pan-Placentalia and Pan-Marsupialia for the total branch names. Eutheria, then, is defined herein as a node-based name that includes the last common ancestor of Placentalia and the early Cretaceous *Eomaia scansoria* (Ji et al., 2002), plus all of its descendants. The name Metatheria is defined as a node-based name that includes the last common ancestor shared by Marsupialia and *Sinodelphys szalayi* (Luo et al., 2003), and all its descendants.

8) Pan-Monotremata (total-clade name): a stem-based name that includes crown Monotremata and all taxa closer to monotremes than to Theria. In the older literature, the term Prototheria was used to include monotremes and fossils hypothesized to be closer to monotremes than to therians. However, that conception of Prototheria proved paraphyletic in virtually all phylogenetic analyses and was abandoned. More recently Australosphenida (Luo et al., 2001) was coined in reference to Monotremata and fossils branching from the monotreme stem. That name was never clearly defined, however, as either a node-based or stem-based name, and in my analysis it is paraphyletic, with some members on the monotreme stem and others on the therian stem. Pan-Monotremata is treated as a total-clade name.

A phylogenetic definition and diagnosis of Monotremata and its major subclades is necessary to interpret the relationships of extinct monotremes to extant monotremes, and to understand the natural history of platypuses and echidnas, and their part in the evolution of mammals. To provide a phylogenetic definition of Monotremata, Tachyglossidae, and Ornithorhynchidae, I ran a parsimony analysis using a previously published morphological character matrix of mammals. For the analysis, I increased the diversity of Monotremata with the addition of three new taxa to the matrix. Those new taxa include the long-beaked echidna, *Zaglossus*, the extinct echidna, *Megalibgwilia*, and the extinct, putative monotreme, *Kryoryctes*. The matrix utilized in this study was written to resolve therian relationships; therefore, some taxa were removed before analysis. The reasoning for the inclusion and exclusion of specific taxa is explained in detail in the **Taxonomic Sampling** section, below. New monotreme characters were also added to the matrix. These characters were written based on comparisons made between extinct and extant monotremes, therians, and their extinct relatives observed in person in museum collections, digitally on DigiMorph.org, or from the literature. A diagnosis for Monotremata and its major subclades was written based on the distribution of synapomorphies resulting from the phylogenetic analysis.

Institutional Abbreviations

AMNH	American Museum of Natural History, New York City, New York
IVPP	Institute of Vertebrate Paleontology and Paleoanthropology, Beijing, China

LACM	Los Angeles County Museum of Natural History, Los Angeles, California
MACN	Museo de Ciencias Naturales, Universidad Nacional de San Juan, Argentina
MAE	Mongolian Academy of Sciences, Ulaanbaatar, Mongolia
MCZ	Museum of Comparative Zoology, Harvard University, Cambridge, Massachusetts
PVSJ	Universidad Nacional de San Juan, San Juan, Argentina
QM	Queensland Museum, South Brisbane, Queensland, Australia
TMM	Vertebrate Paleontology Laboratory, Jackson School of Geosciences, The University of Texas at Austin, Austin, Texas

TAXONOMIC SAMPLING

This section is a narrative of the history of discovery of putative extinct monotremes that is intended to describe both the nature of the fossil record and some of the controversies that have surrounded analysis of these specimens. With this narrative I also attempt to set a context for the selection of taxa used in the analysis. Following the narrative is a list of the specimens that were studied in this analysis.

Fossil Record of Monotremata

Extinct monotremes known from fossils (Appendix 1.B) are either posited to be within the monotreme crown (i.e., fossils sharing the last common ancestor of living *Ornithorhynchus* and *Tachyglossus*), or to be putative members of the monotreme stem

that lie outside the monotreme crown (i.e., members of Pan-Monotremata; see **Taxonomic Conventions**, above). Several fossils have been assigned to both categories by different authors, and determining to which category each of the extinct taxa belongs is one of the goals of my phylogenetic analysis.

The fossil record of therian (and stem-therian) mammals extends from the mid-Jurassic through the Quaternary, and is preserved over broad swaths of global geography. In stark contrast, the fossil record of putative monotremes is quite sparse and confined to only a few Gondwanan localities dating no earlier than the Early Cretaceous.

Throughout the 19th and most of the 20th centuries, monotremes presented paleontologists with an especially tenacious problem, one similar to that presented by turtles. Most or all of the known fossils are highly derived, and they all bear obvious resemblance to their living relatives. This effectively disguised the more distant roots of Monotremata and its constituent clades and, moreover, most fossils were all of Neogene age and were discovered within or close to the biogeographic range of their living relatives. Accordingly, although their allocation to crown-Monotremata was relatively simple, these fossils offered few tangible clues as to the deeper ancestry of Monotremata, or to the ancestral monotreme condition. The living species were separated from their common ancestor by long ghost lineages (Norell, 1992) and monotreme origins remained mysterious (e.g., Musser, 2003, 2005: 378).

Older fossils from Paleogene and Mesozoic localities were eventually discovered in Australia, Argentina, and Madagascar. Unfortunately, those specimens were

fragmentary, and seemed to lack the obvious apomorphic specializations of the living echidnas and platypus. And each one proved controversial with respect to its phylogenetic position. Some were placed along the monotreme stem and even within its crown. But owing to their fragmentary nature, relatively few characters are available to provide robust support for any of the proposed trees. The analysis presented here not only tests the affinities of these controversial fossils, but also examines the robustness of some of the characters upon which previous analyses were based.

Crown-Monotreme Fossils - Putative Echidnas

The majority of fossils of monotremes is from Neogene deposits of Australia, and show close anatomical resemblance to their living relatives. The first monotreme fossil reported was the humerus of a large Pleistocene echidna from fluvial deposits in Darling Downs, Queensland (Krefft, 1868). Since then, more than eighty fossil specimens of large echidnas have been accessioned in museums in Australia, and it is likely that many additional fragmentary specimens now lie unrecognized in unsorted bulk matrix collected from Australian cave deposits (Murray, 1978). Of the specimens represented by cranial remains, most have long beaks and were subsequently referred to *Zaglossus*. Several new species were named from more or less complete cranial material (Appendix 1.B), but it is beyond the scope of the present work to untangle their taxonomy and systematics beyond the achievements of Murray (1978). However, four exceptionally well-preserved skulls from Naracoorte, South Australia were distinguished under the new generic designation *Megalibgwilia ramsayi* Owen, 1884 (Griffiths et al., 1991). The specific epithet

‘*ramsayi’* is entrenched in subsequent literature, but as Helgen et al. (2012) observed, *Megalibgwilia ramsayi* is a junior synonym of *Megalibgwilia owenii* (Krefft, 1868), and that specific epithet will be recognized here. Photographs and anatomical evidence provided by Griffiths et al. (1991) support their conclusion that *Megalibgwilia* is unequivocally distinguishable from all known species of *Zaglossus*, and according to Helgen et al. (2012) *Megalibgwilia* is now recognized in the Pleistocene cave deposits of New South Wales (Wellington Cave), South Australia (Naracoorete), Tasmania (Montagu Caves and King Island), and south-western Western Australia (Tight Entrance Cave). On this basis, *Megalibgwilia owenii* was treated in my phylogenetic analysis as a third nominal echidna clade, in addition to *Zaglossus* and *Tachyglossus*. As detailed below, *Megalibgwilia* was found to lie just outside of crown Tachyglossidae as a stem echidna.

Most of the remaining monotreme fossils (Appendix 1.B) found in Australia in the 19th and early 20th centuries came from Neogene cave deposits that are probably zooarcheological sites (e.g., Owen 1884; Murray, 1978; Musser, 2003; Helgen, 2012). From the moment of their discovery, they were quite obviously allied to the living echidnas and this conclusion was embraced by all subsequent workers. The oldest unquestionable echidna material is from a Miocene locality near Gulgong, New South Wales, a deep lead gold mine that is now collapsed (Murray, 1978; Musser, 2003). It consists of a partial long-snouted skull with an associated humerus that is attributed to *Zaglossus robusta.* The locality was initially thought to be Pleistocene age (Murray,

1978), but more recent dates show it to be middle Miocene (14-13 Mya; Woodburne et al., 1985; Griffiths et al., 1991). In the following decades, a number of other fossils referable to Tachyglossidae were recovered from Australian deposits (Appendix 1.B).

Previous researchers recognized that the fossil echidnas attested to a larger range of sizes than is seen today, but the material provided little information on what more ancestral monotremes might have looked like, or on the circumstances surrounding monotreme origin and diversification. Viewed in the context of a broader phylogenetic analysis of Monotremata presented below, however, it is evident that these fossil echidnas afford important new information not only on tachyglossid evolution, but on the origin of Monotremata itself.

Putative Platypus Fossils

The fossil record for the extinct relatives of the modern platypus is even less complete than that of the echidnas, and took much longer to discover and recognize these fossils for what they are, or might be. On the face of it, this is surprising given that the semi-aquatic platypus lives in riparian habitats that often preserve a rich record of their inhabitants (Weigelt, 1927/1989). Perhaps it is the long tectonic dormancy of the continent of Australia that has preserved only a paucity of Cenozoic fossil localities compared with what one might expect for so large an area (Flannery, 1990; Long et al., 2002).

The first real breakthrough was not until 1971-1972, with the discovery and identification by Michael O. Woodburne and Richard Tedford of two isolated platypus

teeth from Oligocene-Miocene sediments of South Australia. What would become the holotype of *Obdurodon insignis* was recovered in 1972 by screen washing sands of the Etadunna Formation in the locality known as SAM quarry North, near Lake Palankarinna, Etadunna Station, South Australia (Woodburne and Tedford, 1975). The paratype (AMNH 97228) had been collected earlier, in 1971, from the locality known as South Prospect B, Namba Formation, Lake Namba, Frome Downs Station, South Australia (Woodburne and Tedford, 1975). These two teeth were the basis for naming *Obdurodon insignis* (Woodburne and Tedford, 1975), and their preliminary referral to the platypus lineage was soon confirmed by additional data. This included the discovery of beautifully preserved dentary fragments and a partial ilium at the *Obdurodon insignis* type locality which displayed striking and extremely detailed resemblances to the same elements in extant *Ornithorhynchus* (Archer et al., 1978; see also Pascal et al., 1992a). Then came the spectacular discovery of a virtually complete skull and associated teeth and jaw fragments of a second extinct platypus, *Obdurodon dicksoni*, from mid-Miocene freshwater carbonate deposits near Riversleigh Station, northwestern Queensland (Archer et al., 1992). Its broad, flattened bill and bulbous cranium are remarkably similar to the recent *Ornithorhynchus* (Flannery et al., 1995; Musser and Archer, 1998; Musser, 2003).

Additional material of *Obdurodon dicksoni* was later recovered at Riversleigh Station. Most notable was a dentary that extended the unique resemblances between *Obdurodon* and *Ornithorhynchus* to encompass many features of the mandible. This new material further supported the possession of an enlarged dentary canal as a feature unique

to the platypus lineage (Musser and Archer, 1998). Although the resemblances of the dentaries in the two taxa are unmistakable, *Obdurodon* was found to be plesiomorphic in retaining relatively larger coronoid and angular processes, presumably from how it chewed relating to the retention of fully mineralized teeth. More recently, the application of computed tomography to the skull of *Obdurodon dicksoni* enabled digital endocasts of the endocranial cavity to be generated, and these show further apomorphic resemblances shared by *Obdurodon* and *Ornithorhynchus* (Macrini et al., 2006).

The *Obdurodon* specimens clarified three important aspects of monotreme history. First, they established a minimum age for the divergence of *Ornithorhynchus* from Tachyglossidae as being prior to 22.4 $\pm$ 0.05 Ma (Archer et al., 1985). Second, the teeth of *Obdurodon* are fully mineralized with dentine and prismatic enamel crowns, and with several short roots (Lester and Archer, 1986), which set to rest earlier speculation on whether the monotremes had evolved from edentulous ancestors. The relatedness of platypuses and echidnas have often been defended based on a reduced, absent, or lost dentition in adults (e.g., Flower and Lydekker, 1891; Greene, 1937; Romer, 1966; Kemp, 2005). In hindsight it seems odd that the question could arise of whether the ancestors of monotremes had teeth. The hatchlings of *Ornithorhynchus* have three molariform cheek teeth that are fully mineralized with dentine and a prismatic enamel crown (Poulton, 1888; Lester and Boyde, 1986). These are shed early and replaced by keratinous structures that are not mineralized. These structures have been termed ‘horny plates’ or ‘cornules’ and debate as to whether they deserve to be called teeth has continued since

their first description (e.g., Home 1802a; Huxley, 1878; Poulton, 1888; Thomas, 1889; Davit-Béal et al., 2009). Additionally, the egg tooth is present in both *Ornithorhynchus* and echidnas, in which it is mineralized with dentine and has an enamel cap (Hill and de Beer, 1949). Nevertheless, during a time when paleontologists questioned whether monotremes and therians evolved to a mammalian grade independently from Paleozoic ancestors, the possibility of an edentulous monotreme ancestor seemed credible. The discovery of *Obdurodon* refocused debate on what type of dentition the ancestral monotreme might have had (Woodburne, 2003). Additionally, *Obdurodon* showed that a modest diversification of semiaquatic platypuses had occurred in the middle Cenozoic, and that members of the lineage have been hunting fresh-water prey for more than 20 million years (Flannery, et al., 1995; Rowe, et al., 2008).

Another major discovery was Australia's fist Mesozoic mammal, *Steropodon galmani* (Archer et al., 1985), from Early Cretaceous sediments of Lightning Ridge, New South Wales. It was recovered from the Wallangulla Sandstone Member of the Griman Creek Formation, and its age was initially estimated to be more than 85 Ma (Archer et al. 1985). Subsequent researchers dated this unit to middle Albian, at 112.99 Ma (Flannery et al., 1995). The type and only published specimen of *Steropodon* is an opalized right dentary fragment holding three molariform teeth (generally referred to as m1- m3) which superficially resemble the molariform teeth of *Obdurodon*. Also visible is a greatly expanded mandibular canal, a feature unique to the platypus among living mammals which suggested that *Steropodon* had a bill equipped with electroreceptors and that it

hunted in the fresh waters of Australia as its only living relative does today (Archer et al. 1985; Flannery et al., 1995; Rowe et al., 2008).

Unlike *Obdurodon*, whose completeness leaves little doubt that it is a platypus, *Steropodon* is so incomplete that its placement has remained controversial. It was initially said to be an "ornithorhynchid-like monotreme" (Archer et al., 1985: 363) based on the resemblances of its molariform teeth with those of *Obdurodon*: "Its anteroposteriorly very compressed trigonid, absence of a paraconid on m1, high transverse loph-like trigonid and talonoid crests, very large talonid, lack of a hypoconulid, and prominent anterior, posterior and buccal cingula are distinctive features that in combination also occur only in the isolated lower molars of the middle Miocene monotreme *Obdurodon insignis*" (Archer et al., 1985: 364-365). The distinction between crown-monotremes and stem-monotremes had yet to be made at that time, and the primary question asked of *Steropodon* initially regarded its implications for the more general relationships of monotremes to other mammals.

Subsequently, in the taxonomic style of the time, uncertainty surrounding the relationships of *Steropodon* was recognized by ranking this isolated jaw fragment as "Family Steropodontidae" (Flannery, et al., 1995: 419). Further, *Steropodon* has a large mandibular canal which resembles the condition in *Obdurodon* and *Ornithorhynchus* (Flannery et al., 1995). In *Ornithorhynchus* the canal transmits a hugely enlarged branch of the mandibular nerve and arteries, which supply innervation and vascularization to the

bill (Grant, 2007). The presence of the hypertrophied mandibular canal implied a semi-aquatic habitus in all three taxa.

The discovery of a monotreme in the Early Cretaceous of Australia was completely unexpected at that time. Owing more to its great antiquity and less to character data, Flannery et al. (1995) and most later authors concluded that *Steropodon* lies on the monotreme stem (e.g., Luo et al., 2001; Kielan-Jaworowska et al., 2004; Phillips et al. 2009, 2010). However, Rowe et al. (2008) argued that *Steropodon* is a crown-monotreme that lies along the ornithorhynchid stem. There are two major points at stake in the controversy. First, if *Steropodon* is a member of the monotreme crown, it implies that the phylogenetic divergence between Tachyglossidae and Ornithorhynchidae occurred in or before the Early Cretaceous, a date older than any of the molecular clock estimates for this event published prior to 2008 (Rowe et al., 2008). Secondly, if *Steropodon* is in fact a stem-monotreme, its position is more consistent with the molecular clock estimates, but it would suggest that crown Monotremata evolved from a semi-aquatic platypus-like ancestor, and that Tachyglossidae is secondarily terrestrial. Only one group of authors (Phillips et al., 2009, 2010) explicitly stated a semi-aquatic origin for Monotremata. The implications of this controversy are addressed more fully in the **Discussion**, below.

Steropodon also was considered to be a ‘pretribosphenic’ stem-therian (Kielan-Jaworowska et al., 1987). However, that position gained no support beyond its initial

publication, and all other authors have treated *Steropodon* as either a crown- or stem-monotreme.

In 1992, the first non-Australian monotreme, *Monotrematum sudamericanum*, was described (Pascual et al., 1992a, 1992b, 2002). It was discovered in early Paleocene (Danian) sediments of Patagonia, near Punta Peligro, Golfo San Jorje, Chubut Province, Argentina, in the Hansen Member (Blanco Negro Inferior) of the Salmananca Formation. The initial discovery was based on a single tooth, described as an upper right second molar. Soon thereafter, an isolated incomplete left upper first molar and distal ends of the right and left femora were recovered from the type locality (Forasiepi and Martinelli, 2003). The two teeth of *Monotrematum* exhibited resemblance to the teeth of both *Steropodon* and *Obdurodon*. *Monotrematum* was classified as an ornithorhynchid on the basis of dental synapomorphies (Pascual et al., 1992b: 8), although the teeth were not scored in a matrix, nor were the specimens included in a formal cladistic analysis. The distal femora, also provisionally assigned to *Monotrematum sudamericanum,* bore close resemblances to the femur in *Ornithorhynchus* (Forasiepi and Martinelli, 2003). Those authors speculated that the ancestral monotreme may have been a semi-aquatic platypus-like mammal.

In 1995, another purported monotreme fossil, *Kollikodon ritchiei*, was discovered in Australia at Lightning Ridge, from the same Early Cretaceous locality that had produced *Steropodon* (Flannery et al., 1995). The initial discovery was a right dentary fragment with teeth thought to be m1-3 and alveoli for p1-2 and m4. *Kollikodon* was

allied to ornithorhynchids based on an array of features that its dentary and teeth shared with both *Steropodon* and *Obdurodon*. These include

> …an anteroposteriorly compressed m1 trigonid that lacks a paraconid (autapomorphic among Mesozoic mammals), high transverse loph-like trigonid and talonid blades (autapomorphic), very large talonid (autapomorphic among pre-tribosphenic mammals), prominent anterior, posterior and buccal cingula (?symplesiomorphic in mammals), abrupt discontinuity in size between the small P_2 (as indicated by the alveoli) and large m1 (autapomorphic among all Mesozoic mammals) and wide talonids without entoconids (autapomorphic among Mesozoic mammals)….Because all these features, except the transverse, loph-like blades, are also present in *K*[*ollikodon*] *ritchiei*, this taxon is concluded to also be a monotreme. *K*[*ollikodon*] *ritchiei* and *S*[*teropodon*] *galmani* further share very large dental canal size (which suggests a need for relatively extensive innervation and blood supply at the front of the head, as in modern platypuses which have sensitive rhinaria and electrosensory organs). In *K*[*ollikodon*] *ritchiei* the dentary narrows markedly anterior to the position of M1, as it does in *O*[*rnithyrhynchus*] *anatinus*. As in all other monotremes, there is no evidence of a canine alveolus although the specimen is missing much of the anterior portion of the dentary. The teeth have very shallow roots in contrast to those of *S*[*teropodon*] *galmani*, and the premolar (and possibly molar) alveoli invade the canal space, as they do in….*Obdurodon* and *Ornithorhynchus*. (Flannery et al., 1995: 418-419)

As with *Steropodon*, *Kollikodon ritchiei* was accorded its own family (Flannery et al., 1995). Notwithstanding the many resemblances that *Kollikodon* shares alone with *Steropodon*, *Obdurodon*, and *Ornithorhynchus*, Ornithorhynchidae and Tachyglossidae were depicted as each other's closest relatives, with Steropodontidae and Kollikodontidae distributed as successive outgroups to the crown along the monotreme stem (Flannery et al., 1995, fig. 2). None of the dental evidence advanced in support of this scheme of relationships can be assessed in Tachyglossidae, except the autapomorphic state, "complete loss of all teeth" (Flannery et al., 1995: 419), and thus their phylogeny reflects more an opinion on relationships than an analytic result. These authors avoided the larger consequence of the proposed relationships, namely that monotremes arose as semi-aquatic platypus-like mammals, and that echidnas must therefore be secondarily terrestrial. It is easy to understand their reluctance to confront that idea. All the fossil evidence surrounding the origin of Mammalia points to a terrestrial ancestor (e.g., Rowe et al., 2011), and although several semi- and fully-aquatic mammalian clades had evolved (e.g., pinnipeds, cetaceans), there are no compelling examples among mammals of a secondarily terrestrial lineage.

Subsequent to the initial report on *Kollikodon*, a partial maxilla was recovered that possesses highly derived, tubercular multi-cusped upper teeth unlike any other mammal (Musser, 2003, 2005). 'Gestalt' resemblances to tritylodontid mammaliamorphs and multituberculate mammals were evident, but they could not be extended to cusp-to-cusp hypotheses of homology with either clade. As a result, Musser (2003, 2005) came to

doubt whether *Kollikodon* is a monotreme at all, either within the crown or along the stem. More extensive new material of *Kollikodon* was recently recovered, which Musser is now studying in detail. I therefore decided to exclude this taxon from the following analysis until the more complete description is published.

Ambiguous Monotremes

Ambondro mahabo (Flynn et al., 1999) is based on a single dentary fragment preserving three teeth, considered to be the ultimate premolar and first two molars. It was collected from the upper level of the Isalo Group (Isalo III) of the Mahajanga Basin of Madagascar, which is considered Middle Jurassic (Bathonian) age. *Ambondro* was originally assigned to Tribosphenida based on wear facets in a well-developed talonid which suggest occlusion by the protocone and a functionally tribosphenic occlusal condition. It also possesses a strong distal metacristid that tends to place it with Tribosphenida (Davis, 2011: 237). Alternatively, others argued that the tribosphenic condition arose at least twice, and that the presence of a shelf-like mesial cingulid that wraps around the mesiolingual corner of the trigonid is a key feature linking it to other basal stem-monotremes (Kielan-Jaworowska, 2004: 204). There are few data upon which to base a conclusion, but *Ambondro* was included in this analysis, highlighting its importance in debates about the Gondwanan radiation of stem monotremes.

The next important Australian discovery was the recovery of a suite of jaws representing three taxa from the Early Flat Rocks locality of Victoria, Australia (Rich et al., 1997, 1999, 2001). An overlying bed was dated using the fission track method at

between 121-112.5 Ma. (Rich et al., 1999, 2001a). The taxa from the Flat Rocks Locality include *Teinolophos trusleri*, *Ausktribosphenos nyktos*, and *Bishops whitmorei*. *Teinolophos* is known from at least six dentaries, some with teeth, that present a gradation in size, while *Bishops* is known from two dentaries with teeth. All three were initially regarded as tribosphenic therian mammals (Rich et al. 1999, 2001a), but Rich et al. (2001b) subsequently argued that *Teinolophos* is a monotreme (without stating whether it was a crown or stem member) closely related to *Steropodon*. All three Flat Rocks taxa subsequently came to be regarded as stem-monotremes by many authors (Luo et al., 2001, see Fig. 2.1A; Kielan-Jaworowska et al., 2004; Phillips et al. 2009).

After using high-resolution X-ray computed tomography on several of the Flat Rocks jaws, Rowe et al. (2008; Fig. 2.1B) argued that *Teinolophos* is a stem-ornithorhynchid, that properly lies within the monotreme crown. The major evidence pertained to the absence of postdentary elements, a hypertrophied mandibular canal that runs the length of the jaw, similarities of its teeth to both *Steropodon* and *Obdurodon*, a large medial tubercle for attachment of the pterygoideus musculature, and the configuration of the coronoid, condylar, and angular processes of the dentary. Their study of *Teinolophos* also presented several 'relaxed' molecular clock analyses which accounted for possible rate heterogeneities (Rowe et al., 2008, table 1). One of those estimates had credibility intervals that encompassed the age of the Flat Rocks locality.

That interpretation stands in stark contrast to all other molecular clock estimates, which postulate that the platypus and echidna lineages diverged far more recently with

most authors preferring a date in the latter half of the Cenozoic (Table 3). To support their conclusion, Rowe et al. (2008) argued that previously published 'strict' molecular clock estimates failed to account for rate heterogeneities in molecular evolution but that the 'relaxed' model took these into account. Whereas the credibility intervals for the analyses are exceedingly wide, the absence of precision is a more accurate reflection of molecular clock models. It was hypothesized that *Steropodon* and *Teinolophos* are both stem-ornithorhynchids, and that they are evidence not only that Monotremata originated by at least the Early Cretaceous, but that it also split into its two major sister lineages (Rowe et al., 2008).

Several characters in the Rowe et al. (2008) matrix were challenged, and the novel argument that such features as the expanded mandibular canal are plesiomorphic was presented in a response to the conclusion that *Teinolophos* is a crown monotreme (Phillips et al., 2009). Although they agreed that *Teinolophos* as well as *Steropodon* are allied to monotremes, they found them both to occupy a position on the monotreme stem (Fig. 2.1C). They also fully confronted the implications of such a position, and speculated that monotremes were indeed semi-aquatic ancestrally, and that the echidna lineage had secondarily become terrestrial thrust-diggers. They performed yet another molecular clock analysis under a different set of prior assumptions and reached the more conventional conclusion of a mid-Cenozoic date for the origin of monotremes and divergence of the platypus and echidna lines. The response to this by Camens (2010) and

rejoinder (Phillips et al., 2010) are discussed below in light of the results of my phylogenetic analysis.

Although *Ausktribosphenos nyktos*, and *Bishops whitmorei*, were originally considered to be tribosphenic mammals and were allied to placentals (Rich et al., 1999, 2001a), later authors (Luo et al., 2001; Kielan-Jaworowska et al., 2004) allocated them to the monotreme stem. The name Australosphenida has been applied to this group (e.g., Luo et al., 2001; Kielan-Jaworowska et al., 2004), although it is unclear how the name is defined and whether it refers to the total-clade Monotremata (crown + stem) or to some subset. This nomenclatural matter is dealt with below.

Hadrocodium wui (Luo et al., 2001) is known from a single fairly complete skull that was recovered from the Early Jurassic Lower Lufeng Formation, in the Lufeng Basin of Yunnan, China. It was placed near the base of crown-Mammalia, lying just outside the crown (Rowe et al., 2011), or just inside, as the basal-most stem monotreme (Rowe et al., 2008). The skull was CT scanned at The University of Texas, and both its osteology and an endocast are known in considerable detail (Rowe, et al., 2011). However, not a single element of the postcranium is known.

In 2002, an isolated jaw from the Middle to Late Jurassic of Chubut, Argentina was described as another member of Australosphenida and named *Asfaltomylos patagonicus* (Rauhut et al., 2002). It was collected from the Cañadón Asfalto Formation and consists of a left mandible with roots and crown fragments of what they consider to be the last three premolars and three molars. It retains a postdentary trough

(plesiomorphy), and shares with other australosphenidans a lingual cingulid at the base of the paraconid and talonids. It was taken to be further evidence of a mid-Jurassic radiation of Gondwanan australosphenidans.

In 2005, an isolated humerus recovered from the Early Cretaceous Eumeralla Formation at Dinosaur Cove in south-eastern Australia was tentatively attributed to Monotremata and named *Kryoryctes cadburyi* (Pridmore et al., 2005). The humerus is remarkably similar to that of living monotremes, particularly echidnas, in size, torsion, and in its articular surfaces. The major difference with *Kryoryctes cadburyi* is that the radius and ulna articulate on separate condyles as opposed to one bulbous condyle characteristic of monotremes. The assignment of *Kryoryctes* to Tachyglossidae, or the assignment of *Kryoryctes* as a basal tachyglossid would support the hypothesis that ornithorhynchids and tachyglossids diverged as early as the Early Cretaceous. For this reason, it is of interest to add *Kryoryctes cadburyi* to the matrix.

Lastly, there is a clade of small Jurassic mammals known from China and Europe that is characterized by functionally tribosphenic molariform teeth, but in which the talonid basin is positioned in front of, rather than behind, the trigonid. The first to be described was *Shuotherium dongi* based on an isolated partial dentary from the Middle to Late Jurassic of Sichuan, China (Chow and Rich, 1982). Later some isolated lower molars from the Upper Bathonian Forest Marble Formation of England were named *Shuotherium kermacki* (Sigogneau-Russell, 1998), and shortly after, from the same locality as *Shuotherium dongi*, an upper right molar matching the proposed morphology

of the molar of *Shuotherium* was discovered. Due to its larger size, it was named as a new species, *Shuotherium shilongi*. More recently, a partial skeleton with this distinctive dentition was described from the Middle Jurassic of China, named *Pseudotribos robustus* (Luo et al., 2007; holotype CAGS – IG0408-11) from Daohugou Locality, Ningcheng County of Inner Mongolia Autonomous Region of People's Republic of China. The specimen is from bed 3 of the Jiulongshan Formation. A volcanic ash 20 meters above this bed was dated at 164.2 +/- 2.5 Ma from feldspar using 40Ar/39Ar and from zircon by SHRIMP 206Pb/238U dating at 164.2 +/- 2.4Ma (Luo et al., 2007, supplemental material: 3).

More recent phylogenetic analyses consistently placed the shuotheriids within Australosphenida (Luo et al., 2001; Luo et al., 2002; Rauhut et al., 2002; Kielan-Jaworowska et al., 2002; Luo and Wible, 2005; Luo et al., 2007; but see Rowe et al., 2008), which is not surprising given that all these analyses except that by Rowe et al., (2008) utilized the original matrix published by Luo et al. (2001). Although the shuotheriids independently evolved a crushing basin analogous to the talonid of tribosphenic mammals, the Luo et al. (2001, 2007) matrices scored the basin of shuotheriids and its surrounding cusps as homologous structures to those of the tribosphenic molar. Therefore, the reliability of the phylogenetic placement of any shuotheriid taxon is questionable and a reevaluation of dental character scores is needed. Such a reevaluation is beyond the scope of this project, which is to identify new synapomorphies of Monotremata, resolve relationships within Monotremata, and

reconstruct the ancestral monotreme based on new skeletal evidence. For this reason, only *Shuotherium*, to the exclusion of *Pseudotribos*, was included in my analysis to maintain consistency with the analyses of Rowe et al. (2008) and Phillips et al. (2009).

Pan-Therians Used in this Analysis

Fruitafossor windscheffeli (Luo and Wible, 2005) from the Late Jurassic Fruita Formation (sometimes considered a member of the Morrison Formation) was included because it is the most basal stem-therian according to Luo and Wible (2005), and it is represented by a fairly complete skull and skeleton.

Jeholodens jenkinsi (Ji et al., 1999) and *Gobiconodon ostromi* (Jenkins and Schaff, 1988) were included because they are among the most complete and best-known early members of Eutriconodonta, a fairly diverse clade known from Jurassic and Cretaceous fossils in Asia, North America, and South America. In most analyses (e.g., Luo and Wible, 2005), Eutriconodonta lies at the base of the therian stem (Rowe, 1988; Rougier et al., 1996; Kielan-Jaworowska et al., 2004), or just crown-ward relative to *Fruitafossor* (Luo and Wible, 2005). However, some analyses place Eutriconodonta just outside of crown Mammalia (e.g., Ji et al., 2006). Both *Fruitafossor* and *Jeholdens* were CT scanned at The University of Texas, but the scan data did not add appreciably to the scoring of these taxa based on the literature and were therefore not used.

In the pre-cladistic literature, Multituberculates were grouped with monotremes in what is now hypothesized to be a paraphyletic 'Prototheria' (Rowe, 1988, 1993). It is now well established that Multituberculata lies closer to crown Theria than to

Monotremata, but that the clade retains a number of plesiomorphic features compared to crown therians. Several genera of plagiaulacidan and cimolodontan multituberculates are known from numerous specimens with fairly complete crania and post-crania and were scored accordingly (Kielan-Jarowowska, 1989, 1997; Wible and Rougier, 2000). One if these taxa, *Kryptobaatar dashzevegi* (Wible and Rougier, 2000), was scanned at The University of Texas, and the scans helped me interpret scoring decisions that were reflected in published matrices.

Vincelestes neuquenianus is a stem therian known from relatively complete crania and postcrania (Bonaparte, 1986; Bonaparte and Rougier, 1987). It, too, was CT scanned at The University of Texas and used for analysis. *Dryolestes* (Martin, 1999) is another well-studied stem therian from the Upper Jurassic of Portugal, with a fairly complete skull and postcranial skeleton, and it was added to the stem-therians used in the outgroup. *Dryolestes* was scored from the literature (Table 2.3).

For crown therians, *Eomaia* (Ji et al., 2002) and *Sinodelphys* (Luo et al., 2003) are the earliest well-known stem-placentals and stem-marsupials, respectively, and both are known from fairly complete skulls and postcranial skeletons. The interpretation of *Eomaia* as the earliest known therian has recently been challenged, however (O'Leary et al., 2013). *Leptictis*, and the extant mammals *Erinaceus* and *Dasypus*, were selected to represent crown Placentalia, and *Didelphis* and *Vombatus* were selected to represent crown Marsupialia, in keeping with earlier published matrices (Luo and Wible, 2005).

Outgroup Taxa

Because the hypothesized relationships of some of the ingroup taxa varied so widely in their taxonomic allocation in previously published analyses, I chose representatives of crown Theria, pan-therians, and pan-mammals (lying outside the crown) as my outgroups (Table 2.1). Other pan-mammals used in my analysis include the following *Haldanodon expectatus*, *Morganucodon oehleri*, *Kayentatherium wellesi*, and *Pachygenelus monus*.

Haldanodon exspectatus is the most complete and best known member of Docodonta, a diverse clade of Late Triassic and Jurassic mammaliaformes that has been found consistently to lie just outside of crown Mammalia. *Haldanodon* is known from several partial skulls and postcranial skeletons recovered from the Guimarota coal mine of Portugal, of Late Jurassic (Kimmeridgian) age. Its skull and postcranial skeleton are thoroughly described and illustrated (Lillegraven and Krusat, 1991; Martin 2005) and I scored it from descriptions in the literature, taxon-character matrices, and illustrations (Lillegraven and Krusat, 1991; Martin 2005).

The second successive outgroup to crown Mammalia is *Morganucodon oehleri*. Its skull and postcranial skeleton are thoroughly described and illustrated (e.g., Kermack et al. 1973, 1981; Jenkins and Parrington, 1976). In addition, two specimens were CT scanned at The University of Texas (IVPP 8685, and IVPP 358) and the datasets were used in scoring the matrix. They were collected from the Lower Lufeng Formation of the Lufeng Basin, China, and are of Early Jurassic (Hettangian – Sinemurian) age.

The third successive outgroup to crown Mammalia used in the matrix is *Kayentatherium wellesi*, a member of the Late Triassic to Jurassic clade Tritylodontidae. *Kayentatherium* is known from numerous specimens collected from the Early Jurassic Kayenta Formation of North America and well-represented in the collections of UT's Vertebrate Paleontology Laboratory and the Museum of Comparative Zoology at Harvard, where I was able to study specimens first-hand. Its skull (Sues, 1986) and postcranial skeleton (Sues and Jenkins, 2006) were thoroughly described. I was able to score this taxon based on previous descriptions and taxon-character matrices (Rowe, 1988, 1993), and using unpublished drawings and notes by Tim Rowe.

The fourth successive outgroup to crown Mammalia used in my matrix is *Pachygenelus* cf. *monus*, a representative of Tritheledontidae, which I scored based on specimens at the Museum of Comparative Zoology, accounts in the literature (Rowe, 1993), and unpublished drawings and notes by Tim Rowe. The hypothesized placement of Tritheledontidae varies. Some results suggest Tritheledontidae lies just inside or just outside of Mammaliamorpha, which is a node-based clade stemming from the last common ancestor shared by tritylodonts and crown Mammalia, and all its descendants (see Rowe, 1993).

MATERIALS AND METHODS

Sources of Anatomical data

Characters were scored based on personal observation, CT scans, and from published material. Extant monotreme and didelphid taxa were observed in person in the Mammalogy Collections at AMNH, MCZ, and TMM. Extinct taxa outside of Crown Mammalia, including morganucodontids, and tritylodontids, were observed in the Vertebrate Paleontology Collections at MCZ. Specimens observed personally are listed in Table 2.1.

CT scans

Archives of digital morphological datasets from specimens scanned by the X-ray computed tomography scanners at the University of Texas High-Resolution X-ray Computed Tomography Facility (UTCT) included the early pan-mammal *Morganucodon*, the early mammal *Hadrocodium*, the multituberculate *Kryptobaatar*, as well as marsupials, monotremes, and placentals. Specimens that were used for character-scoring were accessed on DigiMorph.org; a list of the URL web addresses for each specimen is listed in Table 2.2.

Literature

Literature was used for interpreting skeletal anatomy and for learning the anatomy of specimens that I could not observe in person or on DigiMorph.org. Table 2.3 lists the

primary literature referenced for cranial and postcranial anatomy of the taxa used in the morphological analysis.

Matrix

The matrix used in this phylogenetic analysis was adapted from Luo and Wible (2005). The original matrix included 96 mammalian and non-mammalian synapsid taxa, and 422 cranial and post-cranial morphological characters. Their taxon list was pared down to the 32 taxa discussed above for this analysis.

Eighteen new characters were added by Rowe et al. (2008) to the Luo and Wible (2005) matrix in order to address specifics with the anatomy of monotremes. Eighty-seven characters were rescored by Rowe et al. (2008) and used in this analysis.

The most recent modifications to the matrix were made by Phillips et al. (2009) where they re-scored four characters, eliminated one character on the basis of redundancy, and added two new characters. The two new characters added by Phillips et al. (2009) related to adult body size (character 440) and mandibular aspect ratio (character 441). Without a matrix to see how these two characters were scored for all of the included taxa, and without time to go over each taxon and make the calculations, these characters were not added to the matrix I received from Dr. Luo.

Characters identified from comparing museum specimens of monotremes were added to the Luo and Wible (2005) matrix and all relevant taxa were scored. Modifications made by Rowe et al. (2008) were made to the matrix along with six

modifications suggested by Phillips et al. (2009). Twenty monotreme characters were rescored based on re-evalutaion of character states or absence of characters in some of the extinct taxa; the new modifications are discussed below.

Character List

All character-state scores utilized in the analysis are identical to those of Luo and Wible (2005) and Rowe et al. (2008) except those itemized below (the numbers in parentheses refer to the character number in the original dataset). For a complete list of characters, see Appendix 2.A.

Modifications to the scoring of Luo and Wible (2005) and Rowe et al. (2008)

Character 7. Angular process of the dentary: (0) Weakly developed to absent; (1) Present, distinctive but not inflected; (2) Present and transversely flaring; (3) present and slightly inflected; (4) Present, strongly inflected, and continuing anteriorly as the mandibular shelf.

Tachyglossus: 1. The mandibular angle is present and distinct. It is aligned in a single plane with the condylar process and is not, therefore, inflected.

Character 8. Position of the angular process of the dentary relative to the dentary condyle: (0) Anterior position (the angular process is below the main body of the coronoid process, separated widely from the dentary condyle); (1) Posterior position (the

angular process is positioned at the level of the posterior end of the coronoid process, either close to, or directly under the dentary condyle).

Tachyglossus: 1. Angular process of the dentary is posterior to the coronoid process.

Character 10. Flat ventral surface of the mandibular angle: (0) Absent; (1) Present.

Teinolophos and ***Obdurodon***: 1. Angular process is horizontal in cross section, giving the angular process a flat surface.

Ambondro and ***Steropodon***: '?.' The angular process is not preserved in known specimens.

Character 27. Shape and relative size of the dentary articulation: (0) Condyle small or absent; (1) Condyle massive, bulbous, and transversely broad in its dorsal aspect; (2) Condyle mediolaterally narrow and vertically deep, forming a broad arc in lateral outline, either ovoid or triangular in posterior view.

Tachyglossus: 3. New character state. The dentary condyle of Tachyglossidae is neither small or absent, bulbous, nor vertically deep. The dentary condyle of Tachyglossidae is anteroposteriorly elongate and vertically thin and relatively flat on its dorsal surface.

Character 31. Position of the dentary condyle relative to the level of the postcanine alveoli:(0) Below or about the same level; (1) Above.

Tachyglossus: 0. The position of the dentary condyle was scored as below the postcanine alveoli (Phillips et al., 2009), which is consistent with my personal observations. Relative to the dorsal surface of the dentary where molar crowns would emerge, the dentary condyle is high above that surface in *Ornithorhynchus* and *Obdurodon*. In *Tachyglossus* and *Zaglossus*, the dentary dips ventrally around the position of the angular process and the dentary peduncle is posteriorly directed so that the condyle is roughly level with the dorsal surface of the dentary.

Character 34. Alignment of the ultimate molar (or posteriormost postcanine) to the anterior margin of the dentary coronoid process (and near the coronoid scar if present): (0) Ultimate molar medial to the coronoid process; (1) Ultimate molar aligned with the coronoid process.

Teinolophos, ***Obdurodon***, and ***Ornithorhynchus***: 0. Although the ultimate molar is positioned anterior to the coronoid process, the tooth is not aligned with the coronoid process because the tooth is directed medially.

Character 222. Fully ossified floor in the acetabulum: (0) Present; (1) Absent.

Obdurodon: '?.' The acetabulum of *Obdurodon* is incomplete and therefore it is difficult to determine whether or not the floor of the acetabulum is ossified. *Tachyglossus* and *Ornithorhynchus* were originally scored as 1 (acetabulum not fully ossified; Luo and Wible, 2005) but then were rescored as 0 (acetabulum fully ossified; Rowe et al., 2008).

Ornithorhynchus should remain as 0, but *Tachyglossus* should be scored as the original scoring because an open acetabulum is a synapomorphy of Tachyglossidae. The acetabulum of *Megalibgwilia* is not known so this character was scored as '?.' An innominate of '*Zaglossus*' *hacketti* is known, however, with a perforate acetabulum (Glauert, 1914) so it is possible that the acetabulum is not fully ossified in *Megalibgilia* as well.

Character 228. Size of the lesser trochanter: (0) Large; (1) Small to absent.

Tachyglossus: 1. Lesser trochanter of femur is small, not large.

Character 277. External size of the cranial moiety of the squamosal: (0) Narrow; (1) Broad; (2) Expanded posteriorly to form the skull roof table.

Tachyglossus: 1. The squamosal is broad in tachyglossids.

Character 285. Position of the craniomandibular joint: (0) Posterior or lateral to the level of the fenestra vestibuli; (1) Anterior to the level of the fenestra vestibuli.

Ornithorhynchus: 0.

Tachyglossus: 1. *Ornithorhynchus* and *Tachyglossus* were originally scored as 0 (Luo and Wible, 2005) but were changed to a new character state 2 (Rowe et al., 2008) though character state 2 was not defined. *Ornithorhynchus* is better suited to character state 0 (craniomandibular joint lateral to the level of the fenestra vestibuli), but *Tachyglossus*

should be scored as 1 (craniomandibular joint anterior to the level of the fenestra vestibuli).

Character 327. "Bifurcation of the paroccipital process" - presence vs. absence (this is modified from the character used in several previous studies): (0) Absent; (1) Present.
Tachyglossus: 0. The paroccipital process is lacking in echidnas (Wible et al., 2001).

Character 328: Posterior paroccipital process of the petrosal: (0) No ventral projection below the level of the surrounding structures; (1) Projecting below the surrounding structures.
Tachyglossus: 0. The paroccipital process is lacking in echidnas (Wible et al., 2001).

Character 371. Ventral opening of the minor palatine foramen:
(0) Encircled by the pterygoid (and ectopterygoid if present) in addition to the palatine; (1) Encircled by the palatine and maxilla, separated widely from the subtemporal margin; (2) Encircled completely by the palatine (or between palatine and maxilla), large, with thin bony bridge from the subtemporal margin; (3) Large, posterior fenestration; (4) Notch.
Tachyglossus: 5. Character state 5 is a new state I added designating the minor palatine foramina that encircled by the palatine, occurring in a single row along the length of each palatine, and separated widely from the subtemporal margin. This character as a whole

needs revision, however. Some of the character states are vague (e.g., ‘large’ used to describe foramen size for state 2 and state 3. How does the large size in the two states differ? If they are different, I would disagree that the palatine foramina are large in the tachyglossids).

Character 375. Exit(s) of the infraorbital canal: (0) Single; (1) Multiple. The character states for this character should be rewritten as: (0) Multiple; (1) Single; (2) More than three, on average between 5 and 10 exits.

Tachyglossus: 2. This character was written by Luo and Wible (2005) as a binary character but should be written as three states for monotremes. *Obdurodon* and *Ornithorhynchus* have as many as three large exits of the infraorbital canal (state 1). In Tachyglossidae, the infraorbital canal branches within the maxilla and the trigeminal nerve exits out of multiple small foramina on the anterior end of the maxilla (state 2). *Tachyglossus* has between five and seven foramina, while *Zaglossus* can have 10 or more. The number of foramina may be positively correlated with electroreception sensitivity. The number of foramina in *Megalibgwilia* is unclear from the published photos and illustrations (Griffiths et al., 1991; Murray, 1978).

Character 376. Composition of the posterior opening of the infraorbital canal (maxillary foramen): (0) Between the lacrimal, palatine, and maxilla; (1) Exclusively enclosed by the maxilla; (2) Enclosed by the maxilla, frontal and palatine.

Obdurodon: 2. Originally scored as '?,' CT data visible on DigiMorph.org (see Table 2.2) suggests that the posterior opening of the maxillary foramen is enclosed by the maxilla, frontal and palatine.

Tachyglossus: 3. The posterior opening of maxillary canal is bordered by frontal and maxilla exclusively in tachyglossids.

Character 383. Frontal-maxilla facial contact: (0) Absent; (1) Present.

Tachyglossus: 0/1. The maxilla and frontal contact in most tachyglossids specimens. In some specimens (e.g., AMNH 65842, MCZ 7393) a small portion of the maxilla and frontal contact outside of the orbit on the face.

Character 396. Anterior ascending vascular channel (for the arteria diploëtica magna) in the temporal region: (0) Open groove; (1) Partially enclosed in a canal; (2) Completely enclosed in a canal or endocranial; (3) Absent.

Tachyglossus: 1. The channel is partially enclosed by the cranium.

Character 397. Posttemporal canal for the arteria and vena diploëtica: (0) Present, large; (1) Small; (2) Absent.

Tachyglossus: 1. The posttemporal canal for the arteria and vena diploëtica is small relative to the size of the posttemporal canal of *Megalibgwilia*, *Ornithorhynchus*, *Obdurodon*, and their extinct relatives.

Character 423. Platypus-type bill: (0) Absent; (1) Present.

Steropodon, ***Teinolophos***: '?.' As described by Phillips et al. (2009), the rostra of *Steropodon* and *Teinolophos* are not known so there is no direct evidence of a platypus-type bill.

Character 424. Electrophoretic capability with snout: (0) Absent; (1) Present.

Obdurodon, ***Teinolophos***: '?.' The electroreceptive capability of *Obdurodon* and *Teinolophos* is only inferred based on morphological similarities with *Ornithorhynchus.*

Tachyglossus: 1. *Tachyglossus* should be scored for presence of electrosensory capability in the snout because echidnas are capable of electroreception.

Characters removed for analysis

Character 35. Direction of lower jaw movement during occlusion (as inferred from teeth): (0) Dorsomedial movement; (1) Dorsomedial movement with a significant medial component; (2) Dorsoposterior movement. Jaw movement was inferred from tooth wear and is not applicable to tachyglossids. Removal of the character did not affect tree topology. Retention of character needlessly increased tree length.

Character 215. Sutures of the ilium, ischium, and pubis within the acetabulum: (0) Present; (1) Fused. This character was removed because the presence of sutures is ontogenetically variable, and the maturity at time of death for many of the fossils is

unknown. Skeletal maturity is not yet adequately characterized for a majority of mammalian taxa, especially extinct species.

Character 385. Posterior width of nasal bones: (0) Narrow; (1) Broader than the width at the mid-length of the nasal. This character from Luo and Wible (2005) is similar to a new character written by Rowe et al. (2008): nasal width as widest anteriorly or posteriorly. This character was removed because the posterior end of the nasals in some taxa can be wide but taper to a fine point making it difficult to score objectively.

Character 439. Dentary symphyseal region: (0) Broad, vertical contact between right and left dentaries; (1) Dentaries taper anteriorly to points that make almost no medial contact; (2) Dentaries flaring into lateral shelves that have a long, thin zone of symphyseal contact. The character added by Rowe et al. (2008) was removed and replaced with a new character describing the dentary symphysis and shape of the terminal ends of the dentaries, as discussed below.

New Characters

New characters were added to the matrices published by Luo and Wible (2005) and Rowe et al. (2008).

Cranial characters

Character 423. Ratio of rostrum length to skull length (rostrum length measured as rostral tip of premaxilla to edge of orbit around the lacrimal foramen region (Fig. 2.2A-

D): (0) Rostrum is less than half the length of the skull (Fig. 2.2A); (1) Rostrum is over half the length of the skull (Fig. 2.2B-D).

Character 424. Jugal: (0) Present, forming anterior end of zygomatic arch; (1) Reduced; (2) Absent.

Character 425. Curvature of rostrum: (0) Straight, protruding anteriorly (Fig. 2.3A); (1) Straight, angled ventrally (Fig. 2.3B); (2) Decurved (Fig.2.3C); (3) Recurved (Fig.2.3D).

Character 426. Roof of nasopharyngeal passageway visible in ventral view because of retraction of secondary palate: (0) Absent (Fig. 2.4B); (1) Anterior-most portion of septomaxillae visible because of minor retraction of secondary palate; (2) Secondary palate significantly receded exposing much of the ventral surface of the septomaxillae (Fig. 2.4A).

Character 427. Dorsal exposure of anterior portion of vomer because of recessive nasals: (0) Absent (Fig. 2.5B); (1) Present (Fig. 2.5A).

Character 428. Posteromedial incision of palatine: (0) Absent (Fig. 2.6B); (1) Present, shallow; (2) Present, deep (Fig. 2.6A).

Character 429. Rostral end of secondary palate: (0) Extends to the tip of the rostrum; (1) Ends at maxillae (Fig. 2.7A, B).

Character 430. Shape of rostral end of maxillary palatal process: (0) 'W'-shaped at the midline (Fig. 2.8B); (1) Slightly concave, or 'V'-shaped (Fig. 2.8A).

Character 431. Shape of secondary palate in cross section: (0) Flat (Fig. 2.9C); (1) Deeply arched (Fig. 2.9A, B); (2) Shallowly arched.

Character 432. Palatal sculpturing: (0) Absent; (1) Prominent transverse bony ridges (see Fig. 3 of Griffiths, 1991); (2) Slight transverse bony ridges.

Character 433. Parietal sculpturing (Fig. 2.10): (0) Absent; (1) Present.

Character 434. Parietal anterior suture: (0) Contacts frontal only (Fig. 2.11B); (1) Contacts or nearly contacts nasal (Fig. 2.11A).

Character 435. Contact of posterior temporal suture of parietal: (0) Squamosal (Fig. 2.12C); (1) Squamosal and periotic (Fig. 2.12A, B).

Character 436. Incisura occipitalis: (0) Absent (Fig. 2.13A); (1) Present (Fig. 2.11B-D).

Character 437. Palatal process of premaxilla (in ventral view): (0) Short, terminating anterior to canine (Fig. 2.14A); (1) Present, sharply pointed, not extending far past rostral end of palate (Fig. 2.14C); (2) Present, long, extending well beyond rostral end of palate (Fig. 2.14B).

Character 438. Position/orientation of middle ear ossicles: (0) Nearly vertical (Fig. 2.15B); (1) Horizontal (Fig. 2.15A).

Character 439. Position of occipital condyles relative to ventral-most surface of skull (visible in lateral view): (0) Slightly rostral to, or closely aligned with, dorsal aspect of occiput and level with ventral surface of skull (Fig. 2.16A, B); (1) Extend farther caudally than occiput, level with ventral surface of skull (Fig. 2.16C); (2) Extend farther caudally than occiput, positioned roughly in the center of the back of the skull (Fig. 2.16D).

Mandibular characters

Character 440. Coronoid process orientation: (0) Dorsal (Fig. 2.17A, B); (1) Lateral (Fig. 2.17C).

Character 441. Position of dentary symphysis: (0) Distal, terminal end of dentary (Fig. 2.18C); (1) Not at the terminal end of the dentary (Fig. 2.18A, B).

Character 442. Terminal end of dentaries: (0) Fused; (1) Free, pointed (Fig. 2.19C); (2) Free, spatulate (Fig. 2.19A, B).

Character 443. Anterior end of dentary with a medial 'foramen mandibulare anterius dorsale' (Zeller, 1989a (Fig. 2.20): (0) Absent; (1) Present.

Character 444. Curvature of dentaries: (0) Curve medially, angle dorsally anterior to angular process (Fig. 2.21C); (1) Bow laterally, relatively flat but angle dorsally at angular process (Fig. 2.21A, B).

Character 445. Dentary condyle shape: (0) No condyle; (1) Round, or anteroposterior axis of curvature (Fig. 2.22A); (2) Axis of curvature is mediolateral (Fig. 2.22B).

Character 446. Composition of craniomandibular joint: (0) Quadrate-articular; (1) Quadrate-articular and dentary-squamosal; (2) Dentary-squamosal.

Character 447. Mandibular tubercle: (0) Absent; (1) Present (Fig. 2.23).

Character 448. Mandibular canal entrance: (0) Single entrance (Fig. 2.24B); (1) Two entrances (Fig. 2.24A).

Postcranial Characters

Character 449 Spinal nerve exit: (0) Between vertebrae; (1) through foramina in neural arches (Fig. 2.25).

Character 450. Ribs: (0) Two heads that articulate with vertebrae; (1) One head that articulates with vertebrae (Fig. 2.26).

Character 451. Cervical zygapophyses: (0) Present; (1) Absent in first five cervicals; (2) Absent.

Character 452. Ventral processes on atlas: (0) Absent; (1) Present (Fig. 2.27).

Character 453. Ossified, imbricating ventral ribs: (0) Absent; (1) Present (Fig. 2.28).

Character 454. Teres major tubercle: (0) Weak structure that does not project medially beyond lesser tubercle (Fig. 2.29B); (1) Robust, projecting beyond lesser tubercle (Fig. 2.29A).

Character 455. Entepicondylar foramen position (ventral/posterior view): (0) Near margin of proximal part of entepicondyle (Fig. 2.30B); (1) Centrally located within the entepicondyle (Fig. 2.30A).

Character 456. Orientation of inter-epicondylar axis (based on position of ectepicondyle to proximal end of humerus, Fig. 2.31): (0) Approximately 90° or greater (Fig. 2.31B); (1) Less than 90° (between 75° and 80°, Fig. 2.31A).

Character 457. Distinct articulation sites for radius and ulna: (0) Present; (1) Absent (Fig. 2.32).

Character 458. Elbow joint aligned with long axis of humerus: (0) Present; (1) Absent, elbow joint off-centered laterally (Fig. 2.33).

Character 459. Radius and ulna: (0) Bowed and separate, allowing for pronation and supination; (1) Straight, appressed along entire length limiting opportunity for pronation and supination (Fig. 2.34).

Character 460. Ulnar contribution to wrist: (0) Minimal; (1) Substantial.

Character 461. Trochlea on distal end of ulna: (0) Absent; (1) Present (Fig. 2.5).

Character 462. Dual concave facets on radius: (0) Absent; (1) Present (Fig. 2.36).

Character 463. Dual processes on olecranon process of ulna: (0) Absent; (1) Present (Fig. 2.37).

Character 464. Rounded, laterally inflected process on distal tibia: (0) Absent; (1) Present (Fig. 2.38).

Phylogenetic Analysis

The morphological data matrix was uploaded into the parsimony analysis software Paup*4b10 (Swofford, 2003). Most-parsimonious trees (MPTs) were estimated with a heuristic search algorithm and 1000 random sequence additions, equal weights for all characters, and tree-bisection and reconnection (TBR) branch swapping. Character settings were optimized for accelerated transformation (ACCTRAN) and delayed transformation (DELTRAN). Nodal support was measured with bootstrapping. Bootstrap analyses included 1000 replications and 10 random input orders per replicate. Trees were viewed in the program FigTree v1.3.1.

RESULTS

Six MPTs were recovered with a tree length of 1261, consistency index of 0.5757, a homoplasy index of 0.4243, retention index of 0.7297 and a rescaled consistency index of 0.4201. A strict consensus tree is shown in Figure 2.39.

Monotremata, including Ornithorhynchidae and Tachyglossidae, was recovered as a monophyletic taxon that is the sister taxon of Pan-Theria. Ornithorhynchidae resolves as a polytomy that includes *Ornithorhynchus*, *Obdurodon*, and *Steropodon*. In both the strict consensus tree and Adams consensus tree, these relationships are unresolved. *Teinolophos* is positioned outside of Ornithorhynchidae as a member of Pan-Ornithorhynchidae. Tachyglossidae consists of the extant *Zaglossus* and *Tachyglossus*, and *Megalibgwilia* lies on the stem (Pan-Tachyglossidae) as a basally divergent echidna.

Pan-Theria is a stem-based total-clade containing Theria and all taxa more closely related to Theria than to Monotremata. Since the definition published by Rowe (1993), Theriiformes was defined as a node-based name that includes the last common ancestor of eutriconodontids and crown Theria, and all of its descendants (Luo and Wible, 2005). *Fruitafossor* is the most basal taxon on the therian stem. *Kryoryctes* is sister to Theriiformes (*sensu* Luo and Wible, 2005).

Appendix 2.B lists the synapomorphies for each node of Monotremata recovered from the parsimony search.

Diagnosis

Diagnoses of Monotremata and clades within Monotremata are based on the distribution of characters under the delayed transformation (DELTRAN) character optimization setting in PAUP*4b10. Owing to the quantity of missing data in some extinct taxa, writing a diagnosis based on the DELTRAN setting minimizes uncertainty. Ambiguous synapomorphies are generally a result of missing data and as a more complete fossil record accumulates they may have a more general distribution than is recovered using DELTRAN optimization; they are indicated with an asterisk (*). All discussed apomorphies are based on characters in the Luo and Wible (2005) matrix except where otherwise noted.

Monotremata

Teeth

The teeth in living monotremes are either vestigial or entirely absent. All known extinct monotremes are either known only from teeth (Archer et al., 1985; Flannery et al., 1995; Rich et al., 1999) or were originally described from teeth (Pascual et al., 1992a, b, 2002) with the exception of *Megalibgwilia* which lacks teeth (Murray, 1978; Griffiths et al., 1991), and '*Zaglossus*' *hacketti* which is based on postcranial remains (Glauert, 1914; Murray, 1978). An unambiguous dental synapomorphy of Monotremata is the lack of incisors or canines. A hypothesized dental formula for erupted mineralized teeth of *Ornithorhynchus* is i0/0 c0/0 p1/0 m2/3 (Green, 1937). These teeth are shed as the maturing platypus is weaned and begins hunting on its own in the water. Evidence of

additional toothbuds that are resorbed before they can erupt was described by Green (1937). Considering the ephemeral 'milk dentition' of young *Ornithorhynchus*, the complete dental formula for *Ornithorhynchus* is i0/5 c1/1 p2/2 m3/3. The upper jaw of *Obdurodon dicksoni* has zero incisors and canines, two premolars, and 2 molars. The terms 'premolar' and 'molar' have been applied to *Obdurodon* by most authors, although there is no substantive evidence regarding tooth replacement. The lower dentition of *Obdurodon* is known from posterior left dentary fragments of both *Obdurodon insignis* and *Obdurodon dicksoni* and two isolated premolars (left p1 and right p2) of *Obdurodon dicksoni*. There is an alveolus for an m3 suggesting that the dental formula for adult *Obdurodon* is i0/0 c0/0 p2/2 m2/3 (Archer et al., 1992 and 1993; Musser and Archer, 1998). The anterior region of the upper and lower jaws of *Teinolophos* and *Steropodon* are unknown so it cannot be definitively stated whether incisors and canines were present or absent in these Early Cretaceous taxa.

Skull

Monotremes are almost unique among mammals (with few exceptions including *Myrmecophaga tridactyla* and cetaceans) for having a snout length greater than half the length of their skull (pers. obs., Fig. 2.2A-D). The narial aperture is dorsally directed at the end of the rostrum* (Rowe et al., 2008). Ventrally, a pointed process of the premaxilla extends far posteriorly along the lateral margin of the rostrum (pers. obs., Fig. 2.14B). Otherwise the premaxilla does not contribute to the secondary bony palate (pers. obs., Fig. 2.7A, B). Instead, the hard palate begins with palatal processes of the maxillae.

The secondary palate extends posteriorly to the basisphenoid-basioccipital synchondrosis, and therefore obscures the basisphenoid from view.

Monotremes retain a lacrimal gland but lack a lacrimal bone, and the lacrimal foramen is bordered by the maxilla and frontal (pers. obs.). Medial processes of each frontal are wedged between the two nasals. The orbital process of each frontal contacts the maxilla within each orbit. There is no contact between the frontal and alisphenoid*. Facial processes of the large parietal extend anteriorly and either contact or nearly contact the nasals (pers. obs., Fig. 2.11A).

The glenoid fossa on the squamosal is dorsoventrally expanded and mediolaterally compressed and contacts the squamosal cranial moiety. The squamosal lacks a post-glenoid depression and a postglenoid process.

The monotreme cochlea is elongate and partly coiled to about 270° rather than being only slightly curved or coiled into a full 360°. A cribriform plate of the internal acoustic meatus is present, which transmits a branch of the VIIth and two branches of the VIIIth nerves*. The foramen ovale is positioned on the ventral surface of the skull along with the middle ear ossicles which lie on a nearly horizontal plane to the base of the skull* (pers. obs., Fig. 2.15A). Externally, the tympanohyal contacts the cochlear housing. The stapedial muscle fossa is lost. The stapes itself is imperforate and columelliform*. The hypoglossal foramen is confluent with the jugular foramen, instead of forming its own distinct foramen. Monotremes lack a pila antotica*.

The brain of monotremes is relatively large; the vermis, or central lobe of the cerebellum, is anteriorly expanded*. This affects the surface topography of the skull overlying the cerebellum such that the lambdoidal and sagittal crests are lost*. Instead, the trigeminal muscles attach to the sub-spherical surface of the skull, leaving distinctive muscle scarring only on the parietal (Van Bemmelen, 1901; Fig. 2.10). This probably also reflects the general reduction of the monotreme dentition and weakly developed masticatory musculature.

A dorsal incision in the margin of the foramen magnum, the incisura occipitalis, is present (pers. obs., 2.13B-D). The incisura occipitalis is present in a few marsupials and immature placentals (Voss and Jansa, 2009). It is persistent in the monotreme specimens that I examined with the exception of a couple of specimens of *Zaglossus* (see Chapter 1). Based on the varying degree of closure of the incisura occipitalis in *Zaglossus*, discussed in Chapter 1, it is unclear whether the presence of an incisura occipitalis in all monotremes represents a mature state, or that the specimens I examined are all immature. Unfortunately, the museum records that accompany the specimens of monotremes do not provide information regarding the age of the specimen when it was collected.

The lower jaw of montremes is composed solely of the dentaries and lacks post-dentary elements including the surangular, prearticular, and coronoid bones. There is some controversy in the literature regarding whether this is a synapomorphy of Mammalia, or if this condition evolved multiple times within mammals (e.g., Rowe, 1988, 1996; Kielan Jaworowska et al., 2004). The coronoid process is oriented laterally

(pers. obs., Fig. 2.17A, B). The mandibular foramen is located in the pterygoid fossa. The dentary peduncle holding the dentary condyle is gracile and vertically directed as opposed to posteriorly directed and the dentary condyle is rounded with an anteroposterior axis of rotation* (pers. obs., Fig. 2.22A). The ventral surface of the mandibular angle is flat* and provides the site of insertion of the detrahens mandibuli muscle, which affords a unique system for depressing the mandible. The terminal ends are spatulate (Fig. 2.19A) and have a medial "foramen mandibulare anterius dorsale" (Zeller, 1989a: fig. 22) present on the dorsal surface (Fig. 2.20A).

Postcranial Skeleton

The atlas vertebra has fused neural arches and intercentrum. Atlantal ribs are present and the postaxial cervical ribs and are fused to their respective vertebrae. The spinal nerves exit from foramina perforating the lamina of the neural arches, as opposed to issuing from between the vertebrae (pers. obs., Fig. 2.25). Monotreme ribs have a single head that articulates with its respective vertebra (pers. obs., Fig. 2.26). Ossified ventral ribs are broad and imbricating (Fig. 2.28), in a pattern unique to monotremes that is associated with their ability to flatten their bodies while moving through confined spaces (Gregory, 1947). The cranial margin of the fused interclavicle/manubrium is emarginated or flat, lacking a median process.

On the scapula, a distinctive fossa for the teres major muscle is present on the lateral aspect of the scapular plate. The orientation of inter-epicondylar axis (measured

from ectepicondyle to proximal end of humerus) is angled between 75° and 80° as opposed to 90° (Pridmore et al., 2005; Fig. 2.31A).

The articulation of the humerus with the radius and ulna is unique in monotremes. The elbow joint is not aligned with the long axis of the humerus* (Pridmore et al., 2005; Fig. 2.33). The capitulum and ulnar trochlea form a continuous synovial surface which is anteroposteriorly cylindrical in shape (pers. obs., Fig. 2.32). The olecranon process is distinctive in monotremes for having dual processes that spread posteromedially to anterolaterally (pers. obs., Fig. 2.37). The radius and ulna are straight and appressed along their entire length, limiting pronation and supination (pers. obs., Fig. 2.34). A substantial portion of the wrist articulates with the ulna where a deep trochlea is formed on the distal surface of the ulna (pers. obs.; Fig. 2.35); this contrasts to most other mammals in which the radius has the broadest contact with the wrist, and the ulna contributes only marginally to the wrist with a somewhat pointed styloid process (pers. obs.). Dual concave facets are present on the distal end of radius (pers. obs., Fig. 2.36).

In the pelvis, the dosal margin of the ischium is concave with a hypertrophied ischiatic tuberosity*. The dorsal margin of acetabulum is closed with a complete rim. A preacetabular tubercle is present on the ilium for the rectus femoris muscle. The lesser psoas muscle leaves a marked tuberosity on the pubis.

On the femur, the third trochanter is present as a continuous ridge connected to the greater trochanter. Despite the presence of a patella (which is absent in most marsupials but present in therians), monotremes lack a patellar groove*.

The calcaneus has a distinct, long, and laterally projecting peroneal process and a distinct, deep peroneal groove. There is no ventral curvature of the calcaneal tubercle. Metatarsal V and the peroneal process of the calcaneus contact side-by-side. The sesamoid bones in the digital flexor tendons are unpaired. The cuboid is skewed to the medial side of the long axis of the calcaneus. An external tarsal spur sheathed in keratin is present in male platypuses, and is connected to a venom gland in the leg (see Grant, 2007). Females can develop a spur sheath (but no spur) that is lost early in captive individuals, and persists no longer than the individual's first breeding season in the wild (Grant, 2007). The spur is present in echidnas, but the gland and duct are vestigial (Augee et al., 2006). The spur is present in some female echidnas but it regresses early in ontogeny (Augee et al., 2006). In male echidnas, the spur is covered in a sheath which is eventually lost as the animal matures (Augee et al., 2006).

Sensory systems

Because *Ornithorhynchus* and extant tachyglossids are electrosensitve (Griffiths, 1978; Manger et al., 1997; Pettigrew, 1999; Augee et al., 2006), electroreception was likely present in Monotremata ancestrally. Although it is impossible to test the electroreceptive capability of extinct monotremes, the large maxillary canal size of *Obdurodon*, and the large mandibular canal size of *Teinolophos*, *Steropodon*, and even the Early Cretaceous monotreme *Kollikodon ritchiei* have led some to speculate that these extinct taxa were also capable of electroreception (Flannery et al., 1995; Rowe et al., 2008).

Pan-Ornithorhynchidae (Node 54)

Pan-Ornithorhynchidae is a total-clade name that that is currently known to contain only *Teinolophos*, *Obdurodon*, *Steropodon*, and *Ornithorhynchus*.

Dentition

Teinolophos, *Obdurodon*, *Steropodon*, and *Ornithorhynchus* share numerous dental characters. The cusps of the posterior molars are slightly triangulated. This differs from the pan-mammalian outgroup taxa and extinct pan-therian taxa that lack triangulated molars, and it also distinguishes therians from the putative pan-monotremes (i.e., 'australosphenidans') with fully triangulated posterior molars. Cusp 'a' (protoconid) and cusp 'c' (metaconid) are nearly equal in height. The anterior mesio-lingual cingular cuspule of the lower molars is absent. The paraconids are lingually positioned and appressed to the metaconid. The paracristid, a crest between cusp 'a' and cusp 'b' (paraconid), is nearly transverse relative to the longitudinal axis of the molar. The paracristid and protocristid on the trigonid form an angle greater than 35°. The trigonid is anteroposteriorly compressed and is 40-45% of the tooth length (rather than up to ¾ of the tooth length) while the talonid is equal to or wider than the trigonid. A deep hypoflexid (concavity between the trigonid and talonid, anterolabial to the hypoconid or cusp d) is present on each lower molar, making up over 65% of the talonid width as opposed to 40% to nearly 50% in other mammals with tribosphenic dentition. The talonid and trigonid of the last lower molars are relatively equal in height. The talonid has two functional cusps forming a 'V-shaped' basin*. There are only two hypertrophied wear

facets, wear facets 3 and 4, on the mesial and distal surfaces of the talonid*. The hypoconid, like other therians and *Vincelestes*, is labially positioned rather than lingually positioned, and elevated above the cingulid level. The hypoconulid is positioned within the lingual 1/3 of the talonid basin. On the anterior lower molars (m1 and m2), the tip of the hypoconulid is procumbent and the posterior wall is vertical. On the ultimate lower molar, the hypoconulid is tall, higher than the hypoconid, and recurved.

Skull

In *Teinolophos*, *Obdurodon*, *Steropodon*, and *Ornithorhynchus*, the angular process of the dentary is present and transversely flaring, forming a shelf that wraps dorsomedially to ventrolaterally. The angular process is relatively high on the dentary, positioned at or near the level of the molar alveolar line, and as in crown Monotremata probably provided the site of insertion of the detrahens mandibuli muscle (Edgeworth, 1935; Rowe, 1986). The angular process of many pan-mammals is level with the base of the jaw. Other extinct Southern Hemisphere taxa, *Ausktribosphenos*, *Asphaltomylos*, *Ambondro*, and *Bishops* (members of Australosphenida sensu Luo et al., 2001) also share a high angular process with the aforementioned taxa. A well-defined and thin crest forms the ventral border of the masseteric fossa. This differs from the unnamed clade stemming from the last common ancestor of therians plus *Vincelestes*, which is the closest extinct pan-therian to the crown therians, which have a low and broad crest forming the ventral border of the masseteric fossa. The crest of the masseteric fossa along the anterior border of the coronoid process is hypertrophied and laterally flaring. The dentary condyle is

above the level of the postcanine alveoli. A mandibular tubercle is present on the medial margin of the mandibular foramen.

Ornithorhynchidae

Known members of Ornithorhynchidae include *Ornithorhynchus*, *Obdurodon*, and *Steropodon*. In this analysis, *Ornithorhynchus*, *Obdurodon*, and *Steropodon* form an unresolved polytomy. Insofar as *Steropodon* is known only from the Early Cretaceous, and *Obdurodon* is Oligocene-Miocene in age, it is possible that, with more complete specimens, *Steropodon* will be resolved as a stem-ornithorhynchid.

Dentition

Ornithorhynchidae was united by many dental synapomorphies in my analysis, despite the highly derived dentition of *Ornithorhynchus*. With more complete knowledge of the osteology of *Steropodon,* these characters may eventually diagnose a more inclusive clade than Ornithorhynchidae. Because nothing besides a partial dentary with teeth is known for either *Steropodon* or *Teinolophos,* all of the cranial and postcranial apomorphies of Ornithorhynchidae are equivocal in their distributions.

The molars are readily diagnosed by the ratio of the talonid to the trigonid, which is almost equal in these taxa*; the talonid is between 60% and 80% the height of the trigonid in *Steropodon*, and equal in height to the trigonid in *Obdurodon*. Mesial cingulids of the molars are above the alveolar margin and are weak and discontinuous with cuspules below the trigonid. A mesial cingulid forms a continuous shelf below the

trigonid, with no relation to the protoconid and paraconid, and has no occlusal function*. The postcingulids cross the lower molars horizontally above the alveolar margin. The molar wear facets are present and occlude upon tooth eruption. Prevallum/postvallid shearing is present, but their facultative dilambdodonty does not involve the protocone, which is lacking in these taxa. Facet 4, on the posterior aspect of the hypoconid, is oriented transversly to the long axis of the tooth rather than being oblique to the long axis of the tooth*. The labial stylar shelf on the penultimate upper molar is present, and is broad. The paracone and metacone are separated at their base.

Skull

The rostrum of *Obdurodon* and *Ornithorhynchus* (unknown in *Steropodon*), is straight, and angled ventrally (pers. obs., Fig. 2.3B). It is anteriorly flattened and is wider than the distance between the orbits* (Rowe et al., 2008). The palatal processes of the premaxillae terminate in a sharp point and are posteriorly elongate* (pers. obs., Fig. 2.14C). The septomaxillae form flattened plates exposed on the dorsal surface of the snout between the nasals and maxillae* (Rowe et al., 2008). The nasals are widest anteriorly around the naris* (Rowe et al., 2008). The fenestra cochleae and jugular foramina are not separated*. Maxillary facial processes have a robust posterolateral maxillary process that buttresses the large lateral maxillary nerve exit and forms the attachment base for the bill* (Rowe et al., 2008). The maxillary canal diameter is greatly hypertrophied and nearly equal to the nasopharyngeal diameter* (Rowe et al., 2008). The posterior opening of the maxillary canal is enclosed by the maxilla, frontal and palatine

rather than between the lacrimal, palatine, and maxilla as in most other mammals and their extinct relatives*. The jugals are reduced to a post-orbital process on the zygomatic arches above the maxillae and squamosals* (Zeller, 1989). The dorsal aspect of the vomer is exposed anteriorly because of the posterior retraction of the nasals* (pers. obs., Fig. 2.5A). The mesethmoid is ossified and forms multiple turbinals and a cribriform plate with only one, or a small number of, large perforations* (Rowe et al., 2008). There is facial contact between the frontal and maxilla*. Within the cranium, the falx cerebri is ossified (Rowe et al., 2008).

The dentaries bend inward, meet at the dentary symphysis, and spread outward so that the dentaries are free at their terminal ends (pers. obs., Fig. 2.21A). In the dentary, the mandibular canal has two entrances, a medial entrance homologous with the mandibular foramen of other mammals and a lateral entrance within the deep masseteric fossa (Fig. 2.24A).

Postcranial Skeleton

The distal tibial malleolus is distinct and medially inflected* (Fig. 2.38).

Pan-Tachyglossidae (Node 56)

Pan-Tachyglossidae is a total-clade name that currently includes only the extinct, basal echidna *Megalibgwilia*, and the extant echidnas, *Zaglossus* and *Tachyglossus*.

Dentition

Apart from the fleeting appearance of an egg tooth around the time of hatching (Green, 1930; Hill and de Beer, 1949), the upper and lower jaws lack teeth for the entirety of their lifespan*.

Skull

The rostrum in the known pan-tachyglossids is long and narrow as opposed to the broad spatulate face in ornithorhynchids (Rowe et al., 2008). The extinct *Megalibgwilia* and extant *Zaglossus* have a decurved rostrum which is primitive for the known pan-tachyglossids, and the curvature becomes more pronounced in *Zaglossus* than in *Megalibgwilia* (pers. obs., Fig. 2.3D). *Tachyglossus* is derived in its recurved (Fig. 2.3C), secondarily shortened rostrum (about equal to or less than half the total skull length, pers. obs., Fig. 2.2C). The facial processes of the septomaxillae surround the nares and meet on the dorsal midline* (Rowe et al., 2008). In ventral view, the surfaces of the septomaxillary facial processes are visible owing to a posteriorly retracted secondary bony palate* (pers. obs., Fig. 2.4A). The rostral end of the bony palate, formed by the palatal processes of the maxillae, is concave and forms a smooth 'V' (Fig. 2.8A) in contrast to other taxa in which the anterior margin of the maxillae forms a 'W' (Fig. 2.8B) An elongate, medial incision at the caudal end of the bony palate separates the left and right palate (pers. obs., Fig. 2.6A). Anteriorly in cross section, the secondary palate is broadly arched (see Griffiths et al., 1991), rather than being flat* (Fig. 2.9 C). Prominent, transverse bony ridges add texture to the palatal surfaces* (Griffiths et al., 1991). The bony ridges in *Megalibgwilia* were likely covered in keratin as in living tachyglossids

(Griffiths et al., 1991). Extant tachyglossids use the keratinized, spiky ridges on the roof of their mouth and the surface of the back of their tongue to grind invertebrates with the aid of their flexible tongue (Augee et al., 2006). The palatal processes of the premaxillae are greatly elongate, extending beyond the narial lacuna (pers. obs., Fig. 2.14B). Primitively, the jugal forms the anterior portion of the zygomatic arch in mammals. *Ornithorhynchus* and *Obdurodon* have a reduced jugal that forms a postorbital process on the zygomatic arch (the jugal is also reduced in multituberculates but is positioned on the medial surface of the zygomatic arch). Tachyglossids, however, lack a jugal (Kuhn, 1971). The squamosal of tachyglossids is distinctive for the anteroposteriorly, and dorsoventrally, broad cranial moiety. The craniomandibular joint is positioned anterior to the fenestra vestibuli*.

The periotic lacks a paroccipital process (Wible et al., 2001). An epitympanic recess is present lateral to the crista parotica. The minor palatine foramina are positioned linearly on the ventral surface of the palatines, separated from the subtemporal margin. The infraobrital canal primitively opens from three foramina in the maxilla for Mammalia. In Tachyglossidae, the maxillae are perforated by multiple maxillary foramina with as few as five in *Tachyglossus* to as many as ten in *Zaglossus* (Chapter 1). Within the maxillae the maxillary branch of the trigeminal nerve, used for both mechanoreception and electroreception in monotremes (Augee et al., 2006), branches intricately (Chapter 1, Fig. 1.9). *Zaglossus* has an estimated 2000 electroreceptors in the skin of its snout and is more sensitive to electroreception than *Tachyglossus* in which

there are only about 400 electroreceptors (Manger et al., 1997; Pettigrew, 1999). The length of the snout and number of maxillary foramina piercing the maxillae are likely correlated with electroreceptive capability in Tachyglossidae (Chapter 1). It was impossible to count accurately the number of maxillary foramina in *Megalibgwilia* from images in the published literature, leaving doubt on the electroreceptive potential for *Megalibgwilia*. The posterior foramen of the maxillary canal pierces only the maxilla. The carotid foramina are positioned within the suture of the basisphenoid and basioccipital as opposed to entirely within the basisphenoid*. The anterior lamina of the periotic in pan-tachyglossids is so greatly expanded that the posterior temporal suture of the parietal contacts both the squamosal and the periotic (pers. obs., Fig. 2.12A, B). In ornithorhynchids and other mammalian taxa and mammal relatives, the parietal does not make contact with the periotic (Fig. 2.12C). The occiput of Tachyglossidae is rounded and the occipital condyles protrude beyond the occiput and are level with the floor of the cranium (pers. obs., Fig. 2.16C). *Tachyglossus*, once again, is derived compared to *Megalibgwilia* and *Zaglossus* with the occipital condyles elevated to near the middle of the back of the skull (Fig. 2.16D).

Postcranial Skeleton

If one accepts that the large, isolated fossil humeri of echidnas are assignable to *Megalibgwilia* (Helgen et al., 2012), then the argument can be made that having the entepicondylar foramen of the humerus positioned centrally within the entepicondyle, rather than close to the margin of the entepicondyle, is diagnostic for Pan-Tachyglossidae

(see Pridmore et al., 2005). Alternatively, if these humeri do not pertain to *Megalibgwilia*, then this feature could be apomorphic for crown Tachyglossidae.

Tachyglossidae

Skull

In basal pan-mammals, pan-therians, Ornithorhynchidae, and *Megalibgwilia*, the posttemporal canal is large (Griffiths et al., 1991; Archer, 1992; Rougier et al., 1992; Archer et al., 1993; Musser and Archer, 1998; Kielan-Jaworowska et al., 2004). In both *Zaglossus* and *Tachyglossus*, the posttemporal canal is relatively small (pers. obs.), which is convergent with a reduced-to-absent condition seen in extant crown therians (Wible et al., 2001). The tachyglossid secondary palate is somewhat retracted anteriorly, exposing more of the roof of the nasopharyngeal passageway than in *Megalibgwilia** (Griffiths et al., 1991; Fig. 2.4A). The palatal roof is more shallowly curved, compared to the deep curvature in *Megalibgwilia** (Griffiths, 1991). In tachyglossids, bony palatal sculpturing is reduced to absent, although the soft palate features rows of keratinized ridges (Chapter 1, Fig. 1.3). The pterygoids are small, positioned on the dorsolateral surface of the nasopharyngeal passageway and fail to meet at the midline*. Although this is likely a synapomorphy of all pan-tachyglossids, the pterygoids of *Megalibgwilia* are not described. The arteria diploëtica magna passes through a partially enclosed canal along the squamosal (Rougier et al., 1992; Wible and Hopson, 1995; Wible et al., 2001). In

some specimens of *Zaglossus*, this blood vessel is entirely enclosed in a canal that forms between the squamosal and orbitosphenoid (Chapter 1).

The ethmoidal cribriform plate is ossified, and there are more ossified endoturbinal plates in tachyglossids than in any other known mammal (see Chapter 1, Fig. 18, 19). The armadillo *Dasypus* approaches this condition, but tachyglossids appear to have the largest surface area for olfactory epithelium of any mammal (Rowe et al., 2011).

The dentary condyle of tachyglossids is dorsoventrally shallow and anteroposteriorly elongate with a mediolaterally directed arc in cross-section* (pers. obs.). The angular process is noticeably posterior to the posterior end of the reduced coronoid process, close to the dentary condyle*.

Postcranial skeleton

Zygapophyses are absent in the first five cervical vertebrae*. The lesser trochanter on the femur is small*. The pelvis of *Tachyglossus* and *Zaglossus* differs from *Ornithorhynchus* and other mammals in its perforate acetabulum.

DISCUSSION

Evolution

In contrast to several molecular analyses that called into question the monophyly of monotremes as traditionally conceived, my analysis unequivocally supported a monophyletic Monotremata that is the sister taxon to pan-therian mammals. Under the

popular ‘Australosphenida’ hypothesis (Luo et al., 2001; Kielan Jaworowska et al., 2004) it was argued that a number of Cretaceous and Paleogene mammals from the Southern Hemisphere lie along the monotreme stem, including *Steropodon* and *Teinolophos*, and that the most basal dichotomy in Mammalia was the divergence of ‘Australosphenida’ (southern mammals which include the common ancestor of monotremes) from ‘Boreosphenida’ (northern mammals which include the common ancestor of therians). Superficially, this scheme resembles the taxonomic conventions followed here, in which Pan-Monotremata and Pan-Theria are sister taxa. My phylogenetic analysis differs from the ‘Australosphenida – Boreosphenida’ hypothesis in some subtle yet important ways.

The most significant differences involve the various extinct taxa proposed as members of Australosphenida. My analysis failed to identify any known fossils that can confidently be placed on the monotreme stem. Instead, my analysis corroborates the position of *Teinolophos* as a pan-ornithorhynchid (Rowe et al., 2008), and includes both *Teinolophos* and *Steropodon* as members of crown Monotremata. All of the other putative stem-monotremes allocated to ‘Australosphenida’ (*Ambondro, Shuotherium, Asfaltomylos, Ausktrobosphenos,* and *Bishops*) were found to lie along the therian stem. This is consistent with the findings of Rowe et al. (2008) that placed these taxa within the therian crown. In spite of their lability between the therian crown and stem, no evidence was found in my analysis to support the placement of those taxa on the monotreme stem.

Because the names Australosphenida and Boreosphenida were never formally defined, it is unclear whether they were intended as total-clade names or as node-based

names, or as some other entity. The name ‘Prototheria’ is deeply entrenched in the literature as a possible synonym to Pan-Monotremata, but it suffers the same equivocation in meaning as does Australosphenida. Whereas Theriimorpha (Rowe, 1993) was explicitly defined as a total-clade name, Rowe (pers. comm.), chose to abandon the name he coined in favor of the greater taxonomic simplicity embodied in the Pan-convention, and he now prefers Pan-Theria for the total therian clade. Given the lack of phylogenetic support for the Australosphenida - Boreosphenida hypothesis, and in light of the evidence discussed above that Australosphenida is paraphyletic, it appears that a new interpretation of early mammalian history is warranted.

My analysis corroborates the basal dichotomy in mammlian evolution is between Pan-Monotremata and Pan-Theria. Although the terminology is new, this view conforms closely to the conventional picture of early mammalian evolution described in the Introduction. The oldest recognized crown mammal is the pan-therian *Phascolotherium bucklandi*, from the Middle Jurassic (Bathonian) Stonesfield Slate of England (Rowe, 1988, 1993). Another ancient pan-therian is *Juramaia sinensis*, from the Middle-Late Jurassic of China (Luo et al., 2011). These fossils indicate that the monotreme stem extends minimally at least into the Middle Jurassic, as a ghost lineage.

The divergence of crown Monotremata into Pan-Ornithorhynchidae and Pan-Tachyglossidae occurred by the Early Cretaceous, approximately 112-121 Ma. To date, all fossils assignable to Pan-Monotremata occur in the Southern Hemisphere. Until the phylogenetic positions are more robustly established for the other southern taxa once

assigned to ‘Australoshpenida,’ (most importantly *Ambondro, Asfaltomylos, Ausktrobosphenos, and Bishops*), however, it remains possible that the earliest dichotomy in mammalian history took place in the Southern Hemisphere. My analysis suggests that platypuses and echidnas were evolving independently since at least the Early Cretaceous, and since then that these two clades have been confined to the Southern Hemisphere.

Molecular estimates for the platypus and echidna divergence vary significantly and have little temporal overlap. A divergence time between 64 and 80 Ma was estimated with DNA-DNA hybridization and molecular clock methods (Westerman and Edwards, 1992). Later, a divergence time between 50 and 57 mya was estimated with α-actalbumin, with a split between monotremes and therians estimated between 163 and 186 Ma (Messer et al., 1998), which overlaps with the age of the oldest therian fossils, *Phascolotherium bucklandi* (Rowe, 1988) and *Juramaia sinensis*, from the Middle Jurassic (Luo et al., 2011). One study using protamine P1 genes estimated the time of divergence between the two monotreme families to be as recent as 22.3 Ma (Retief et al., 1993), while mitochondrial 12S RNA sequences were used to estimate a divergence date between 14 and 15 Ma, though thought the authors admitted that this could be an underestimate (Gemmell and Westerman, 1994). Using a relaxed-molecular-clock method from a five-nuclear gene dataset from van Rheede et al. (2006), Rowe et al. (2008) estimated a broad range of divergence dates that overlapped with the Early Cretaceous date obtained from the Flat Rocks locality (Rich et al., 2001). Increased precision of the relaxed molecular clock methods was attempted with the addition of two

other nuclear genes alongside complete mitochondrial genome sequences, recovering a median estimate of 27.7 Ma (Phillips et al., 2009).

Unfortunately, because *Kryoryctes* was not resolved to be within Monotremata, there is no evidence of a tachyglossid-like monotreme dating to the Early Cretaceous. It is possible that discovery of more complete skeletal material attributable to *Kryoryctes*, currently only known from a single humerus, will recover a relationship within Monotremata.

To the degree that my findings are correct, because Tachyglossidae is a sister group to the platypuses, it must have a ghost lineage from the Early Cretaceous to the Miocene. Relatively complete skulls of extinct monotremes are not known until the latter half of the Cenozoic. Two diagnostic characters of tachyglossids, absence of teeth and a thin, reduced jaw, probably explain why fossil echidnas are not yet known from older deposits, and why it is not surprising that the fossil record of echidnas stretches only as far back as the Miocene.

With the Miocene fossil *Megalibgwilia* positioned as the sister taxon to Tachyglossidae it is possible that *Zaglossus* and *Tachyglossus* diverged relatively recently. The possibility of a recent divergence between *Zaglossus* and *Tachyglossus* is supported by molecular estimates ranging from 100,000 years ago (Westerman and Edwards, 1992) to 2 mya (Gemmell and Westerman, 1994). However, the entire Cenozoic fossil record of Pan-Monotremata is fragmentary and it is entirely unrepresented over long spans of geological time. In light of all the conflicting, non-

overlapping molecular clock estimates for the platypus-echidna divergence, it is difficult to place confidence in similar methods when used to date the *Zaglossus*-*Tachyglossus* divergence.

CONCLUSIONS: A PORTRAIT OF THE ANCESTRAL MONOTREME

In light of the diagnosis of Monotremata presented above, the ancestral monotreme was likely a small, insectivorous, terrestrial scratch-digger. It had an elongated face whose surface was covered with skin that held hundreds to thousands of individual electroreceptor cells. If *Steropodon, Kollikodon*, or *Teinolophos* resemble the ancestral condition, given the shape of their dentaries, it is unlikely that the ancestral monotreme had a 'duck-bill' in spite of its electoreceptive capabilities. Instead, the shape of its snout was probably intermediate in width between that of *Ornithorhynchus* and the echidnas. Although it is commonly asserted that monotremes have no teeth, the fossil evidence indicates that the ancestral monotreme had a fully developed dentition which it used in mastication.

The ancestral monotreme used electroreception along with a highly developed sense of olfaction to hunt prey that probably included terrestrial vertebrates, arthropods, and other animals. That the ancestral monotreme had a fairly well-developed system of electroreception suggests that it may have hunted for prey in moist environments, such as the moist understory of the rainforests in which *Zaglossus* lives today and into which it probes its long snout while searching for prey. *Tachyglossus* is derived in reducing its electroreception capability, and in restricting its diet to myrmecophagy.

The monotreme ancestor gave rise to the semi-aquatic platypus lineage, in which electroreception reached the pinnacle of sensitivity. Concomitant with this was a diminution of the olfactory system. Having lost its masticatory teeth, the echidna lineage may be secondarily specialized in its diet of worms, small arthropods, termites and ants. Some echidnas remain in their ancestral terrestrial habit, possessing large claws for digging and a large olfactory system developed to a far greater degree than in other mammals. Although *Tachyglossus* is commonly used in phylogenetic analyses, in many regards it is the most specialized of all, possessing a snout shorter than half the length of its skull, reducing the number of electroreceptors, and in the capacity to thrive in arid environments. The important message here is that *Zaglossus* and *Ornithorhynchus* together present a far more accurate picture of Monotremata when choosing representative taxa for phylogenetic analysis.

If *Steropodon* and *Teinolophos* are indicative of the true size of the ancestral monotreme, then size increase has characterized both daughter clades. *Obdurodon* and *Ornithorhynchus anatinus* are both considerably larger than these early ornithorhynchids. Among pan-tachyglossids, the largest-bodied monotremes known are *Zaglossus* and the more robust *Megalibgwilia*. The largest monotreme yet reported, '*Zaglossus*' *hacketti* Glauert, 1914, is based on an isolated humerus and is estimated to weigh 20 kg (Murray, 1978; Helgen et al., 2012).

The platypus lineage is equally sensational in its transformations from the ancestral condition. Its development of a widened snout and the fleshy bill that encloses

an array of 40,000 electroreceptors and 60,000 pressure receptors is unique among mammals. Now that we understand just how its sensory system works, the nick-name 'duck-billed' platypus is a misnomer at best. And the profound modification of its dentition that occurred since it branched from its close relative *Obdurodon* remains an enigma to the many paleontologists who rely upon dental characters to reconstruct mammalian phylogeny, and have done so for more than a century; it is still the subject of controversy.

Many questions surrounding monotreme evolution remain to be answered. Perhaps the most important is whether there ever was a diversification of this clade approaching that of the pan-therians. Whereas the entire tally of living and extinct monotremes amounts to only about a dozen species, extant Theria alone comprises nearly 5000 species, and there is probably an equal number of extinct species. The marked asymmetry of these clades only invites speculation, and encourages more fieldwork in the Southern Hemisphere.

Table 2.1: List of specimens observed in museum collections.

Taxon	Specimen number
Tritylodontidae	
Kayentatherium	MCZ 8812
Monotremata	
Ornithorhynchus anatinus	AMNH 200255
	AMNH 252512
	MCZ 29073
	MCZ 42718
	TMM M-5899
Obdurodon dicksoni	AMNH 128800 (plastotype)
Tachyglossus aculeatus	AMNH 35679
	AMNH 65833
	AMNH 65842
	AMNH 107185
	AMNH 105202
	MCZ 29075
	MCZ 29163
	TMM M-1741
	TMM M-1826
	TMM M-2949
Zaglossus bartoni	AMNH 157072
	AMNH 190862
Zaglossus brujni	MCZ 7397
	MCZ 12414
	MCZ 59685
Megalibgwilia ramsayi	AMNH 18353 (cast)
Theria	
Didelphis marsupialis	AMNH 240520
	TMM M-1197
	TMM M-2164
	TMM M-2205
Didelphis virginiana	AMNH 217744
Erinaceous europaeus	TMM M-3670

Table 2.2: Table of URL codes for specimens accessed on DigiMorph.org. Specimens listed in alphabetical order by taxon.

Specimen	DigiMorph.org URL
Dasypus novemcinctus TMM M-7417	http://digimorph.org/specimens/Dasypus_novemcinctus/
Didelphis virginiana TMM M-2517	http://digimorph.org/specimens/Didelphis_virginiana/
Hadrocodium wui IVPP 8275	http://digimorph.org/specimens/Hadrocodium_wui/
Kryptobaatar dashzevegi PSS-MAE 101	http://digimorph.org/specimens/Kryptobaatar_dashzevegi/
Morganucodon oehleri IVPP 8685	http://digimorph.org/specimens/Morganucodon_oehleri/
Obdurodon dicksoni QM F20568	http://digimorph.org/specimens/Obdurodon_dicksoni/
Ornithorhynchus anatinus AMNH 200255	http://digimorph.org/specimens/Ornithorhynchus_anatinus/adult/
Ornithorhynchus anatinus AMNH 252512	http://digimorph.org/specimens/Ornithorhynchus_anatinus/juvenile/
Probainognathus sp. PVSJ 410	http://digimorph.org/specimens/Probainognathus_sp/
Tachyglossus aculeatus AMNH 154457	http://digimorph.org/specimens/Tachyglossus_aculeatus/skull/
Vincelestes neuquenianus MACN-N 04	http://digimorph.org/specimens/Vincelestes_neuquenianus/
Vombatus ursinus TMM M-2953	http://digimorph.org/specimens/Vombatus_ursinus/
Zaglossus bartoni AMNH 157072	http://digimorph.org/specimens/Zaglossus_bartoni/
Zaglossus bruijni MCZ 7379	http://digimorph.org/specimens/Zaglossus_bartoni/

Table 2.3: List of literature references for cranial and postcranial anatomy of various taxa used in the morphological analysis. Literature is organized by taxon. Taxa arranged alphabetically.

Taxon	Citation(s)
Ambondro mahabo	Flynn et al., 1999; Luo et al., 2001
Asfaltomylos patagonicus	Rauhut et al., 2002
Ausktribosphenos nyktos	Rich et al., 1997; Kielan-Jaworowska et al., 1998; Luo et al., 2001
Bishops whitmorei	Rich et al., 2001
dryolestoids	Martin, 1999; Asher et al., 2007; Rougier et al., 2011, 2012
early mammals	Kielan-Jaworowska et al., 2004
Eomaia scansoria	Ji et al., 2002
Fruitafossor windscheffeli	Luo and Wible, 2005
Gobiconodon ostromi	Jenkins and Schaff, 1988
Haldanodon expectatus	Martin, 2005
Jeholodens jenkinsi	Qiang et al., 1999

Table 2.3 (continued)

Kayentatherium wellesi	Sues, 1986
Kryoryctes cadburyi	Pridmore et al., 2005
Obdurodon insignis and *Obdurodon dicksoni*	Archer et al., 1978; Archer, 1992, 1993; Musser and Archer, 1998
Ornithorhynhcus anatinus	Kesteven, 1940; Kuhn and Zeller, 1987 1989a, b, 1993
Megalibgwilia ramsayi	Murray, 1978; Griffith et al., 1991
Monodelphis brevicaudata	Wible, 2003
Monotremata (comparative across different taxa)	Van Bemmelen, 1901; Watson, 1916; Simpson, 1938; Gregory, 1947; Griffiths, 1978; Kielan-Jaworowska et al., 1987; Pridmore et al., 2005
Morganucodonta (comparative across different taxa)	Jenkins and Parrington, 1976; Wible and Hopson, 1995
Multituberculata (comparative across different taxa)	Jenkins and Krause, 1983; Kielan-Jaworowska, 1989; Wible and Hopson, 1995; Kielan-Jaworowska, 1997; Wible and Rougier, 2000; Hurum and Kielan-Jaworowska, 2008
Sinodelphys szalayi	Luo et al., 2003

Table 2.3 (continued)

Steropodon galmani	Archer et al., 1985
Tachyglossus aculeatus	Kuhn, 1971
Vincelestes neuquenianus	Rougier et al., 1992
Zaglossus bruijni	Gervais, 1877-1878; Allen, 1912; Griffiths et al., 1991

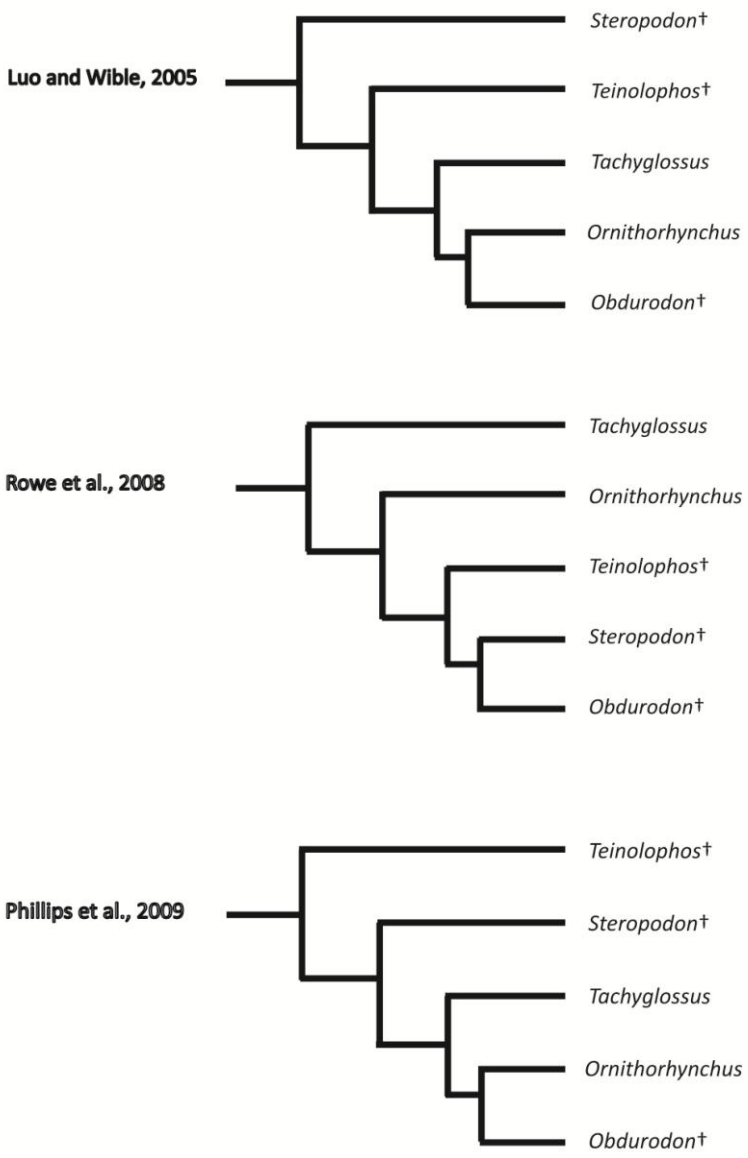

Figure 2.1: Three recently published hypotheses of monotreme relationships. The hypothesis proposed by Luo and Wible (2005) and the hypothesis proposed by Phillips et al. (2009) are similar in that the two Early Cretaceous monotreme fossils included in the analysis are positioned as basal monotremes and differ from the hypothesis proposed by Rowe et al. (2008) where the two Early Cretaceous monotreme taxa are positioned as derived ornithorhynchids. Tachyglossids positioned as basal monotremes (Rowe et al., 2008), suggests a divergence between tachyglossids and ornithorhynchids as far back as the Early Cretaceous.

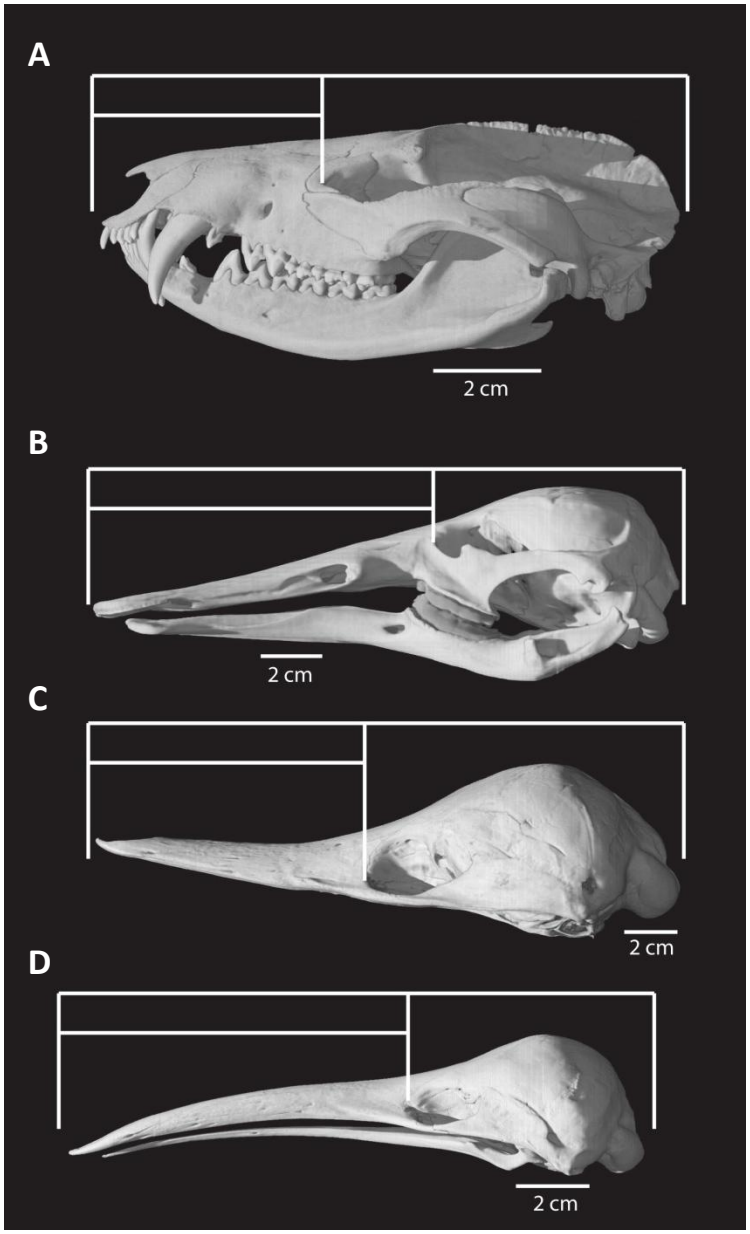

Figure 2.2: Rostrum length in *Didelphis virginiana* TMM M-2517 (A), *Ornithorhynchus anatinus* AMNH 200255 (B), *Tachyglossus aculeatus* AMNH 154457 (C), and *Zaglossus bartoni* AMNH 157072 (D). Rostrum length is measured from terminal end of premaxillae to lacrimal foramen. A rostrum length of less than half the length of the skull is typical of mammals and mammal relatives. A rostrum length longer than half the length of the skull is characteristic of monotremes with the exception of *Tachyglossus*. *Myrmecophago* and cetaceans also have a rostrum length longer than half the length of the skull.

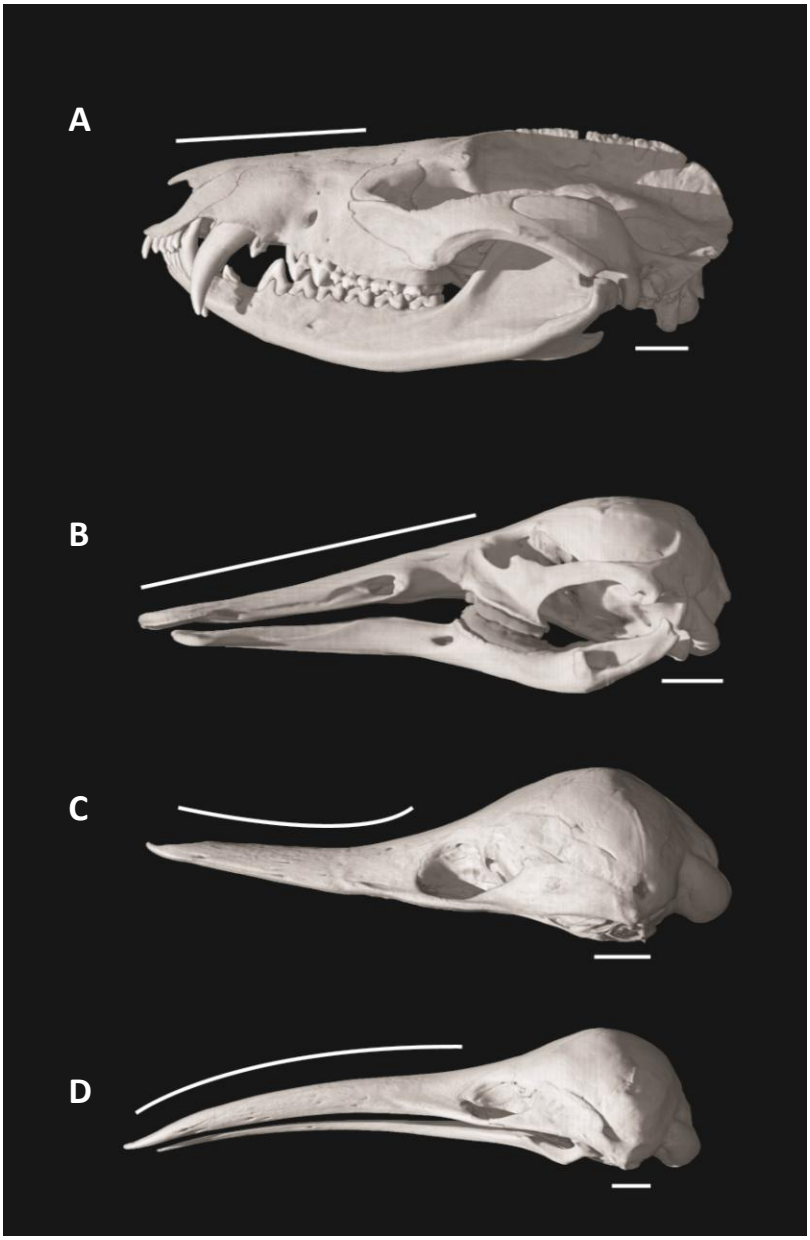

Figure 2.3: Curvature of rostrum (emphasized by white line) in *Didelphis virginiana*, TMM M-2517 (A), *Ornithorhynchus anatinus* AMNH 200255 (B), *Tachyglossus aculeatus* AMNH 154457 (C), and *Zaglossus bartoni* AMNH 157072 (D). *Didelphis* has a short and straight rostrum common in mammals and mammal relatives. *Ornithorhynchus* is an example of a straight, and ventrally directed, rostrum. The recurved rostrum is an autapomorphy of *Tachyglossus*. The decurved rostrum is illustrated here in *Zaglossus*. Scale bar = 1 cm.

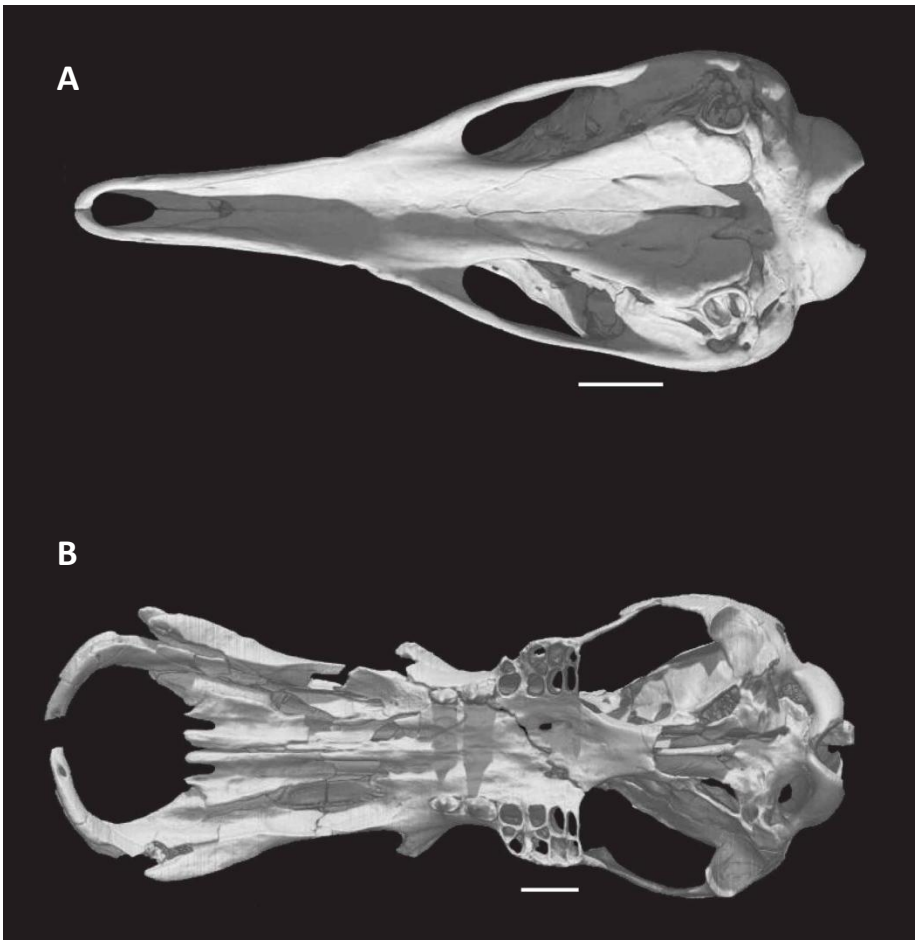

Fig. 2.4. Roof of nasopharyngeal passageway visible in ventral view is a synapomorphy of Tachyglossidae. *Tachyglossus aculeatus* AMNH 154457 (A) illustrates the rostral exposure of the roof of the nasopharyngeal passageway from an anteriorly retracted secondary palate. In the extinct tachyglossid, *Megalibgwilia*, the anterior end of the secondary palate does not recede as far posteriorly as it does in *Tachyglossus* and *Zaglossus* exposing only a small portion of the roof of the nasopharyngeal passageway. *Obdurodon dicksoni* QM F20568 (B) illustrates the plesiomorphic condition where the secondary palate extends anteriorly to cover the nasopharyngeal passageway in ventral view. Scale bars = 1 cm.

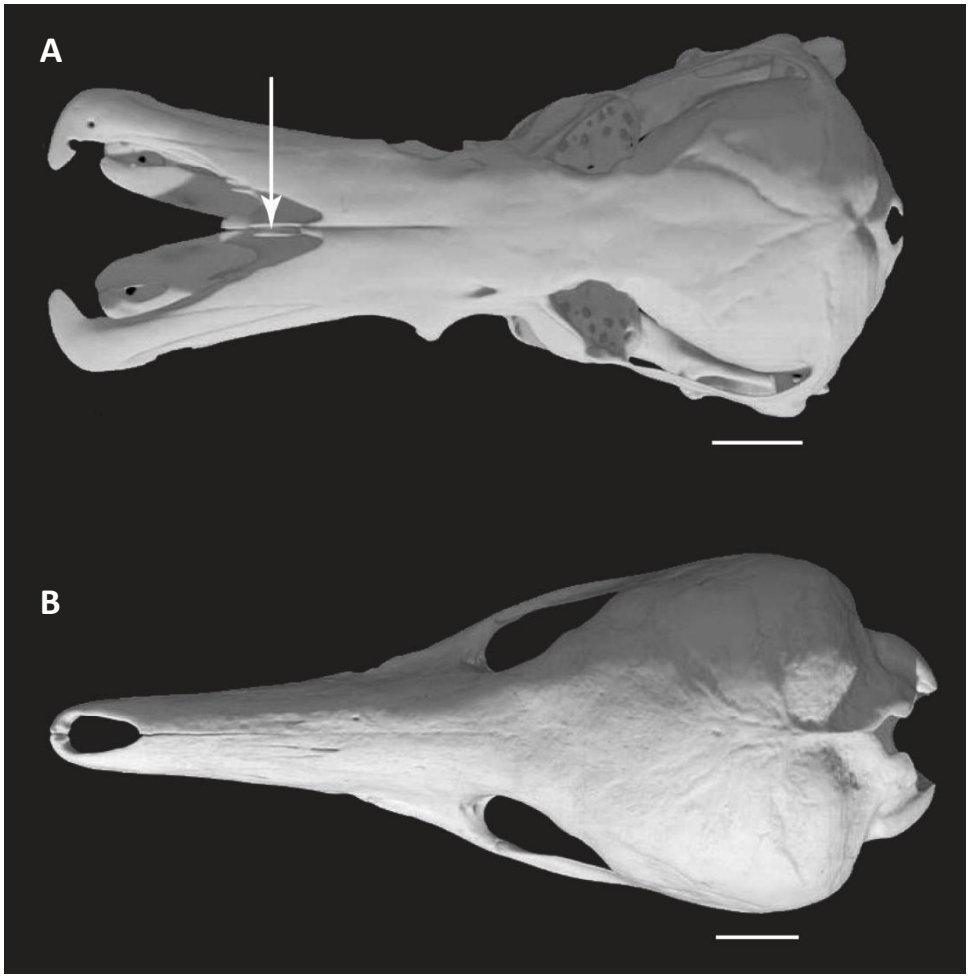

Figure 2.5: Exposure of vomer in dorsal view is a synapomorphy of Ornithorhynchidae. *Ornithorhynchus anatinus* AMNH 200255 (A) illustrates the vomer, visible in dorsal view because the medial portion of the nasal does not expand far anteriorly as in other mammals and mammal relatives. In tachyglossids such as *Tachyglossus aculeatus* AMNH 154457 (B), the nasals and septomaxilla cover the vomer in dorsal view. Scale bar = 1 cm.

Figure 2.6: Medial incision on the posterior margin of the palate, outlined in white is a tachyglossids synapomorphy. In *Tachyglossus aculeatus* AMNH 154457 (A), a medial incision cuts through the posterior end of the secondary palate so that the posterior ends of the palatines do not contact one another medially. In other mammals including *Ornithorhynchus* AMNH 200255 (B), the posterior margin of the secondary palate is relatively straight and entire, with the palatines contacting medially along their lengths. Skulls are shown to scale. Scale bar = 1 cm.

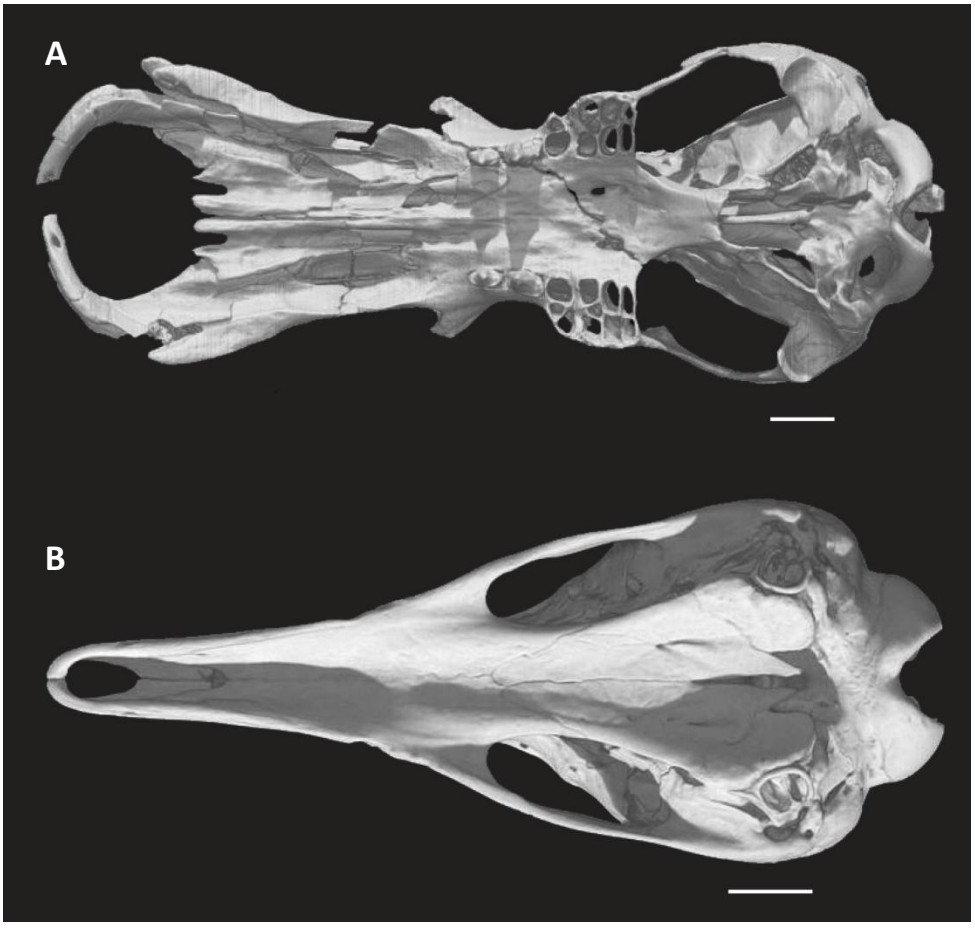

Figure 2.7: Anterior margin of secondary palate is formed by maxilla in monotremes. For mammals, the secondary palate is primitively composed of the premaxillae, maxillae, and palatines. In monotremes, the palatal processes of the premaxillae do not grow medially and contribute to the secondary palate as shown by *Obdurodon dicksoni* QM F20568 (A) and *Tachyglossus aculeatus* AMNH 154457 (B). Instead, the maxillae form the anterior margin of the secondary palate. Scale bar = 1 cm.

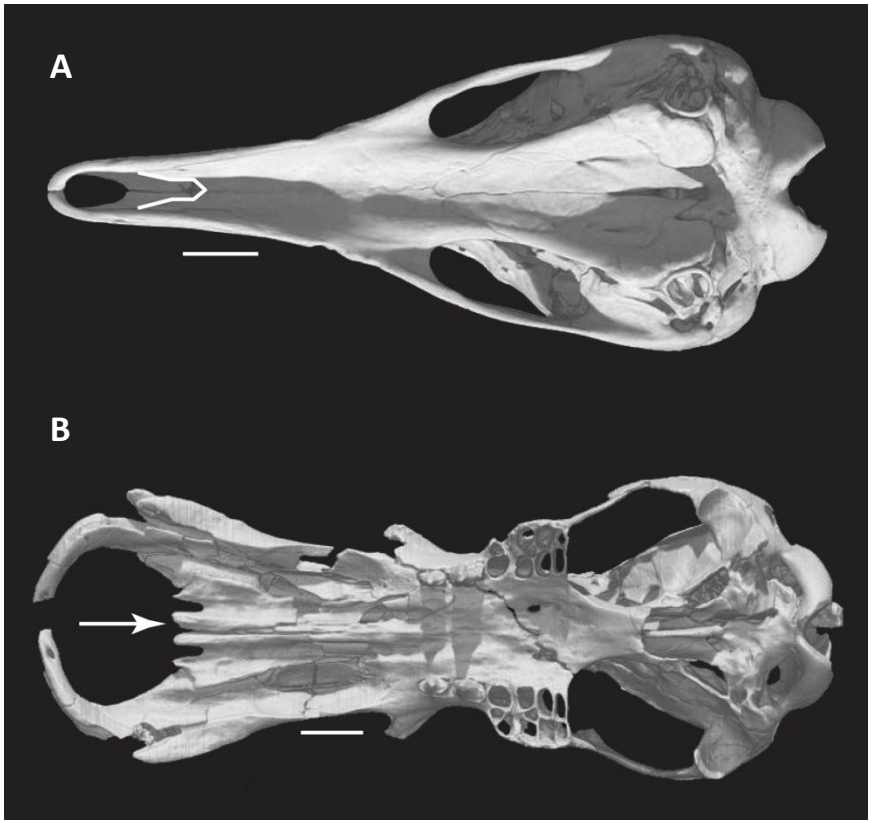

Figure 2.8: A synapomorphy of Tachyglossidae is for the palatal processes of the maxillae to be smooth and form a concave, 'V'-shaped anteroventral margin of the maxillae, as shown by the white outline on *Tachyglossus aculeatus* AMNH 154457 (A). *Obdurodon dicksoni* QM F20568 (B) illustrates the plesiomorphic condition for mammals with the anteroventral margin of the maxillae forming a zig-zag, 'W' shape, indicated by the arrow. Scale bar = 1 cm.

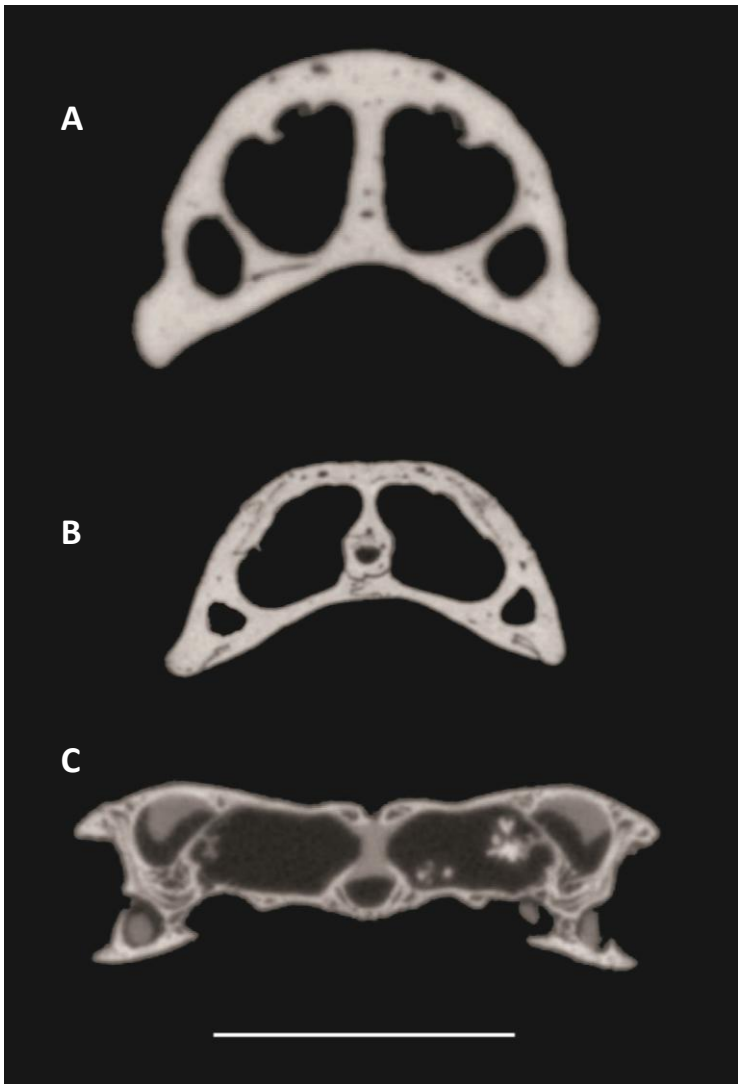

Figure 2.9: In Tachyglossidae, the anterior end of the hard palate is narrowly arched, as seen in *Tachyglossus aculeatus* AMNH 154457 (A) and *Zaglossus bartoni* AMNH 507072 (B). A flat hard palate is plesiomorphic for mammals, as illustrated by *Ornithorhynchus anatinus* AMNH 200255 (C). The hard palate in the extinct tachyglossid, *Megalibgwilia* (not shown), is broadly arching in cross section (Griffiths et al., 1991). Scale bar = 1 cm.

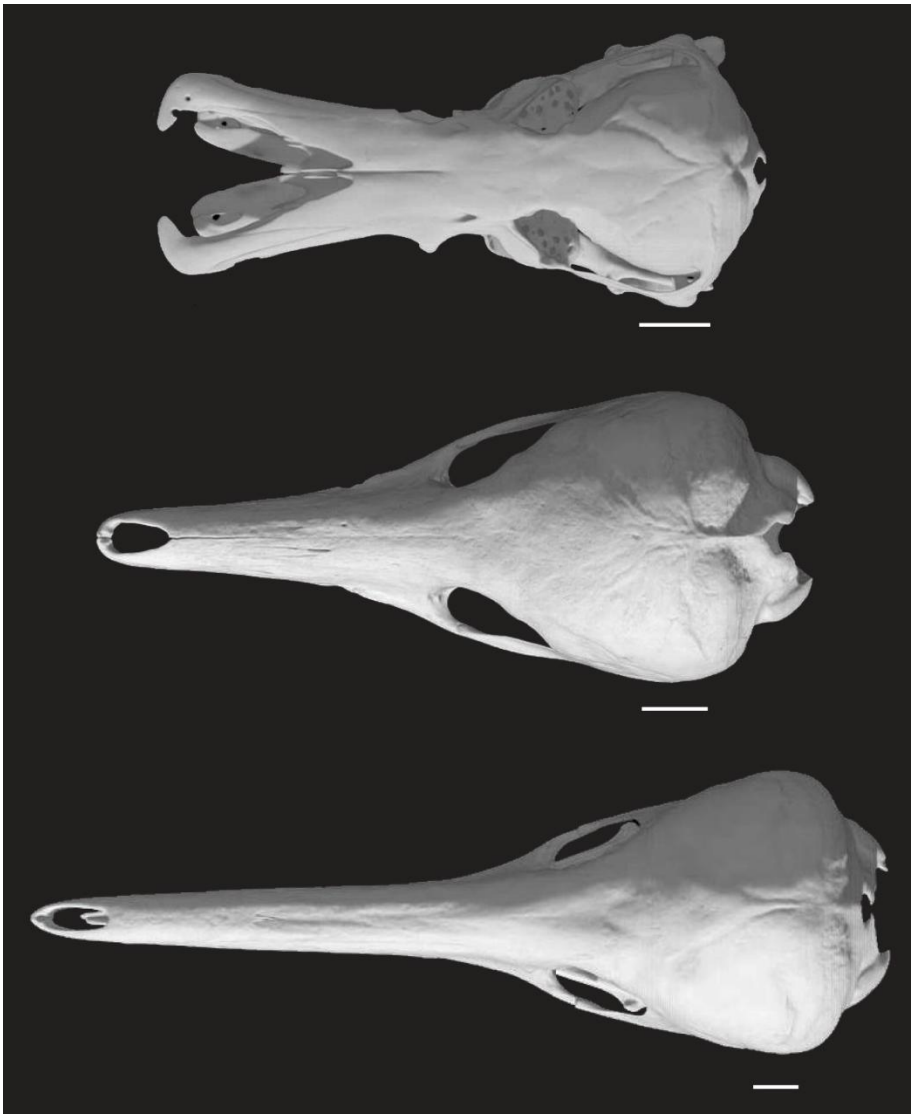

Figure 2.10: Parietal sculpturing in *Ornithorhynchus anatinus* AMNH 200255 (top), *Tachyglossus aculeatus* AMNH 154457 (middle), and *Zaglossus bartoni* AMNH 507072 (bottom). In mammals, the sagittal crest is a site of muscle attachment. Monotremes, which lack a prominent sagittal crest and lambdoidal crest, develop sculpturing on the parietal where muscles of the head attach and leave scars (Van Bemmelen, 1901). Scale bar = 1 cm.

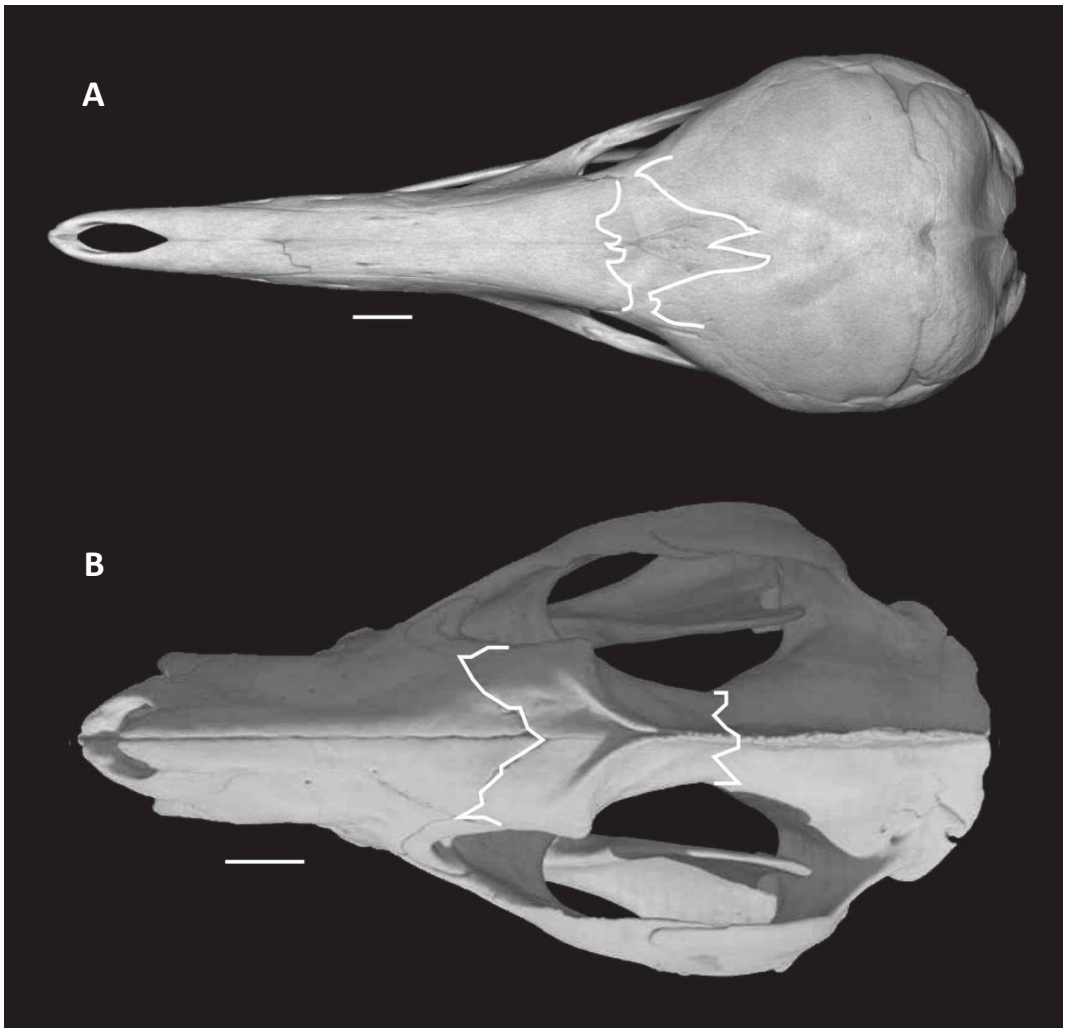

Figure 2.11: Anterior parietal suture nearly contacts, and occasionally contacts, the nasals in monotremes, as seen *Zaglossus bartoni* AMNH 157072 (A). *Didelphis virginiana* TMM M-2517 (B) illustrates the plesiomorphic condition where parietal and nasals are greatly separated by the frontal. The posterior nasal suture and anterior parietal suture are outlined in red. Scale bar = 1 cm.

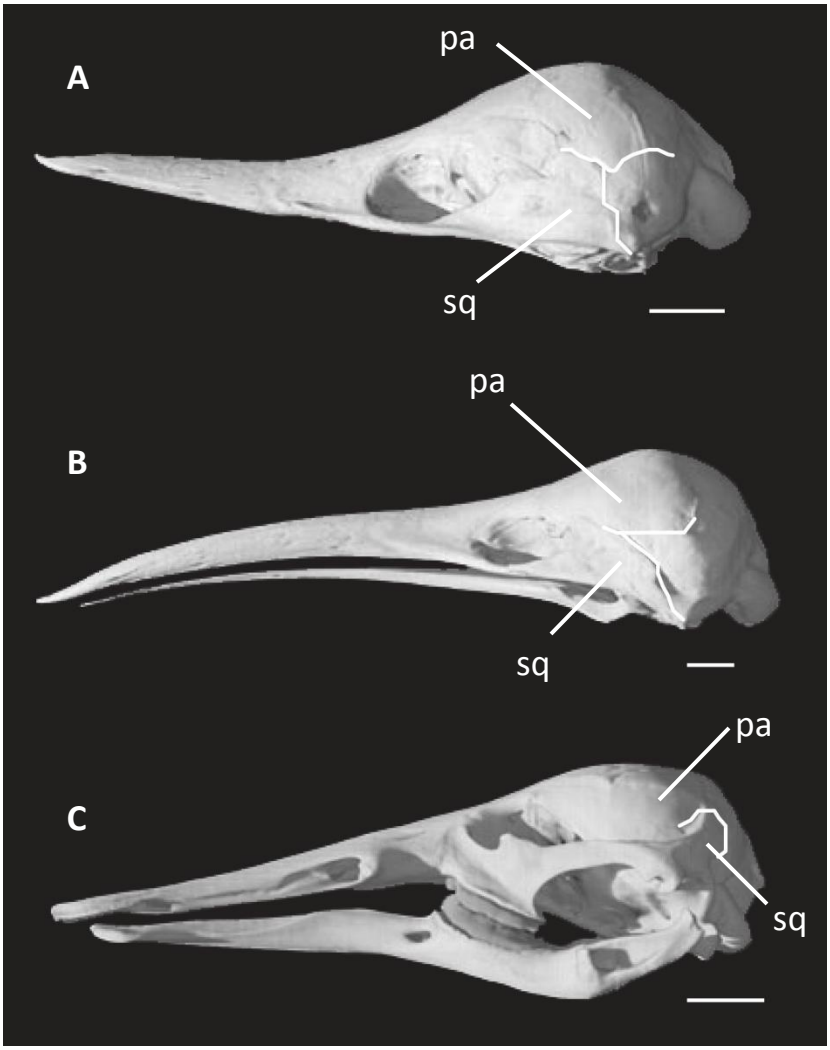

Figure 2.12: Contact of the posterior portion of the parietal temporal suture differs between tachyglossids and ornithorhynchids. In Tachyglossidae, the posteroventral margin of the parietal contacts both the squamosal and the periotic, as seen in *Tachyglossus aculeatus* AMNH 154457 (A) and *Zaglossus bartoni* AMNH 507072 (B). *Ornithorhynchus anatinus* AMNH 200255 (C) illustrates the primitive condition of a parietal that only contacts the squamosal and not the periotic simultaneously. Scale bar = 1 cm. pa = parietal, sq = squamosal.

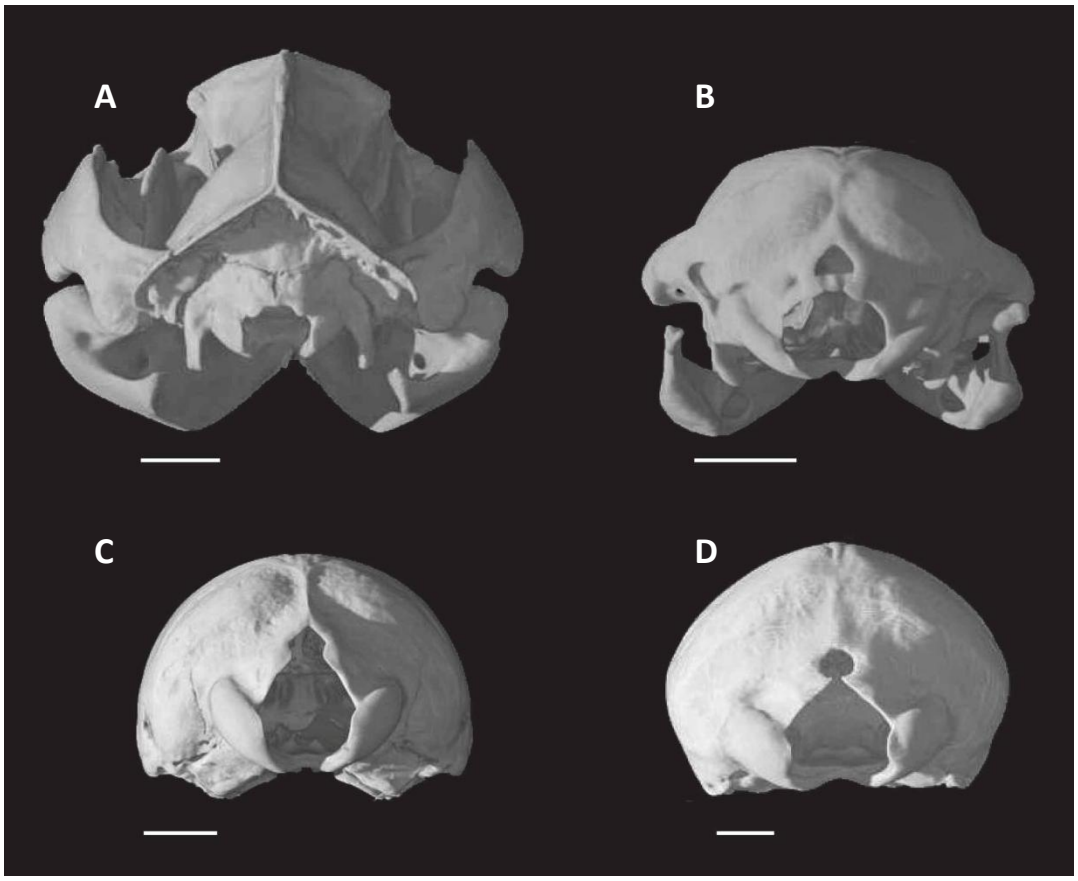

Figure 2.13: The incisura occipitalis is present in monotremes but not in all other mammals. The foramen magnum is typically an entire, circular opening in the back of the skull as seen in *Didelphis virginiana* TMM M-2517 (A). All monotremes known from complete skulls however, have a large incision on the dorsomedial margin of the foramen magnum, shown in *Ornithorhynchus anatinus* AMNH 200255 (B), *Tachyglossus aculeatus* AMNH 154457 (C), and *Zaglossus bartoni* AMNH 157072 (D). Scale bars = 1 cm.

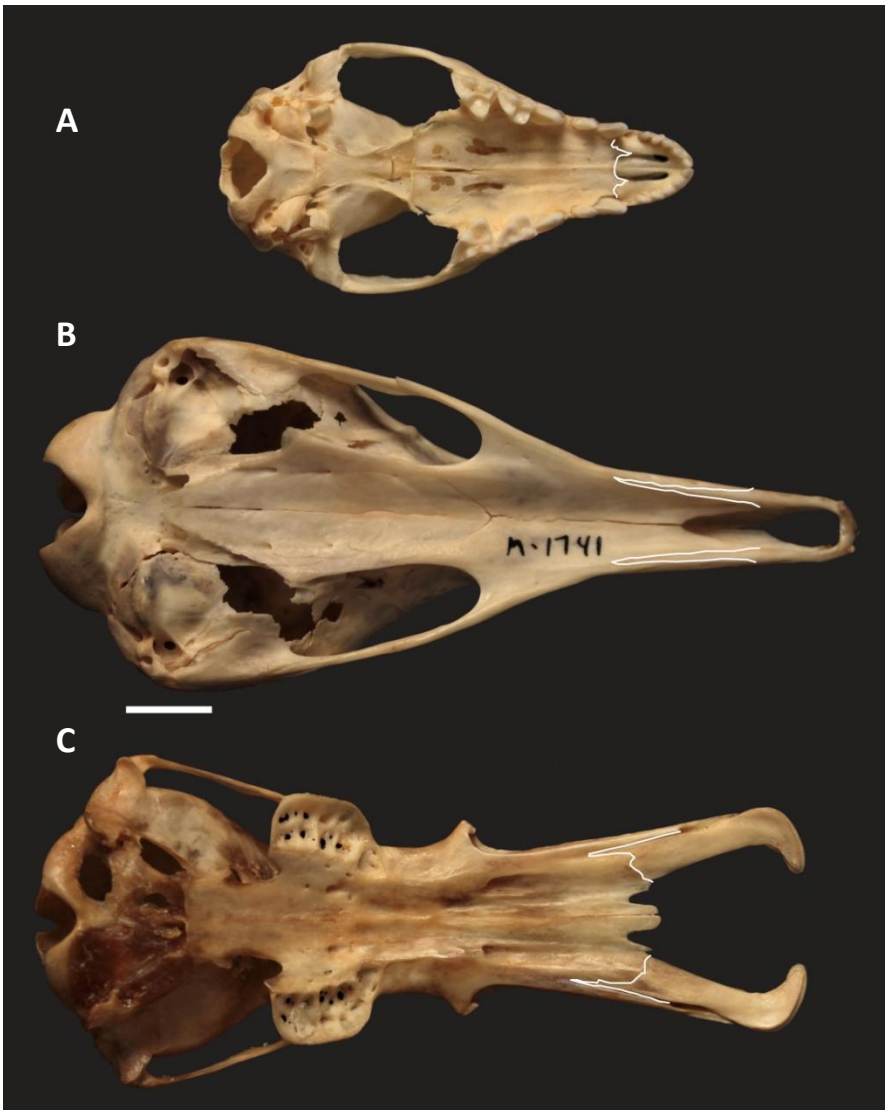

Figure 2.14: In therians such as *Didelphis virginiana* TMM M-2164 (A), the palatal processes are short and terminate at or before the upper canines. In monotremes the palatal processes of the premaxillae are unhindered by the presence of canines and extend far posterior. In *Tachyglossus aculeatus* TMM M-1741 (B) and other tachyglossids, the processes extend relatively farther posterior than in *Ornithorhynchus anatinus* TMM M-5899 (C) and other ornithorhynchids, measuring approximately the entire length of the snout. The palatal processes of the premaxillae are outlined in white. Skulls are shown to scale; scale bar = 1 cm.

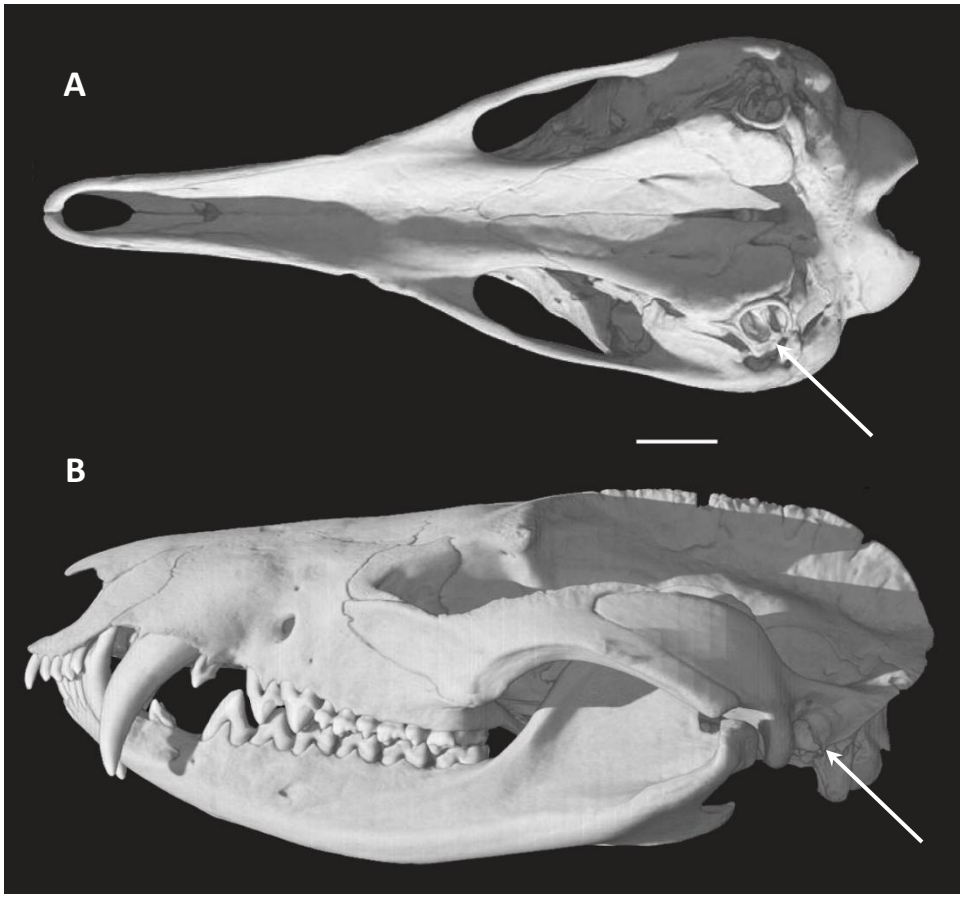

Figure 2.15: Middle ear ossicles are oriented on a horizontal plane in the monotremes. In monotremes such as *Tachyglossus aculeatus* AMNH 154457 (A), the relatively large middle ear ossicles are oriented in a horizontal plane on the ventral surface of the skull, indicated by the white arrow. In therians including *Didelphis virgiana* TMM M-2517 (B), the small middle ear ossicles are enclosed within the ectotympanic and are positioned laterally on the skull, indicated by white arrow. Skulls are shown to scale. Scale bar = 1 cm.

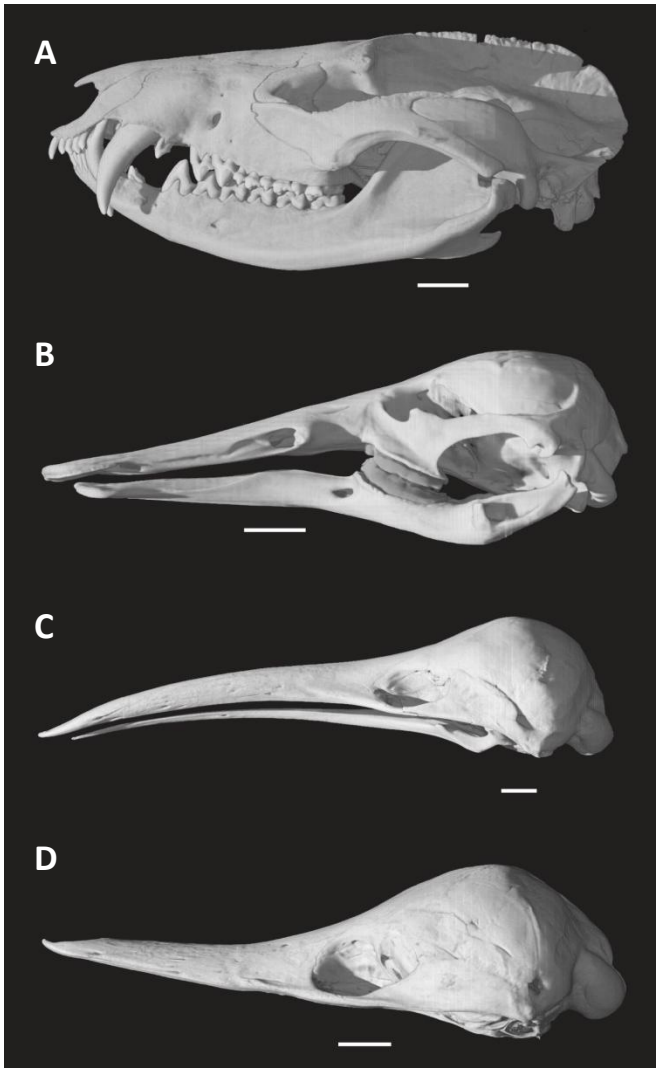

Figure 2.16: Position of occipital condyles in *Didelphis virginiana* TMM M-2517 (A), *Ornithorhynchus anatinus* AMNH 200255 (B), and *Zaglossus bartoni* AMNH 157072 (C), are lower on the skull than in *Tachyglossus aculeatus* AMNH 154457 (D). The bottom of the occipital condyles is typically aligned with the most ventral portion of the skull. In *Tachyglossus aculeatus*, however, the bottom of the occipital condyles is positioned above the most ventral portion of the skull. Scale bar = 1 cm.

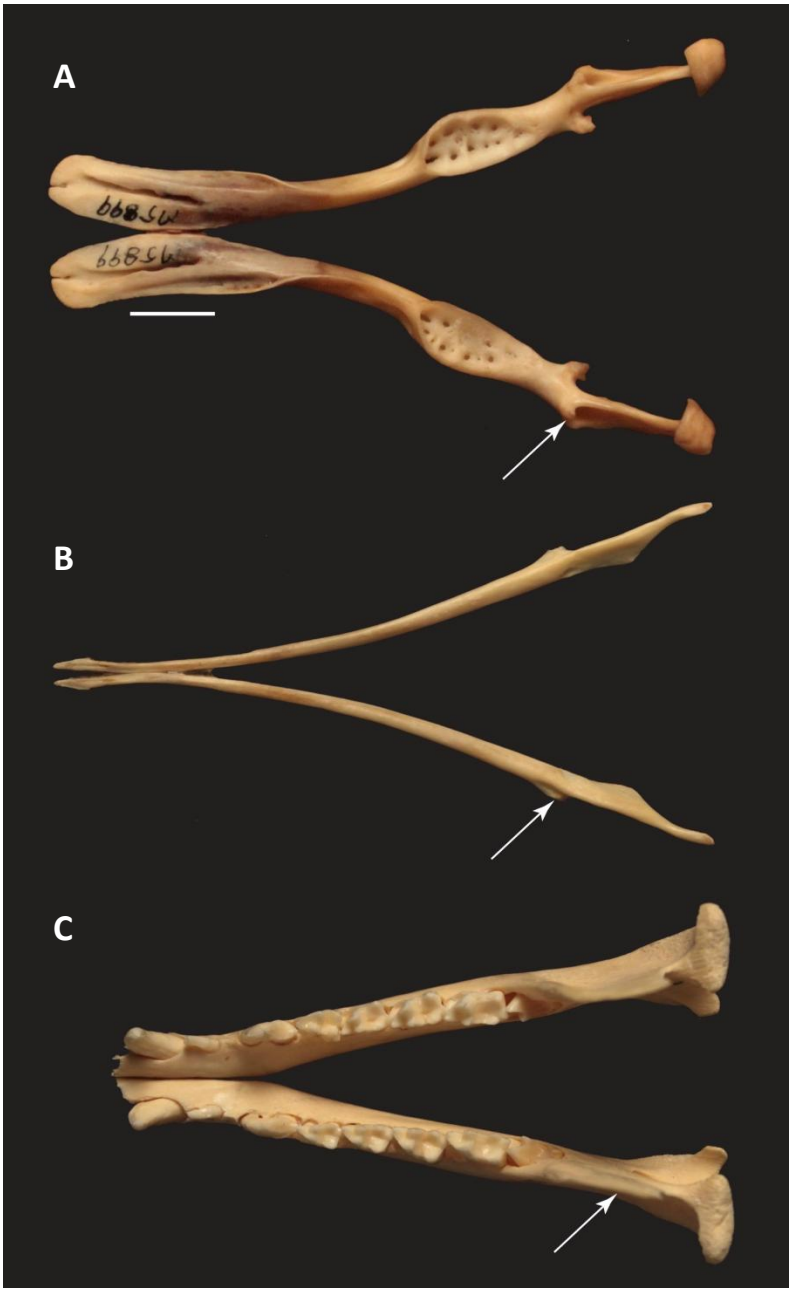

Figure 2.17: Lateral orientation of coronoid process in the mandibles of *Ornithorhynchus anatinus* TMM M-5899 (A), *Tachyglossus aculeatus* TMM M-1826 (B), and *Didelphis virginiana* TMM M-2205 (C). In extant monotremes, the coronoid process, though reduced, is oriented laterally as opposed to oriented dorsally so that it is in alignment with the long axis of the dentary. Lower jaws are shown to scale. Scale bar = 1 cm.

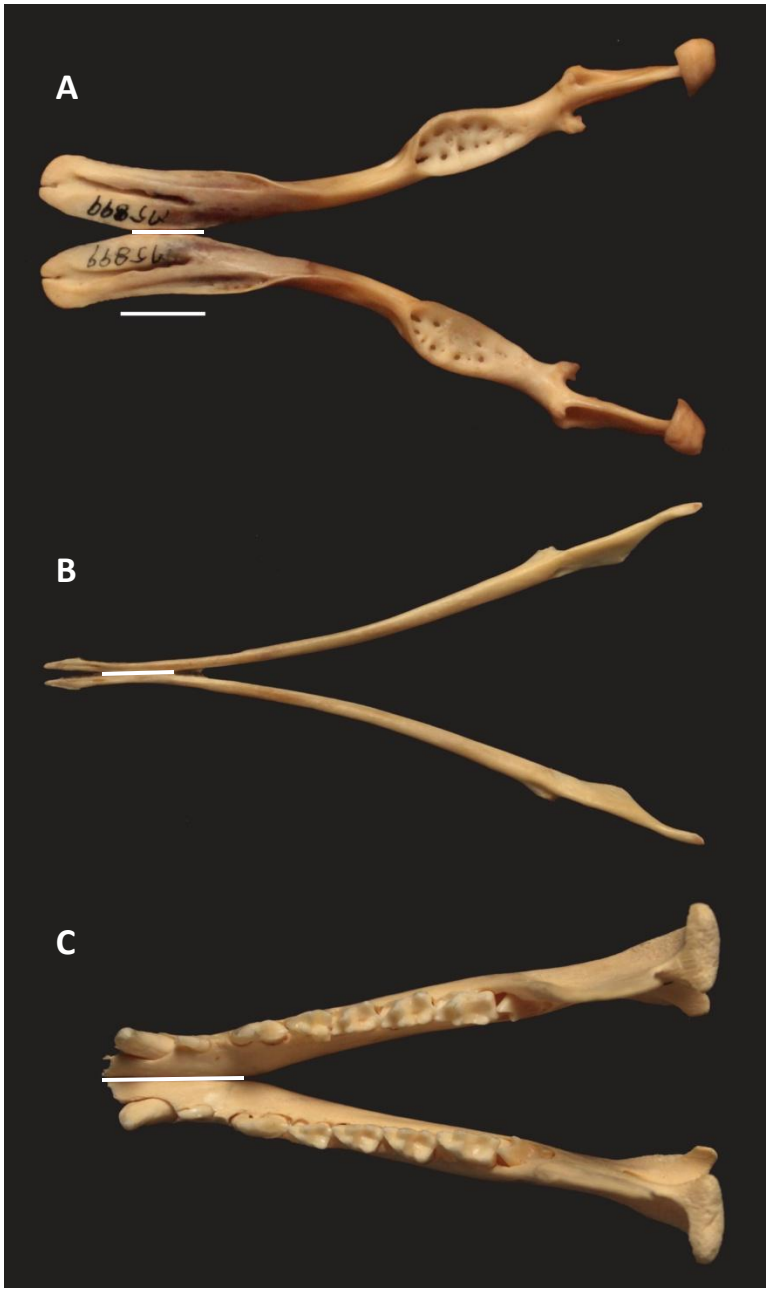

Figure 2.18: The dentary symphysis in monotremes such as *Ornithorhynchus anatinus* TMM M-5899 (A) and *Tachyglossus aculeatus* TMM M-1826 (B), does not reach the terminal ends of the dentaries. The dentary symphysis in *Didelphis virginiana* TMM M-2205 (C) is in the plesiomorphic position, anterior and connecting the terminal ends of the dentaries. Lower jaws are shown to scale. Scale bar = 1 cm.

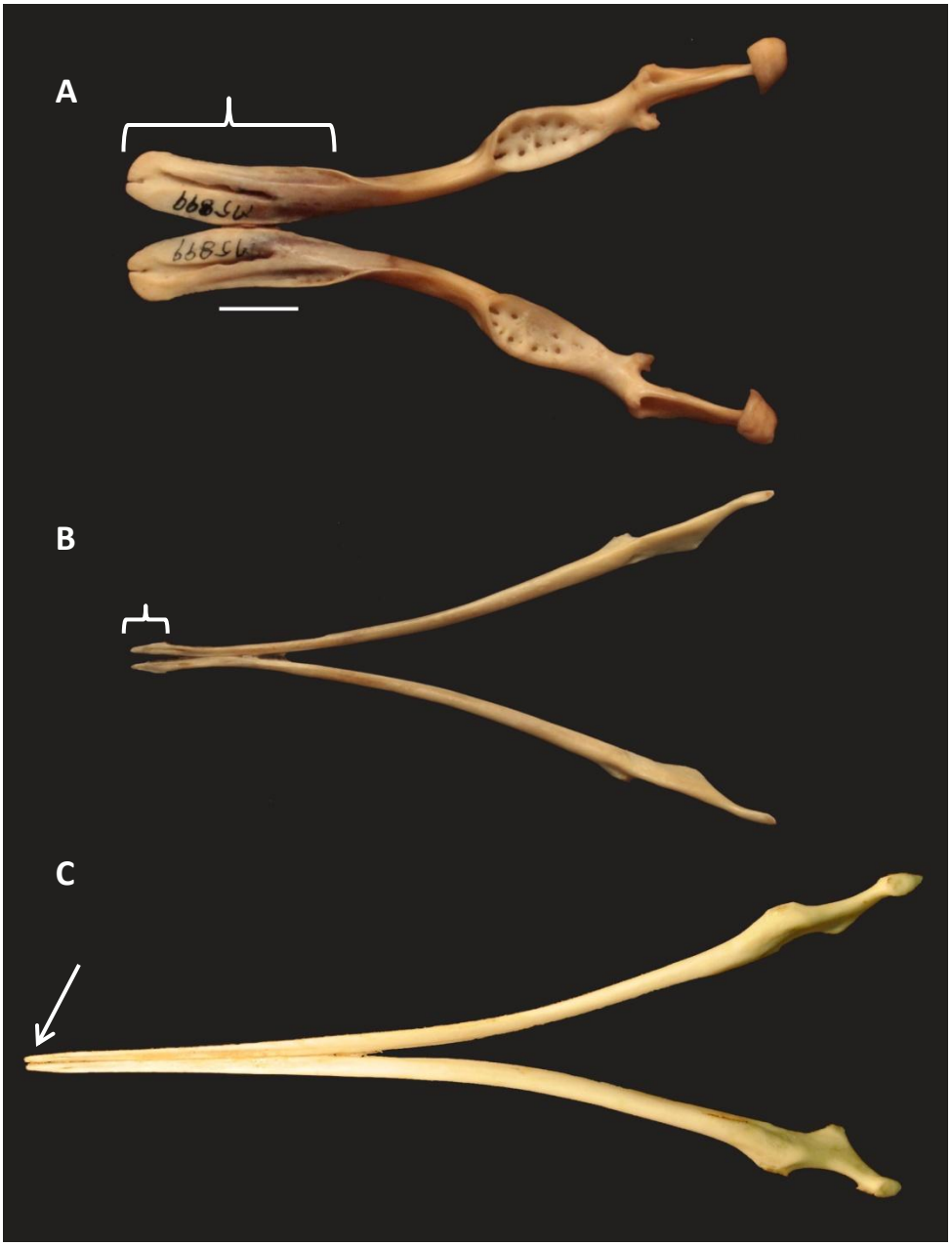

Figure 2.19: Varying shapes of terminal end of dentaries in *Ornithorhynchus anatinus* TMM M-5899 (A), *Tachyglossus aculeatus* TMM M-1826 (B) and *Zaglossus bartoni* AMNH 194702 (C). The terminal end of the dentaries in *Ornithorhynchus* and *Tachyglossus* are dorsoventrally flattened and laterally expanded, giving them a spatulate shape. In *Zaglossus*, the terminal ends of the dentaries are thin splints that are circular in cross section. Lower jaws are shown to scale. Scale bar = 1 cm.

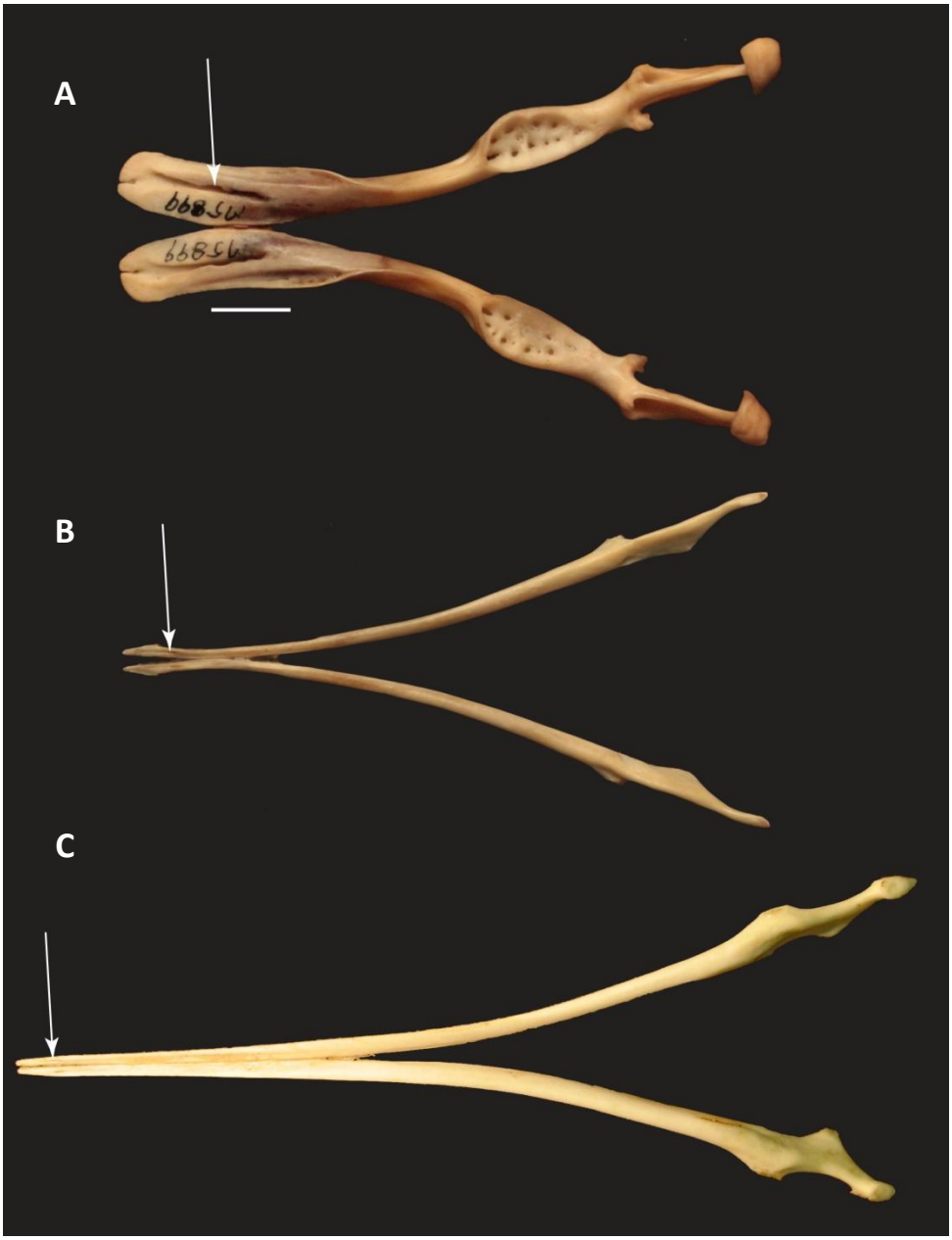

Figure 2.20: Medial "foramen mandibulare anterius dorsale" (Zeller, 1989a: fig. 22) in *Ornithorhynchus anatinus* TMM M-5899 (A), *Tachyglossus aculeatus* TMM M-1826 (B), and *Zaglossus bartoni* AMNH 194702 (C). Having a medial foramen on the dorsal side of the anterior end of the dentaries is a synapomorphy of Monotremata. It may be homologous with the mesial foramen located in the symphysis of each dentary in other mammals. Jaws are shown to scale. Scale bar = 1 cm.

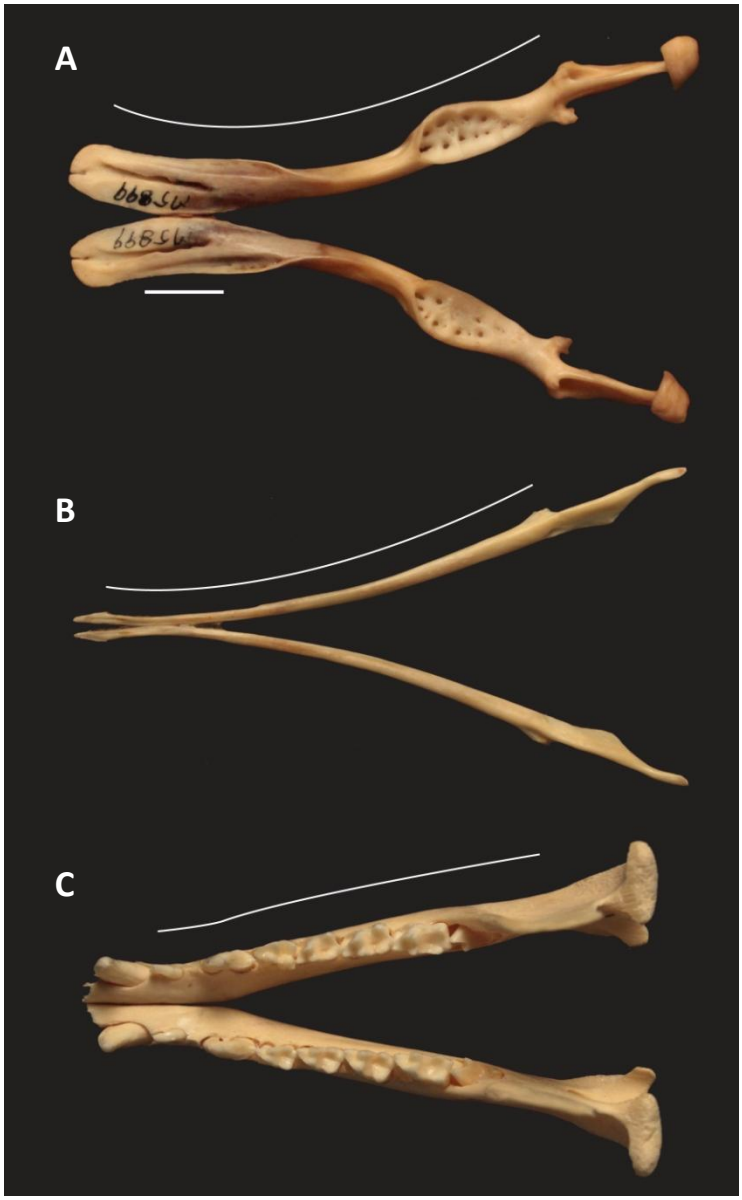

Figure 2.21: Curvature of dentaries in *Ornithorhynchus anatinus* TMM M-5899 (A) and *Tachyglossus aculeatus* TMM M-1826 (B). The mandibles of ornithorhynchids and *Tachyglossus aculeatus* curve medially, emphasized by floating white line, rather than having no curve as in *Didelphis virginiana* TMM M-2205 (C). The curvature is most exaggerated in *Ornithorhynchus anatinus* and more subtle in *Tachyglossus*. The dentaries of *Zaglossus* are anteriorly elongate and greatly reduced and appear to have the most subtle degree of curvature though it is difficult to determine in dried specimens. Lower jaws are shown to scale. Scale bar = 1 cm.

Figure 2.22: The axis of rotation in monotremes is mediolateral, as illustrated by *Ornithorhynchus anatinus* TMM M-5899 (A). *Didelphis virginiana* TMM M-2205 (B) illustrates the plesiomorphic dorsoventral axis of rotation of the dentary condyle for mammals. Scale bar = 1 cm.

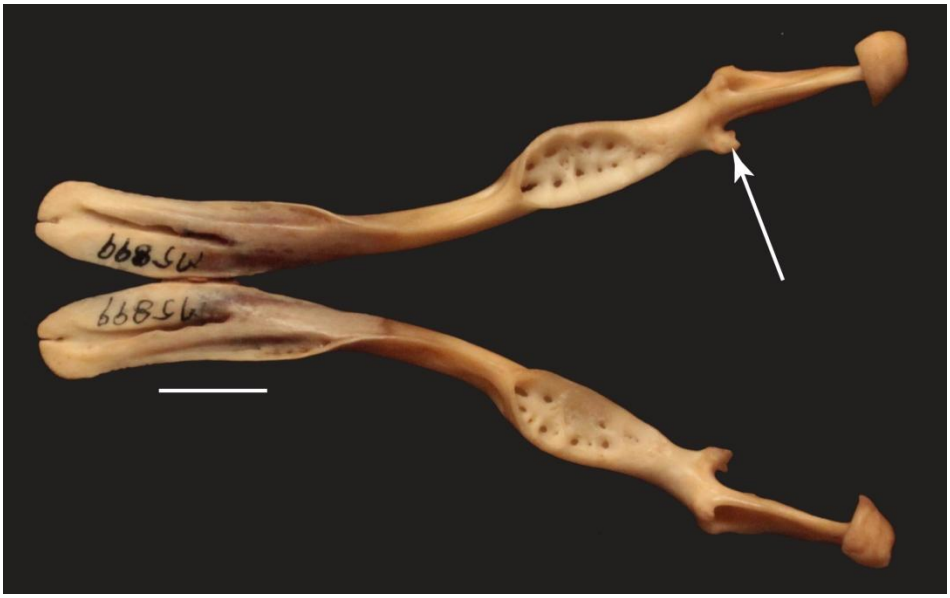

Figure 2.23: The mandibular tubercle is a synapomorphy of Ornithorhynchidae and is illustrated here in *Ornithorhynchus anatinus* TMM M-5899. Scale bar = 1 cm.

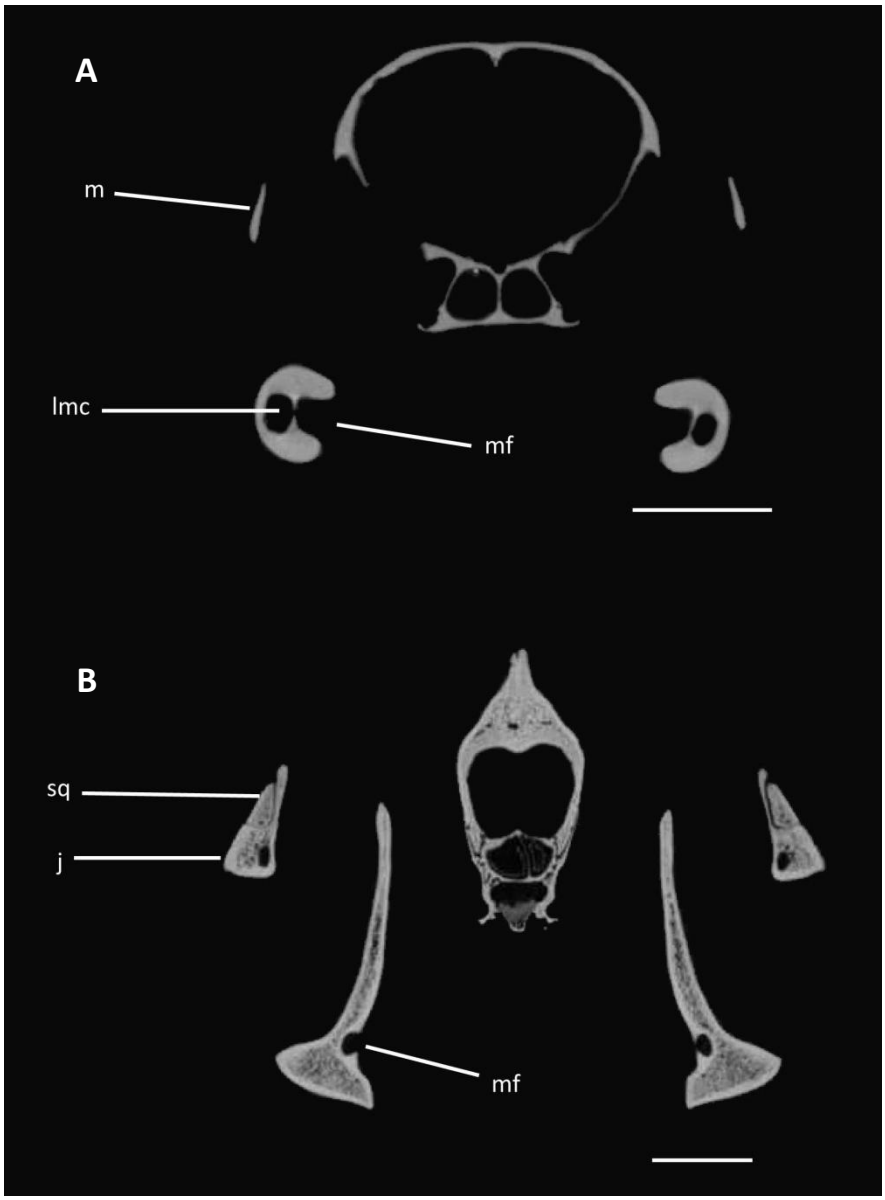

Figure 2.24: In *Ornithorhynchus anatinus* AMNH 200255 (A), two mandibular canals pass through the posterior end of the dentary. The foramen for the entrance to the lateral mandibular canal in *Ornithorhynchus* is positioned within the deep masseteric fossa. *Obdurodon* also has a lateral mandibular canal. *Didelphis virginiana* TMM M-2517 (B) is pictured in cross section at the entrance of the mandibular canal with no lateral mandibular canal present. Cross sections are not shown to scale. Scale bar = 1 cm. j = jugal, lmc = lateral mandibular canal, m = maxilla, mf = mandibular foramen.

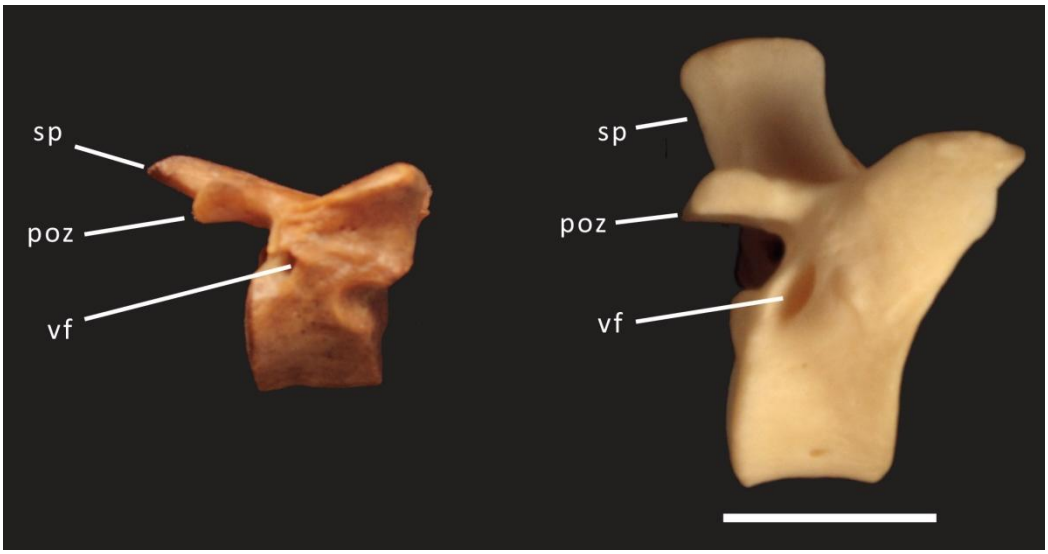

Figure 2.25: Vertebral foramina in *Ornithorhynchus anatinus* TMM M-5899 (right) and *Tachyglossus aculeatus* TMM M-2949 (left) for the exit of the spinal nerve. Thoracic vertebrae shown to scale. Scale bar = 1 cm. poz = postzygapophysis, sp = spinous process, vf = vertebral foramen.

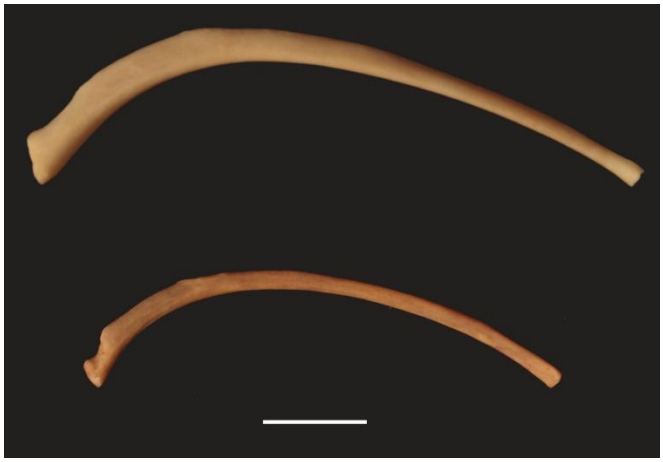

Figure 2.26: The ribs of monotremes articulate with the vertebrae solely with the capitulum rather than with the capitulum and tuberculum. Top: *Tachyglossus aculeatus* TMM M-2949. Bottom: *Ornithorhynchus anatinus* TMM M-5899. Scale bar = 1 cm.

Figure 2.27: Posterior view of the atlas of *Ornithorhynchus anatinus* TMM M-5899 illustrating the paired ventral processes. Gregory (1947) refers to these processes as hypapophyseal horns for attachment of depressor muscles for the head. Scale bar = 1 cm.

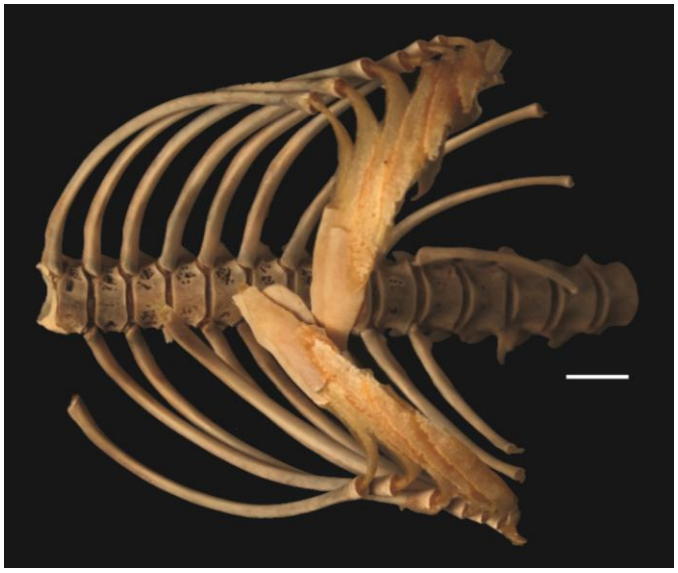

Figure 2.28: Thoracic region of a young *Tachyglossus aculeatus* TMM M-1826 illustrating the ossified, imbricating ventral ribs; a synapomorphy of Monotremata. Scale bar = 1 cm.

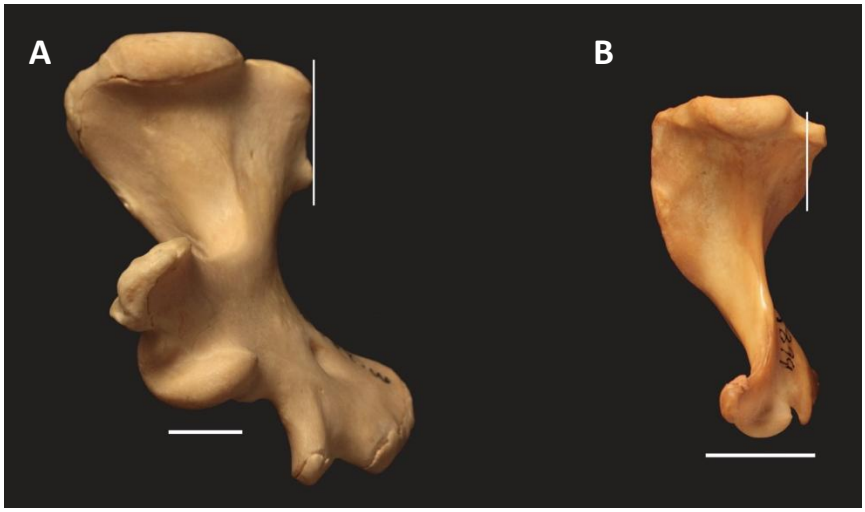

Figure 2.29: Comparison of teres major tubercle of the left humeri of *Tachyglossus aculeatus* TMM M-2949 (A) and *Ornithorhynchus anatinus* TMM M-5899 (B). Left humerus of *Tachyglossus aculeatus* TMM M-2949 in posterior view illustrating robust teres major tubercle, diagnostic of Tachyglossidae. A vertical white line is drawn from the teres major tubercle to the lesser tubercle to demonstrate the relative position of the process between the two monotreme species. Scale bars = 1 cm.

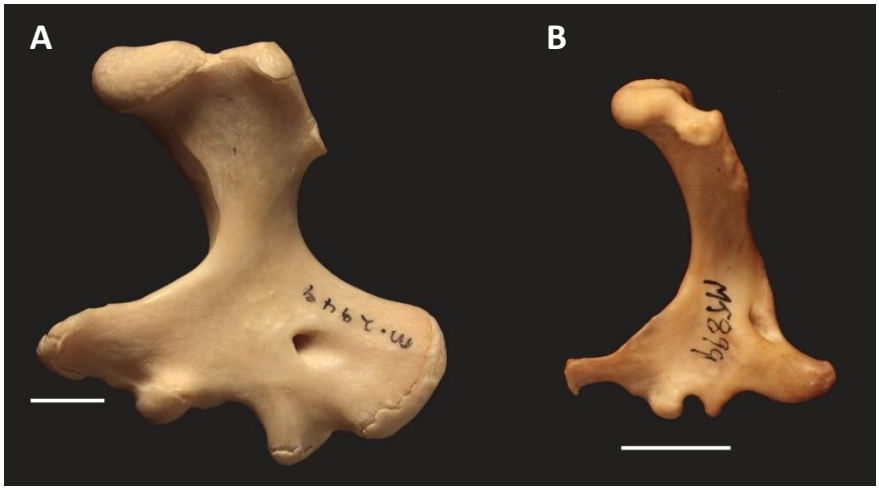

Figure 2.30: Left humeri of *Tachyglossus aculeatus* TMM M-2949 (A) and *Ornithorhynchus anatinus* TMM M-5899 (B) comparing the position of the entepicondylar foramen. Rather than an entepicondylar foramen positioned far medially on the humerus as seen in *Ornithorhynchus*, the entepicondylar foramen of tachyglossids is more centrally located on the distal end of the humerus. Scale bar = 1 cm.

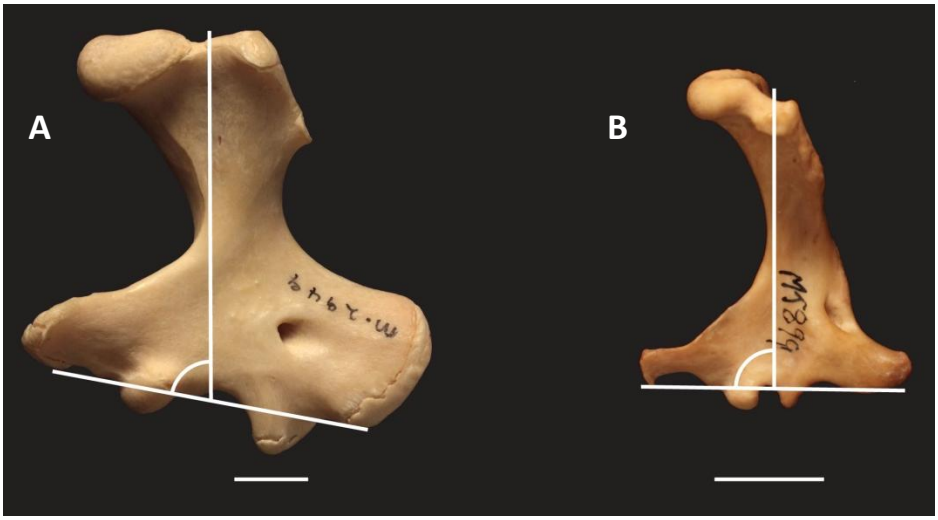

Figure 2.31: Orientation of epicondylar axis shown in the left humeri of *Tachyglossus aculeatus* TMM M-2949 (A) and *Ornithorhynchus anatinus* TMM M-5899 (B). The angle of the inter-epicondylar axis is measured as the angle between the epicondyles and the proximodistal axis of the humerus from the ectepicondyle relative to the proximal end of the humerus. In many mammalian taxa, the angle is approximately 90°, as in *Ornithorhynchus*, while in tachyglossids the angle is less than 90°. Scale bar = 1 cm.

Figure 2.32: The elbow joint in Monotremata is unique among mammals and their relatives for having a single, synovial condyle (indicated by the arrows) where both the radius and ulna articulate, rather than having a trochlea and capitulum for the ulna and radius, respectively. Left: left humerus of *Tachyglossus aculeatus*, TMM M-2949. Right: left humerus of *Ornithorhynchus anatinus*, TMM M-5899. Scale bar = 1 cm.

Figure 2.33: The elbow joint in Monotremata is lateral to the long axis of the humerus, as illustrated in the left humerus of *Tachyglossus aculeatus* TMM M-2949 (left) and *Ornithorhynchus anatinus* TMM M-5899 (right), rather than in alignment with the long axis of the humerus as in non-monotreme mammals. Scale bar = 1 cm.

Figure 2.34: In monotremes, the radius and ulna are tightly appressed to one another as illustrated by *Ornithorhynchus anatinus* TMM M-5899 (top) and *Tachyglossus aculeatus* TMM M-1826 (bottom). Radii and ulni are shown to scale. Scale bar = 1 cm.

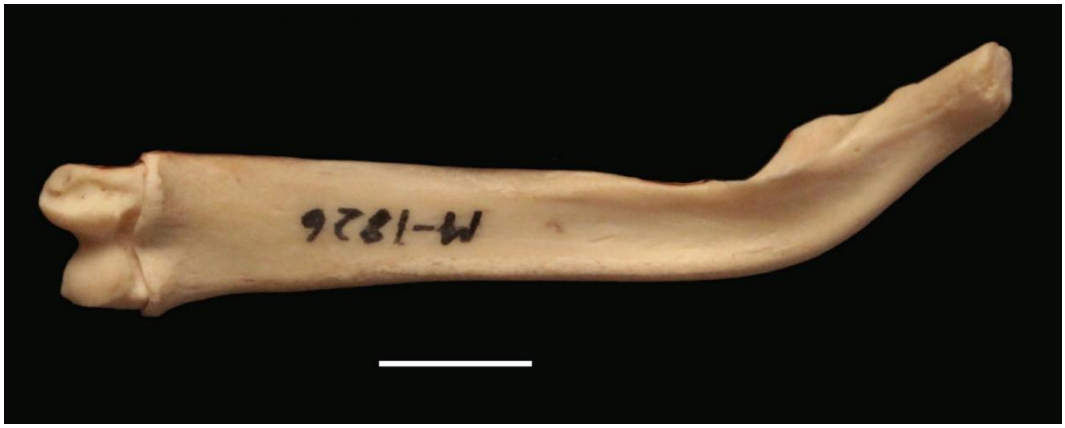

Figure 2.35: Posterior view of right ulna of *Tachyglossus aculeatus* TMM M-1826 illustrating the trochlear shape of the distal end for articulation with the proximal carpals. Scale bar = 1 cm.

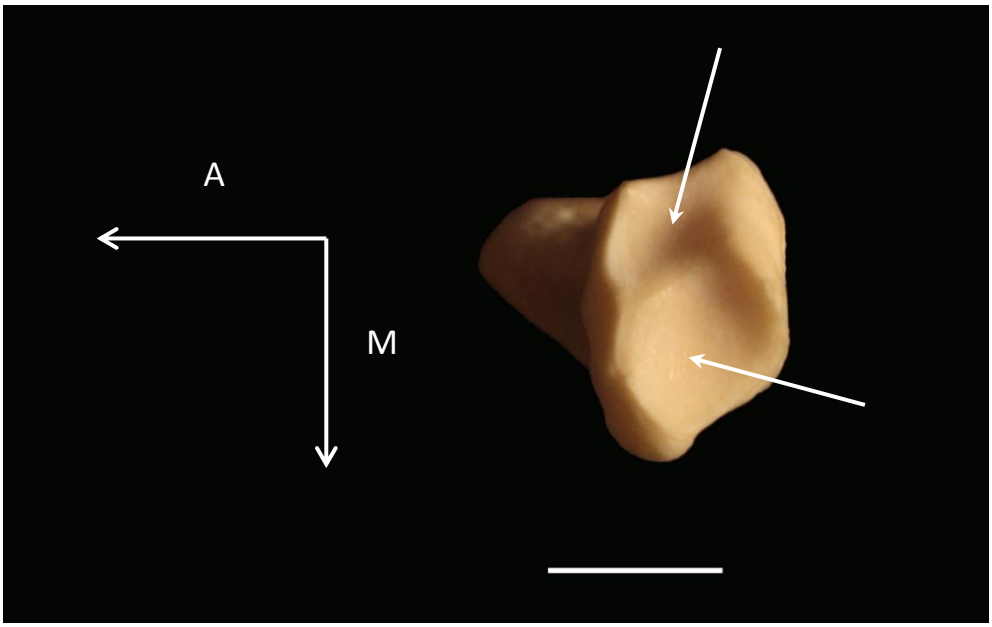

Figure 2.36: Distal end of left radius in *Tachyglossus aculeatus* TMM M-1741 illustrating two distinct surfaces for articulation with carpals are present on the radii in monotremes. Scale bar = 1 cm. A = anterior. M = medial.

Figure 2.37: In monotremes, the olecranon process of the ulna has two prominent processes projecting anteriorly and posteriorly. Shown here is the right ulna of *Ornithorhynchus anatinus* TMM M-5899. Scale bar = 1 cm.

Figure 2.38: Laterally inflected process on distal end of left tibia of *Ornithorhynchus anatinus* TMM M-5899. Scale bar = 1 cm.

Figure 2.39: Strict consensus tree showing relationships of monotreme taxa to one another and to other extinct and extant mammals (next page). Significant bootstrap values are shown on the monotreme stem and stems of monotreme clades. CI = 0.5759, HI = 0.4241, CI excluding uninformative characters = 0.5568, HI excluding uninformative characters = 0.4432, RI = 0.7296, RC = 0.4202.

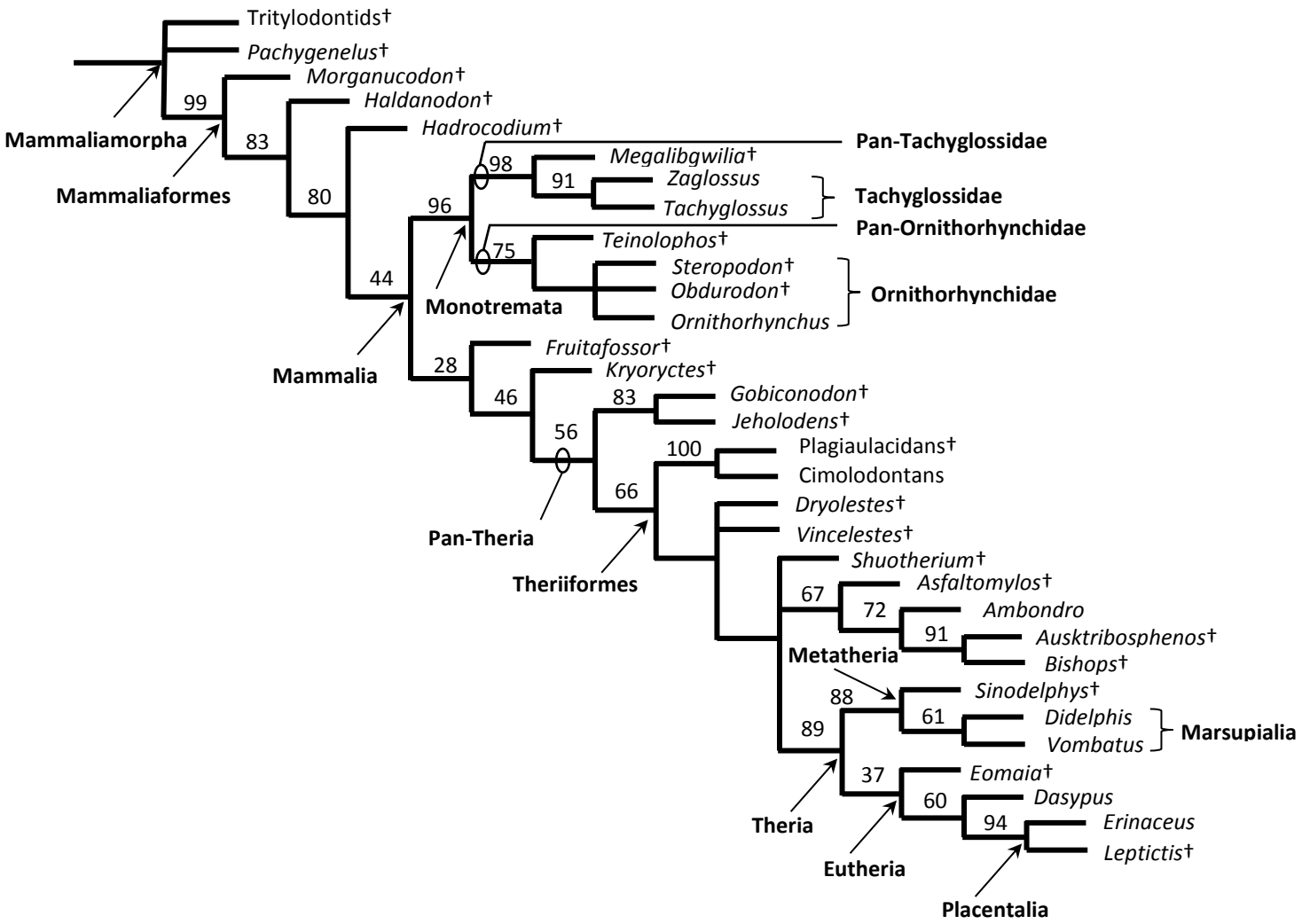
Tritylodontids†
Pachygenelus†
Morganucodon†
Haldanodon†
Hadrocodium†
Megalibgwilia†
Zaglossus
Tachyglossus
Teinolophos†
Steropodon†
Obdurodon†
Ornithorhynchus
Fruitafossor†
Kryoryctes†
Gobiconodon†
Jeholodens†
Plagiaulacidans†
Cimolodontans
Dryolestes†
Vincelestes†
Shuotherium†
Asfaltomylos†
Ambondro
Ausktribosphenos†
Bishops†
Sinodelphys†
Didelphis
Vombatus
Eomaia†
Dasypus
Erinaceus
Leptictis†
99
83
80
44
98
91
96
75
28
46
56
83
100
66
67
72
91
88
61
89
37
60
94
Mammaliamorpha
Mammaliaformes
Mammalia
Monotremata
Pan-Tachyglossidae
Tachyglossidae
Pan-Ornithorhynchidae
Ornithorhynchidae
Pan-Theria
Theriiformes
Metatheria
Marsupialia
Theria
Eutheria
Placentalia

Appendices

APPENDIX 1.A. TABLE SUMMARIZING THE HISTORY OF THE TAXONOMY OF EXTANT MONOTREMES

Class	Subclass	Order	Family	Genus	Species	Subspecies	Synonyms	Original Citation	Source	Range
Mammalia								Linnaeus 1758	Classification of Mammals	
							Zootoka	Aristotle 330 B.C.	Classification of Mammals	
							Vivipera	Ray 1693	Classification of Mammals	
							Mastodia	Rafinesque 1814	Classification of Mammals	
							Thricozoa	Oken 1847	Classification of Mammals	
							Aistheseaozoa	Oken 1847	Classification of Mammals	
							Pilifera	Bonnet 1892	Classification of Mammals	
							Mammalea	Kinman 1994	Classification of Mammals	
	Prototheria						Reptantia	Illiger 1811	Classification of Mammals	
							Ornithodelphia	de Blainville 1834	Classification of Mammals	
							Monotremata	Bonaparte 1837	Classification of Mammals	
							Amasta	Haeckel 1866	Classification of Mammals	
							Sauropsidelphia	Roger 1887	Classification of Mammals	
							Ornithostomi	Cope 1889	Classification of Mammals	
							Monotremiformes	Kinman 1994	Classification of Mammals	
		Monotremata						Bonaparte, 1837	Mammal species of the World	
		Platypoda						Gill 1872	Classification of Mammals	
							Ornithorhynques	Gervais 1854	Classification of Mammals	
			Ornithorhynchidae					Gray, 1825	Mammal species of the World, Classification of Mammals	

Class	Subclass	Order	Family	Genus	Species	Subspecies	Synonyms	Original Citation	Source	Range
							Ornithoryncina	Gray 1825	Classification of Mammals	
							Ornithorhynchidae	Burnett 1830	Classification of Mammals	
							Ornithorhynchina	Bonaparte 1837	Classification of Mammals	
				Ornithorhynchus			*Dermipus*, Wiedermann 1800; *Platypus*, Shaw 1799	Blumenbach, 1800	Mammal species of the World	
					Ornithorhynchus anatinus		O. breviirostris, Ogilby 11832; O. crispus, Macgillivray 1827; O. fuscus, Peron 1807; O. laevis, Macgillivray 1827; O. novaehollandiae, Lacepede 1800; O. paradoxus, Blumenbach 1800; O. phoxinus, Thomas 1923; O. rufus, Peron 1807; O. triton, Thomas 1923	Shaw 1799	Mammal species of the World	
		Tachyglossa						Gill 1872	Classification of Mammals	
							Echidnes	Gervais 1854	Classification of Mammals	
			Tachyglossidae					Gill 1872	Mammal species of the World	
							Aculeata	Geoffroy Saint-Hilaire 1795	Classification of Mammals	
							Echidnidae	Burnett 1830	Classification of Mammals	
							Echidnina	Bonaparte 1837 (as subfamily)	Classification of Mammals	
							Echidnida	Haeckel 1866	Classification of Mammals	

Class	Subclass	Order	Family	Genus	Species	Subspecies	Synonyms	Original Citation	Source	Range
				Tachyglossus				Illiger 1811	Mammal species of the World, Classification of Mammals	
							Acanthonotus	Goldfuss 1809	Mammal species of the World, Classification of Mammals	
							Echidna	G. Cuvier 1797	Mammal species of the World, Classification of Mammals	
							Echinopus	G. Fischer de Waldheim 1814	Mammal species of the World, Classification of Mammals	
							Syphonia	Rafinesque 1815	Mammal species of the World, Classification of Mammals	
					Tachyglossus aculeatus			Shaw 1792; *Shaw and Nodder 1792	Mammal species of the World, *Mammals of New Guinea	
							*Echidna** *australiensis*, Lesson 1827		Mammal species of the World, *Mammals of New Guinea	
							*Echidna** *australis*, Lesson 1836		Mammal species of the World, *Mammals of New Guinea	
							*Echidna** *corealis*, Krefft 1872		Mammal species of the World, *Mammals of New Guinea	
							*Ornithorhynchus** *eracinius*, Mudie 1829		Mammal species of the World, *Mammals of New Guinea	
							*Ornithorhynchus** *hystrix*, Home 1802		Mammal species of the World, *Mammals of New Guinea	

Class	Subclass	Order	Family	Genus	Species	Subspecies	Synonyms	Original Citation	Source	Range
							*Echidna** *longiaculeata*, Tiedemann 1808		Home, 1802b	
							*Acanthonotus** *myrmecophagus*, Goldfuss 1809		Mammal species of the World, *Mammals of New Guinea	
							*Echidna** *novaehollandiae*, Lacepede 1799		Mammal species of the World, *Mammals of New Guinea	
							*Echidna** *orientalis*, Krefft 1872		Mammal species of the World, *Mammals of New Guinea	
							*Echidna** *sydneiensis*, Kowarzik 1909		Mammal species of the World, *Mammals of New Guinea	
							T. typica, Thomas 1885		Mammal species of the World	
							T. acanthion, Collett 1884		Mammal species of the World	
							T. ineptus, Thomas 1906		Mammal species of the World	
							T. lawesii, Ramsay 1877		Mammal species of the World	
							T. multiaculeatus, W. Rothschild 1905		Mammal species of the World	
							setosus, E. Geoffroy St. Hilaire 1803		Mammal species of the World	
							*Echidna** *breviaculeata*, Tiedermann 1808		Mammal species of the World, *Mammals of New Guinea	

Class	Subclass	Order	Family	Genus	Species	Subspecies	Synonyms	Original Citation	Source	Range
							Echidna hobartensis* Kowarzik, 1909		Mammal species of the World, *Mammals of New Guinea	
							Platypus longirostrus*, Perry 1810		Mammal species of the World, *Mammals of New Guinea	
							**Platypus longirostra*, Perry 1810		Mammal species of the World, *Mammals of New Guinea	
						T. a. setosus		Geoffroy 1803	Mammals of New Guinea	Tasmania
						T. a. lawesi		Ramsay 1877e	Mammals of New Guinea	
						T. a. acanthion		Collett 1884	Mammals of New Guinea	central Australia
						T. a. multiaculeatus		Rothschild 1905	Mammals of New Guinea	
						T. a. ineptus		Thomas 1906a	Mammals of New Guinea	Western Australia
				Zaglossus				Gill 1877	Mammal Species of the World	
							Tachyglossus bruijnii	Peters and Doria 1876 (type species)	Mammal Species of the World	
							Acanthoglossus	Gervais 1877	Mammal Species of the World	
							Bruynia	Dubois 1882	Mammal Species of the World	
							Proechidna	Dubois 1884, Gervais 1877*	Mammal species of the World, Classification of Mammals	
							Prozaglossus	Kerbert 1913	Mammal Species of the World	
							Bruijnia	Thomas 1883	Classification of Mammals	
							Megalibgwilia	Griffiths, Wells & Barrie 1991	Classification of Mammals	
					Zaglossus attenboroughi			Flannery and Groves 1998	Mammal Species of the World	*Cyclops Mountains*

Class	Subclass	Order	Family	Genus	Species	Subspecies	Synonyms	Original Citation	Source	Range
					Zaglossus bartoni			Thomas, 1907	Mammal Species of the World	
							Z. bubuensis	Laurie 1952	Mammal Species of the World	
						Z. b. bartoni		Flannery and Groves 1998	Flannery and Groves 1998	*intermediate size*
						Z. b. clunius		Thomas and W. Rothschild 1922	Mammal Species of the World	
						Z. b. diamondi		Flannery and Groves 1998	Mammal Species of the World	
						Z. b. smeenki		Flannery and Groves 1998	Mammal Species of the World	Nanneau Range
					Zaglossus bruijnii		*Tachyglossus bruijnii, Peters and Doria 1876* (type species)	Gill 1877	Mammal Species of the World	
							Acanthoglossus bruijnii, Gervais 1877			
							Bruynia tridactyla	Dubois 1882	Griffiths et al. 1991, Mammal Species of the World, Flannery and Groves 1998	
							Bruijnia		Griffiths et al. 1991	
							Prozaglossus		Griffiths et al. 1991	
							Z. goodfellowi	Thomas, 1907	Mammal Species of the World	
							*Z. bruijnii** *gularis*	W. Rothschild 1922	Mammal species of the World, *Mammals of New Guinea	
							Z. (*Proechidna**) *nigro-aculeatus*	W. Rothschild 1892	Mammal species of the World, *Mammals of New Guinea and Flannery and Groves 1998	
							*Z. bruijnii** *pallidus*	W. Rothschild 1922	Mammal species of the World, *Mammals of New Guinea	

Class	Subclass	Order	Family	Genus	Species	Subspecies	Synonyms	Original Citation	Source	Range
							Z. (*Proechidna**) *villosissima*	Dubois 1884	Mammal species of the World, *Mammals of New Guinea and Flannery and Groves 1998	
							Z. bartoni clunius	Thomas and W. Rothschild 1922	Mammals of New Guinea	
							Z. bubuensis	Laurie 1952	Mammals of New Guinea	
						Z. b. bruijnii		Peters and Doria 1876b	Mammals of New Guinea	Irian Jaya
						Z. b. bartoni		Thomas 1907a	Mammals of New Guinea	Papua New Guinea
						Z. b. goodfellowi		Thomas 1907b	Mammals of New Guinea	Salawati

APPENDIX 1.B. TABLE SUMMARIZING EXTINCT MAMMALS CLASSIFIED AS MONOTREMES.

Name	Synonym(s)	Specimen	Material	Geography	Locality	Formation	Age	Classification	Citation
Kollikodon ritchiei		A.M. F.96602 (Holotype)	right dentary frag w/ m1-3, alveoli for p1-2 and m4	N.S.W. Australia	Lightning Ridge	Wallangulla Sandstone Member, Griman Creek Formation	Early Cretaceous, middle Albian	Kollikodontidae	Flannery et al. 1995
Teinolophos trusleri		MSC 148 (=NMV P208231) (Holotype)	left mandible frag w/ penultimate molar	south-eastern Australia	Flat Rocks site		Early Cretaceous, Early Aptian	Eupantotheria, Monotremata, Ornithorhynchidae	Rich et al. 1999
Steropodon galmani		A.M. F.66763	right dentary fragment with m1-3	N.S.W. Australia	Lightning Ridge	Wallangulla Sandstone Member, Griman Creek Formation	Early Cretaceous, middle Albian (~112-99 My)	Ornithorhynchidae (Archer et al. 1985), Steropodontidae (Flanntery et al. 1995)	Archer et al. 1985
Monotrematum sudamericanum		MLP 91-I-1-1	right M2	Golfo de San Jorge Basin of central Patagonia	Banco Negro Inferior exposures		Banco Negro Inferior SALMA, 63.2-61.8 My, late early Paleocene	Ornithorhynchidae	Pascual et al. 1992
		MPEF-PV 1634	right M2	Punta Peligro, Golfo San Jorge, Chubut Province, Argentina	Hansen Member ("Banco Negro Inferior")	Salamanca Formation	Early Paleocene (Danian)		Pascual et al. 2002
		MPEF-PV 1635	frag left M1	Punta Peligro, Golfo San Jorge, Chubut Province, Argentina	Hansen Member ("Banco Negro Inferior")	Salamanca Formation	Early Paleocene (Danian)		Pascual et al. 2003

Name	Synonym(s)	Specimen	Material	Geography	Locality	Formation	Age	Classification	Citation
		MACN-Pv CH 1888	complete distal end of left femur	Punta Peligro, Golfo San Jorge, Chubut Province, Argentina	Hansen Member ("Banco Negro Inferior")	Salamanca Formation	Early Paleocene (Danian)		Forasiepi and Martinelli, 2003
		MPEF-PV 1728	medial distal end of right femur	Punta Peligro, Golfo San Jorge, Chubut Province, Argentina	Hansen Member ("Banco Negro Inferior")	Salamanca Formation	Early Paleocene (Danian)		Forasiepi and Martinelli, 2003
Obdurodon insignis		SAM P18087 (Holotype)	right upper molar	South Australia	SAM Quarry North, U of Cal. Riverside Loc. RV-7247	Etadunna Formation	Batesfordian or Balcombian age: Mid-Miocene	Ornithorhynchidae	Woodburne and Tedford 1975
		AMNH 97228 (Paratype)	right upper molar	W of Lake Namba, South Australia.	South Prospect B, grid zone 6, ref. 320135	Namba Formation	Batesfordian or Balcombian age: Mid-Miocene		Woodburne and Tedford 1976
		QM F9558	left dentary (posterior portion)	Lake Palankarinna, Etadunna Station, South Australia	SAM Quarry North	Etadunna Formation	Batesfordian or Balcombian age: Mid-Miocene		Archer et al. 1978
		QM F9559	left ilium	Lake Palankarinna, Etadunna Station, South Australia	SAM Quarry North	Etadunna Formation	Batesfordian or Balcombian age: Mid-Miocene		Archer et al. 1979
Obdurodon dicksoni		QM F20564	Complete skull, partial dentary with upper and lower dentitions	Riversleigh, northwestern Queensland	Ringtail Site, Ray's Amphitheatre		Middle Miocene		

Name	Synonym(s)	Specimen	Material	Geography	Locality	Formation	Age	Classification	Citation
Zaglossus hacketti			atlas, clavicles, episternum, pelvic girdle, two femora, a tibia and radius	Mammoth Cave			Upper Pleistocene (Merrilees 1968, Murray 1978)	Tachyglossidae	Glauert 1914
Megalibgwilia ramsayi		SAM P20488	skull (Peters and Doria 1876),	Naracoorte, South Australia	Ossuary of Victoria Cave		Pleistocene	Sister to *T. aculeatus* and *Zaglossus* (Murray 1978)	Murray 1978, Griffiths et al. 1991
		HJD III 271 AN D272, HSD 25, D.J. Barrie, Coonalpyn, SA	skull	Naracoorte, South Australia	Henschke Cave		16,700-90,000 to 120,000=Uranium dating of bones in Victoria Cave (Oligocene-Miocene=limestone age)	Tachyglossidae	Griffiths et al. 1991
	**Zaglossus robusta* (Murray 1978), *Echidna ramsayi* (Murray 1978)	T.M. Z.2031	skull, humeri, femora, tibiae, etc. (14 elements total)	north western Tasmania	Montagu Caves, NW Tas.		20000 (Murray 1978)-13000	Tachyglossidae	Griffiths et al. 1991
	Echidna owen(i)i, Krefft 1868	A.M. F.11017 (Holotype)	distal portion of right humerus (Krefft 1868)?	Darling Downs, Queensland			Pleistocene	Tachyglossidae	Murray 1978
	Echidna ramsayi, Owen 1884	A.M. F.10948 (Holotype for all of *E. ramsayi*)	humerus	Wellington Caves, N.S.W.	Wellington cave breccia		Pleistocene	Tachyglossidae	Murray 1978
	Echidna gigantea, Roger 1887							Tachyglossidae	

Name	Synonym(s)	Specimen	Material	Geography	Locality	Formation	Age	Classification	Citation
	Zaglossus harrissoni, Scott and Lord 1921	Q.V.M. 1965:39:5 (Holotype)	femora	King Island	Egg Lagoon			Tachyglossidae	
	Zaglossus ramsayi, Murray, 1978b							Tachyglossidae	
	Echidna (*Proechidna*) *robusta*, Dun 1895.	A.M. F.51451 (Holotype)	cranial fragment	Gulgong, N.S.W.	Canadian Deep Lead Mine Shaft		Pliocene, but possibly Upper Pleistocene	Tachyglossidae	Murray 1978
	Ornithorhynchus maximus, Dun 1895		humerus					Tachyglossidae	Murray 1978
	Zaglossus robusta, Murray 1978a							Tachyglossidae	

APPENDIX 1.C. SCANNING PARAMETERS FOR *ZAGLOSSUS BRUIJNI* MCZ 7397

Univeristy of Texas High-Resolution X-ray Facility Archive 1840

Bhullar:

7397_: Scans of the skull and mandibles of *Zaglossus bruijni* (MCZ 7397; New Guinea, Mt Arfak) for Anjan Bhullar of The University of Texas at Austin Department of Geological Sciences. Specimen scanned by Jessie Maisano and Matthew Colbert 15 April 2008. This specimen was scanned in two passes. The second pass overlapped the first set by one rotation (19 slices) with original slice 200 from the first set corresponding to original slice 8 from the second set. After deleting duplicate slices, slices 1-156 from the first pass were nudged three pixels up and one pixel to the left in Photoshop to align with slices 157-1139 from the second set.

16bit: 1024x1024 16-bit TIFF images. II, 210 kV, 0.15 mA, intensity control off, high-power mode, no filter, empty container wedge, no offset, slice thickness 2 lines (= 0.125 mm), S.O.D. 180 mm, 1400 views, 2 samples per view, inter-slice spacing 2 lines (= 0.125 mm), field of reconstruction 57 mm (maximum field of view 59.68304 mm), reconstruction offset 4000, reconstruction scale 6300. Acquired with 19 slices per rotation and 15 slices per set. Drift- and ring-removal processing done by Rachel Racicot based on correction of raw sinogram data using IDL routines "RK_SinoDeDrift" with parameter "driftlength=21, goodfile=95" using the 95th file from the first pass, and "RK_SinoRingProcSimul" with parameters "bestof5=11, binwidth=21". Second pass reconstructed with rotation of 1 degree. Deleted last four duplicate slices of each rotation. Total final slices = 1139.

8bitjpg: 8bit jpg version of the above images.

specimenphotos: JPG images of the specimen.

APPENDIX 1.D. SCANNING PARAMETERS FOR *ZAGLOSSUS BARTONI* AMNH 157072

Macrini:

Zaglossus: Scans of the skull of *Zaglossus bruijni* (AMNH 157072; New Guinea: Papua; Milne Bay Prov, Mt. Dayman N. slopes, midd. Comp.; H.M. Van Deusen #12445 c. 1540; 22 June 1953) for Ted Macrini of the Department of Geological Sciences, The University of Texas at Austin. Specimen scanned by Matthew Colbert 31 October 2003.

16bitrot: 1024x1024 16-bit TIFF images. II, 180 kV, 0.133 mA, no filter, empty container wedge, no offset, slice thickness 3 lines (= 0.175 mm), S.O.D. 168 mm, 1000 views, 2 samples per view, inter-slice spacing 3 lines (= 0.175 mm), field of reconstruction 55 mm (maximum field of view 55.0039 mm), reconstruction offset 5300, reconstruction scale 1900. Acquired with 9 slices per rotation. Flash-removal processing done by Rachel Racicot based on correction of raw sinogram data using IDL routine "RK_SinoDeSpike" with default parameters. Rotation correction processing done by Rachel Racicot using IDL routine "DoRotationCorrection". Total slices = 909.

This specimen was too long to scan in one pass, and was scanned in two parts, overlapping one set of 9 slices. Slices 1-135 are from the first pass, and were nudged one pixel left and one pixel up in Photoshop by Rachel Racicot to align with the slices of the second pass (slices 136-909).

8bitjpg: 8-bit JPG version of the above images.

specimenphotos: JPG images of the specimen.

APPENDIX 2.A: CHARACTER LIST

Mandible (36 characters)

1. Post-dentary trough (behind the tooth row): (0) Present; (1) Absent.

2. Separate scars for the surangular/prearticular in the post-dentary trough: (0) Present; (1) Absent.

3. Overhanging medial ridge above the post-dentary trough (behind the tooth row): (0) Present; (1) Absent.

4. Degree of development of Meckel's sulcus: (0) Well developed; (1) Weakly developed; (2) Vestigial or absent.

5. Curvature of Meckel's sulcus (under the tooth row): (0) Parallel to the ventral border of the mandible; (1) Convergent on the ventral border of the mandible.

6. Groove for the replacement dental lamina (= Crompton's groove): (0) Present; (1) Absent.

7. Angular process of the dentary: (0) Weakly developed to absent; (1) Present, distinctive but not inflected; (2) Present and transversely flaring (This is different from character state {4} in having a lateral expansion of the angle and in lacking the anterior

shelf); (3) Present and slightly inflected; (4) Present, strongly inflected, and continuing anteriorly as the mandibular shelf.

8. Position of the angular process of the dentary relative to the dentary condyle: (0) Anterior position (the angular process is below the main body of the coronoid process, separated widely from the dentary condyle); (1) Posterior position (the 8 angular process is positioned at the level of the posterior end of the coronoid process, either close to, or directly under the dentary condyle).

9. Vertical elevation of the angular process of the dentary relative to the molar alveoli: (0) Angular process low, at or near the level of the ventral border of the mandibular horizontal ramus; (1) Angular process high, at or near the level of the molar alveolar line (and far above the ventral border of the mandibular horizontal ramus).

10. Flat ventral surface of the mandibular angle: (0) Absent; (1) Present.

11. Coronoid bone (or its attachment scar): (0) Present; (1) Absent.

12. Location of the mandibular foramen (posterior opening of the mandibular canal): (0) Within the postdentary trough or in the posterior part of Meckel's sulcus; (1) In the pterygoid fossa and offset from Meckel's sulcus (the intersection of Meckel's sulcus at the pterygoid margin is ventral and posterior to the foramen); (2) In the

pterygoid fossa and in alignment with the posterior end of Meckel's sulcus; (3) In the pterygoid fossa but not associated with Meckel's sulcus; (4) Not associated with any of the above structures.

13. Vertical position of the mandibular foramen: (0) Below the alveolar plane; (1) At or above the alveolar plane.

14. Concavity (fossa) for the reflected lamina of the angular bone on the medial side of the dentary angular process: (0) Present; (1) Absent.

15. Splenial bone as a separate element (as indicated by its scar on the dentary): (0) Present; (1) Absent.

16. Relationship of the "postdentary" complex (surangular-articular-prearticular) to the craniomandibular joint (CMJ) [CMJ is made of several bones in the stem groups of mammals or mammaliaforms, whereas the temporomandibular joint 9 (TMJ) is the medical and veterinary anatomical term applicable to living mammals in which the jaw hinge is made only of the temporal (squamosal) bone and the dentary. CMJ and TMJ are used interchangeably here as appropriate to the circumstances]: (0) Participating in CMJ; (1) Excluded from CMJ.

17. Contact of the surangular bone (or associated postdentary element) with the squamosal: (0) Absent; (1) Present.

18. Pterygoid muscle fossa on the medial side of the ramus of the mandible: (0) Absent; (1) Present.

19. Medial pterygoid ridge (shelf) along the ventral border of the ramus of the mandible: (0) Absent; (1) Present; (2) Pterygoid shelf present and reaching the dentary condyle via a low crest.

20. Ventral border of the masseteric fossa: (0) Absent; (1) Present as a low and broad crest; (2) Present as a well-defined and thin crest.

21. Crest of the masseteric fossa along the anterior border of the coronoid process: (0) Absent or weakly developed; (1) Present and laterally flaring; (2) Hypertrophied and laterally flaring.

22. Anteroventral extension of the masseteric fossa: (0) Absent; (1) Extending anteriorly onto the body of the mandible; (2) Further anterior extension below the ultimate premolar.

23. Labial mandibular foramen inside the masseteric fossa: (0) Absent; (1) Present.

24. Posterior vertical shelf of the masseteric fossa connected to the dentary condyle: (0) Absent; (1) Present as a thin crest along the angular margin of mandible; (2) Present as a thick, vertical crest.

25. Posterior-most mental foramen: (0) In the canine and anterior premolar (premolariform) region (in the saddle behind the canine eminence of the mandible); (1) Below the penultimate premolar (under the anterior end of the functional postcanine row); (2) Below the ultimate premolar; (3) At the ultimate premolar and the first molar junction; (4) Under the first molar.

26. Articulation of the dentary and the squamosal: (0) Absent; (1) Present, but without condyle/glenoid; (2) Present, but with condyle/glenoid.

27. Shape and relative size of the dentary articulation: (0) Condyle small or absent; (1) Condyle massive, bulbous, and transversely broad in its dorsal aspect; (2) Condyle mediolaterally narrow and vertically deep, forming a broad arc in lateral outline, either ovoid or triangular in posterior view.

28. Orientation of the dentary peduncle (condylar process) and condyle: (0) Dentary peduncle more posteriorly directed; (1) Dentary condyle continuous with the semicircular posterior margin of the dentary; the condyle is facing up due to the up-turning of the

posterior-most part of the dentary; (2) Dentary articulation extending vertically for the entire depth of the posterior mandibular ramus; it is confluent with the ramus and without a peduncle; the dentary articulation is posteriorly directed; (3) More vertically directed dentary peduncle.

29. Ventral (inferior) border of the dentary peduncle: (0) Posteriorly tapering; (1) Columnar and with a lateral ridge; (2) Ventrally flaring; (3) Robust and short; (4) Ventral part of the peduncle and condyle continuous with the ventral border of the mandible.

30. Gracile and elongate dentary peduncle: (0) Absent; (1) Present.

31. Position of the dentary condyle relative to the level of the postcanine alveoli: (0) Below or about the same level; (1) Above.

32. Tilting of the coronoid process of the dentary (measured as the angle between the anterior border of the coronoid process and the horizontal alveolar line of all molars): (0) Coronoid process strongly reclined and the coronoid angle obtuse (≥150°); (1) Coronoid process less reclined (135°-145°); (2) Coronoid process less than vertical (110°-125°); (3) Coronoid process near vertical (95° to 105°).

33. Size of the coronoid process of the dentary: (0) Not reduced; (1) reduced.

34. Alignment of the ultimate molar (or posteriormost postcanine) to the anterior margin of the dentary coronoid process (and near the coronoid scar if present): (0) Ultimate molar medial to the coronoid process; (1) Ultimate molar aligned with the coronoid process.

35. Dentary symphysis: (0) Fused; (1) Unfused.

36. Rostral mandibular spout: (0) Absent; (1) Present.

Premolars (16 characters)

37. Ultimate upper premolar - metastylar lobe: (0) Reduced or absent; (1) Enlarged and wing-like.

38. Ultimate upper premolar - metacone or metaconal swelling: (0) Absent; (1) Present.

39. Ultimate upper premolar - protocone or protoconal swelling: (0) Little or no lingual swelling; (1) Present.

40. Penultimate upper premolar - protocone or protoconal swelling: (0) Little or no lingual swelling; (1) Protoconal swelling; (2) Distinctive and functional protocone.

41. Position of the tallest posterior upper premolar within the premolar series: (0) Absent; (1) In ultimate premolar position; (2) In penultimate premolar position.

42. Diastema posterior to the first upper premolar (applicable to taxa with premolar-molar differentiation): (0) Absent; (1) Present.

43. Ultimate lower premolar - symmetry of the main cusp a (= protoconid): (0) Asymmetrical (anterior edge of cusp a is more convex in outline than the posterior edge); (1) Symmetrical (anterior and posterior cutting edges are equal or subequal in length; neither edge is more convex or concave than the other in lateral profile).

44. Ultimate lower premolar - anterior cusp b (= paraconid): (0) Absent or indistinctive; (1) Present and distinctive; (2) Enlarged.

45. Ultimate lower premolar - arrangement of principal cusp a, cusp b (if present), and cusp c (assuming the cusp to be c if there is only one cusp behind the main cusp a): (0) Aligned in a single straight line or at a slight angle; (1) Distinctive triangulation; (2) Premolar multicuspate in longitudinal row(s).

46. Ultimate lower premolar - posterior (distal) cingulid or cingular cuspule (in addition to cusp c or the metaconid if the latter cusp is present on a triangulated trigonid). (0) Absent or indistinctive; (1) Present; (2) Present, in addition to cusp c or the c swelling; (3) Presence of the continuous posterior (distal) cingulid at the base of the crown.

47. Ultimate lower premolar - outline: (0) Laterally compressed (or slightly angled); (1) Transversely wide (by trigonid); (2) Transversely wide (by talonid).

48. Ultimate lower premolar - labial cingulid: (0) Absent or vestigial; (1) Present (at least along the length of more than half of the crown).

49. Ultimate lower premolar - lingual cingulid: (0) Absent or vestigial; (1) Present.

50. Ultimate lower premolar - relative height of primary cusp a to cusp c (measured as the height ratio of a and c from the bottom of the valley between the two adjacent cusps): (0) Posterior cusp c distinctive but less than 30% of the primary cusp a; (1) Posterior cusp c and primary cusp a equal or subequal in height (c is 40%-100% of a).

51. Penultimate lower premolar - paraconid (=cusp b): (0) Absent; (1) Present but not distinctive; (2) Present and distinctive.

52. Penultimate lower premolar - arrangement of principal cusp a, cusp b (if present), and cusp c (we assume the cusp to be c if there is only one cusp behind the main cusp a): (0) Cusps in straight alignment (for a tooth with a single cusp, the anterior and posterior crests from the main cusp are in alignment); (1) Cusps in reversed triangulation; (2) With multicusps in longitudinal row(s).

Molar Morphology (69 characters)

53. Alignment of the main cusps of the anterior lower molar(s) (justification for separating this feature from the next character on the list): Several taxa of "obtuse-angled symmetrodonts" and eutriconodont amphilestids show a gradient of variation in cusp triangulation along the molar series; the degree of triangulation may be different between the anterior and posterior molars). (0) Single longitudinal row; (1) Reversed triangle–acute (≤90o); (2) Multiple longitudinal multicuspate rows.

54. Triangulation of cusps in the posterior molars: (0) Absent; (1) Multi-row and multi-cuspate; (2) Posterior molars slightly triangulated; (3) Posterior molars fully triangulated.

55. Postvallum/prevallid shearing (angle of the main trigonid shear facets, based on the second lower molar): (0) Absent; (1) Present, weakly developed, slightly oblique; (2) Present, strongly developed and more transverse; (3) Present, strongly developed, short and slightly oblique.

56. Development of postvallum shear (on the upper second molar; applicable to molars with reversed triangulation of cusps) (increasing the ranks of postvallum shear and can be ordered): (0) Present but only by the first rank: postmetacrista; (1) Present, with the addition of a second rank (postprotocrista below postmetacrista) but the second rank does not reach labially below the base of the metacone; (2) Metacingulum/metaconule present, in addition to postprotocrista, but the metacingulum crest does not extend beyond the

base of the metacone*;* (3) Metacingulum extended beyond metacone; (4) Metacingulum extended to the metastylar lobe; (5) Second rank postvallum shear forming a broad shelf (as in selenodonty).

57. Postcingulum: (0) Absent or weak; (1) Present; (2) Present and reaching past the metaconule; (3) Formed by the hypoconal shelf raised to near the level of the protocone.

58. Precise opposition of the upper and lower molars:(0) Absent; (1) Present (either one-to-one, or occluding at the opposite embrasure or talonid); (2) Present (one lower molar contacts sequentially more than one upper molar).

59. Relationships between the cusps of the opposing upper and lower molars: (0) Absent; (1) Present, lower primary cusp a occludes in the groove between upper cusps A, B; (2) Present, lower main cusp a occludes in front of the upper cusp B and into the embrasure between the opposite upper tooth and the preceding upper tooth; (3) Present, parts of the talonid occluding with the lingual face (or any part) of the upper molar; (4) Lower multicuspate rows alternately occluding between the upper multicuspate rows; (5) Columnar tooth without cusps and with beveled wear across the entire crown contact surface.

60. Protoconid (cusp a) and metaconid (cusp c) height ratio (on the lower second

molar): (0) Protoconid distinctively higher; (1) Protoconid and metaconid nearly equal in height.

61. Relative height and size of the base of the paraconid (cusp b) and metaconid (cusp c) (on the lower second molar): (0) Paraconid distinctively higher than the metaconid; (1) Paraconid and metaconid nearly equal in height; (2) Paraconid lower than metaconid; (3) Paraconid reduced or absent.

62. Elevation of the cingulid base of the paraconid (cusp b) relative to the cingulid base of the metaconid (cusp c) on the lower molars: (0) Absent; (1) Present.

63. Cristid obliqua (sensu Fox 1975: defined as the oblique crest anterior to, and connected with, the labial-most cusp on the talonid heel, the leading edge of facet3): presence vs. absence and orientation (applicable only to the molar with at least a hypoconid on the talonid or a distal cingulid cuspule): (0) Absent; (1) Present, contact closest to the middle posterior of the metaconid; (2) Present, contact closest to the lowest point of the protocristid; (3) Present, contact closest to the middle posterior of the protoconid.
Fruitafossor windscheffeli: (?) Not applicable.

64. Lower molar - medial and longitudinal crest (=‘pre-entocristid’ or ‘prehypoconulid’) on the talonid heel (only applicable to taxa with talonid or at least a cusp d): (0) Talonid

(or cusp d) has no medial and longitudinal crest; (1) Medial-most cristid (‘pre-entoconid cristid’) of the talonid in alignment with the metaconid or with the post-metacristid if the latter is present (the postmetacristid is defined as the posterior crest of metaconid that is parallel to the lingual border of the crown), but widely separated from the latter; (2) Medial-most cristid of the talonid (‘pre-hypoconulid’ cristid, based on cusp designation of Kielan- Jaworowska et al. 1987) is hypertrophied and in alignment with the postmetacristid and abuts the latter by a V-notch; (3) ‘Pre-entocristid’ crest is offset from the metaconid (and postmetacristid if present), and the ‘preentocristid’ extending anterolingually past the base of the metaconid.

65. Posterior lingual cingulid of the lower molars: (0) Absent or weak; (1) Distinctive; (2) Strongly developed, crenulated with distinctive cuspules (such as the kuhneocone).

66. Anterior internal (mesio-lingual) cingular cuspule (e) on the lower molars: (0) Present as an anterior cuspule but not at the cingulid level; (1) Present, at the cingulid level; (2) Present, positioned above the cingulid level; (3) Absent.

67. Anterior and labial (mesio-buccal) cingular cuspule (f): (0) Absent; (1) Present.

68. Mesial cingulid features above the gum: (0) Absent; (1) Weak and discontinuous, with individualized cuspules below the trigonid (as individual cuspule e, f, or both, but e and f are not connected); (2) Present, in a continuous shelf below the trigonid (with no

relations to the protoconid and paraconid), without occlusal function; (3) Present, with occlusal contact to the upper molar.

69. Cingulid shelf wrapping around the anterolingual corner of the molar to extend to the lingual side of the trigonid below the paraconid: (0) Absent; (1) Present, without occlusal function to the upper molars; (2) Present, with occlusal function to the upper molars.

70. Postcingulid (distal transverse cingulid above the gum level) on the lower molars: (0) Absent; (1) Present, horizontal above the gum level.

71. Interlocking mechanism between two adjacent lower molars: (0) Absent; (1) Present, posterior cingular cuspule d (or the base of the hypoconulid) of the preceding molar fits in between cingular cuspules e and f of the succeeding molar; (2) Present, posterior cingular cuspule d fits between cingular cuspule e and cusp b of the succeeding molar; (3) Present, posterior cingular cuspule d of the preceding molar fits into an embayment or vertical groove of the anterior aspect of cusp b of the succeeding molar (without any involvement of distinctive cingular cuspules in interlocking).

72. Size ratio of the last three lower molars: (0) Ultimate molar is smaller than the penultimate molar (m1≥m2≥m3; or m2≥m3≥m4; or m3≥m4≥m5; or m4≥m5≥m6); (1) Penultimate molar is the largest of the molars (m1≤m2≤m3≥m4; or m1≤m2>m3)*;* (2) Ultimate molar is larger than the penultimate molar (m1≤m2≤m3); (3) Equal size.

73. Paraconid position relative to the other cusps of the trigonid on the lower molars (based on the lower second molar): (0) Paraconid in anterolingual position; (1) Paraconid lingually positioned (within lingual 1/4 of the trigonid width); (2) Paraconid lingually positioned and appressed to the metaconid; (3) Paraconid reduced in the selenodont/lophodont patterns.

74. Orientation of the paracristid (crest between cusps a and b) relative to the longitudinal axis of the molar (from Hu et al. 1998) (This is separated from the previous character ["lingual" vs. "labial" position of the paraconid] because of the different distribution of the a-b crest among mammals with non-triangulated molars sampled in this study): (0) Longitudinal orientation; (1) Oblique; (2) Nearly transverse.

75. Angle of the paracristid and the protocristid on the trigonid: (0) > 90°; (1) 90° ~ 50°; (2) < 35°.

76. Mesiolingual vertical crest of the paraconid on the lower molars (applicable only to taxa with reversed triangulation of the molar cusps): (0) Rounded; (1) Forming a keel.

77. Anteroposterior shortening at the base of the trigonid relative to the talonid (applicable only to taxa with a talonid heel with a distal cusp d; measured at the lingual base of the lower second molar trigonid where possible): (0) Trigonid long (extending

over 3/4 of the tooth length); (1) Swelling on the side walls of the trigonid (taxa assigned to this character state have a trigonid length ratio 45%~50%; but their morphology is different from all other states in that their side walls are convex); (2) No shortening (trigonid 50-65% of tooth length); (3) Some shortening (the base of trigonid < 50% of tooth length); (4) Anteroposterior compression of trigonid (trigonid 40~45% of the tooth length).

78. Molar (the lower second molar measured where possible) trigonid/talonid heel width ratio: (0) Narrow (talonid ≤40% of trigonid); (1) Wide (talonid is 40-70% of the trigonid in width); (2) Talonid is equal or wider than trigonid.

79. Lower molar hypoflexid (concavity anterolabial to the hypconid or cusp d): (0) Absent or shallow (all "triconodont-like" teeth are coded as "0" here as long as they have cuspule d); (1) Deep (40~50% of talonid width); (2) Very Deep (>65%).

80. Morphology of the talonid (or the posterior heel) of the molar: (0) Absent; (1) Present, as an incipient heel, a cingulid, or cingular cuspule (d); (2) Present, as a transverse ‘V-shaped’ basin with two functional cusps; (3) Present, as an obtuse ‘V-shaped’ triangle; (4) Present, as a functional basin, rimmed with 3 functional cusps (if the entoconid is vestigial, there is a functional crest to define the medial rim of the basin).

81. Hypoconid (we designate the distal cingulid cuspule d as the homolog to the hypoconid in the teeth with linear alignment of the main cusps; we assume the cusp to be the hypoconid if there is only a single cusp on the talonid in the teeth with reversed triangulation):
(0) Present, but not elevated above the cingulid level; (1) Present (as distal cusp d, *sensu* Crompton 1971), elevated above the cingulid level, labially positioned (or tilted in the lingual direction); (2) Present (larger than cusp d, with occlusal contact to the upper molar), elevated above the cingulid level, lingually positioned.

82. Hypoconulid (if there are only two functional cusps on the talonid, we assume that the second and more lingual cusp on the talonid to be the hypoconulid, following the rationale of Kielan-Jaworowska et al. 1987): (0) Absent; (1) Present, and median (near the mid-point of the transverse talonid width); (2) Present, and placed within the lingual 1/3 of the talonid basin; (3) Incorporated into the crest of lophodont or selenodont conditions.

83. Anterior lower molar (preferably the first, or the second if the first is not available) - hypoconulid - anteroposterior orientation: procumbent vs. reclined (applicable to the taxa with at least two cusps on the talonid): (0) Cusp tip reclined and the posterior wall of the hypoconulid is slanted and overhanging the root; (1) Cusp tip procumbent and the posterior wall of the cusp is vertical; (2) Cusp tip procumbent and the posterior wall is gibbous.

84. Hypoconulid labial postcingulid (shelf) on the lower molars (definition following Cifelli 1993; non-homologous with the postcingulid coded elsewhere in this list because of the different relationship to the talonid cusps; applicable to taxa with identifiable hypoconid and hypoconulid only): (0) Absent; (1) Present as a crest descending mesiolabially from the apex of the hypoconulid to the base of the hypoconid.

85. Last lower molar - hypoconulid - orientation and relative size (applicable to the taxa with at least a talonid heel; scored on the third molar for Peramus and eutherians, the fourth molar for Kielantherium and metatherians; justification for separating this character from the character of the anterior molar hypoconulids is that the ultimate molar shows different morphology and distribution, especially in taxa in which there is posteriorly decreasing size gradient, e.g. Deltatheridium): (0) Short and erect; (1) Tall (higher than hypoconid) and recurved.

86. Entoconid (if there are three functional cusps on the talonid, we assume that the third and the lingual-most functional cusp on the talonid is the entoconid, following the rationale given by Kielan-Jaworowska et al. 1987): (0) Absent; (1) Present, about equal distance to the hypoconulid as to the hypoconid*;* (2) Present, with slight approximation to the hypoconulid (distance between the hypoconulid and entoconid noticeably shorter than between the hypoconulid and hypoconid); (3) Present, and twinned with the hypoconulid.

87. Height ratio of the medial side of the crown (apex of the hypoconid to the base of the labial crown) vs. the most lingual cusp on the talonid to the base of the labial crown (this character can be based either on the entoconid if the entoconid is present or the hypoconulid if the entoconid cannot be scored): (0) Entoconid absent on the talonid heel; (1) Entoconid lower than the hypoconid; (2) Entoconid near the height of the hypoconid; (3) Entoconid near the height of the hypoconid and linked to the hypoconid by a transverse crest.

88. Alignment of the paraconid, metaconid, and entoconid on the lower molars (applicable only to taxa with triangulation of the trigonid cusps and the entoconid present on the talonid): (0) Cusps not aligned; (1) Cusps aligned.

89. The length vs. width ratio of the functional talonid basin of the lower molars (in occlusal view, measured at the cingulid level, and based on the second molar): (0) Longer than wide (or narrows posteriorly); (1) Length equals width.

90. Elevation of the talonid (measured as the height of the hypoconid from the cingulid on the labial side of the crown) relative to the trigonid (measured as the height of protoconid from the cingulid) (applicable only to the teeth with reversed triangulation): (0) Hypoconid/protoconid height ratio less than 20% (hypoconid or cusp d is on the cingulid); (1) Hypoconid/protoconid height ratio between 25% and 35% (talonid cusp elevated above the cingulid level); (2) Hypoconid/protoconid height ratio between 40%

and 60%; (3) Hypoconid/protoconid height ratio between >60% and 80%; (4) Equal height.

91. Size (labiolingual width) of the upper molar labial stylar shelf on the penultimate molar: (0) Absent; (1) Present and narrow; (2) Present and broad.

92. Presence vs. absence of the ectoflexus on the upper second molar (or postcanines in the middle portion of the postcanine row). Comments: justification for separating this character from the next is that only a single upper molar is known for three taxa that are otherwise crucial for assessing the timing and biogeography of the divergence of earliestknown crown therians: Murtoilestes, Atokatheridium, and Kokopellia. Nanolestes and Shuotherium are also only represented by isolated upper molars. Therefore, the gradient character of the ectoflexus along the tooth row is not applicable for these taxa. Presence vs. absence of the ectoflexus alone does not exhaust the systematic distribution of the ectoflexus-related characters among taxa with isolated upper molars. (0) Absent or weakly developed; (1) Present.

93. Ectoflexus gradient along the molar series (see the above for justification of separating presence/absence from the gradient of the ectoflexus on the upper molar(s)): (0) Present on penultimate molar, but weakly developed or absent on the anterior molars; (1) Present on the penultimate and preceding molars.

94. Morphological features on the labial cingulum or stylar shelf of the upper molars (excluding the parastyle and metastyle): (0) Indistinctive; (1) Distinctive cingulum, without cuspules; (2) Individualized or even hypertrophied cuspules; (3) W-pattern on stylar shelf; (4) Cingulum crenulated with distinctive and even-sized multiple cuspules.

95. Upper molar protocone: (0) Functional cusp and lingual swelling absent; (1) Functional cusp absent, but the lingual side is more swollen than the labial side at the cingular level; (2) Functional cusp present.

96. Degree of labial shift of the protocone (distance from the protocone apex to the lingual border vs. the total tooth width, in %) (applicable only to those taxa with reversed triangulation):
(0) Protocone present but no labial shift (10%-20%); (1) Moderate labial shift (25%-30%); (2) Substantial labial shift (≥ 40%).

97. Morphology of the protocone (applicable only to those taxa with reversed triangulation and a lingual swelling of the upper molar): (0) Protoconal region present but no distinct protocone; (1) Protocone present, its apical portion anteroposteriorly compressed; (2) Apical portion slightly expanded; (3) Apical portion expanded; (4) Apical portion forming an obtuse triangle with the protoconal cristae.

98. Height of the protocone relative to the paracone and metacone (whichever is highest of the latter two): (0) Protocone markedly lower (less than 70%); (1) Protocone of intermediate height (70%~80%); (2) Protocone near the height of paracone and metacone (within 80%).

99. Height and size of the paracone (cusp B) and metacone (cusp C) (based on the upper second molar if available): (0) Paracone noticeably higher and larger at the base than metacone; (1) Paracone slightly larger than metacone; (2) Paracone and metacone of equal size or paracone lower than metacone.

100. Metacone position relative to paracone: (0) Metacone labial to paracone; (1) Metacone about the same level as paracone; (2) Metacone lingual to paracone.

101. Base of the paracone and metacone (based on the upper second molar if available, applicable only to triangulated molars): (0) Merged; (1) Separated.

102. Centrocrista between the paracone and the metacone of the upper molars (applicable only to taxa with well-developed metacone and distinctive wear facets 3 and 4): (0) Straight; (1) V-shaped, with labially directed postparacrista and premetacrista.

103. Anteroposterior width of the conular region (with or without conules) on the upper molars (applicable only to taxa with reversed triangulation and an occluding lingual

portion of the upper molar; for the taxa with conules, this is measured between the paraconule and metaconule; for those taxa without conules, this is measured as the length of the tooth medial to the base of paracone; the upper second molar measured where possible): (0) Narrow (anteroposterior distance medial to the paracone and metacone less than 0.30 of total tooth length); (1) Moderate development (distance between position of conules = 0.31—0.50 of total tooth length); (2) Wide (distance between conules greater than 0.51 of total tooth length); (3) Expanded.

104. Presence of the paraconule and metaconule on the upper molars: (0) Absent; (1) Present.

105. Relative position of the paraconule and metaconule on the upper first and second molars (character adopted from Archibald et al. 2001): (0) Paraconule and metaconule closer to the protocone; (1) Both positioned near the midpoint of the protocone-metacone; (2) Paraconule and metaconule labial to the midpoint.

106. Internal conular cristae: (0) Cristae indistinctive; (1) Cristae distinctive and wing-like.

107. Parastylar groove (on upper second molar): (0) Weak or absent; (1) Moderately to well developed.

108. Stylar cuspule “A”, the parastyle, on the upper molars (of the Bensley- Simpson system; cuspule “E” of the Crompton designation): (0) Present (at least a swelling is present); (1) Absent.

109. Preparastyle on the upper first molar (applicable to molars with triangulation): (0) Absent; (1) Present.

110. Stylar cuspule “B” (opposite the paracone) (based on the upper second molar if available):
(0) Vestigial to absent; (1) Small but distinctive; (2) Subequal to the parastyle; (3) Large (subequal to parastyle), with an extra "B-1" cuspule in addition to "B".

111. Stylar cuspule "C" (near the ectoflexus) on the penultimate upper molar: (0) Absent; (1) Present.

112. Stylar cuspule "D" (opposite the metacone) on the penultimate upper molar: (0) Absent; (1) Present.

113. Absence vs. presence and size of the stylar cuspule “E” (Bensley-Simpson designation; not the Crompton cusp E): (0) Absent or poorly developed; (1) Present, less developed than or subequal to stylar cuspule “D”; (2) Present and better developed than cuspule “D”.

114. Position of the stylar cuspule “E” relative to cusp “D” or “D-position”: (0) “E” more lingual to “D” or “D-position”; (1) “E” distal to or at same level as “D” or “D-position”.

115. Upper molar interlock: (0) Absent; (1) Tongue-in-groove interlock; (2) Parastylar lobe of a succeeding molar lumbricated with the metastylar region of a preceding molar.

116. Size and labial extent of the metastylar lobe and parastylar lobe (based on the upper first molar if available; if not, then based on upper second): (0) Metastylar lobe smaller than the parastylar lobe; (1) Metastylar lobe of similar size and labial extent to the parastylar lobe; (2) Metastylar lobe much larger than the parastylar lobe; (3) Metastylar lobe absent.

117. Salient postmetacrista on the upper molars (applicable to taxa with reversed triangulation): (0) Absent or weakly developed; (1) Well-developed but no longer than the metaconeprotocone distance; (2) Hypertrophied and longer than the metacone-protocone distance.

118. Selenodont molar pattern: (0) Absent; (1) Present.

119. Outline of the lower first molar crown (in crown view): (0) Laterally compressed; (1) Oblong with slight labial bulge; (2) Triangular or tear-drop shaped; (3) Rectangular (or rhomboidal); (4) Circular.

120. Aspect ratio and outline of the upper first molar: (0) Laterally compressed; (1) Longer than transversely wide (oval-shaped or spindle shaped); (2) Transversely wider than long (triangular outline); (3) Rectangular or nearly so; (4) Circular.

121. Carnassial shearing blades on last upper premolar and first lower molar: (0) Absent; (1) Present.

Molar Wear Pattern (12 characters)

122. Functional development of occlusal facets on individual molar cusps: (0) Absent; (1) Absent at eruption but developed later by crown wear; (2) Wear facets match upon tooth eruption (inferred from the flat contact surface upon eruption).

123. Topographic relationships of wear facets to the main cusps: (0) Lower cusps a, c support two different wear facets (facets 1 and 4) that contact the upper primary cusp A; (1) Lower cusps a, c support a single wear facet (facet 4) that contacts the upper primary cusp B (this facet extends onto cusp A as wear continues, but 1 and 4 do not develop simultaneous in these taxa);
(2) Multicuspate series, each cusp may support 2 wear facets.

124. Development and orientation of prevallum/postvallid shearing (based on either upper or the lower molar structures): (0) Absent; (1) Present and obtuse; (2) Present, hypertrophied and transverse.

125. Wear facet 1 (a single facet supported by cusp a and cusp c) and facet 2 (a single facet supported by cusp a and cusp b): (0) Absent; (1) Present.

126. Upper molars - development of facet 1 and the preprotocrista (applicable to molars with reversed triangulation): (0) Facet 1 (prevallum crest) short, not extending to the stylocone area; (1) Facet 1 extending into the hook-like area near the stylocone; (2) Preprotocrista long, extending labially beyond the paracone.

127. Differentiation of wear facet 3 and facet 4 (applicable to taxa with a distal cusp d or "hypoconulid"): (0) Absent; (1) Present; (2) Facets 3 and 4 hypertrophied on the flanks of the strongly V-shaped talonid.

128. Orientation of facet 4 (on the posterior aspect of the hypoconid): (0) Present and oblique to the long axis of the tooth; (1) Present and forming a more transverse angle to the long axis of the tooth.

129. Morphology of the posterolateral aspect of the talonid (the labial face of the hypoconid or equivalent area of Crompton facet 4, applicable to taxa with fully basined talonid): (0) Gently rounded; (1) Angular.

130. Wear pattern within the talonid basin (applicable to those taxa with triangulated molars): (0) Absent; (1) Present; (2) Present apically on the crests of the talonid; (3) Apical wear on crest and lophodont.

131. Development of the distal metacristid (applicable only to taxa with reversed triangulation): (0) Present; (1) Absent.

132. Differentiation of wear facets 5 and 6 on the labial face of the entoconid: (0) Absent; (1) Present.

133. Surficial features on the occluding surfaces on the talonid (only applicable to taxa with reversed triangulation): (0) Smooth surface on the talonid heel (or on cusp d); (1) Multiple ridges within the talonid basin; (2) Talonid present, but wear occurs apically on the crests of cristid obliqua and hypoconid cristid (V-shaped talonid crests).

Other Dental Features (28 characters)

134. Number of lower incisors: (0) Five or more; (1) Four; (2) Three; (3) Two; (4) One; (5) No incisors.

135. Number of upper incisors: (0) Five; (1) Four; (2) Three; (3) Two or one; (4) No incisors.

136. Upper canine - presence vs. absence, and size: (0) Present and enlarged; (1) Present and small; (2) Absent.

137. Number of upper canine roots: (0) One; (1) Two.

138. Lower canine - presence vs. absence and size: (0) Present and enlarged; (1) Present and small; (2) Absent.

139. Number of lower canine roots: (0) One; (1) Two.

140. Number of upper premolars (only applicable to taxa with premolar vs. molar differentiation): (0) Five or more; (1) Four; (2) Three; (3) Two or less.

141. Number of lower premolars: (0) Five or more; (1) Four; (2) Three; (3) Two or less.

142. Number of lower molars or molariform postcanines: (0) Six or more; (1) Five; (2) Four; (3) Three; (4) Two or less.

143. Number of upper molars or molariform postcanines (applicable only to those taxa that do not have multiple dental replacements): (0) Six or more; (1) Five; (2) Four; (3) Three; (4) Two or less.

144. Total number of upper postcanine loci: (0) More than 8 (including the loci plus the alveoli of shed anterior postcanines); (1) Eight; (2) Seven, (3) Six; (4) Five or less.

145. Number of lower postcanine loci: (0) Eight or more; (1) Seven; (2) Six; (3) Five or less.

146. Procumbency and diastema of first (functional) upper premolar or postcanine in relation to the upper canine: (0) Not procumbent and without diastema; (1) Procumbent and with diastema.

147. Diastema separating the lower first and second premolars (defined as the first and second functioning premolar or premolariform postcanine): (0) Absent (gap less than one tooth root for whichever is smaller of the adjacent teeth); (1) Present, subequal to one tooth-root diameter or more; (2) Present, equal to or more than one-tooth length.

148. Ultimate premolar bladed or crenulated: (0) Absent; (1) Present.

149. Upper anterior-most incisor: (0) Subequal to the remaining incisors, no diastema with the second incisor; (1) Anteriorly projecting, separated from the second incisor by a diastema; (2) Absent (as evidenced by a median gap between the mesial-most incisors).

150. Ultimate and penultimate upper incisors are relatively compressed laterally: (0) Absent; (1) Present, and spoon-shaped to rhomboid-shaped in lateral view; (2) Present, and spatulate in lateral view; (3) Ultimate and/or penultimate upper incisors bicuspate or tricuspate.

151. Staggered lower incisor (Hershkovitz 1982): (0) Absent; (1) Present.

152. Replacement pattern of incisors and canines: (0) More than one replacement; (1) One replacement; (2) No replacement.

153. Replacement of at least some posterior functional molariform postcanines: (0) Present; (1) Absent.

154. Procumbency and enlargement of the lower anterior-most incisor: (0) Absent; (1) Present (at least 50% longer than the adjacent incisor).

155. Enlarged diastema in the lower incisor-canine region (better developed in older individuals): (0) Absent; (1) Present and behind the canine; (2) Present and behind the posterior incisor.

156. U-shaped ridge in the lower multi-rowed molars: (0) Absent; (1) Present.

157. Single-aligned and the labial row of multi-cusp or multi-rowed lower molar - Cusp ratio: (0) Second mesial cusp (b2 of Butler 2000) highest; (1) Mesial cusp (b1 of Butler 2000) highest.

158. Multi-rowed upper premolar/molar - cusp ratio in the labial row of multicusp row: (0) Distal cusp highest, with a gradient of anteriorly decreasing height; (1) Cusps in same row of equal height.

159. Alignment of multi-cuspate upper first and second molars: (0) Second lingually offset from the first so that the lower second molar lingual row occludes with the lingual side of the upper second labial row; (1) Lower second molar labial row occludes with the labial side of the upper second labial row.

160. Enamel microstructure (character state definition following Wood et al. 1999; distribution following Clemens 1997; Sander 1997; Wood and Stern 1997): (0) Synapsida columnar enamel (prismless); (1) ‘Transitional’ (sheath indistinct, ‘prismatic’ crystallites

inclined at less than 45o to the ‘interprismatic’ matrix); (2) Full prismatic enamel; (3) Enamel absent.

161. Open root end of the postcanines (0) Absent; (1) Present.

Vertebrae and Ribs (10 characters)

162. Fusion of the atlas neural arch and intercentrum: (0) Absent; (1) Present.

163. Atlas rib: (0) Present; (1) Absent.

164. Fusion of dens to the axis: (0) Absent; (1) Present.

165. Axis rib: (0) Present; (1) Absent (rib fused to form the transverse process).

166. Postaxial cervical ribs: (0) Unfused; (1) Fused.

167. Number of thoracic vertebrae: (0) 13 or less; (1) 15 or more.

168. Anticlinal vertebra: (0) Absent; (1) Present.

169. Mobile lumbar ribs: (0) Present; (1) Absent.

170. Orientation of lumbar ribs or transverse processes: (0) Posterolaterally directed; (1) Laterally or anterolaterally directed.

171. Xenarthrous articulation in addition to the pre- and post-zygapophyses of lumbar vertebrae: (0) Absent; (1) Present.

Shoulder Girdle (20 characters)

172. Interclavicle: (0) Present; (1) Absent.

173. Contact relationships between the interclavicle (embryonic membranous element) and the sternal manubrium (embryonic endochondral element) (assuming the homologies of these elements by Klima 1973, 1987): (0) Two elements distinct from each other, posterior end of the interclavicle abuts with the anterior border of manubrium; (1) Two elements distinct from each other, the interclavicle broadly overlaps the ventral side of the manubrium; (2) Complete fusion of the embryonic membranous and endochondral elements resulting in a single and enlarged manubrium.

174. Cranial margin of the interclavicle/manubrium (assuming the interclavicle is fused to the sternal manubrium in living therians, Klima 1987): (0) Emarginated or flat; (1) With a median process.

175. Sternoclaviclular joint (assuming that homologous elements of the interclavicle and the manubrium are fused to each other in therians, Klima 1973, 1987): (0) Immobile; (1) Mobile.

176. Acromioclavicular joint: (0) Extensive articulation; (1) Limited articulation (either pointed acromion, pointed distal end of clavicle, or both).

177. Curvature of the clavicle: (0) Boomerang-shaped; (1) Slightly curved.

178. Scapula - supraspinous fossa: degree of development along the length: (0) Present only in the “acromional region” of the scapula, and on the cranial (dorsal) border of the scapula and positioned anterior to the glenoid); (1) Weakly developed (present only along a part of the scapula and positioned lateral to the glenoid); (2) Fully developed (present along the entire dorsal border of the scapula).

179. Proportion of supraspinous vs. infraspinous fossae (width measured across the "saddle region" of the spine, or near the mid-length of the scapula): (0) Supraspinous “fossa” on the cranial aspect of the scapula and much narrower than infraspinous fossa; (1) Supraspinous width is 50% to 80% that of infraspinous fossa; (2) Fossae subequal; (3) Supraspinous over 150% that of infraspinous fossa.

180. Scapula - acromion process: (0) Short stump, level with or behind the glenoid; (1) Hook-like and extending below the glenoid.

181. Scapula - a distinctive fossa for the teres major muscle on the lateral aspect of the scapular plate: (0) Absent; (1) Present.

182. Procoracoid: (0) Present; (1) Fused to the sternal apparatus (Klima 1973) .

183. Procoracoid foramen: (0) Present; (1) Absent (assuming the procoracoid is fused to the sternal apparatus in living therians, Klima 1973).

184. Coracoid: (0) Large, with posterior process; (1) Small, without posterior process.

185. Anterior process of the coracoid: (0) Indistinctive; (1) Distinctive; (2) Distinctive and forming a broad plate.

186. Coracoid process bridging over posteriorly toward the vertebral border of scapula (or fused with the latter): (0) Absent; (1) Present.

187. Size of the anterior-most element (‘manubrium’) relative to the subsequent sternebrae in the sternal apparatus: (0) Large; (1) Small.

188. Orientation (‘facing’ of the articular surface) of the glenoid (relative to the plane or the long axis of the scapula): (0) Nearly parallel and facing posterolaterally; (1) Oblique and facing more posteriorly; (2) Perpendicular.

189. Shape and curvature of the glenoid: (0) Saddle-shaped, oval and elongate; (1) Uniformly concave and more rounded in outline.

190. Medial surface of the scapula: (0) Convex; (1) Flat.

191. Suprascapular incisure (defined as the prominent emargination on the cranial border of the supraspinus fossa): (0) Absent; (1) Present.

Forelimb and Manus (15 characters)

192. Humeral head: (0) Subspherical, weakly inflected; (1) Spherical, strongly inflected.

193. Intertubercular groove of the humerus: (0) Shallow and broad; (1) Narrow and deep.

194. Size of the lesser tubercle of the humerus relative to the greater tubercle: (0) Wider; (1) Narrower.

195. Torsion between the proximal and distal ends of the humerus: (0) Strong (≥30°); (1) Moderate (30° –15°); (2) Weak.

196. Ventral extension of the deltopectoral crest or the position of the deltoid tuberosity: (0) Short and limited to the proximal part of the humeral shaft; (1) Extending ventrally (distally) at least 1/3 the length of the shaft.

197. Teres tuberosity on medial side of humerus. (0) Absent; (1) Present; (2) Hypertrophied.

198. Ulnar articulation on the distal humerus: (0) Bulbous ulnar condyle; (1) Cylindrical trochlea in posterior view with a vestigial ulnar condyle in anterior view; (2) Cylindrical trochlea without an ulnar condyle (cylindrical trochlea extending to the anterior/ventral side).

199. Radial articulation on the distal humerus: (0) Distinct and rounded radial condyle in both anterior (ventral) and posterior (dorsal) aspects (that does not form a continuous synovial surface with the ulnar articulation in the ventral/anterior view of the humerus); (1) Rounded radial condyle anteriorly but cylindrical posteriorly; (2) Capitulum (forming a continuous synovial surface with the ulnar trochlea; cylindrical in both anterior and posterior aspects).

200. Entepicondyle and ectepicondyle of the humerus: (0) Robust; (1) Weak.

201. Sigmoidal shelf for the supinator ridge extending proximally from the ectepicondyle: (0) Absent; (1) Present.

202. Styloid process of the radius: (0) Weak; (1) Strong.

203. Enlargement of the scaphoid: (0) Not enlarged (scaphoid ≤150% of the lunate); (1) Enlarged (scaphoid twice the size of the lunate); (2) Enlarged with a distolateral process.

204. Size and shape of the hamate (unciform): (0) About equal size to the triquetrum, anteroposteriorly compressed; (1) Hypertrophied, much larger than the triquetrum, mediolaterally compressed.

205. Trapezium morphology and proportion: (0) Elongate to cuboidal, larger than or subequal to the trapezoid; (1) Bean-shaped or fusiform, smaller than the trapezoid.

206. Triquetrum-lunate proportion: (0) Triquetrum nearly twice the size of the lunate; (1) Triquetrum subequal to the lunate.

Pelvic Girdle (11 characters)

207. Anterior process of the ilium: (0) Short (less than the diameter of the acetabulum); (1) Long, 1-1.5 times the diameter of the acetabulum (following Hopson and Kitching 2001); (2) Elongate, more than 1.5 times the diameter of the acetabulum.

208. Posterior process of the ilium: (0) Present; (1) Reduced or absent.

209. Acetabular dorsal emargination: (0) Open (emarginated); (1) Closed (with a complete rim).

210. Ischiatic dorsal margin and tuberosity: (0) Dorsal margin concave (emarginated) and ischiatic tuberosity present; (1) Dorsal margin concave and ischiatic tuberosity hypertrophied; (2) Dorsal margin straight and ischiatic tuberosity small.

211. Posterior spine of the ischium: (0) Elongate; (1) Short and blunt.

212. Epipubic bone: (0) Present; (1) Absent.

213. Fusion of the sacral vertebrae with the proximal caudal vertebrae: (0) Absent; (1) Present.

214. Fusion of the ischium with the caudal vertebrae: (0) Absent; (1) Present.

215. Preacetabular tubercle on the ilium for M. rectus femoris: (0) Absent; (1) Present.

216. Fully ossified floor in the acetabulum: (0) Present; (1) Absent.

217. Lesser psoas tuberosity or process on the pubis: (0) Absent; (1) Present.

Hindlimb and Pes (49 characters)

218. Inflected head of the femur set off from the shaft by a neck: (0) Neck absent and head oriented dorsally; (1) Neck present, head spherical and inflected medially.

219. Fovea for the acetabular ligament on the femoral head: (0) Absent; (1) Present.

220. Orientation of the greater trochanter: (0) Directed dorsolaterally; (1) Directed dorsally.

221. Position of the lesser trochanter: (0) On medial side of the shaft; (1) On the ventromedial or ventral side of the shaft.

222. Size of the lesser trochanter: (0) Large; (1) Small to absent.

223. The third trochanter of femur: (0) Absent; (1) Present; (2) Present as a continuous ridge connected to the greater trochanter.

224. Patellar facet (‘groove’) of the femur: (0) Absent; (1) Shallow and weakly developed; (2) Well-developed.

225. Proximo-lateral tubercle or tuberosity of the tibia: (0) Large and hook-like; (1) Indistinct.

226. Distal tibial malleolus: (0) Weak; (1) Distinct.

227. Fibula contacting the distal end of the femur: (0) Present; (1) Absent; (2) Fibula fused with the tibia.

228. Fused distal portions of the tibia and fibula: (0) Absent; (1) Present.

229. Distal fibular styloid process: (0) Weak or absent; (1) Distinct.

230. Fibula contacting the calcaneus (= 'tricontact in upper ankle joint' of Szalay 1994): (0) Extensive contact; (1) Reduced; (2) Absent.

231. Superposition (overlap) of the astragalus over the calcaneus (lower ankle joint): (0) Little or absent; (1) Weakly developed; (2) Present.

232. Astragalar neck: (0) Absent; (1) Weakly developed (asymmetrical: present only on the lateral side of the "neck region", or Szalay's [1994] comment on "necklessness").

233. Astragalar neck basal width (justification for separating this character from the navicular facet expansion is that the latter concerns symmetry, whereas this character deals with proportion; the distributions of these two character are different in some stem eutherians and crown marsupials): (0) Neck narrower than the head; (1) Neck about same width as the head (with parallel sides, constricted posterior to navicular facet); (2) Widest point of neck at mid-length (widening is not developed near the base of the neck); (3) Astragalar neck widest at the base.

234. Astragalonavicular facet aspect ratio: (0) Navicular facet transversely wider than dorsoventrally thick; (1) Navicular facet dorsoventrally thicker than transversely wide.

235. Navicular facet expansion in the astragalar head region: (0) Restricted anteriorly; (1) Asymmetrical spread only to the medial side of the astragalar "head-neck region"; (2) Astragalar head supersedes navicular so the navicular facet shifted ventrally; (3) Symmetrical spread of the navicular facet to both the lateral and the medial sides of the neck (symmetrical with regards to the main axis of the neck).

236. Astragalar trochlea (defined as a saddle-shaped upper ankle joint): (0) Absent; (1) Present, but weak (defining crest on the medial astragalo-tibial facet weakly developed); (2) Present, with clear separation of the medial and lateral tibial facets.

237. Well-defined medio-tibial crest (more or less parallel to the tibio-fibular crest) on the astragalus: (0) Absent; (1) Present.

238. Astragalar medial plantar tuberosity (AMPT of Szalay 1994 and Horovitz 2000): (0) Absent; (1) Present, but weakly developed; (2) Present, and ventrally flaring or protruding.

239. Distal end of the calcaneal tubercle: (0) Short, without a terminal swelling; (1) Elongate, vertically deep, and mediolaterally compressed, with a terminal swelling.

240. Morphology of the peroneal process of the calcaneus: (0) Laterally expanded shelf, larger than the combined length of the sustentacular and astragalar facets, lateral to the astragalar facet; (1) With a distinct and long peroneal process, laterally projecting; (2) With a distinct peroneal process, demarcated by a deep peroneal groove at the base; (3) Laterally directed, small peroneal shelf demarcated from the anterior (cuboidal) edge of the calcaneus; (4) Anterolaterally directed, hypertrophied peroneal process/shelf; (5) Peroneal structure laterally reduced (lateral surface is straight from the calcaneal tubercle).

241. Placement of the base of the peroneal process relative to the level of the cuboid facet of the calcaneus: (0) Peroneal structure posterior to the level of the cuboid facet; (1)

Peroneal structure developed anteriorly at the same level as the cuboid facet; (2) Peroneal structure hypertrophied, extending anteriorly beyond the level of the cuboid facet.

242. Peroneal groove of the calcaneus: (0) Indistinct, on the anterolateral aspect of the lateral shelf; (1) Distinct, deep separation of the peroneal process; (2) Weakly developed, with shallow groove on the lateral side of the process; (3) Distinct, on the anterolateral corner of the peroneal process.

243. Alignment of the cuboid to the main axis of the calcaneus: (0) On the anterior (distal) end of the calcaneus (the cuboid is aligned with the long axis of the calcaneus); (1) On the anteromedial aspect of the calcaneus (the cuboid is skewed to the medial side of the long axis of the calcaneus):

244. Orientation of the calcaneocuboid joint: (0) Calcaneocuboid facet on the calcaneus oriented ventrally (more visible in the plantar view than in dorsal view); (1) Calcaneocuboid facet oriented anteriorly (distally); (2) Calcaneocuboid facet oriented ventromedially or medio-obliquely.

245. Saddle-shaped calcaneocuboid joint: (0) Calcaneocuboid facet on the calcaneus relatively flat to slightly concave; (1) Saddle-shaped (differentiation of dorsal vs. proximal calcaneocuboid “facets” so that the whole calcaneocuboidal joint is saddle-shaped).

246. Lower ankle joint - orientation of the sustentacular facet of the calcaneus in relation to the horizontal plane: (0) Nearly vertical; (1) Oblique (≤70o) to nearly horizontal.

247. Antero-posterior placement of the sustentacular facet relative to the astragalar facet on the calcaneus: (0) Directly anterior to the astragalar facet and vertically oriented on the medial edge of the calcaneus; (1) On the dorsal aspect and positioned anteromedial to the astragalar facet on the calcaneus; (2) On the dorsal aspect, medial to the astragalar facet; (3) On the dorsal aspect, anterior to the astragalar facet.

248. Confluence of the sustentacular facet and the astragalar facet on the calcaneus: (0) Absent; (1) Present.

249. Ventral outline of the sustentacular process of the calcaneus: (0) Indistinctive; (1) Medially directed shelf, with rounded outline; (2) Protruding triangle, posteromedially directed;

250. Antero-posterior position of the sustentacular facet/process (using the most salient point of the facet/process in ventral view as landmark) relative to the length of the calcaneus:
(0) Near the mid-point; (1) Near the anterior (proximal) one-third.

251. Shape of posterior calcaneo-astragalar process/protuberance and its contiguous fibular contact (if the fibula contact is present) on the calcaneus: (0) Confluent with fibular contact and kidney-shaped (best viewed medially); (1) Oblong to ellipsoidal; (2) Nearly spherical and bulbous, more transversely developed than character state 1; (3) Transversely confluent with the sustentacular facet.

252. Placement of the CAF structure (structure of the calcaneoastragalar contact): (0) On the medial side of the body of the calcaneus; (1) On the dorsal side of the body of the calcaneus, but bordering on the body's medial margin (without a protruding outline); (2) On the dorsal side of the body of the calcanues and protruding beyond the body's medial margin; (3) Withdrawn and separated from the medial margin and placed along the lateral margin of the body of the calcaneus.

253. Anterior ventral (plantar) tubercle of the calcaneus: (0) Absent; (1) Present, at the anterior edge (just lateral to the cuboid facet); (2) Present, set back from the anterior edge.

254. Anteroventral groove or depression of the calcaneus: (0) Absent; (1) Present.

255. Cross-sectional shape of the body of the calcaneus at the level of the posterior calcaneoastragalar facet: (0) Dorso-ventrally compressed; (1) Mediolaterally compressed.

256. Ventral curvature of the calcaneal tubercle: (0) Present; (1) Absent.

257. Proportion of the navicular and cuboid (measured in transverse width in dorsal view): (0) Navicular narrower or subequal to cuboid; (1) Navicular wider than cuboid.

258. Proportion of the entocuneiform, mesocuneiform, and ectocuneiform (in ventral view): (0) Mesocuneiform and ectocuneiform small, their combined width smaller than the width of the entocuneiform; (1) Mesocuneiform and ectocuneiform large, their combined width (in dorsal view) exceeding the width of the entocuneiform.

259. Medio-plantar aspect of the cuboid deeply notched by the peroneus longus tendon: (0) Absent; (1) Present.

260. Prehallux: (0) Absent; (1) Present.

261. Side-by-side contact of metatarsal V and the peroneal process of the calcaneus: (0) Absent; (1) Present.

262. Relationships of the proximal end of metatarsal V to the cuboid: (0) Metatarsal V is off-set to the medial side of the cuboid; (1) Metatarsal V is so far off-set to the side of the cuboid that it contacts the calcaneus; (2) Metatarsal V is level with the anterior end of the cuboid.

263. Ventrolateral tubercle at the proximal end of metatarsal V: (0) Absent; (1) Present, at the anterior edge of the calcaneus; (2) Present, off-set posteriorly from the anterior edge of the calcaneus.

264. Angle of metatarsal III to the calcaneus (which indicates how much the sole of the foot is 'bent' from the long axis of the ankle): (0) Metatarsal III aligned with (or parallel to) the long axis of the calcaneus; (1) Metatarsal III arranged obliquely from the long axis of the calcaneus.

265. Metatarsal II and metatarsal III proximal ends: (0) II and III even or II more proximal than III; (1) III more proximal than II.

266. Opposable hallux: (0) Absent; (1) Present.

Other Postcranial Characters (4 characters)

267. Ossified patella: (0) Absent; (1) Present.

268. Sesamoid bones in the digital flexor tendons: (0) Absent; (1) Present, unpaired; (2) Present, paired.

269. External pedal (tarsal) spur: (0) Absent; (1) Present.

270. Pes digital grouping: (0) Didactylous; (1) Syndactylous.

Basicranium (68 characters)

271. External size of the cranial moiety of the squamosal: (0) Narrow; (1) Broad; (2) Expanded posteriorly to form the skull roof table.

272. Participation of the cranial moiety of the squamosal in the endocranial wall of the braincase: (0) Absent; (1) Present.

273. Multiple vascular foramina (for rami temporales) in the squamosal and parietal: (0) Absent; (1) Present.

274. Topographic relationships of the dentary-squamosal contact (or glenoid) and the cranial moiety of the squamosal (only applicable to taxa with the dentarysquamosal joint; this character is best seen in ventral view): (0) Contact on the internal aspect of the zygoma, without a constricted neck; (1) Contact on the zygoma, with a constricted neck; (2) Contact on the cranial moiety of squama; (3) On zygoma, without a constricted neck.

275. Cross-section profile of the squamosal anterior to its zygomatic root: (0) Rounded or triangular and tapering anteriorly; (1) Dorsoventral expanded and mediolaterally compressed, and not tapering anteriorly.

276. Postglenoid depression on the squamosal: (0) Present as the post-craniomandibular joint sulcus (“external auditory meatus” on the zygoma); (1) Absent; (2) Present on the skull base.

277. Squamosal - entoglenoid process: (0) Absent or vestigial; (1) Present, but separated from the postglenoid process; (2) Present, enlarged and connected to the postglenoid process.

278. Position of the craniomandibular joint: (0) Posterior or lateral to the level of the fenestra vestibuli; (1) Anterior to the level of the fenestra vestibuli.

279. Orientation of the glenoid on the squamosal: (0) On the inner side of the zygoma and facing ventromedially; (1) On the platform of the zygoma and facing ventrally.

280. Postglenoid process of the squamosal: (0) Absent; (1) Postglenoid crest raised below the fossa, but without a distinctive process; (2) Distinctive process; (3) Distinctive process buttressed by ectotympanic.

281. Postglenoid foramen presence vs. absence and composition: (0) Absent; (1) Present, in the squamosal; (2) Present, between the squamosal and petrosal; (3) Present, between the squamosal and ectotympanic.

282. Medial margin of the glenoid fossa: (0) Formed by the squamosal; (1) Formed by the alisphenoid.

283. Squamosal - epitympanic recess (this character may be ordered): (0) No contribution to the “epitympanic area” of the petrosal; (1) Small contribution to the posterolateral wall of the epitympanic recess; (2) Large contribution to the lateral wall of the epitympanic recess; (3) Squamosal forming a large part of enlarged epitympanic sinus.

284. Contribution of the basisphenoid wing (parasphenoid ala) to the external bony housing of the cochlea: (0) Participates in the rim of the fenestra vestibuli; (1) Does not reach the rim of the fenestra vestibuli; (2) Absent or excluded from the cochlear housing.

285. Relationship of the cochlear housing to the lateral lappet of the basioccipital: (0) Entirely covered by the basioccipital; (1) Medial aspect covered by the basioccipital; (2) Partially (~about half width on the medial side) covered by the basioccipital; (3) Fully exposed as the promontorium.

286. Thickened rim of the fenestra vestibuli: (0) Present; (1) Absent.

287. Cochlear housing fully formed by the petrosal: (0) Absent; (1) Present.

288. Ventromedial surface of the promontorium: (0) Flat; (1) Inflated and convex.

289. Lateral wall and overall external outline of the promontorium: (0) Triangular, with a steep and slightly concave lateral wall; (1) Elongate and cylindrical; (2) Bulbous and oval shaped.

290. Cochlea: (0) Cochlear recess (without a canal); (1) Short canal; (2) Elongate canal, to the fullest extent of the promontorium; (3) Curved; (4) Elongate and partly coiled; (5) Elongate and coiled to at least 360°.

291. Internal acoustic meatus - cribriform plate: (0) Absent; (1) Present.

292. Internal acoustic meatus depth: (0) Deep with thick prefacial commissure; (1) Shallow with thin prefacial commissure.

293. Primary bony lamina within the cochlear canal: (0) Absent; (1) Present.

294. Secondary bony lamina for the basilar membrane within the cochlear canal: (0) Absent; (1) Present.

295. Crista interfenestralis: (0) Horizontal, broad, and extending to the base of the paroccipital process; (1) Vertical, delimiting the back of the promontorium; (2) Horizontal, narrow, and connecting to the caudal tympanic process.

296. Post-promontorial tympanic recess: (0) Absent; (1) Present.

297. Rostral tympanic process of the petrosal: (0) Absent or low ridge; (1) Tall ridge, but restricted to the posterior half of the promontorium; (2) Well-developed ridge reaching the anterior pole of the promontorium.

298. Caudal tympanic process of the petrosal: (0) Absent; (1) Present; (2) Present, notched; (3) Present, hypertrophied and buttressed against the exoccipital paracondylar process.

299. Petrosal - tympanic process (Kielan-Jaworowska- 1981): (0) Absent; (1) Present.

300. Rear margin of the auditory region: (0) Marked by a steep wall; (1) Extended onto a flat surface.

301. Prootic canal: (0) Absent; (1) Present, vertical; (2) Present, horizontal and reduced.

302. Position of the sulcus for the anterior distributary of the transverse sinus relative to the subarcuate fossa. (0) Anterolateral; (1) Posterolateral.

303. Lateral trough floor anterior to the tympanic aperture of the prootic canal and/or the primary facial foramen: (0) Open lateral trough, no bony floor; (1) Bony floor present; (2) Lateral trough absent.

304. Anteroventral opening of the cavum epiptericum: (0) Present; (1) Present, with reduced size (due to the anterior expansion of the lateral trough floor); (2) Present, partially enclosed by the petrosal; (3) Present, enclosed by the alisphenoid and petrosal; (4) Present, as large piriform fenestra.

305. Enclosure of the geniculate ganglion by the bony floor of the petrosal in the cavum supracochleare: (0) Absent; (1) Present.

306. Hiatus Fallopii: (0) Present, in the petrosal roof of the middle ear; (1) Present, at the anterior end of the petrosal; (2) Absent (applicable only to those taxa with a cavum supracochleare).

307. Foramen ovale - composition: (0) Between the petrosal and alisphenoid; (1) Secondary foramen partially or fully enclosed by the alisphenoid, in addition to the

primary foramen between the petrosal and alisphenoid; (2) In the petrosal (anterior lamina); (3) Between the alisphenoid and squamosal; (4) Within the alisphenoid.

308. Foramen ovale - position: (0) On the lateral wall of the braincase; (1) On the ventral surface of the skull.

309. Number of exit(s) for the mandibular branch of the trigeminal nerve (V3): (0) One; (1) Two.

310. Quadrate ramus of the alisphenoid: (0) Forming a rod underlying the anterior part of the lateral flange; (1) Absent.

311. Alisphenoid canal (for the ramus inferior and/or ramus infraorbitalis): (0) Absent; (1) Present.

312. Anterior lamina exposure on the lateral braincase wall: (0) Present; (1) Reduced or absent.

313. Orientation of the anterior part of the lateral flange: (0) Horizontal shelf; (1) Ventrally directed; (2) Medially directed and contacting the promontorium; (3) Vestigial or absent.

314. Vertical component of the lateral flange ('L-shaped' and forming a vertical wall to the pterygoparoccipital foramen): (0) Present; (1) Absent.

315. Vascular foramen in the posterior part of the lateral flange (and anterior to the pterygoparoccipital foramen): (0) Present; (1) Absent.

316. Relationship of the lateral flange to the crista parotica (or the anterior paroccipital process that bears the crista): (0) Widely separated; (1) Narrowly separated; (2) Continuous.

317. Pterygoparoccipital foramen (for the ramus superior of the stapedial artery): (0) Laterally open notch; (1) Foramen enclosed by the petrosal or squamosal; (2) Absent.

318. Position of the pterygoparoccipital foramen relative to the level of the fenestra vestibuli: (0) Posterior or lateral; (1) Anterior.

319. "Bifurcation of the paroccipital process" - presence vs. absence (this is modified from the character used in several previous studies): (0) Absent; (1) Present.

320. Posterior paroccipital process of the petrosal: (0) No ventral projection below the level of the surrounding structures; (1) Projecting below the surrounding structures.

321. Morphological differentiation of the anterior paroccipital region: (0) Anterior paroccipital is bulbous and distinctive from the surrounding structures; (1) Anterior paroccipital region has a distinct crista parotica.

322. Epitympanic recess lateral to the crista parotica: (0) Absent; (1) Present.

323. Tympanohyal contact with the cochlear housing: (0) Absent; (1) Present.

324. Relationship of the squamosal to the paroccipital process: (0) Squamosal covers the entire paroccipital region; (1) No squamosal cover on the anterior paroccipital region; (2) Squamosal covers a part of the paroccipital region, but not the crista parotica (the squamosal wall and the crista parotica are separated by the epitympanic recess).

325. Medial process of the squamosal reaching toward the tympanic cavity: (0) Absent; (1) Present (near or bordering on the foramen ovale).

326. Stapedial artery sulcus on the petrosal: (0) Absent; (1) Present.

327. Transpromontorial sulcus for the internal carotid artery on the cochlear housing: (0) Absent; (1) Present.

328. Deep groove on the anterior pole of the promontorium (Muizon 1994): (0) Absent; (1) Present.

329. Epitympanic wing medial to the promontorium: (0) Absent; (1) Present.

330. Ectopterygoid process of the alisphenoid: (0) Absent; (1) Present.

331. Tympanic process of the alisphenoid: (0) Absent; (1) Present, but limited to the "piriform" region of the basicranium; (2) Intermediate; (3) Well-developed, extending to near the jugular foramen.

332. Hypotympanic recess in the junction of the alisphenoid, squamosal, and petrosal: (0) Absent; (1) Present.

333. Separation of the fenestra cochleae from the jugular foramen: (0) Absent; (1) Separate but within the same depression; (1) Separate (not within the same depression).

334. Channel of the perilymphatic duct: (0) Open channel and sulcus; (1) At least partially enclosed channel.

335. Jugular foramen size relative to the fenestra cochleae (applicable only to those taxa with a jugular foramen fully separated from the fenestra cochleae): (0) Jugular subequal to the fenestra cochleae; (1) Jugular larger than the fenestra cochleae.

336. Relationship of the jugular foramen to the opening of the inferior petrosal sinus: (0) Confluent; (1) Separate.

337. Stapedial muscle fossa size: (0) Absent; (1) Present, small; (2) Present, large (twice the size of the fenestra vestibuli).

338. Hypoglossal foramen: (0) Indistinct, either confluent with the jugular foramen or sharing a depression with the jugular foramen; (1) Separated from the jugular foramen; (2) Separated from the jugular foramen; the latter has a circular, raised external rim.

Middle Ear Ossicle Characters (16 Characters)

339. Geometry (shape) of the incudo-mallear contact: (0) Trochlear (convex and cylindrical) surface of the incus; (1) Trough; (2) Saddle-shaped contact on the incus; (3) Flat surface.

340. Alignment of the incus and the malleus: (0) Posterior-anterior; (1) Posterolateral to anterior medial; (2) Dorsoventral.

341. Twisting of the dorsal plate relative to the trochlea on the quadrate: (0) Dorsal plate aligned with the trochlea; (1) Dorsal plate twisted relative to the trochlea, (2) Dorsal plate twisted and elevated from the trochlea; (3) Dorsal plate reduced to a conical process (crus longum).

342. Presence of a quadrate/incus neck (slightly constricted region separating the dorsal plate or crus brevis from the trochlea; this represents the differentiation between the 'body' and crus brevis of the incus): (0) Absent; (1) Present.

343. Dorsal plate (= crus brevis) of the quadrate/incus: (0) Broad plate; (1) Pointed triangle; (2) Reduced.

344. Incus - angle of the crus brevis to crus longum of the incus (this is equivalent to the angle between the dorsal plate and the stapedial process of the quadrate): (0) Alignment of the stapedial process (crus longum) and the dorsal plate (crus brevis) (or an obtuse angle between the two structure) (distinctive process is lacking, stapes/incus contact is on the medial side of the quadrate trochlea); (1) Perpendicular or acute angle of the crus brevis and crus longum ("A-shaped" incus).

345. Primary suspension of the incus/quadrate on the basicranium: (0) By quadratojugal in addition to at least one other basicranial bone; (1) By squamosal only; (2) By petrosal

(either by the preserved direct contact of the incus or by inference from the presence of a well-defined crista parotica).

346. Quadratojugal: (0) Present; (1) Absent.

347. Morphology of the stapes: (0) Columelliform–macroperforate; (1) Columelliform–imperforate (or microperforate); (2) Bicrurate–perforate.

348. Stapedial ratio: (0) Less than 1.4; (1) 1.4-1.8; (2) ≥1.8.

349. Bullate stapedial footplate: (0) Absent; (1) Present.

350. Malleolar neck: (0) Absent; (1) Present.

351. Ectotympanic ring (may be ordered): (0) Plate-like; (1) Curved and rod-like; (2) Ring-shaped; (3) Slightly expanded (fusiform); (4) Expanded; (5) Tube-like.

352. Entotympanic and its contribution to the bullar structure: (0) Absent; (1) Present.

353. Position/orientation of the incisura tympanica: (0) Posteroventral; (1) Posterior; (2) Postero-dorsal; (3) Dorsal.

354. Fusion of the ectotympanic to other bones: (0) Absent; (1) Fused to other bones.

Other Cranial Characters (44 characters)

355. Posterior extent of the bony secondary palate: (0) Anterior to the posterior end of the tooth row; (1) Level with the posterior end of the tooth row; (2) Extending posterior to the tooth row; (3) Extending to the basisphenoid-basioccipital suture.

356. Posterior median spine (or torus) on the palate: (0) Absent; (1) Present.

357. Pterygopalatine ridges: (0) Present; (1) Absent.

358. Transverse process of the pterygoid: (0) Present and massive; (1) Present but reduced (as the hamulus); (2) Greatly reduced (with a vestigial crest on pterygoid) or absent.

359. Pterygoids contact on midline: (0) Present; (1) Absent.

360. Ventral opening of the minor palatine foramen: (0) Encircled by the pterygoid (and ectopterygoid if present) in addition to the palatine; (1) Encircled by the palatine and maxilla, separated widely from the subtemporal margin; (2) Encircled completely by the palatine (or between palatine and maxilla), large, with thin bony bridge from the subtemporal margin; (3) Large, posterior fenestration; (4) Notch.

361. Transverse canal foramen: (0) Absent; (1) Present.

362. Carotid foramen position: (0) Within the basisphenoid; (1) Within the basisphenoid/basioccipital suture; (2) Within the basisphenoid/petrosal suture; (3) Through the opening of the cavum epiptericum.

363. Overhanging roof of the orbit: (0) Absent; (1) Present, formed by the frontal.

364. Exit(s) of the infraorbital canal: (0) Single; (1) Multiple.

365. Composition of the posterior opening of the infraorbital canal (maxillary foramen): (0) Between the lacrimal, palatine, and maxilla; (1) Exclusively enclosed by the maxilla; (2) Enclosed by the maxilla, frontal and palatine.

366. Size and shape of the lacrimal: (0) Small, oblong-shaped on the facial part of the rostrum; (1) Large, triangleshaped on the facial portion of rostrum; (2) Crescent shaped on the facial portion of the rostrum; (3) Reduced to a narrow strap; (4) Absent from the facial portion of the rostrum.

367. Location of the lacrimal foramen: (0) Within the orbit; (1) On the facial side of the lacrimal (anterior to or on the anterior orbital margin).

368. Number of lacrimal foramina: (0) One; (1) Two.

369. Lacrimal foramen composition: (0) Within the lacrimal; (1) Bordered by or within the maxilla.

370. Maximum vertical depth of the zygomatic arch relative to the length of the skull (this character is designed to indicate the robust vs. gracile nature of the zygomatic arch): (0) Between 10-20%; (1) Between 5-7%; (2) Zygoma incomplete.

371. Frontal/alisphenoid contact: (0) Dorsal plate of the alisphenoid contacting the frontal at the anterior corner; (1) Dorsal plate of the alisphenoid with more extensive contact with the frontal (~50% of its dorsal border); (2) Absent.

372. Frontal-maxilla facial contact: (0) Absent; (1) Present.

373. Nasal-frontal suture - medial process of the frontals wedged between the two nasals: (0) Absent; (1) Present.

274. Pila antotica: (0) Present; (1) Absent.

375. Fully ossified medial orbital wall of the orbitosphenoid: (0) Absent; (1) Present, forming the ventral floor of the braincase but not the entire orbital wall; (2) Present, forming both the braincase floor and the medial orbital wall.

376. Separation of the optic foramen from the sphenorbital fissure: (0) Absent; (1) Present.

377. Orbital opening for the minor palatine nerve: (0) Absent; (1) Present.

378. Anterior part of the jugal on the zygoma: (0) Anterior part of the jugal extends to the facial part of the maxilla and forms a part of the anterior orbit; (1) Anterior part of the jugal does not reach the facial part of the maxilla and is excluded from the anterior orbit margin.

379. Posterior part of the jugal: (0) Contributes to the squamosal glenoid; (1) Borders on but does not contribute to the squamosal glenoid; (2) Terminates anterior to the squamosal glenoid.

380. Maxillary in the sub-temporal margin of the orbit: (0) Absent; (1) Present; (2) Present and extensive.

381. Orbital process of the frontal borders on the maxilla within orbit: (0) Absent; (1) Present.

382. Anterior ascending vascular channel (for the arteria diploëtica magna) in the temporal region: (0) Open groove; (1) Partially enclosed in a canal; (2) Completely enclosed in a canal or endocranial; (3) Absent.

383. Posttemporal canal for the arteria and vena diploëtica: (0) Present, large; (1) Small; (2) Absent.

384. Nuchal crest: (0) Overhanging the concave or straight supraoccipital; (1) Weakly developed with convex supraoccipital.

385. Sagittal crest: (0) Prominently developed; (1) Weakly developed; (2) Absent.

386. Tabular bone: (0) Present; (1) Absent.

387. Occipital slope: (0) Occiput sloping posterodorsally (or vertically oriented) from the occipital condyle; (1) Occiput sloping anterodorsally from the occipital condyle (such that the lambdoidal crest is leveled anterior to the occipital condyle and condyle is fully visible in dorsal view of the skull).

388. Occipital artery groove on the occiput extending dorsal to the posttemporal foramen: (0) Absent; (1) Present.

389. Foramina on the dorsal surface of the nasals: (0) Absent; (1) Present.

Fruitafossor windscheffeli: (?) Unknown.

390. Septomaxilla: (0) Present, with the ventromedial shelf; (1) Present, without the ventromedial shelf; (2) Absent.

391. Internarial process of the premaxilla: (0) Present; (1) Absent.

392. Posterodorsal process of the premaxilla: (0) Does not extend beyond canine ("short or absent"); (1) Extends beyond canine ("intermediate"); (2) Contacts frontal posteriorly (“long”).

393. Facial part of the premaxilla borders on the nasal: (0) Absent; (1) Present.

394. Premaxilla - palatal process relative to the canine alveolus: (0) Does not reach to the level of the canine alveolus; (1) Reaches the level of the canine alveolus.

395. Palatal vacuities: (0) Absent; (1) Present, near palatomaxillary border; (2) Present, either positioned near or extended to the posterior edge of bony palate.

396. Major palatine foramina: (0) Absent; (1) Present.

397. Ossified ethmoidal cribriform plate of the nasal cavity: (0) Absent; (1) Present.

398. Posterior excavation of the nasal cavity into the bony sphenoid complex: (0) Absent; (1) Present; (2) Present and partitioned from the nasal cavity.

Cranial Vault and Brain Endocast Characters (7 characters)

399. External bulging of the braincase in the parietal region: (0) Absent; (1) Expanded (the parietal part of the cranial vault is wider than the frontal part, but the expansion does not extend to the lambdoidal region); (2) Greatly expanded (expansion of the cranial vault extends to the lambdoidal region).

400. Anterior expansion of the vermis (central lobe of the cerebellum): (0) Absent; (1) Present.

401. Overall size of the vermis: (0) Small; (1) Enlarged.

402. Lateral cerebellar hemisphere (excluding the paraflocculus): (0) Absent; (1) Present.

403. External division on the endocast between the olfactory lobe and the cerebral hemisphere (well-defined transverse sulcus separating the olfactory lobes from the

cerebrum): (0) Absence of external separation of the olfactory lobe from cerebral hemisphere; (1) Enlarged olfactory lobes; (2) Clear division of transverse sulcus.

404. Anterior expansion of the cerebral hemisphere: (0) Absent; (1) Present.

405. Expansion of the posterior cerebral hemisphere (for each hemisphere, not the combined width of the posterior hemispheres): (0) Absent; (1) Present.

Soft-tissue characters (2 characters)

406. Trophoblasts in the placenta: (0) Absent; (1) Present.

407. Mullerian ducts (oviduct and uterus) pass in between the ureters (Renfree, 1993): (0) Absent; (1) Present.

New characters added by Rowe et al., 2008 (15 characters)

408. Platypus-type bill: (0) Absent; (1) Present.

409. Electrophoretic capability with snout: (0) Absent; (1) Present.

410. Narial aperture: (0) Facing anteriorly; (1) Dorsally; (2) Anteroventrally where plane of perpendicular reference is defined by the narial circumference or rim.

411. Rostrum shape: (0) Tubular and narrowing anteriorly, its tip narrower in width than the distance between the orbits; (1) Flattened and wider than distance between the orbits; (2) Conically narrowed to elongate sharp point.

412. Premaxilla facial process: (0) Separated from nasal by septomaxilla, (1) Premaxilla contacting nasal; (2) Premaxillary facial process absent.

413. Premaxilla: (0) With palatine process continuous and connected to premaxillary alveolar process; (1) Lacking palatine process.

414. Septomaxilla facial process: (0) Forming vertical process exposed on lateral surface of face between nasal and maxilla; (1) Flattened plate exposed on dorsal surface of snout between nasal and maxilla; (2) Facial processes surrounding nares and meeting on dorsal midline; (3) Septomaxilla facial process absent.

415. Nasals width: (0) Widest posteriorly, near orbits; (1) Widest anteriorly around naris.

416. Maxilla facial process: (0) Smooth and unelaborated around perforations for maxillary nerve; (1) Having a robust posterolateral maxillary process that buttresses the large lateral maxillary nerve exit and forms attachment base for the bill.

417. Maxillary canal diameter: (0) Comparatively narrow and much smaller than nasopharyngeal passageway; (1) Greatly hypertrophied and nearly equal to nasopharyngeal diameter.

418. Vomer: (0) Tall Y-shaped element with groove running along tall longitudinal midline plate; (1) Short V- shaped bone lacking longitudinal plate.

419. Roof of nasopharyngeal passageway: (0) Nasals form plates of bone largely confined to the roof of the nasopharyngeal passageway; (1) Nasals with a ventral process that curves down and medial to maxilla and forms extensive medial wall and partial floor to nasopharyngeal passageway.

420. Faux cerebri: (0) Not ossified between cerebral hemispheres; (1) Forming a deep ossified septum between cerebral hemispheres.

421. Mesthmoid: (0) Not ossified; (1) Ossifies to form multiple turbinals and a cribriform plate with many small foramina; (2) Ossifies to form multiple turbinals and a cribriform plate with only one, or a small number of, large perforations.

422. Mandibular foramen and canal diameter: (0) Comparatively narrow; (1) Greatly hypertrophied to half or more the diameter of dentary.

New characters

Cranial characters (17 characters)

423. Ratio of rostrum length to skull length (rostrum length measured as rostral tip of premaxilla to edge of orbit around the lacrimal foramen region Fig. 2.2): (0) Rostrum is less than half the length of the skull; (1) Rostrum is over half the length of the skull.

424. Jugal: (0) Present, comprising anterior end of zygomatic arch; (1) Reduced; (2) Absent.

425. Curvature of rostrum (Fig. 2.3): (0) Straight, protruding anteriorly; (1) Straight, angled ventrally; (2) Decurved; (3) Recurved.

426. Roof of nasopharyngeal passageway visible in ventral view due to recession of secondary palate (Fig. 2.3): (0) Absent; (1) Anterior-most portion of septomaxillae visible due to minor recession of secondary palate; (2) Secondary palate is significantly receded exposing much of the ventral surface of the septomaxillae.

427. Dorsal exposure of anterior portion of vomer due to recessive nasals (Fig. 2.4): (0) Absent; (1) Present.

428. Posteromedial incision of palatine (Fig. 2.5): (0) Absent; (1) Present, shallow; (2) Present, deep.

429. Rostral end of secondary palate (Fig. 2.6): (0) Extends to the tip of the rostrum; (1) Ends at maxillae.

430. Shape of rostral end of maxillary palatal process (Fig. 2.7): (0) “W”-shaped at the midline; (1) Slightly concave, or “V”-shaped.

431. Shape of secondary palate in cross section (Fig. 2.8): (0) Flat; (1) Broadly arched; (2) Narrowly arched.

432. Palatal sculpturing: (0) Absent; (1) Prominent transverse bony ridges (see fig. 3 of Griffiths, 1991); (2) Slight transverse bony ridges.

433. Parietal sculpturing (Fig. 2.9): (0) Absent; (1) Present.

434. Parietal anterior suture (Fig. 2.10): (0) Contacts frontal only; (1) Contacts or nearly contacts nasal.

435. Contact of posterior temporal suture of parietal (Fig. 2.11): (0) Squamosal; (1) Squamosal and periotic.

436. Incisura occipitalis (Fig. 2.12): (0) Absent; (1) Present.

437. Palatal process of premaxilla (in ventral view, Fig. 2.13): (0) Extremely short, terminating anterior to canine; (1) Present, sharply pointed, not extending far past rostral end of palate; (2) Present, very long, extending well beyond rostral end of palate.

438. Position/Orientation of middle ear ossicles (Fig. 2.14): (0) Nearly vertical; (1) Horizontal.

439. Occipital condyles position relative to ventral-most surface of skull (visible in lateral view, Fig. 2.15): (0) Slightly rostral to, or closely aligned with, dorsal aspect of occiput and level with ventral surface of skull; (1) Extends further caudally than occiput, level with ventral surface of skull; (2) Extends further caudally than occiput, positioned roughly in the middle of the back of the skull.

Mandibular characters (9 characters)

440. Coronoid process orientation (Fig. 2.16): (0) Dorsal; (1) Lateral.

441. Position of dentary symphysis (Fig. 2.17): (0) Distal, terminal end of dentary; (1) Not at the terminal end of the dentary.

442. Terminal end of dentaries (Fig. 2.18): (0) Fused; (1) Free, pointed; 2) Free, spatulate.

443. Medial ‘foramen mandibulare anterius dorsale’ from Zeller, 1989a (Fig. 2.19): (0) Absent; (1) Present.

444. Curvature of dentaries (Fig. 2.20): (0) Curve medially, angle dorsally anterior to angular process; (1) Bow laterally, relatively flat but angle dorsally at angular process.

445. Dentary condyle shape (Fig. 2.21): (0) No condyle; (1) Round, or anteroposterior axis of curvature; (2) Axis of curvature is mediolateral.

446. Composition of CMJ: (0) Quadrate-articular; (1) Quadrate-articular and dentary-squamosal; (2) Dentary-squamosal.

447. Mandibular tubercle (Fig. 2.22): (0) Absent; (1) Present.

448. Mandibular canal entrance (Fig. 2.23): (0) Single entrance; (1) Two entrances.

Postcranial Characters (16 characters)

449. Spinal nerve exit (Fig. 2.24): (0) Between vertebrae; (1) through foramina in neural arches.

450. Ribs (Fig. 2.25): (0) Two heads that articulate with vertebrae; (1) One head that articulates with vertebrae.

451. Cervical zygapophyses: (0) Present; (1) Absent in first 5 cervicals; (2) Absent.

452. Ventral processes on atlas (Fig. 2.26): (0) Absent; (1) Present.

453. Ossified, imbricating ventral ribs (Fig. 2.27): (0) Absent; (1) Present.

454. Teres major tubercle (Fig. 2.28): (0) Weak structure that does not project medially beyond lesser tubercle; (1) Robust, projecting beyond lesser tubercle.

455. Entepicondylar foramen position (ventral/posterior view, Fig. 2.29): (0) Near margin of proximal part of entepicondyle; (1) Centrally within the entepicondyle.

456. Disposition of inter-epicondylar axis (based on position of ectepicondyle to proximal end of humerus, Fig. 2.30): (0) Approximately 90° or greater; (1) Less than 90° (between 75° and 80°).

457. Distinct articulation sites for radius and ulna (Fig. 2.31): (0) Present; (1) Absent.

458. Elbow joint aligned with long axis of humerus (Fig. 2.32): (0) Present; (1) Absent, elbow joint off-centered laterally.

459. Radius and ulna (Fig. 2.33): (0) Bowed and separate, allowing for pronation and supination; (1) Straight, appressed along entire length limiting opportunity for pronation and supination.

460. Ulnar contribution to wrist: (0) Minimal; (1) Substantial.

461. Trochlea on distal end of ulna (Fig. 2.34): (0) Absent; (1) Present.

462. Dual concave facets on radius (Fig. 2.35): (0) Absent; (1) Present

463. Dual processes on olecranon (Fig. 2.36): (0) Absent; (1) Present.

464. Rounded, laterally inflected process on distal tibia (Fig. 2.37): (0) Absent; (1) Present.

APPENDIX 2.B. APOMORPHY LIST

Below is a list of synapomorphies for each node at and within Monotremata recovered from the parsimony search. The left column identifies the node at which the synapomorphies occur. The preceeding column identifies the character number corresponding to the character matrix and the description of that character as it is written in the character matrix. The consistency index (CI) is listed next followed by the change in character state. A double-lined arrow indicates an unambiguous character state change while a single-lined arrow indicates an ambiguous synapomorphy.

Node	Character # (description)	CI	Character state change
Monotremata	2 (SA/PRA scars)	0.500	0 ==> 1
	10 (Ang ventral s)	0.250	0 --> 1
	11 (Coronoid foss)	0.250	0 ==> 1
	12 (Man for post)	0.500	0 --> 3
	28 (Den peduncle)	0.500	0 ==> 3
	30 (Gracile denta)	1.000	0 ==> 1
	134 (# of lower i)	0.455	1 ==> 5
	135 (# upper inci)	0.455	0 --> 4
	136 (Up. canine p)	0.222	0 --> 2
	138 (Lower canine)	0.286	0 --> 2
	162 (Atlas interc)	0.500	0 ==> 1
	163 (Atlas rib)	0.500	0 ==> 1

164 (Dens of axis)	0.500	0 --> 1
166 (Cervical rib)	0.500	0 ==> 1
174 (Front interc)	0.250	1 ==> 0
181 (Teres m foss)	0.500	0 ==> 1
199 (Hu radial co)	0.500	0 ==> 2
201 (S-shape supi)	0.250	0 --> 1
209 (Acebatular n)	0.500	0 ==> 1
210 (Ischium tube)	0.750	0 --> 1
215 (Preacetabula)	1.000	0 ==> 1
217 (Lesser psoas)	1.000	0 ==> 1
223 (3rd Trochant)	1.000	0 ==> 2
226 (Tibial malle)	0.167	0 ==> 1
240 (Pero-Proc-Mo)	0.714	0 ==> 1
242 (Peroneal gro)	0.400	0 ==> 1
243 (Cal/cub bone)	0.333	0 --> 1
256 (Cal-tuber cu)	0.250	0 ==> 1
261 (Cal-Pero-MT)	1.000	0 ==> 1
267 (Ossified pat)	0.333	0 ==> 1
268 (Flexor Sesam)	1.000	0 ==> 1
269 (Extarsal spu)	0.333	0 --> 1
274 (SQ/glenoid r)	0.600	1 ==> 2
275 (SQ zygo-prof)	0.333	0 ==> 1

276 (SQ PG depres)	0.500	2 ==> 1
280 (SQ Postgleno)	0.500	1 ==> 0
290 (Cochlear can)	0.800	3 ==> 4
291 (IAM cribrifo)	0.500	0 ==> 1
308 (FO position)	0.333	0 ==> 1
323 (Tympanohyal)	1.000	0 ==> 1
337 (Stapedial fo)	0.500	1 ==> 0
338 (XII foramen)	0.667	1 ==> 0
347 (Stapedial mo)	0.667	0 --> 1
355 (2nd palate)	0.500	2 ==> 3
366 (Size/shape l)	0.667	1 ==> 4
369 (Lacr fo comp)	0.500	0 ==> 1
371 (Fr/Al contac)	0.667	0 --> 2
373 (Medial Frt/n)	0.500	0 ==> 1
374 (Pila antotic)	0.333	0 --> 1
381 (Fron/Mx in o)	0.500	0 ==> 1
384 (Lambdoidal c)	0.333	0 --> 1
400 (Vermis anter)	0.500	0 --> 1
409 (Electrorecep)	1.000	0 --> 1
410 (Narial apert)	1.000	0 ==> 1
412 (Pmx facial p)	0.667	0 --> 2
413 (Pmx pal proc)	1.000	0 ==> 1

423 (Rostrum-skul)	0.500	0 ==> 1
429 (Rostral end)	1.000	0 ==> 1
433 (Parietal scu)	1.000	0 ==> 1
434 (Parietal ant)	1.000	0 ==> 1
436 (Incisura occ)	1.000	0 ==> 1
438 (Pos/Orient o)	1.000	0 --> 1
440 (Coronoid pro)	1.000	0 ==> 1
442 (Terminus of)	1.000	0 ==> 2
443 (Medial MAD f)	1.000	0 ==> 1
444 (Dentary curv)	1.000	0 ==> 1
445 (dentary cond)	1.000	0 --> 1
449 (Spinal nerve)	1.000	0 ==> 1
450 (rib heads)	1.000	0 ==> 1
453 (Ossified ven)	1.000	0 ==> 1
456 (Inter-epicon)	1.000	0 ==> 1
457 (Trochlear-fo)	1.000	0 ==> 1
458 (Elbow joint)	0.500	0 --> 1
459 (Radius + uln)	1.000	0 ==> 1
460 (Ulnar contri)	1.000	0 ==> 1
461 (Distal ulna)	1.000	0 ==> 1
462 (Distal radiu)	1.000	0 ==> 1
463 (Olecranon du)	1.000	0 ==> 1

Pan-Ornithorhynchidae	7 (Dent angl pres	0.400	1 ==> 2
	9 (Vertical lvl o)	0.500	0 ==> 1
	20 (Masse fossa v)	0.400	0 ==> 2
	21 (Ant border ms)	0.400	0 ==> 2
	31 (Cond level to)	0.333	0 ==> 1
	54 (Post molar tr)	0.750	0 --> 2
	59 (Cusps/wears)	0.556	1 --> 3
	60 (M Prtd-mecd r)	0.250	0 --> 1
	66 (Ant-Ling cusp)	0.375	0 --> 3
	73 (trigonid patt)	0.750	0 --> 2
	74 (Paracristid)	0.667	0 --> 2
	75 (Paratd/protid)	0.667	0 --> 2
	77 (Trigonid shor)	0.750	0 --> 4
	78 (m2 trg/ta wid)	0.500	0 --> 2
	79 (Hypoflexid)	0.400	0 --> 2
	80 (Talonid morph)	0.714	0 --> 2
	81 (Hypoconid)	0.667	0 --> 1
	82 (Hypoconulid)	0.600	0 --> 2
	83 (Hypcld orient)	0.400	0 --> 1
	85 (Ultimate-l-m)	0.333	0 --> 1
	90 (Talonid eleva)	0.667	1 --> 4
	127 (Molar facet)	1.000	0 --> 2

	129 (post-lat tal)	0.500	0 --> 2
	133 (Surface in t)	1.000	0 --> 2
	422 (Mandibular c)	1.000	0 ==> 1
	447 (Mandibular t)	1.000	0 ==> 1
Ornithorhynchidae	33 (Reduced denta)	0.500	0 --> 1
	53 (lw m-1 triang)	0.500	0 --> 1
	61 (M Pacd-mecd r)	0.375	2 ==> 1
	63 (Cristid obliq)	0.750	0 ==> 1
	64 (M Pre-entocri)	0.500	0 --> 1
	68 (Mesial cingul)	0.375	0 --> 2
	70 (Postcingulid)	0.500	0 ==> 1
	91 (Lab Styl Shel)	0.667	0 --> 2
	94 (stylar shelf)	0.444	0 --> 1
	101 (Para/meta ba)	0.333	0 --> 1
	120 (outline of u)	0.444	0 --> 3
	122 (Wear develop)	0.400	1 ==> 2
	124 (Prevallum/po)	0.750	0 ==> 3
	128 (Orient facet)	0.250	0 --> 1
	320 (Ventral Proj)	0.250	0 --> 1
	333 (JF/FC separa)	0.500	1 --> 0
	365 (IOF composit)	0.500	0 --> 2
	372 (Frontal-max)	0.333	0 --> 1

	382 (Ascending ch)	0.750	1 --> 0
	408 (Bill)	1.000	0 --> 1
	411 (Rostrum shap)	1.000	0 --> 1
	414 (Smx facial p)	0.750	0 --> 1
	415 (Nasals width)	0.500	0 --> 1
	416 (Maxillary ne)	1.000	0 --> 1
	417 (Maxillary ca)	1.000	0 --> 1
	420 (Faux cerebri)	0.250	0 --> 1
	421 (Mesethmoid)	0.667	1 --> 2
	424 (Jugal)	0.667	0 --> 1
	425 (Curvature of)	1.000	0 --> 1
	427 (Vomer exposu)	1.000	0 --> 1
	437 (palatal proc)	1.000	0 --> 1
	441 (Dentary symp)	0.500	0 --> 1
	448 (Mandibular n)	1.000	0 ==> 1
	464 (Medial proce)	1.000	0 --> 1
Pan-Tachyglossidae	142 (# lower mola)	0.400	3 --> 4
	271 (SQ cranial s)	0.500	0 ==> 1
	278 (SQ CMJ posit)	0.250	0 --> 1
	319 (PP bifurcati)	0.500	1 ==> 0
	322 (Epitym Reces)	0.333	0 --> 1
	360 (Minor pal on)	0.667	1 ==> 5

	364 (infr-orb for)	0.500	0 ==> 2
	365 (IOF composit)	0.500	0 --> 1
	411 (Rostrum shap)	1.000	0 --> 2
	414 (Smx facial p)	0.750	0 --> 2
	424 (Jugal)	0.667	0 --> 2
	425 (Curvature of)	1.000	0 --> 2
	428 (Palatine inc)	0.667	0 ==> 1
	430 (Rostral end)	1.000	0 ==> 1
	435 (Parietal pos)	1.000	0 ==> 1
	437 (palatal proc)	1.000	0 --> 2
	439 (OC position)	1.000	0 ==> 1
	441 (Dentary symp)	0.500	0 --> 1
	455 (Entepicondyl)	0.500	0 ==> 1
Tachyglossidae	8 (Dent angle pos)	0.333	0 --> 1
	27 (Size of Den c)	0.600	1 --> 3
	33 (Reduced denta)	0.500	0 --> 1
	216 (Acetabular f)	1.000	0 --> 1
	222 (Less troch s)	0.500	0 --> 1
	359 (Ptgd meet mi)	0.500	0 --> 1
	383 (PTC size)	0.500	0 ==> 1
	397 (Ossified cri)	0.333	0 --> 1
	419 (roof of nasa)	1.000	0 ==> 1

426 (Nasopharyng)	1.000	0 --> 2
431 (Hard palate)	0.667	0 --> 2
432 (Palatal scul)	1.000	0 --> 2
451 (Cervical zyg)	1.000	0 --> 1

References

Allen, G. M. 1912. Zaglossus. *Memoirs of the Museum of Comparative Zoology at Harvard College* **40**: 253-307, Plates 1-2.

Archer, M., M. D. Plane, and N. S. Pledge. 1978. Additional evidence for interpreting the Miocene *Obdurodon insignis* Woodburne and Tedford, 1975, to be a fossil platypus (Ornithorhynchidae: Monotremata) and a reconsideration of the status of *Ornithorhynchus agilis* De Vis, 1885. *Australian Zoologist* **20**: 9-27.

Archer, M., T. F. Flannery, A. Ritchie, and R. E. Molnar. 1985. First Mesozoic mammal from Australia—an early Cretaceous monotreme. *Nature* **318**: 363-366.

Archer, M., F. A. Jenkins Jr, S. J. Hand, P. Murray, and H. Godthelp. 1992. Description of the skull and non-vestigial dentition of a Miocene platypus (*Obdurodon dicksoni* n. sp.) from Riversleigh, Australia, and the problem of monotreme origins. In M. L. Augee (Ed.), *Platypus and echidnas* (pp.15-27). Mosman, New South Wales, Australia: The Royal Zoological Society of New South Wales.

Archer, M., P. Murray, S. J. Hand, and H. Godthelp. 1993. Reconsideration of monotreme relationships based on the skull and dentition of the Miocene *Obdurodon dicksoni*. In F. S. Szalay, M. J. Novacek, and J. C. McKenna (Eds.), *Mammal Phylogeny: Mesozoic Differentiation, Multituberculates, Monotremes, Early Therians, and Marsupials* (pp. 75-94). New York, New York: Springer-Verlag, New York, Inc.

Asher, R. J., I. Horovitz, T. Martin, and M. R. Sánchez-Villagra. 2007. Neither a rodent nor a platypus: reexamination of *Necrolestes patagonensis* Ameghino. *American Museum Novitates* **3546**: 1-40.

Ashwell, K. W. S. 2006a. Chemoarchitecture of the monotreme olfactory bulb. *Brain, Behavior and Evolution* **67**: 69-84.

Ashwell, K. W. S. 2006b. Cyto- and chemoarchitecture of the monotreme olfactory bulb. *Brain, Behavior and Evolution* **67**: 85-102.

Ashwell, K. W. S. 2012. Development of the cerebellum in the platypus (*Ornithorhynchus anatinus*) and short-beaked echidna (*Tachyglossus aculeatus*). *Brain, Behavior and Evolution* **79**: 237-251.

Ashwell, K. W. S., C. D. Hardman, and P. Giere. 2012. Distinct development of peripheral trigeminal pathways in the platypus (*Ornithorhynchus anatinus*) and short-beaked echidna (*Tachyglossus aculeatus*). *Brain, Behavior and Evolution* **79**: 113-127.

Augee, M. L., B. Gooden, and A. Musser. 2006. *Echidna: Extraordinary egg-laying mammal*. Collingwood, Victoria, Australia: CSIRO Publishing.

Bell, C. J., J. A. Gauthier, and G. S. Bever. 2010. Covert biases, circularity, and apomorphies: A critical look at the North American Quaternary Herpetofaunal Stability Hypothesis. *Quaternary International* **217**:30–36.

Bellmer, E. H. 1963. The time of embryonic fusion of the malleus and incus in the guinea pig. *American Midland Naturalist* **69**: 426-434.

Bemmelen, J. F. van. 1901. Der Schädelbau der Monotremen. *Semon's Zoologische Forschungsreisen* **3**: 729-798.

Bever, G. S. 2005. Variation in the ilium of North American *Bufo* (Lissamphibia: Anura) and its implications for species-level identification of fragmentary anuran fossils. *Journal of Vertebrate Paleontology* **25**: 548–560.

Bonaparte, C. L. 1827. A new systematic arrangement of vertebrated animals. *Transactions of the Linnean Society of London* **18**: 247-304.

Bonaparte, J. F. 1986. Sobre *Mesungulatum houssayi* y nuevos mamíferos Cretácicos de Patagonia, Argentina. *Actas IV Congreso Argentino Paleontología y Bioestratigrafía* **2**: 48-61.

Bonaparte, J. F., and G. Rougier. 1987. Mamíferos del Cretácico inferior de Patagonia. *Actas IV Congreso Latinoamericano de Paleontología, Bolivia* **1**: 343-359.

Broom, R. 1914. On the origin of mammals. *Philosophical Transactions of the Royal Society of London. Series B, Biological Sciences* **206**: 1-48.

Burrell, H. 1927. *The Platypus: Its Discovery, Zoological Position, Form and Characteristics, Habits, Life History, Etc*. Sydney, New South Wales, Australia: Angus & Robertson Limited.

Camen, A. B. 2010. Were early Tertiary monotremes really all aquatic? Inferring paleobiology and phylogeny from a depauperate fossil record. *Proceedings of the National Academy of Sciences* **107**: E12.

Carroll, R. L. 1988. *Vertebrate Paleontology and Evolution*. New York, New York: W. H. Freeman and Company.

Chow, M., and T. H. Rich. 1982. *Shuotherium dongi*, n. gen. and sp., a therian with pseudo-tribosphenic molars from the Jurassic of Sichuan, China. *Australian Mammalogy* **5**: 127-142.

Davit-Béal, T., A. S. Tucker, and J.-Y. Sire. 2009. Loss of teeth and enamel in tetrapods: Fossil record, genetic data and morphological adaptations. *Journal of Anatomy* **214**: 477–501.

de Beer, G. R. 1929. The development of the skull of the shrew. *Philosophical Transactions of the Royal Society of London. Series B, Containing Papers of a Biological Character*: 411-480.

de Beer, G. R., and M. A. Fell. 1936. The development of the Monotremata. —Part III. The development of the skull of *Ornithorhynchus*. *The Transactions of the Zoological Society of London* **23**: 1-42.

de Queiroz, K. 1994. Replacement of an essentialistic perspective on taxonomic definitions as exemplified by the definition of "Mammalia." *Systematic Biology* **43**: 497-510.

de Queiroz, K. 2007. Toward an integrated system of clade names. *Systematic Biology* **56**: 956-974.

de Queiroz, K., and J. Gauthier. 1992. Phylogenetic taxonomy. *Annual Review of Ecology and Systematics* **23**: 449-480.

de Queiroz, K., and J. Gauthier. 1994. Toward a phylogenetic system of biological nomenclature. *Trends in Ecology & Evolution* **9**: 27-31

Donoghue, M. J., J. Doyle, J. A. Gauthier, A. G. Kluge, and T. B. Rowe. 1989. Importance of fossils in phylogeny reconstruction. *Annual Review of Ecology and Systematics* **20**: 431-460.

Dun, W. S. 1895. Notes on the occurrence of monotreme remains in the Pliocene of New South Wales. *Records of the Geological Survey of New South Wales* **4**: 118-126.

Edgeworth, F. H. 1935. *The Cranial Muscles of Vertebrates*. Cambridge, Massachusetts: Cambridge University Press.

Edinger, T. 1941. The brain of *Pterodactylus*. *American Journal of Science* **239**: 665-682.

Fitzinger, L. J. F. J. 1826. *Neue classification der reptilian nach ihren natürlichen Verwandtsschaften nebst einer Verwandschafts-Tafel und einem Verzeichnisse der Reptilien-Sammlung des K. K. zoologischen Museums zu Wien*. Vienna, Austria: J. G. Heubner.

Flannery, T. 1990. Pleistocene faunal loss: implications of the aftershock for Australia's past and future. *Archaeology in Oceania* **25**: 45–67.

Flannery, T. 1995. *Mammals of New Guinea*. Ithica, New York: Cornell University Press.

Flannery, T. F., M. Archer, T. H. Rich, and R. Jones. 1995. A new family of monotremes from the Cretaceous of Australia. *Nature* **377**: 418-420.

Flannery, T. F., and C. P. Groves. 1998. A revision of the genus *Zaglossus* (Monotremata, Tachyglossidae), with description of new species and subspecies. *Mammalia* **62**: 367-396.

Flynn, J. J., J. M. Parrish, B. Rakotosamimanana, W. F. Simpson, and A. R. Wyss. 1999. A middle Jurassic mammal from Madagascar. *Nature* **401**: 57-60.

Forasiepi, A. M., and A. G. Martinelli. 2003. Femur of a monotreme (Mammalia, Monotremata) from the Early Paleocene Salamanca Formation of Patagonia, Argentina. *Ameghiniana* **40**: 625-630.

Fuchs, H. 1910. Über das Pterygoid, Palatinum und Parasphenoid der Reptilien und Säugetiere, nebst einigen Betrachtungen über die Beziehungen zwischen Nerven und Skeletteilen. *Anatomischer Anzeiger* **36**: 33-95.

Gaupp, E. 1908. Zur Entwicklungsgeschichte und vergleichenden Morphologie des Schädels von *Echidna aculeata* var. typical. *Jenaische Denkschriften* **6**: 539-788.

Gauthier, J. A., A. G. Kluge, and T. B. Rowe. 1988. Amniote phylogeny and the importance of fossils. *Cladistics* **4**:105-209.

Gemmell, N. J., and M. Westerman. 1994. Phylogenetic Relationships within the Class Mammalia: A study using mitochondrial 12S RNA sequences. *Journal of Mammalian Evolution* **2**: 3-23.

Gervais, P. 1877-1878. Ostéographie des monotrèmes vivants et fossils comprenant la description et l'iconographie du squelette et du système dentaire de ces animaux ainsi que des documents relatifs à leur histoire naturelle. Chapitre deuxième. *Les échidnés de la Nouvelle-Guinée* (pp. 41-56, Plates 6-9). Paris, France: Librairie Scientifique et Maritime.

Gill, T. 1872. Arrangement of the families of mammals with analytical tables. *Smithsonian Miscellaneous Collections* **11**: 1-98.

Gill, T. 1903. Origin of the name Monotremes. *Science* **17**: 433-434.

Glauert, L. 1914. The mammoth cave. *Records of the Western Australian Museum VI* **1**: 11-38.

Goodrich, E. S. 1916. On the classification of the Reptilia. *Proceedings of the Royal Society of London. Series B, Containing Papers of a Biological Character* **89**: 261-276.

Grant, T. R. 1992. Historical and current distribution of the platypus, *Ornithorhynchus anatinus*, in Australia. In M. L. Augee (Ed.), *Platypus and Echidnas* (pp. 232-254). Mosman, New South Wales, Australia: The Royal Zoological Society of New South Wales.

Grant, T. R. 2007. *Platypus* (4th ed.). Collingwood, Victoria, Australia: CSIRO Publishing.

Gray, J. E. 1825. Outline of an attempt at the disposition of the Mammalia into tribes and families with the list of the genera apparently appertaining to each tribe. *Annals of Philosophy, n. s.* **10**: 336–344.

Green, H. L. 1930. A description of the egg tooth of *Ornithorhynchus*, together with some notes on the development of the palatine processes of the premaxillae. *Journal of Anatomy* **64**: 512-522.

Green, H. L. H. H. 1937. The development and morphology of the teeth of Ornithorhynchus. *Philosophical Transactions of the Royal Society of London. Series B, Biological Sciences* **228**: 367-420.

Gregory, W. K. 1910. The orders of mammals. *Bulletin of the American Museum of Natural History* **27**: 1-524.

Gregory, W. K. 1947. Monotremes and the palimpsest theory. *Bulletin of the American Museum of Natural History* **88**: 1-52.

Griffiths, M. 1968. *Echidnas*. Oxford, United Kingdom: Pergamon Press Ltd.

Griffiths, M. 1978. *The biology of the monotremes*. New York, New York: Academic Press.

Griffiths, M., R. T. Wells, and D. J. Barrie. 1991. Observations on the skulls of fossil and extant echidnas (Monotremata: Tachyglossidae). *Australian Mammalogy* **14**: 97-101.

Grutzner, F, R. Willem, E. Tsend-Ayush, N. El Mogharbel, P. C. M. O'Brien, R. C. Jones, M. A. Ferguson-Smith, and J. A. M. Graves. 2004. In the platypus a meiotic chain of ten sex chromosomes shares genes with bird Z and mammal X chromosomes. *Nature* **432**: 913-917.

Haeckel, E. 1897. *The Evolution of Man*. New York, New York: Appleton and Company.

Helgen, K. M., R. P. Miguez, J. L. Kohen, and L. E. Helgen. 2012. Twentieth century occurrence of the Long-Beaked Echidna *Zaglossus bruijnii* in the Kimberley region of Australia. *ZooKeys* **255**: 103-132.

Hill, J.P., and G.R. de Beer. 1949. The development and structure of the egg-tooth and caruncle in the monotremes and on the occurrences of vestiges of the egg-tooth and caruncle in marsupials. *Transactions of the Zoological Society of London*, **26**: 503-544.

Home, E. 1802a. Description of the anatomy of *Ornithorhynchus paradoxus*. *Philosophical Transactions of the Royal Society of London* **92**: 67-84, Plates 2-4.

Home, E. 1802b. Description of the anatomy of *Ornithorhynchus hystrix*. Description of the anatomy of *Ornithorhynchus hystrix*. *Philosophical Transactions of the Royal Society of London* **92**: 348-364, Plates 10-13.

Huber, E. 1930a. Evolution of facial musculature and cutaneous field of trigeminus. Part I. *Quarterly Review of Biology* **5**: 133–188.

Huber, E. 1930b. Evolution of facial musculature and cutaneous field of trigeminus. Part II. *Quarterly Review of Biololgy* **5**: 389–437.

Hurum, J. H., and Z. Kielan-Jaworowska. 2008. Postcranial skeleton of a Cretaceous multituberculate mammal *Catopsbaatar*. *Acta Palaeonotologica Polonica* **5**: 545-566.

International Code for Phylogenetic Nomenclature (version 4c). 2010. http://www.ohio.edu/phylocode/

Janke, A., N. J. Gemmell, G. Feldmaier-Fuchs, A. von Haeseler, and S. Pääbo. 1996. The mitochondrial genome of a monotreme—the platypus (*Ornithorhynchus anatinus*). *Journal of Molecular Evolution* **42**: 153-159.

Janke, A., X. Xu, and U. Arnason. 1997. The complete mitochondrial genome of the wallaroo (*Macropus robustus*) and the phylogenetic relationship among Monotremata, Marsupialia and Eutheria. *Proceedings of the National Academy of Sciences* **94**: 1276-1281.

Janke, A., O. Magnell, G. Feldmaier-Fuchs, A. von Haeseler, and S. Pääbo. 2002. Phylogenetic analysis of 18S rRNA and the mitochondrial genomes of the wombat, *Vombatus ursinus*, and the spiny anteater, *Tachyglossus aculeatus*:

Increased support for the Marsupionta hypothesis. *Journal of Molecular Evolution* **54**: 71-80.

Jenkins Jr., F. A., and F. R. Parrington. 1976. The postcranial skeletons of the Triassic mammals, *Eozostrodon*, *Megazostrodon*, and *Erythrotherium*. *Philosophical Transactions of the Royal Society of London. Series B, Biological Sciences* **273**: 387-431.

Jenkins Jr., F. A., and D. W. Krause. 1983. Adaptations for climbing in North American Multituberculates (Mammalia). *Science* **220**: 712-715.

Jenkins Jr, F. A., and C. R. Schaff. 1988. The Early Cretaceous mammal Gobiconodon (Mammalia, Triconodonta) from the Cloverly Formation in Montana. *Journal of Vertebrate Paleontology* **8**: 1-24.

Ji, Q., Z.-X. Luo, and S. Ji. 1999. A Chinise triconodont mammal and mosaic evolution of the mammalian skeleton. *Nature* **398**: 326-330.

Ji, Q., Z.-X. Luo, C.-X. Yuan, J. R. Wible, J.-P. Zhang, and J. A. Georgi. 2002. The earliest known eutherian mammal. *Nature* **416**: 816-822.

Ji, Q., Z.-X. Luo, C.-X Yuan, and A. R. Tabrum. 2006. A swimming mammaliaform from the Middle Jurassic and ecomorphological diversification of early mammals. *Science* **311**: 1123-1127.

Kermack, K. A., F. Mussett, and H. W. Rigney. 1973. The lower jaw of *Morganucodon*. *Zoological Journal of the Linnean Society* **53**: 87-175.

Kermack, K. A., F. Mussett, and H. W. Rigney. 1981. The skull of *Morganucodon*. *Zoological Journal of the Linnean Society* **71**: 1-158.

Kesteven, H. L. 1918. The homology of the mammalian alisphenoid and of the echidna-pterygoid. *Journal of Anatomy* **52**: 449-466.

Kesteven, H. L. 1940. On the interpretation of certain features of an embryonic skull of platypus. *From the Proceedings of the Linnean Society of New South Wales* **65**: 144-154.

Kielan-Jaworowska, Z. 1989. Postcranial skeleton of a Cretaceous multituberculate mammal. *Acta Palaeontologica Polonica* **34**: 75-85.

Kielan-Jaworowska, Z. 1997. Characters of multituberculates neglected in phylogenetic analyses of early mammals. *Lethaia* **29**: 249-266.

Kielan-Jaworowska, Z., A. W. Crompton, and F. A. Jenkins, Jr. 1987. The origin of egg-laying mammals. *Nature* **326**: 871-873.

Kielan-Jaworowska, Z., R. L. Cifelli, and Z.-X. Luo. 1998. Alleged Cretaceous placental from down under. *Lethaia* **31**: 267-268.

Kielan-Jaworowska, Z., R. L. Cifelli, and Z.-X. Luo. 2002. Dentition and relationships of the Jurassic mammal Shuotherium. *Acta Palaeontologica Polonica* **47**: 479-486.

Kielan-Jaworowska, Z., R. Cifelli, and Z.-X. Luo. 2004. *Mammals from the age of dinosaurs: Origins, evolution, and structure*. New York, New York: Columbia University Press.

.Kirsch, J. A. W. and G. C. Mayer. 1998. The platypus is not a rodent. *Philosophical Transactions of the Royal Society of London. Series B: Biological Sciences* **353**: 1221-1237.

Koyabu, D., W. Maier, and M. R. Sánchez-Villagra. 2012. Paleontological and developmental evidence resolve the homology and dual embryonic origin of a mammalian skull bone, the interparietal. *Proceedings of the National Academy of Sciences* **109**: 14075-14080.

Krefft, G. 1868. On the discovery of a new and gigantic fossil species of *Echidna* in Australia. *Annals and Magazine of Natural History* **1**: 113–114.

Kuhn, H.-J. 1971. Die Entwicklung und Morphologie des Schädels von *Tachyglossus aculeatus*. *Abhandlungen der Senckenburgischen Naturforschenden Gesellschaft* **528**: 1-192.

Kuhn, H.-J., and U. Zeller. 1987. The cavum epiptericum in monotremes and therian mammals: Morphogenesis of the mammalian skull. *Mammalia Depicta* **13**: 51-70.

Kühne, W. G. 1973. The systematic position of monotremes reconsidered (Mammalia). *Zeitschrift fur morphologie der tiere* **75**: 59-64.

Kühne, W. G. 1974. On the Marsupionta, a reply to Dr. Parrington. *Journal of Natural History* **11**: 225-228.

Kumanzawa, Y. and M. Nishida. 1999. Complete mitochondrial DNA sequences of the green turtle and blue-tailed mole skink: Statistical evidence for archosaurian affinities of turtles. *Molecular Biology and Evolution* **16**:784-792.

Landry, S. O. 1964. The form and phylogenetic history of the mammalian interparietal bone. *American Zoologist* **4**: 400.

Laurin, M. and R. R. Reisz. In press. Synapsida. In P. Cantino, K. de Queiroz, and J. A. Gauthier (Eds.), *Phylocode*. Berkeley, California: University of California Press.

Leary, T., Seri, L., Flannery, T., Wright, D., Hamilton, S., Helgen, K., Singadan, R., Menzies, J., Allison, A., James, R., Aplin, K., Salas, L. & Dickman, C. 2008. *Zaglossus bartoni*. In IUCN 2012. IUCN Red List of Threatened Species. Version 2012.2. <www.iucnredlist.org>. Downloaded on 04 January 2013.

Lefèvre, C. M., J. A. Sharp, and K. Nicholas. 2009. Characterization of monotreme caseins reveals lineage-specific expansion of an ancestral casein locus in mammals. *Reproduction, Fertility and Development* **21**: 1015-1027.

Lester, K. S. and M. Archer. 1986. A description of the molar enamel of a middle Miocene monotreme (*Obdurodon*, Ornithorhynchidae). *Anatomy and Embryology* **174**: 145-151.

Lester, K. S. and A. Boyde. 1986. Scanning microscopy of platypus teeth. *Anatomy and Embryology* **174**: 15-26.

Long J., M. Archer, T. Flannery, and S. Hand. 2002. *Prehistoric mammals of Australia and New Guinea: 100 million years of evolution.* Sydney, New South Wales, Australia: University of New South Wales Press.

Lightoller, G. S. 1942. Matrices of the facialis musculature homologization of the musculature in monotremes with that of marsupials and placentals. *Journal of Anatomy* **76**: 258–269.

Lillegraven, J. A., and G. Krusat. 1991. Cranio-mandibular anatomy of *Haldanodon exspectatus* (Docodonta: Mammalia) from the Late Jurassic of Portugal and its implications to the evolution of mammalian characters. *Contributions to Geology, University of Wyoming* **28**: 39-138.

Linnaeus, C. 1758. Systema Natura per Regna tria Naturae, secundum Classes, Ordines, Genera, Species, cum Characteribus, differentiis, Synonymis, Locis. Editio Decima. Holmiae.

Lubosch, W. 1907. Das Kiefergelenk der Edentaten und Marsupialier. *Denkschriften der medicinisch - naturwissenschaftlichen. Gesellschaft. Jena* **7**: 1-38.

Luo, Z.-X., R. L. Cifelli, and Z. Kielan-Jaworowska. 2001. Dual origin of tribosphenic mammals. *Nature* **409**: 53-57.

Luo, Z.-X., Z. Kielan-Jaworowska, and R. L. Cifelli. 2002. In quest for a phylogeny of Mesozoic mammals. *Acta Palaeontologica Polonica* **47**: 1-78.

Luo, Z.-X., Q. Ji, J. R. Wible, and C.-X. Yuan. 2003. An Early Cretaceous tribosphenic mammal and metatherian evolution. *Science* **302**: 1934-1940.

Luo, Z.-X., and J. R. Wible. 2005. A Late Jurassic digging mammal and early mammalian diversity. *Science* **308:** 103–107.

Luo, Z.-X., J. Quang, and C.-X. Yuan. 2007. Convergent dental adaptations in pseudotribosphenic and tribosphenic mammals. *Nature* **450**: 93-97.

Luo, Z.-X., C.-X. Yuan, Q.-J. Meng, and Q. Ji. 2011. A Jurassic eutherian mammal and divergence of marsupials and placentals. *Nature* **476**: 442-445.

MacIntyre, G. 1967. Foramen pseudovale and quasi-mammals. *Evolution* **21**: 834-841.

Macrini, T. 2006. Description of a cranial endocast from a fossil platypus, *Obdurodon dicksoni* (Monotremata, Ornithorhynchidae), and the relevance of endocranial characters to monotreme monophyly. *Journal of Morphology* **267**: 1000-1015.

Macrini, T. E., T. B. Rowe, and M. Archer. 2006. Description of a cranial endocast from a fossil platypus, *Obdurodon dicksoni* (Monotremata, Ornithorhynchidae), and the relevance of endocranial characters to monotreme monophyly. *Journal of Morphology* **267**:1000-1015.

Manger, P. R., R. Collins, J. D. Pettigrew. 1997. Histological observations on presumed electroreceptors and mechanoreceptors in the beak skin of the long-beaked echidna, *Zaglossus bruijnii*. *Proceedings of the Royal Society of London. Series B, Containing Papers of a Biological Character* **264**: 165-172.

Martin, T. 1999. Dryolestidae (Dryolestoidea, Mammalia) aus dem Oberen Jura von Portugal. *Abhandlungen der Senckenbergischen Naturfor-schenden Gesellschaft* **550**: 1-119.

Martin, T. 2005. Postcranial anatomy of *Haldanodon expectatus* (Mammalia, Docodonta) from the Late Jurassic (Kimmeridgian) of Portugal and its bearing for mammalian evolution. *Zoological Journal of the Linnean Society* **145**: 219-248

McKenna, M. C., and S. K. Bell. 1997. Classification of mammals above the species level. New York: Columbia University Press. Print.

Messer, M., A. S. Weiss, D. C. Shaw, and M. Westerman. 1998. Evolution of the monotremes: phylogenetic relationship to marsupials and eutherians, and estimation of divergence dates based on α-lactalbumin amino acid sequences. *Journal of Mammalian Evolution* **5**: 95-105.

Murray, P. F. 1978. Late Cenozoic monotreme anteaters. In: M.L. Augee (ed.), Monotreme Biology. *The Australian Zoologist* **20**: 29-55.

Murchison, E. P., P. Kheradpour, R. Sachidanandam, C. Smith, E. Hodges, Z. Xuan, M., Kellis, F. Grützner, A. Stark, and G. J. Hannon. 2008. Conservation of small RNA pathways in platypus. *Genome Research* **18**: 995-1004.

Murray, P. F. 1978. Late Cenozoic monotreme anteaters. *Australian Zoologist* **20**: 29-55.

Musser, A. M. 2003. Review of the monotreme fossil record and comparison of paleontological and molecular data. *Comparative Biochemistry and Physiology Part A* **136**: 927-942.

Musser, A. M. 2005. *Investigations into the evolution of Australian mammals with a focus on Monotremata* (Doctoral Dissertation). School of Biological, Earth & Environmental Sciences, University of New South Wales, Sydney, New South Wales, Australia.

Musser, A. M., and M. Archer. 1998. New information about the skull and dentary of the Miocene platypus *Obdurodon dicksoni*, and a discussion of ornithorhynchid relationships. *Philosophical Transactions of the Royal Society of London. Series B, Biological Sciences* **353**: 1063-1079.

Nilsson, M. A., U. Arnason, P. B. Spencer, and A. Janke. 2004. Marsupial relationships and a timeline for marsupial radiation in South Gondwana. *Gene* **340**:189-196.

Norell, M. A. 1992. Taxic origin and temporal diversity: The effect of phylogeny. In M. J. Novacek and Q. D. Wheeler (Eds.), *Extinction and phylogeny* (pp. 89-118). New York, New York: Columbia University Press.

Novacek, M. J., and A. Wyss. 1986. Origin and transformation of the mammalian stapes. *Rocky Mountain Geology* **24**, special paper 3: 35-53.

O'Leary, M. A., J. I. Bloch, J. J. Flynn, T. J. Gaudin, A. Giallombardo, N. P. Giannini, S. L. Goldberg, B. P. Kraatz, Z.-X. Luo, J. Meng, X. Ni, M. J. Novacek, F. A. Perini, Z. S. Randall, G. W. Rougier, E. J. Sargis, M. T. Silcox, N. B. Simmons, M. Spaulding, P. M. Velazco, M. Weksler, J. R. Wible, and A. L. Cirranello. 2013. The placental mammal ancestor and the post-K-PG radiation of placentals. *Science* **339**: 662-667.

Olson, E. C. 1944. Origin of mammals based upon cranial morphology of the therapsid suborders. *Geological Society of America Special Papers* **55**: 1-136.

Osborn, H. F. 1903a. On the primary divisions of the Reptilia into two sub-classes, Synapsida and Diapsida. *Science* **17**: 275-276.

Owen, R. 1861. *Essays and observations on natural history, anatomy, physiology, psychology, and geology by John Hunter, F. R. S.; being his posthumous papers on those subjects arranged and revised with notes: To which are added, the introductory lectures on the hunterian collection of fossil remains, delivered in the theatre of the royal college of surgeons of England, March 8th, 10th, and 12th, 1855* (Vols. 1-2). London, United Kingdom: John van Voorst.

Owen, R. 1884. Evidence of a large extinct Monotreme (*Echidna Ramsayi*, Ow.) from the Wellington Breccia Cave, New South Wales. *Philosophical Transactions of the Royal Society of London* **185**: 273-274.

Parker, J. T., and W. A. Haswell. 1897. *A Text-Book of Zoology* (Vols. 1-2). London, United Kingdom: Macmilland and Co., Ltd.

Parrington, F. R. 1974. The problem of the origin of the monotremes. *Journal of Natural History* **8**: 421-426.

Parrington, F. R., and T. S. Westoll. 1940. On the evolution of the mammalian palate. *Philosophical Transactions of the Royal Society of London. Series B, Biological Sciences* **230**: 305-355.

Pascual, R., M. Archer, E. Ortiz-Jaureguizar, J. L. Prado, H. Godthelp, and S. J. Hand. 1992a. First discovery of monotremes in South America. *Nature* **356**: 704-706.

Pascual, R., M. Archer, E. Oritz-Jaureguizar, J. L. Prado, H. Godthelp, and S. J. Hand. 1992b. The first non-Australian monotreme: an early Paleocene South American platypus (Monotremata, Ornithorhynchidae). In M. L. Augee (Ed.), *Platypus and echidnas* (pp. 2-15). Mosman, New South Wales, Australia: The Royal Zoological Society of New South Wales.

Pascual, R., F. J. Goin, L. Balarino, and D. U. Sauthier. 2002. New data on the Paleocene monotreme Monotrematum sudamericanum, and the convergent evolution of triangulate molars. *Acta Palaeontologica Polonica* **47**: 487-492.

Penny, D., and M. Hasegawa. 1997. Molecular systematics: the platypus put in its place. *Nature* **387**: 549-550.

Penny, D., M. Hasegawa, P. J. Wadell, and M. D. Hendy. 1999. Mammalian evolution: timing and implications from using LogDeterminant transform for proteins of differing amino acid composition. *Systematic Biology* **48**:76-93.

Peters, W. C. H., and Doria, G. 1876. Descrizione di una nuova specie di *Tachyglossus* proveniente dalla Nuova Guinea settentrionale. *Annali del Museo Civico di Storia Naturale di Genova* **9**: 183-185.

Phillips, M. J., & Penny, D. 2003. The root of the mammalian tree inferred from whole mitochondrial genomes. *Molecular phylogenetics and evolution* **28**: 171-185.

Phillips, M. J., T. H. Bennett, and M. S. Lee. 2009. Molecules, morphology, and ecology indicate a recent, amphibious ancestry for echidnas. *Proceedings of the National Academy of Sciences* **106**: 17089-17094.

Phillips, M. J., T. H. Bennett, and M. S. Lee. 2010. Reply to Camens: How recently did modern monotremes diversify? *Proceedings National Academy of Sciences* **107**: E13

Poulton, E. B. 1888. The true teeth and the horny plates of *Ornithorhynchus*. *Quarterly Journal of the Microscopal Society* **29**: 9–48.

Presley, R., and F. L. D. Steel. 1976. On the homology of the alisphenoid. *Journal of Anatomy* **121**: 441-459.

Presley, R., and F. L. D. Steel. 1978. The pterygoid and ectopterygoid in mammals. *Anatomy and Embryology* **154**: 95-110.

Proske, U., J. E. Gregory, and A. Iggo. 1998. Sensory receptors in monotremes. *Philosophical Transactions of the Royal Society of London. Series B, Biological Sciences* **353**: 1187-1198.

Pridmore, P. A., T. H. Rich, P. Vickers-Rich, and P. P. Gambaryan. 2005. A tachyglossid-like humerus from the Early Cretaceous of south-eastern Australia. *Journal of Mammalian Evolution* **12**: 359-378.

Qiang, J., Z.-X. Luo, and J. Shu-an. 1999. A Chinese triconodont mammal and mosaic evolution of the mammalian skeleton. *Nature* **338**: 326-330.

Rafinesque, C. S. 1815. *Analyse de la nature* (p. 224). Aux dépens de l'auteur, Palerme.

Rauhut, O. W. M., T. Martin, E. Ortiz-Jaureguizar, and P. Puerta. 2002. A Jurassic mammal from South America. *Nature* **416**: 165-168.

Rens, W., F. Grutzner, P. C. O'brien, H. Fairclough, J. A. Graves, and M. A. Ferguson-Smith. 2004. Resolution and evolution of the duck-billed platypus karyotype with an X1Y1X2Y2X3Y3X4Y4X5Y5 male sex chromosome constitution. *Proceedings of the National Academy of Sciences* **101**: 12257-16261.

Retief, J. D., R. J. Winkfein, and G. H Dixon. 1993. Evolution of the monotremes. The sequences of the protamine P1 genes of platypus and echidna. *European Journal of Biochemistry* **218**: 457-461.

Rich, T. H., P. Vickers-Rich, A. Constantine, T. F. Flannery, L. Kool, and N. van Klaveren. 1997. A tribosphenic mammal from the Mesozoic of Australia. *Science* **278**: 1438-1442.

Rich, T. H., P. Vickers-Rich, A. Constantine, T. F. Flannery, L. Kool, and N. van Klaveren. 1999. Early Cretaceous mammals from Flat Rocks, Victoria, Australia. *Records of the Queen Victoria Museum* **106**: 1-35.

Rich, T. H., T. F. Flannery, P. Trusler, L. Kool, N. van Klaveren, and P. Vickers-Rich. 2001. A second tribosphenic mammal from the Mesozoic of Australia. *Records of the Queen Victoria Museum* **110**: 1-9.

Rougier, G. W., J. R. Wible, and J. A. Hopson. 1992. Reconstruction of the cranial vessels in the Early Cretaceous mammal Vincelestes neuquenianus: implications for the evolution of the mammalian cranial vascular system. *Journal of Vertebrate Paleontology* **12**: 188-216.

Rougier, G. W., S. Apesteguía, and L. C. Gaetano. 2011. Highly specialized mammalian skulls from the Late Cretaceous of South America. *Nature* **479**: 98-102.

Rougier, G. W., J. R. Wible, R. M. D. Beck, and S. Apesteguía. 2012. The Miocene mammal *Necrolestes* demonstrates the survival of a Mesozoic nontherian lineage into the late Cenozoic of South America. *Proceedings of the National Academy of Sciences* **109**: 20053-20058.

Rowe, T. B. 1986. *Osteological diagnosis of Mammalia Linnaeus, 1758, and its relationship to extinct Synapsida* (Doctoral Dissertation). Department of Paleontology, University of California, Berkeley, California.

Rowe, T. B. 1987. Definition and diagnosis in the phylogenetic system. *Systematic Zoology* **36**: 208-211.

Rowe, T. B. 1988. Definition, diagnosis and origin of Mammalia. *Journal of Vertebrate Paleontology* **8**: 241-264.

Rowe, T. B. 1993. Phylogenetic systematics and the early history of mammals. In F. S. Szalay, M. J. Novacek, and M. C. McKenna (Eds.), *Mammal Phylogeny:*

Mesozoic Differentiation, Multituberculates, Monotremes, Early Therians, and Marsupials (pp. 129–145). New York, New York: Springer-Verlag New York, Inc.

Rowe, T. B. 2004. Chordate phylogeny and development. In J. Cracraft and M. J. Donoghue (Eds.), *Assembling the Tree of Life* (pp. 384-409). Oxford, United Kingdom and New York, New York: Oxford University Press.

Rowe, T. B. In press-a. Mammalia. In P. Cantino, K. de Queiroz, and J. A. Gauthier (Eds.), *Phylocode*. Berkeley, California: University of California Press.

Rowe, T. B. In press-b. Pan-Mammalia. In P. Cantino, K. de Queiroz, and J. A. Gauthier (Eds.), *Phylocode*. Berkeley, California: University of California Press.

Rowe, T. B. and J. Gauthier. 1992. Ancestry, paleontology, and definition of the name Mammalia. *Systematic Biology* **41**: 372-378.

Rowe, T. B., T. H. Rich, P. Vickers-Rich, M. Springer, and M. O. Woodburne. 2008. The oldest platypus and its bearing on divergence timing of the platypus and echidna clades. *Proceedings of the National Academy of Sciences* **105**: 1238-1242.

Rowe, T. B., T. E. Macrini, and Z.-X. Luo. 2011. Fossil evidence on the origin of the mammalian brain. *Science* **332**: 955-957.

Shaw, G. 1792. The porcupine ant-eater. *The Naturalist's Miscellany* **3**: 109-111, Plate 109.

Shaw, G. 1799. The duck-billed platypus. *The Naturalist's Miscellany* **10**: 228-232, Plate 385.

Sigogneau-Russell, D. 1998. Discovery of a Late Jurassic Chinese mammal in the Upper Bathonian of England. *Comptes Rendus de l'Académie des Sciences, Paris* **327**: 571–576.

Simpson, G. G. 1938. Osteography of the ear region in monotremes. *American Museum Novitates* **978**: 1-15.

Simpson, G. G. 1971. Concluding remarks: Mesozoic mammals revisited. In D. M. Kermack, and K. A. Kermack (Eds.), *Early mammals* (pp. 181-198). *Zoological Journal of the Linnean Society* **50**, supplement 1 London, England: Academic Press.

Sues, H.-D. 1986. The skull and dentition of two tritylodontid synapsids from the lower Jurassic of western North America. *Bulletin of the Museum of Comparative Zoology* **151**: 217-268.

Sues, H.-D. and F. A. Jenkins. 2006. The Postcranial Skeleton of *Kayentatherium wellesi* from the Lower Jurassic Kayenta Formation of Arizona and the Phylogenetic Significance of Postcranial Features in Tritylodontid Cynodonts. In M. T. Carrano, T. J. Gaudin, R. W. Blob, and J. R. Wible (Eds.), *Amniote Paleobiology: Perspectivers on the Evolution of Mammals, Birds, and Reptiles* (pp. 114-152). Chicago, Illinois: The University of Chicago Press.

Swofford, D. L. 2003. "PAUP*: phylogenetic analysis using parsimony, version 4.0 b10."

Thomas, O. 1889. On the dentition of Ornithorhynchus. *Proceedings of the Royal Society of London. Series B, Containing Papers of a Biological Character* **46**: 126-131

Van Kampen, P. N. 1922. Parasphenoid und Basisphenoid der Säugetiere. *Bijdragen tot de Dierkunde* **22**: 53-58.

Van Bemmelen, J. F. 1900. Über den schädel der monotremen. *Zoologischer Anzeiger* **23**: 449-461.

Van Bemmelen, J. F. 1901. Der Schädelbau der Monotremen. *Semon's Zoologische Forschungsreisen* **3**: 729-798.

van Rheede, T., T. Bastiaans, D. N. Boone, S. B. Hedges, W. W. de Jong, and O. Madsen. 2006. The platypus in its place: Nuclear genes and indels confirm the sister group relation of monotremes and therians. *Molecular Biology and Evolution* **23**: 587-597.

Vernesson, M., M. Aveskogh, B. Munday, and L. Hellman. 2002. Evidence for an early appearance of modern post-switch immunoglobin isotypes in mammalian evolution (II): cloning of the IgE, IgG1 and IgG2 from a monotreme, the duck-billed platypus, *Ornithorhynchus anatinus*. *European Journal of Immunology* **32**: 2145-2155.

Voss, R. S., and S. A. Jansa. 2009. Phylogenetic relationships and classification of didelphid marsupials, an extant radiation of new world metatherian mammals. *Bulletin of the American Museum of Natural History* **322**: 1-177.

Watson, D. M. S. 1916. The monotreme skull: a contribution to mammalian morphogenesis. *Philosophical Transactions of the Royal Society of London. Series B, Biological Sciences* **207**: 311-374.

Weigelt, J. 1989. *Recent vertebrate carcasses and their paleobiological implications*. (J. Schaefer, Trans.). Chicago and London: University of Chicago Press. (Original work published 1927).

Weisbecker, V. 2011. Monotreme ossification sequences and the riddle of mammalian skeletal development. *Evolution* **65**: 1323-1335.

Werneburg, I., and M. R. Sánchez-Villagra. 2011. The early development of the echidna, *Tachyglossus aculeatus* (Mammalia: Monotremata), and patterns of mammalian development. *Acta Zoologica* **92**: 75-88.

Westerman, M., and D. Edwards. 1992. DNA hybridization and the phylogeny of monotremes. In M. L. Augee (Ed.), *Platypus and echidnas* (pp. 28-34). Mosman, New South Wales, Australia: The Royal Zoological Society of New South Wales.

Wible, J. R, Miao, D., and J. A. Hopson. 1990. The septomaxilla of fossil and recent synapsids and the problem of the septomaxilla of monotremes and armadillos. *Zoological Journal of the Linnean Society* **98**: 203-228.

Wible, J. R., and J. A. Hopson. 1995. Homologies of the prootic canal in mammals and non-mammalian cynodonts. *Journal of Vertebrate Paleontology* **15**: 331-356.

Wible, J. R., and G. W. Rougier. 2000. Cranial anatomy of *Kryptobaatar dashzevegi* (Mammalia, Multituberculata), and its bearing on the evolution of mammalian characters. *Bulletin of the American Museum of Natural History* **247**: 1-120.

Wible, J. R., G. W. Rougier, M. J. Novacek, and M. C. McKenna. 2001. Earliest eutherian ear region: a petrosal referred to *Prokennalestes* from the Early Cretaceous of Mongolia. *American Museum Novitates* **3322**: 1-44.

Wilson, D. E., and D. M. Reeder (Eds.). 2005. *Mammal species of the World* (3rd ed.). Baltimore, Maryland: The Johns Hopkins University Press.

Winge, H. 1941. *The Interrelationships of the Mammalian Genera. Translated from Danish by E. Deichmann and G. Allen. Volume I – Monotremata, Marsupialia, Insectivora, Chiroptera, Edentata*. Copenhagen, Denmark: C. A. Reitzels Forlag.

Woodbrne, M. O. 2003. Monotremes as pretribosphenic mammals. *Journal of Mammalian Evolution* **10**: 195-248.

Woodburne, M. O., and R. H Tedford. 1975. The first Tertiary monotreme from Australia. *American Museum Novitates* **2588**: 1-11.

Woodburne, M. O., R. H. Tedford, M. Archer, W. D. Turnbull, M. D. Plane, and E. L. Lundelius. 1985. Biochronology of the continental mammal record of Australia and New Guinea. *Special Publication, South Australia Department of Mines and Energy* **5**: 347-363.

Young, J. Z. 1962. *The Life of Vertebrates*. Oxford, United Kingdom: Oxford University Press.

Zardoya, R., and A. Meyer 1998. Complete mitochondrial genome suggests diapsid affinities of turtles. *Proceedings of the National Acadeny of Sciences* **95**: 14226-14231.

Zeller, U. 1988. The lamina cribrosa of *Ornithorhynhcus* (Monotremata, Mammalia). *Anatomy and Embryology* **178**: 513-519.

Zeller, U. 1989a. Die Entwicklung und Morphologie des Schädels von *Ornithorhynchus anatinus* (Mammalia: Prototheria: Monotremata). *Abhandlungen Senckenbergischen Naturforschenden Gesellschaft* **545**: 1-188.

Zeller, U. 1989b. The braincase of *Ornithorhynchus*. *Fortschritte der Zoologie* **35**: 386-391.

Zeller, U. 1993. Ontogenetic evidence for cranial homologies in monotremes and therians, with special reference to *Ornithorhynchus*. In F. S. Szalay, M. J. Novacek, and J. C. McKenna (Eds.), *Mammal Phylogeny: Mesozoic Differentiation, Multituberculates, Monotremes, Early Therians, and Marsupials* (pp. 95-107). New York: Springer-Verlag, New York, Inc.

Vita

Rachel Veronica Simon Wallace (née Rachel Veronica Simon) was born and raised in the Pacific Northwest, also known as God's Country. She grew up in the charming city of Tacoma, Washington. Rachel earned her Bachelors of Science degree in General Biology from the University of Washington, Seattle. Under the mentorship of Dr. Christian Sidor, she published her first paper with Christian on the first fossils of tapinocephalid dinocephalians from the Ruhuhu Formation in Tanzania. This project grounded her interests in synapsid evolution. After graduating from the University of Washington, Rachel worked for one year as a lab manager for Dr. Gregory Wilson. The lab focused on the extinction and radiation of mammals before and after the K-T boundary, exposing Rachel to Mesozoic-aged mammals.

One year after graduating, Rachel was admitted to the Rowe lab at The University of Texas at Austin, where she was able to study the anatomy and natural history of monotremes and earn her Master's degree. Rachel will be continuing to study the evolution of early mammals and earn her doctorate with Dr. Rowe.

email: rvsimon@utexas.edu

This thesis was typed by Rachel Veronica Simon Wallace.